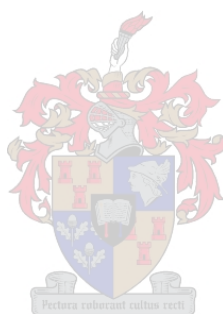


***Investigation of the antifungal activity of tryptophan-rich
cyclic peptides***

by

Precious Gamuchirai Muchaneta Mamhende
BSc Honours (Biochemistry)



Dissertation approved for the degree
Magister Scientiae (Biochemistry)

in the
Faculty of Science
at the
University of Stellenbosch

Supervisor: Prof. Marina Rautenbach
Department of Biochemistry
University of Stellenbosch

April 2019

Declaration

By submitting this thesis electronically, I *Precious Gamuchirai Muchaneta Mamhende* declare that the entirety of the work contained therein is my own, original work, that I am the sole author thereof (save to the extent explicitly otherwise stated), that reproduction and publication thereof by Stellenbosch University will not infringe any third party rights and that I have not previously, in its entirety or in part, submitted it for obtaining any qualification.

*Precious Gamuchirai
Muchaneta Mamhende*

10 January 2019

.....

.....

Name

Date

Copyright © 2019 Stellenbosch University

All rights reserved

Summary

The global population of immunocompromised individuals has been rising due to the immunosuppressive nature of advanced medical interventions such as chemotherapy for cancer and immunosuppressive conditions such as HIV infection. Concurrent with this is the increasing incidence of life threatening systemic fungal infections as well as the growing resistance towards existing antifungal drugs. As a result, there is an urgent need for the discovery and development of novel drugs of antifungal therapy. Antimicrobial peptides present as promising candidates for this role due to their broad-spectrum antimicrobial activity and the limited potential for the evolution of resistance against them.

In this study, the potential of small AMPs to serve as therapeutic agents against fungal infections was investigated by characterising the antifungal activity and mode of action of natural cyclodecapeptides and synthetic RW-hexapeptides against a human fungal pathogen, *Aspergillus fumigatus*. In addition, biophysical characterisation of their structures was conducted to evaluate the role of structure in antifungal activity.

Biophysical characterisation of the secondary structure of cyclodecapeptides confirmed their conserved β -sheet structure. Structural characterisation of cyclic RW-hexapeptides highlighted their secondary structure to be quite stable and to consist of β -sheet and β -turns. On the other hand, the secondary structure of the linear analogues was shown to be flexible, changing from highly irregular (undefined) structures to more defined structures as the polarity of the environment was altered.

The cyclodecapeptides and RW-hexapeptides potently inhibited the germination and growth of *A. fumigatus* spores highlighting the potential of both peptide groups as antifungal agents. However, the cyclodecapeptides exhibited pronounced haemolytic activity which compromised their selectivity for the fungal target. In contrast, the RW-hexapeptides had little to no haemolytic activity which translated to a greater selectivity for the fungal pathogen.

A partial characterisation of the mode action employed by the cyclodecapeptides and the RW-hexapeptides was done. The cyclodecapeptide, tryptocidine C (WC), rapidly induced the uptake of the membrane impermeable dye, SYTOX Green (SG) in *A. fumigatus* hyphae. This result confirmed the previously described membranolytic mode of action of the cyclodecapeptides. In contrast, RW-hexapeptides were not as effective at inducing the uptake of SG, indicating that membrane lysis is not their principal mode of action. Thus, the mode of action of RW-hexapeptides remains unknown but ROS could potentially be involved in the antifungal mechanism of action as one of the cyclohexapeptides, cWWW, significantly increased the accumulation of endogenous ROS in *A. fumigatus* hyphae. Furthermore, the slightly antagonistic interactions between WC and the most active RW-hexapeptide analogues, especially cWWW, in the peptide combination studies could indicate that the two groups of peptides may share a target but act on it differently. While RW-hexapeptides may not be lytic, the membrane could still be their target meaning that the lytic activity of WC prevents them from acting on their target hence the antagonistic interactions. In conclusion, the demonstrated selectivity of the RW-hexapeptides renders them very attractive for potential development as antifungal agents for systemic use.

Opsomming

Die globale bevolking van individue met 'n onderdrukte immuunstelsel het gestyg as gevolg van die immunonderdrukkende aard van gevorderde mediese ingrypings soos chemoterapie vir kanker en immunonderdrukkende toestande soos MIV-infeksie. Gepaardgaande hiermee is daar 'n toename in die voorkoms van lewensbedreigende sistemiese swaminfeksies asook 'n toename weerstand teen bestaande antifungale middels. As gevolg hiervan is daar 'n dringende behoefte aan die ontdekking en ontwikkeling van nuwe middels vir antifungiese behandelings. Antimikrobiese peptiede (AMPe) is belowende kandidate vir hierdie rol weens hul breë spektrum antimikrobiese aktiwiteit en die beperkte potensiaal vir die ontwikkeling van weerstand.

In hierdie studie is die potensiaal van klein AMPe om as middels teen swaminfeksies te dien, ondersoek deur die antifungale aktiwiteit en werking van natuurlike siklodekapeptiede en sintetiese RW-heksapeptiede teen 'n menslike swampatogeen, *Aspergillus fumigatus*, te karakteriseer. Daarbenewens is die biofisiese karakterisering van hul strukture uitgevoer om die rol van struktuur in antifungale aktiwiteit te evalueer.

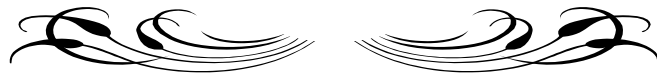
Biofisiese karakterisering van die sekondêre struktuur van siklodekapeptiede het hul bewaarde β -plaatstruktuur bevestig. Strukturele karakterisering van die RW-heksapeptiede het beklemtoon dat die sekondêre struktuur van die sikliese analoë redelik stabiel is en uit reëlmatige sekondêre strukturelemente (β -plaat en β -draaie) bestaan. Daarteenoor is die sekondêre strukture van die lineêre analoë meer buigsam, wat vanaf hoogs onreëlmatige (ongedefinieerde) strukture tot meer gedefinieerde strukture omsskakel, soos die polariteit van die omgewing verander.

Die siklodekapeptiede en RW-heksapeptiede verhinder moontlik die ontkieming en groei van *A. fumigatus*-spore, wat die potensiaal van beide peptiedgroepe as antifungale middels beklemtoon. Die siklodekapeptiede het egter uitgesproke hemolitiese aktiwiteit getoon, wat hul selektiwiteit vir die swamteiken benadeel het. Daarteenoor het die RW-heksapeptiede min of geen hemolitiese aktiwiteit getoon wat 'n groter selektiwiteit vir die swampatogeen beteken.

'n Gedeeltelike karakterisering van die meganisme van aksie wat deur die siklodekapeptiede en die RW-heksapeptiede gebruik word, is gedoen. Die siklodekapeptiede, triptosidien C (WC), het 'n vinnige opname van die membraan-deurdringbare kleurstof, SYTOX Groen (SG) in *A. fumigatus* hife veroorsaak. Die resultaat het die voorheen beskryfde litiese membraan werking van die siklodekapeptiede bevestig. In teenstelling hiermee het RW-heksapeptiede nie effektief die opname van SG veroorsaak nie, wat aandui dat membraanlise nie hul hoofmeganisme van aksie is nie. Die werkingsmeganisme van RW-heksapeptiede bly dus onbekend, maar ROS (reaktiwe suurstof spesies) kan moontlik by die antifungale aktiwiteit betrokke wees, aangesien die sikloheksapeptied, cWWW, die toename van endogene ROS in *A. fumigatus* hife aansienlik verhoog het. Verder kan die effense antagonistiese interaksies tussen WC en die twee aktiefste sikoheksapeptiede, spesifiek cWWW, in die peptiedkombinasie studies aandui dat die twee groepe peptiede 'n teiken kan deel, maar verskil in interaksie. Terwyl RW-heksapeptiede nie lities is nie, kan die membraan steeds hul teiken wees, wat beteken dat die litiese aktiwiteit van WC hulle verhoed om op hul teiken te reageer, wat die antagonistiese interaksies tot gevolg het. As afsluitende gevolgtrekking maak gedemonstreerde selektiwiteit van die RW-heksapeptiede hulle baie aantreklik vir die potensiële ontwikkeling vir sistemiese gebruik as antifungiese middels.



*“The difference between ordinary and extraordinary
is that little extra”*



Acknowledgements

I would like to express my thanks and gratitude to the following persons and institutions:

- Prof Marina Rautenbach, my beloved supervisor, for allowing me the opportunity to study under her mentorship and for her unwavering support throughout my research journey thus far, especially in the writing of my MSc thesis
- My colleagues in the BIOPEP Peptide group for their assistance and support in the laboratory and for making the laboratory a pleasant working environment
- Dr Helba Bredell, the BIOPEP laboratory manager, for her assistance and support in the laboratory and her efficient management of the laboratory
- Dr Margitta Dathe (Leibniz Institute, Germany), for her guidance in the conceptualisation of the project and for donating the cyclic RW-hexapeptides, without which this research could not have been conducted
- Dr Marietjie Stander and her colleagues at the Central Analytical Facilities (CAF), Stellenbosch University for their expertise and technical assistance during mass spectrometry (MS) analysis
- Dr Jaco Brand (CAF, Stellenbosch University), for his expertise and assistance with circular dichroism (CD) spectroscopy
- The National Research Foundation, Stellenbosch University Faculty of Science and BIOPEP Peptide Fund for their financial support in achieving my MSc
- My family and friends for their unconditional love and support throughout this entire journey.

Table of Contents

DECLARATION	I
SUMMARY	III
ACKNOWLEDGEMENTS	VI
TABLE OF CONTENTS	VII
LIST OF ABBREVIATIONS AND ACRONYMS	IX
PREFACE.....	XIII
<i>Aims and objectives</i>	xiv
<i>Thesis Content</i>	xv
OUTPUTS OF MSc STUDY	XVI
CHAPTER 1 LITERATURE REVIEW: INVASIVE FUNGAL INFECTIONS AND ANTIFUNGAL PEPTIDES.....	1
1.1 INTRODUCTION	1
1.2 HUMAN FUNGAL PATHOGENS CAUSING INVASIVE AND/OR SYSTEMIC INFECTIONS	2
<i>Aspergillus fumigatus and invasive Aspergillosis</i>	2
<i>Candida albicans and Candidemia</i>	3
<i>Cryptococcus neoformans and Cryptococcosis</i>	4
1.3 THE CLINICAL ARSENAL OF ANTIFUNGAL DRUGS	5
<i>Polyenes</i>	5
<i>Pyrimidines</i>	6
<i>Azoles</i>	6
<i>Echinocandins</i>	8
1.4 ANTIMICROBIAL PEPTIDES	8
1.5 ANTIFUNGAL PEPTIDES	9
<i>Antifungal peptides of plant origin</i>	12
<i>Insect-derived antifungal peptides</i>	13
<i>Antifungal peptides of animal origin</i>	13
<i>Antifungal peptides of microbial origin</i>	15
1.6 ANTIFUNGAL POTENTIAL OF SMALL AROMATIC PEPTIDES.....	17
<i>Natural cyclodecapeptides: Tyrocidines and analogues</i>	17
<i>Synthetic Arginine and Tryptophan rich peptides: The RW-hexapeptides</i>	22
1.7 CONCLUDING REMARKS	26
1.8 REFERENCES	26
CHAPTER 2 PRODUCTION, PURIFICATION AND CHEMICAL CHARACTERISATION OF NATURAL AND SYNTHETIC PEPTIDES.....	1
2.1 INTRODUCTION	1
2.2 MATERIALS.....	3
<i>Peptide production</i>	3
<i>Extraction, purification and analysis of peptides</i>	3
2.3 METHODS	3
<i>Pre-culturing of the producer organism</i>	3
<i>Production and extraction of peptides from cultures of Brevibacillus parabrevis</i>	4
<i>Semi-preparative RP-HPLC of tyrocidines and analogues</i>	4
<i>ESMS and UPLC-MS analysis of peptides</i>	5
<i>Data Analysis</i>	6
2.4 RESULTS AND DISCUSSION	6
<i>Part 1: Production, purification and characterisation of tyrocidines and analogues</i>	6
<i>Part two: Chemical characterisation of the synthetic hexapeptides</i>	17
2.4 CONCLUSIONS.....	35
2.5 REFERENCES	36

CHAPTER 3 STRUCTURAL CHARACTERISATION OF NATURAL CYCLO-DECAPEPTIDES AND SYNTHETIC HEXAPEPTIDES.....	1
3.1 INTRODUCTION	1
3.2 MATERIALS.....	2
3.3 METHODS	3
<i>Molecular modelling of RW-hexapeptide structures</i>	3
<i>Circular dichroism spectroscopy</i>	4
<i>Fluorescence spectroscopy</i>	4
<i>Data analysis</i>	4
3.4 RESULTS AND DISCUSSION	5
<i>Molecular models of natural cyclo-decapeptides</i>	5
<i>Molecular modelling of RW-hexapeptide structures</i>	7
<i>Analysis of peptide structure by Circular Dichroism</i>	12
<i>Characterisation of the Trp environment using fluorescence spectroscopy</i>	24
3.5 CONCLUSION	30
3.6 REFERENCES.....	31
CHAPTER 4 CHARACTERISATION OF BIOLOGICAL ACTIVITY AND MODE OF ACTION OF NATURAL CYCLODECAPEPTIDES AND SYNTHETIC RW-HEXAPEPTIDES	1
4.1 INTRODUCTION	1
4.2 MATERIALS.....	2
4.3 METHODS	3
<i>Peptide preparation</i>	3
<i>Culturing of fungi and spore harvesting</i>	3
<i>Microdilution broth assays to investigate inhibition of the germination and growth of A. fumigatus spores</i>	3
<i>Microdilution broth assays to determine metabolic inhibition of A. fumigatus hyphae</i>	4
<i>Haemolysis assay</i>	4
<i>Time course kinetic study to investigate membrane permeabilisation</i>	5
<i>Spectrofluorometric determination of ROS production</i>	5
<i>Data Analysis</i>	6
4.4 RESULTS AND DISCUSSION	7
<i>Part 1: Characterisation of biological activity</i>	7
<i>Part 2: Mode of action studies</i>	18
4.5 CONCLUSION	22
4.6 REFERENCES.....	23
4.7 ADDENDUM	27
CHAPTER 5 CONCLUSIONS AND RECOMMENDATIONS FOR FUTURE STUDIES.....	1
5.1 INTRODUCTION	1
5.2 EXPERIMENTAL CONCLUSIONS.....	1
<i>Production, purification and chemical characterisation of natural cyclodecapeptides</i>	1
<i>Chemical characterisation of RW-hexapeptides</i>	2
<i>Structural characterisation of cyclodecapeptides</i>	3
<i>Structural characterisation of RW-hexapeptides</i>	3
<i>Biological activity of peptides</i>	4
5.3 LAST WORD.....	5
5.4 REFERENCES	6

List of Abbreviations and Acronyms

[M+H] ⁺	singly charged molecular ion
[M+2H] ²⁺	doubly charged molecular ion
[M+3H] ³⁺	triply charged molecular ion
[M+K+2H] ³⁺	triply charged potassium adduct
<i>A. clavatus</i>	<i>Aspergillus clavatus</i>
<i>A. flavus</i>	<i>Aspergillus flavus</i>
<i>A. fumigatus</i>	<i>Aspergillus fumigatus</i>
<i>A. giganteus</i>	<i>Aspergillus giganteus</i>
<i>A. nidulans</i>	<i>Aspergillus nidulans</i>
<i>A. terreus</i>	<i>Aspergillus terreus</i>
ACN	acetonitrile
Ac-KRKFW	N-Acetyl-KRKFW-NH ₂
Ac-RKKFW	N-Acetyl-RKKFW-NH ₂
Ac-RRRFW	N-Acetyl-RRRFW-NH ₂
Ac-RWRWRW	N-Acetyl-RWRWRW-NH ₂
Ac-RRRWWW	N-Acetyl-RRRWWW-NH ₂
Ac-RRRWYW	N-Acetyl-RRRWYW-NH ₂
AIDS	acquired immunodeficiency syndrome
AMP(s)	antimicrobial peptide(s)
ATCC	American type culture collection
<i>B. aneurinolyticus</i>	<i>Bacillus aneurinolyticus</i>
<i>B. subtilis</i>	<i>Bacillus subtilis</i>
<i>B. cinerea</i>	<i>Bortrytis cinerea</i>
<i>Br. parabrevis</i>	<i>Brevibacillus parabrevis</i>
<i>C. albicans</i>	<i>Candida albicans</i>
<i>C. glabrata</i>	<i>Candida glabrata</i>
<i>C. parapsilosis</i>	<i>Candida parapsilosis</i>
<i>C. krusei</i>	<i>Candida krusei</i>
<i>C. neoformans</i>	<i>Cryptococcus neoformans</i>
CD	circular dichroism

CH ₂	methylene group
CO	carbonyl group
cKRR	cyclo-KRKFW
cRKK	cyclo-RKKFW
cWFW	cyclo-RRRFW
cWRW	cyclo-RWRWRW
cWWW	cyclo-RRRWWW
cWYW	cyclo-RRRWYW
<i>D. melanogaster</i>	<i>Drosophila melanogaster</i>
DNA	deoxyribonucleic acid
<i>E. coli</i>	Escherichia coli
ESMS	electrospray mass spectrometry
EtOH	ethanol
FA	phenycidine A
FIC	fractional inhibition concentration
FICI	fractional inhibition concentration index
FS	fluorescence spectroscopy
<i>F. moniliforme</i>	<i>Fusarium moniliforme</i>
<i>F. oxysporum</i>	<i>Fusarium oxysporum</i>
<i>F. solani</i>	<i>Fusarium solani</i>
GS	gramicidin S
HC ₅₀	concentration leading to 50% haemolysis
HIV	human immunodeficiency virus
HPLC	high performance liquid chromatography
H ₂ DCFDA	2',7'-dichlorofluorescein diacetate
IA	invasive aspergillosis
IC ₅₀	peptide concentration leading to 50 % microbial growth inhibition
IC _{max}	peptide concentration leading to maximal microbial growth inhibition
LC	liquid chromatography
LC ₅₀	peptide concentration leading to 50% cytotoxicity
LCMS	liquid chromatography mass spectrometry
<i>M. luteus</i>	<i>Micrococcus luteus</i>
<i>m/z</i>	mass over charge ratio

MIC	minimum inhibitory concentration
M(IP) ₂ C	mannosyldiinositolphosphorylceramide
MOA	mode of action
M_r	relative molar mass
MS	mass spectrometry
MV	molecular volume
<i>N. crassa</i>	<i>Neurospora crassa</i>
NCTC	national collection of type cultures
NMR	nuclear magnetic resonance
NH/NH ₂	amino group
OD	optical density
Orn/O	ornithine
<i>P. aeruginosa</i>	<i>Pseudomonas aeruginosa</i>
PBS	phosphate buffered saline
PDA	potato dextrose agar
PDB	potato dextrose broth
<i>P. digitatum</i>	<i>Penicillium digitatum</i>
<i>P. falciparum</i>	<i>Plasmodium falciparum</i>
Phc(s)	phenycidine(s)
POPC	palmitoyloleyphosphatidylcholine
POPE	palmitoyloleyphosphatidylethanolamine
POPG	palmitoyloleyphosphatidylglycerol
<i>P. pastoris</i>	<i>Pichia pastoris</i>
QC	quality control
RBC	red blood cell (erythrocyte)
RMSD	root-mean-square deviation
RNA	ribonucleic acid
ROS	reactive oxygen species
RP-HPLC	reverse phase high performance liquid chromatography
RPMI	Roswell Park Memorial Institute (medium)
R_t	retention time of analyte in column chromatography
RW-hexapeptide(s)	Arg- and Trp-rich hexapeptide(s)
SASA	solvent accessible surface area

SAV	solvent accessible volume
<i>S. cerevisiae</i>	<i>Saccharomyces cerevisiae</i>
SEM	standard error of the mean
SG	SYTOX Green
spp.	species
<i>S. aureus</i>	<i>Staphylococcus aureus</i>
<i>S. pyogenes</i>	<i>Streptococcus pyogenes</i>
Tcn	tyrothricin
Tmix	tyrocidine mixture
TFA	trifluoroacetic acid
TFE	2,2,2-trifluoroethanol
TGS	tryptone glucose and salts culture medium
TOF	time of flight
Tpc(s)	tryptocidine(s)
Trc(s)	tyrocidine(s)
TSB	tryptone soy broth
UPLC	ultraperformance liquid chromatography
UPLC-MS	ultraperformance liquid chromatography linked to mass spectrometry
UV	ultraviolet
WA	tryptocidine A
WB	tryptocidine B
WC	tryptocidine C
WC ₁	tryptocidine C ₁
YA	tyrocidine A
YA ₁	tyrocidine A ₁
YB	tyrocidine B
YB'	tyrocidine B'
YB ₁	tyrocidine B ₁
YC	tyrocidine C
YC ₁	tyrocidine C ₁

Standard 3-letter and 1-letter abbreviations were used for the natural amino acids, with uppercase 1-letter abbreviations for L-amino acid residues and lower case 1-letter abbreviations for D-amino acid residues in peptide sequences

Preface

The increasing frequency of multi-drug resistant pathogens has become an issue of great medical concern worldwide, especially since the population of immunocompromised individuals continues to rise due to immunosuppressive infections such as HIV, post-surgery immunosuppressive therapies and chemotherapy of cancer patients. Immunocompromised patients are often susceptible to life threatening systemic fungal infections such as those caused by *Aspergillus fumigatus*, *Candida albicans* and *Cryptococcus neoformans*. Systemic fungal infections are extremely fatal and are associated with high mortality rates that exceed 50%, even when treatment is administered. The currently available antifungal agents have demonstrated inefficacy in the treatment of systemic fungal infections and/or toxicity towards the host. Moreover, fungal pathogens are increasingly acquiring resistance against these antifungal agents. As such novel therapeutic agents are urgently needed in order to address the global health burden of systemic fungal infections.

Antimicrobial peptides (AMPs) are attractive candidates for potential development as alternative antifungal therapeutic agents. They have broad spectrum activity which compromises the efficient functioning of components of the microbial cell that are essential for survival such as the cell membrane. In addition, antimicrobial activity is swiftly elicited upon encountering a microbial challenge which leaves little room for the development of resistance.

Tyrocidines and analogues are small cyclodecapeptides that are produced by the soil bacterium, *Brevibacillus parabrevis*. They have exhibited potent lytic activity against a plethora of pathogens, including filamentous fungi. They are also components of tyrothricin, an antibiotic that has been used for topical and oral applications in the management of microbial infections for the last 70 years without resistance development. RW-hexapeptides are another group of small AMPs that can potentially be developed as novel antifungal therapeutic agents based on their potent antibacterial activity. They have shown activity against Gram-positive and Gram-negative bacteria. However, the antifungal of most of RW-hexapeptide analogues remains to be characterised.

Therefore, the goal of this research was to elucidate the potential of selected AMPs (natural cyclodecapeptides and synthetic RW-hexapeptides) to serve as alternative antifungal agents in an effort to contribute to the ongoing search for novel therapeutic agents to combat fungal pathogens. To achieve this goal, the aims and objectives listed below had to be met.

Aims and objectives

Aim 1: Production, purification and chemical characterisation of natural cyclodecapeptides and RW-hexapeptides.

1. Acquire a selection of linear and cyclic synthetic RW-hexapeptides and chemically characterise all peptides via electrospray mass spectrometry (ESMS) and ultra-performance liquid chromatography linked to ESMS (UPLC-MS).
2. Produce selected cyclodecapeptide analogues using cultures of *Brevibacillus parabrevis* 5618 supplemented with selected aromatic amino acids and purify peptides via established extraction and semi-preparative HPLC methodologies. Chemically characterise all peptides via ESMS and UPLC-MS.

The results of these objectives are reported in Chapter 2

Aim 2: Biophysical structural characterisation of natural cyclodecapeptides and RW-hexapeptides

1. Analyse secondary structures of RW-hexapeptides and cyclodecapeptides and determine physicochemical parameters from *in silico* molecular models
2. Analyse the secondary structure of cyclodecapeptides and RW-hexapeptides using circular dichroism spectroscopy and determine the influence of different solvent environments on the secondary structures
3. Investigate the effect of different solvent environments on the tertiary structure of cyclodecapeptides and RW-hexapeptides by tracking the fluorescence of Trp residues using fluorescence spectroscopy

The results of these objectives are reported in Chapter 3

Aim 3: Characterisation of the antifungal activity and mode of action of natural cyclodecapeptides and RW-hexapeptides against *Aspergillus fumigatus*

1. Establish the growth inhibition parameters of RW-hexapeptides and natural cyclodecapeptides towards *A. fumigatus* spores and hyphae
2. Establish the inhibition parameters of combinations of RW-hexapeptides with natural cyclodecapeptides to determine if peptide interactions are synergistic, additive or antagonistic towards *A. fumigatus*

3. Determine peptide selectivity by using established haemolytic assays
4. Determine whether the mode of antifungal action of cyclodecapeptides and RW-hexapeptides is lytic or non-lytic
5. Investigate induction of endogenous reactive oxygen species (ROS) by the most active cyclodecapeptides and RW-hexapeptides

The results of these objectives are reported in Chapter 4

Thesis Content

This thesis consists of five chapters and was structured so that each chapter is a standalone unit consisting of the following sections: introduction, materials and methods, results and discussion, conclusion and references. This was done for the purpose of making the publication of findings easier. A literature background on fungal infections and antifungal peptides is presented in Chapter 1. This is followed by Chapter 2-4 where the details of the experimental investigations of each of the three aims are discussed separately. The last chapter (Chapter 5) summaries the findings from this entire investigation and gives recommendations for future work. Due to the structuring of the thesis into independent chapter units, some repetitions were inevitable, but these were kept to a minimum.

Outputs of MSc study

- Mamhende PGM* (2016) Tryptophan-rich cyclic peptides, BIOPEP Forum, Department of Biochemistry, Stellenbosch University, Oral presentation
- Mamhende PGM* (2017) Investigation of the antifungal activity of tryptophan-rich cyclic peptides, Biochemistry Forum, Department of Biochemistry, Stellenbosch University, Oral presentation
- Mamhende PGM*, (2018) Small, aromatic amino acid containing peptides exhibiting antifungal activity, SASBMB 2018 Conference, Potchefstroom, South Africa
- Mamhende PGM* (February 2019) Investigation of the antifungal activity of tryptophan-rich cyclic peptides, Biochemistry Forum, University of Stellenbosch, Oral defence of MSc thesis
- Mamhende PGM, Dathe M, Rautenbach M* (2019) Comparison of the antifungal activity of linear and cyclic Arg-Trp rich hexapeptides, manuscript in preparation for submission to *Frontiers in Microbiology*

*Presenter/Corresponding author

Chapter 1

Literature Review: Invasive fungal infections and antifungal peptides

1.1 Introduction

Fungi are a diverse group of eukaryotic microorganisms; roughly estimated to be around five million species worldwide [1]. They exist either as unicellular organisms known as yeasts or as multicellular filamentous organism known as moulds. The ecological niche of fungi varies, with several species living either as saprophytes in the soil and environment or as commensal organisms within humans and animals. As a result, they can influence the health of other organisms present in these ecological niches or the host which they infect.

Unlike bacteria, fungi were previously regarded as predominantly phytopathogens which has led to a detrimental oversight of their impact on human health. Fungi infect over a billion people each year and millions succumb to these infections [1,2]. Approximately 600 fungal species have been identified as potentially pathogenic towards humans and/or animals [3], but only 20-25 species are frequent etiologic agents of disease [1].

The infections caused by pathogenic fungi are split into two distinct categories namely superficial mycoses and invasive/systemic mycoses. Of the two types, superficial infections are the most common affecting approximately 1.7 billion of the global human population [2]. Infections of this kind normally affect the skin and nails of individuals regardless of immune status; often causing conditions such as athlete's foot, ringworm of the scalp and nail infections. Also common are the infections of the mucosal lining of the oral cavity and female urogenital tract known as oral thrush and vulvovaginal thrush respectively [2]. Fortunately, despite their high incidence, superficial infections are easily treatable and rarely result in mortality; but the quality of life of the afflicted individuals is adversely affected [4].

In contrast, invasive fungal infections have a lower incidence but are usually life threatening and have an unacceptably high overall mortality rate (often exceeding 50%)[2]. Invasive fungal infections are characterised as a severe, life-threatening systemic infections that have disseminated into visceral organs of the body such as, but not limited to the lungs, liver, kidneys and brain. Invasive fungal infections affect mostly immunocompromised individuals. In recent years there has been a surge in the population of immunocompromised individuals due to underlying immunosuppressive conditions such as HIV infection and cancer and aggressive

medical interventions [5]. This has translated to an increase in the occurrence of invasive fungal infections. It should be noted, though, that true mortality rates remain unknown because of lack of good epidemiological data [3]. The estimated annual mortality rate is comparable to that of malaria or tuberculosis; approximately one and half million deaths occur each year due to invasive fungal infections[2]. This indicates that fungi have since evolved into becoming a major health problem and therefore the burden they impose on global health system can no longer be ignored. Because of this, more research must be devoted to combating fungal pathogens and the mycoses they cause.

Although several fungal species are implicated in the pathogenesis of these invasive fungal infections, the top three causative agents are members of the *Candida*, *Aspergillus* and *Cryptococcus* species. These species account for over 90% of all invasive fungal infections [2][6], and by extension fungi-related deaths. The following section has been devoted to reviewing each of the three above-named pathogens and the invasive infections in greater depth.

1.2 Human fungal pathogens causing invasive and/or systemic infections

***Aspergillus fumigatus* and invasive Aspergillosis**

Aspergillus fumigatus is a ubiquitous saprophyte that commonly grows on decaying organic debris and produces airborne spores. Its spores enter the human body via the respiratory system making the lung the primary site of infection although any organ in the body can be affected [7,8]. *A. fumigatus* causes a spectrum of disease conditions in immunocompromised hosts which include acute or chronic invasive aspergillosis (IA), aspergilloma and allergic bronchopulmonary aspergillosis [9]. Of greatest medical concern is acute IA, which is often a fatal infection that progresses rapidly [10]. The mortality rate associated with IA is very high, more than 50% even when diagnosed and treated. However, if there is a delay in diagnosis and or treatment, the fatality rate can be as high as 100% [2,11].

Invasive aspergillosis affects a narrow spectrum of immunosuppressed individuals who usually are recipients of transplants or have underlying haematological malignancies [7,12]. According to a study by Patterson *et al.* [12], approximately 61% of the patients diagnosed with IA had either a haematological cancer or had received a bone marrow transplant (BMT). The estimated incidence of IA is 5-25% in patients with acute leukaemia, 5-10% in recipients of allogeneic BMT and 0.5-5% after solid organ transplantation [7]. Of those who have undergone solid

organ transplantation, the incidence of IA is highest amongst heart or lung transplant recipients (14-18%). Furthermore, an increasing frequency of IA has been observed in immunocompromised patients without an underlying haematological disease such as those diagnosed with advanced AIDS (1-12%) and those with chronic granulomatous disease (25-40%) [7,13]. Recently, the risk of IA has also been associated with diabetes mellitus and the use of corticosteroid therapy [13].

A. fumigatus is the predominant etiologic agent of invasive aspergillosis, accounting for approximately 90% of all human infections. However, other *Aspergillus* species such as *A. flavus*, *A. terreus* and *A. niger* are sometimes implicated as pathogens [7,9,14]. For the purposes of the research presented in this thesis, the focus is entirely on *A. fumigatus* since it is the most common agent of infection.

***Candida albicans* and Candidemia**

The yeast *Candida* is a commensal organism that forms part of the normal flora found on mucosal membranes of healthy individuals. Unfortunately, in the immunocompromised host, *Candida* species have the potential to cause infections and are therefore deemed opportunistic pathogens [15]. According to the Centres for Disease Control and prevention (CDC), *Candida* species pose a serious threat to human health as they are increasingly becoming resistant to antifungal drugs [16].

The invasive fungal infections caused by yeast belonging to the *Candida* genus are termed invasive candidiasis and are the prevalent type of fungal infections in Western countries. The most common clinical presentation of invasive candidiasis is candidemia (bloodstream infection) [17]. It has been reported that *Candida* species are responsible for approximately 8-10% of all health care related blood stream infections [13] and are the fourth most frequent cause of nosocomial bloodstream infection in the United States [18]. Although a multitude of *Candida* species are implicated as etiologic agents of invasive candidiasis, approximately 95-97% of all infections are caused by the following five species: *C. albicans*, *C. glabrata*, *C. krusei*, *C. tropicalis* and *C. parapsilosis* [13,19]. Of these, *C. albicans* remains the leading cause of human infections both in Europe and the United States, accounting for approximately 60% of all infections. However, epidemiology trends have been changing over the years and the incidence of infections due non-*albicans Candida* is increasing [17,20,21].

The development of candidemia is largely associated with prolonged hospitalisation of vulnerable population groups with certain underlying medical conditions which include hematologic malignancies, severe neutropenia, gastrointestinal surgery, premature birth and advanced age (over 70 years). In addition, the presence of a venous catheter, renal failure, extended use of broad-spectrum antibiotics and parenteral nutrition have also been identified as secondary risk factors within these high-risk population groups [13,22–24]. Despite therapeutic intervention, the mortality rate of candidemia has remained very high. Candidemia is associated with a crude mortality exceeding 60% and an attributable mortality between 10%-49% [25].

***Cryptococcus neoformans* and Cryptococcosis**

Cryptococcosis is an opportunistic infection that is primarily caused by *Cryptococcus neoformans*, a ubiquitous fungal pathogen [2]. It is the second most common yeast species to cause opportunistic infections in immune compromised patients [21]. Infection occurs via inhalation and typically manifests itself as meningoencephalitis, also known as meningitis [26]. In regions that are highly prevalent in HIV/AIDS, *C. neoformans* has evolved to become the leading cause of meningitis [27–30]. Incidence of HIV related cryptococcal infections is about 95% in middle and low-income countries and 80% in high income countries. This indicates that HIV infection is the predominant predisposing factor to cryptococcal infections throughout the world [31]. Other factors that also increase one's susceptibility to acquiring a cryptococcal infection include solid organ transplantation, exposure to corticosteroid or other immunosuppressive therapy, hematologic cancers and diabetes mellitus [26].

According to the CDC, the global burden of cryptococcal meningitis stands at an estimated one million cases each year with more than 600 000 mortalities occurring in Sub-Saharan Africa. The disease accounts for 55-70% of AIDS related deaths in Sub-Saharan Africa and Latin America; thereby making it the fourth leading cause of deaths in AIDS patients [29]. These statistics are clearly indicative of how huge the disease burden of cryptococcal meningitis is in Sub-Saharan Africa and how well it compares with the health burden imposed by the continent's well recognised killer diseases such as tuberculosis (350,000 deaths), childhood diarrhoeal diseases (525,000 deaths) and malaria (405,000 deaths) [32]. What is disturbing, though, is that such a fatal infection has not received the same degree of attention as the other diseases of comparable health burden.

1.3 The clinical arsenal of antifungal drugs

The high mortalities associated with invasive fungal infections are a direct result of the shortcomings in their clinical management. Fungal cells, being eukaryotic organisms, bear a strong evolutionary resemblance to human and animal cells. Because of this, the discovery of unique molecular targets that can be exploited for drug development without the risk of inducing toxicity in the host is rather difficult [4,6,33]. As a result, only a few drug classes (polyenes, pyrimidines, azoles and echinocandins) are currently available for clinical use to tackle fungal pathogens [4,6,34]. Refer to Figure 1.1 for chemical structures of selected antifungal drug in clinical use. In addition, toxicity and resistance issues preclude the use of some of the antifungal agents available in the already scant antifungal drug repository further constraining the choice of therapeutics.

Polyenes

Polyenes were the first class of antifungal agents to be approved for clinical use against invasive fungal infections. They are natural, macrocyclic, amphipathic molecules that were isolated from cultures of *Streptomyces* [4]. The exact mechanism of action through which polyenes exert their antifungal activity remains unclear despite their long history in clinical use [35]. For a long time, the consensus in the scientific community was that polyenes act by inserting into and permeabilising ergosterol containing membranes which then leads to leakage of cell contents and ultimately cell death [36,37]. However, recent reports indicate that polyenes act as ergosterol sponges which extract ergosterol out of the lipid bilayer thereby disrupting the integrity of the membrane [38]. The three polyenes that are in clinical use are amphotericin B, nystatin and natamycin. Out of the three, only amphotericin B is used for the treatment of invasive and/or systemic fungal infections [4].

Amphotericin B has the widest spectrum of fungicidal activity and is regarded as the mainstay of antifungal therapy due to its potent fungicidal activity. Unfortunately, its slight affinity for cholesterol-containing membranes often causes nephrotoxicity and infusion related side effects in the host [39]. These toxic side effects are observed in 50-90% of cases [34] which often leads to the discontinuation of treatment. Three lipid formulations of amphotericin B were created to circumvent the toxicity issues and they have greatly improved the toxicity profile of amphotericin B [1]. Nonetheless, the use of amphotericin B is limited to only those infections that cannot be treated with the other therapeutic options

Pyrimidines

Flucytosine is a fungistatic pyrimidine that is licensed for the treatment of invasive mycoses [34]. It is a synthetic fluorinated analogue of cytosine that is readily converted into 5-fluorouracil, a toxic antimetabolite which is a potent inhibitor of nucleic acid metabolism as well as protein synthesis in fungal pathogens [1,6]. Flucytosine is highly selective for fungi because the enzyme that catalyses its conversion into 5-fluorouracil is absent in humans [1]. The rapid onset of resistance, however, limits its clinical usage as primary therapy [1,6,34]. Its combination with amphotericin B is the gold standard for the treatment of cryptococcal meningitis [40]

Azoles

The azoles are the most widely used form of antifungal agents [4,6,41]. They are divided into two classes namely the imidazoles (e.g miconazole and ketoconazole) and triazoles (e.g fluconazole, itraconazole, voriconazole and posaconazole). The imidazoles were the first of the two classes to be deployed for clinical use against invasive infections but were later replaced by the newer triazoles due to the latter's improved spectrum of activity, safety profile and pharmacokinetics [1,41]. Imidazoles are exclusively licensed for topical use [6].

The azoles exert their antifungal activity by interfering with the biosynthetic pathway of ergosterol; a lipid that is crucial to the maintenance of fungal membrane structure and function [42][6]. This interference leads to the accumulation of toxic sterol intermediates as well as depletion of ergosterol which induces severe membrane stress and ultimately, inhibition of fungal cell growth [43]. The mechanism of action of most azoles is fungistatic and is the reason for the evolution of resistance against them [44]. Voriconazole is the only drug in this family that is fungicidal. It is also the recommended therapeutic option for the treatment of invasive aspergillosis [6,34]. It is also worth noting that some *Candida* spp. such as *C. krusei* and *C. glabrata* are inherently resistant to azole therapy [6].

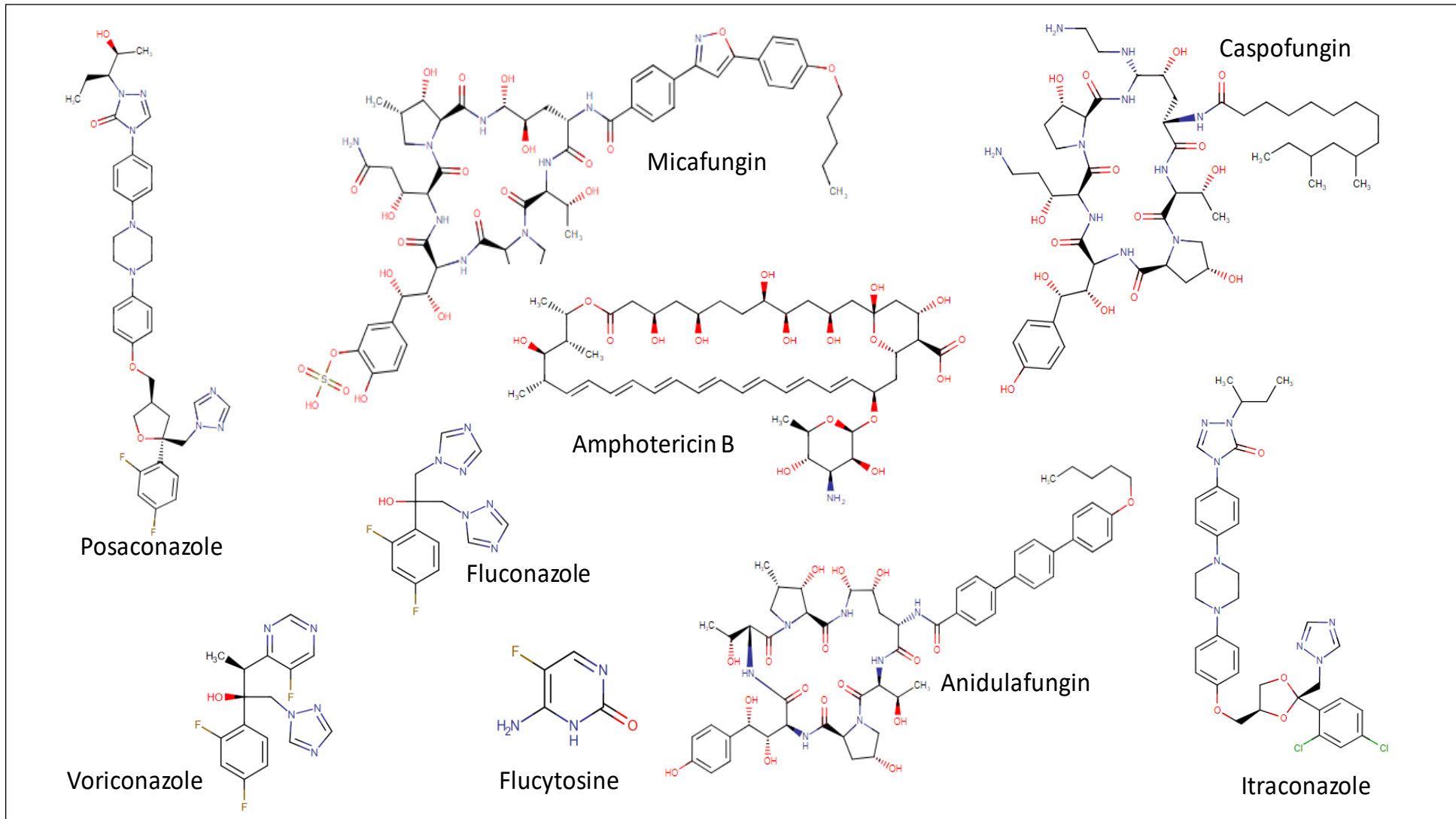


Figure 1.1: Structures of selected antifungal drugs currently in clinical use

Echinocandins

This family of lipopeptide-based antifungal agents are the most recent addition to the antifungal arsenal even though they were first introduced into the clinical scene almost two decades ago [45]. They function by non-competitively inhibiting the synthesis of 1,3 β -D-glucans, an essential polysaccharide in the fungal cell wall. This inhibition of 1,3 β -D-glucan synthase compromises the structural integrity of the growing cell wall leading to osmotic instability and cell death [4,46,47]. The absence of 1,3 β -D-glucans in mammalian cells makes it a unique target in fungi which accounts for the little host toxicity that is associated with the clinical usage of echinocandins [1,6]. At present, three echinocandins are FDA approved and licensed for use in the clinical setting namely caspofungin, micafungin and anidulafungin [6,43,45]. Echinocandins are typically fungicidal towards *Candida* spp. hence are currently the prescribed first line treatment for invasive candidiasis and nosocomial candidemia. On the contrary, they exhibit a fungistatic mode of action towards filamentous fungi including *Aspergillus* spp. [48,49]. As such, they are only used as alternative or second line therapy for invasive aspergillosis [35]. Echinocandins are virtually ineffective against *C. neoformans* [35,46].

This brief review of the existing antifungal therapeutics has highlighted that all the drugs that are currently in clinical use have limitations, therefore novel classes of therapeutics with alternative modes of action are urgently required to alleviate the health burden imposed by fungal infections.

1.4 Antimicrobial peptides

Antimicrobial peptides (AMPs) - Nature's own broad-spectrum antibiotics, could potentially be the solution to the problematic invasive fungal infections. AMPs are natural defence molecules forming part the innate immune system of multicellular organisms and are widely produced by microorganisms as part of their competitive survival strategy [50–52]. They are very diverse in terms of amino acid sequence, secondary structure, origin and activity spectra. However, many of them share a few similarities. They are small, from seven residues up to at about 100 amino acid residues. Most are cationic peptides with at least one positively charged amino acid residue. Hydrophobic residues account for 40-60% of total amino acid composition thus making these compounds amphipathic. Many of them fall into one of the following secondary structural categories: alpha helices, beta sheet, extended helices or loops, as well mixtures of secondary structures [50,53–55].

To date, a multitude of AMPs have been identified with exceptional *in vitro* and *in vivo* activities against various bacterial, fungal, protozoan and viral pathogens. The most prominent AMPs have exhibited low MICs against pathogens (1-8 μ M), even against antibiotic resistant pathogens [53]. This potency, together with many other desirable properties, highlights the potential of AMPs as alternative therapeutics against microbial pathogens. AMPs kill pathogens much more rapidly than conventional antibiotics and in a fashion that involves fundamental structural components of pathogenic cells such as the cell membrane or multiple targets. This mechanism of action renders the development of resistance highly improbable [53,56]. It has been shown that AMPs are able to enhance the activities of classical antibiotics thus making them attractive candidates for combination therapy [53,57]. Because of their omnipresence and natural composition, AMPs could be an eco-friendly means to deal with the pathogenic challenge. Lastly, it is relatively easy to modify the structure of existing natural AMPs to produce synthetic analogues with improved desirable characteristics such as reduced toxicity and enhanced stability.

1.5 Antifungal peptides

Within the large family of AMPs is found a smaller group of peptides known as antifungal peptides (AFPs), targeting mainly fungal pathogens. These peptides are not as widely distributed as peptides with broad spectrum antimicrobial activity [58]. Out of the 1900 AMPs that are registered on the online database of AMPs, a mere 34% are antifungal peptides versus 79% which were classified as antibacterial [59]. A summary on selected antifungal peptides is given in Table 1.1

Like the rest of the AMP family, antifungal peptides have varied amino acid sequences and structures. However, they do seem to possess a relatively large proportion of polar and neutral amino acid residues [55]. In contrast to the well characterised bactericidal AMPs, little is known about the properties and mechanism of action of AFPs making their classification a daunting task [58]. For the purposes of this review, the AFPs have been classified according to their sources which include microorganisms, plants and animals (Table 1.1). It should be noted, however, that this review is not exhaustive and only a few examples of antifungal peptides are discussed in each category

Table 1.1: Examples of antifungal peptides from various sources.

Peptide	Source/Origin	Structural description	Typical target organisms	Mode of action	Reference(s)
<i>Plant peptides</i>					
DmAMP1	<i>Dahlia merckii</i>		<i>S. cerevisiae</i>	Membrane permeabilisation by interaction with sphingolipids	[60]
RsAFP2	<i>Raphanus sativus</i>	51 amino acids	<i>C. albicans</i> , <i>P. pastoris</i>	Membrane permeabilisation by interaction with glucosylceramides, induction of ROS	[61,62]
PvD1	<i>Phaseolus vulgaris</i>	50 amino acids	<i>C. albicans</i> , <i>F. oxysporum</i>	Membrane permeabilisation by interaction with glucosylceramides, induction of ROS and NO	[63]
NaD1	<i>Nicotiana glauca</i>	α -helix and β -sheet	<i>F. oxysporum</i>	Interaction with cell wall, membrane permeabilisation and granulation of cytoplasm	[64]
<i>Insect peptides</i>					
Drosomycin	<i>Drosophila melanogaster</i>	5kDa, Cys-rich 44 amino acids,	<i>F. oxysporum</i> , <i>B. cinerea</i> , <i>N. crassa</i>	Membrane permeabilisation by interaction with sphingolipids	[65,66]
Cecropin A and B	<i>Hyalopora cecropia</i>	Linear, 4 kDa, 35-37 amino acids	<i>Fusarium spp.</i> <i>Aspergillus spp.</i>	Membrane lysis	[67]
Thanatin	<i>Posidus maculiventris</i>	β -sheet, cyclic, 21 amino acids,	<i>N. crassa</i> , <i>A. fumigatus</i> , <i>B. cinerea</i>	Unknown	
<i>Amphibian peptides</i>					
Magainin 2	<i>Xenopus laevis</i>	α -helical, Gly and Ser-rich, 23 amino acids	<i>S. cerevisiae</i> , <i>C. albicans</i> , <i>C. neoformans</i>	Membrane permeabilisation, DNA damage	[68]
Dermaseptins B and S	<i>Phyllomedusa sauvagii</i>	α -helical, Lys-rich, 27-34 amino acids	<i>F. oxysporum</i> , <i>C. albicans</i> , <i>C. neoformans</i>	Membrane lysis by interaction with sterols	[67,69]

<i>Mammalian peptides</i>					
HNP1-3	Human neutrophils	β -sheet, 29-30 amino acids	<i>C. albicans</i> , <i>C. neoformans</i>	Membrane permeabilisation, Inhibition of protein and DNA synthesis	[56,70]
NP1 and NP2	Rabbit neutrophils	β -sheet, 33 amino acids	<i>C. albicans</i> , <i>A. fumigatus</i>	Interaction with chitin	[71]
Lactoferrin	Mammalian secretions	18 amino acids	<i>C. albicans</i> , <i>A. fumigatus</i>	Iron sequestration	[72,73]
Histatin1 and 3	Human saliva	His-rich, 32-38 amino acids	<i>C. albicans</i> , <i>A. fumigatus</i> , <i>C. neoformans</i>	Interaction with energised membrane	[74]
<i>Bacterial peptides</i>					
Iturin A	<i>Bacillus subtilis</i>	Cyclic lipopeptide	<i>A. flavus</i> , <i>F. moniliforme</i>	Membrane permeabilisation	[75,76]
Bacillomycin F	<i>Bacillus subtilis</i>	Cyclic lipopeptide	<i>A. niger</i> , <i>C. albicans</i> , <i>S. cerevisiae</i>	Membrane permeabilisation	[77]
Nikkomycin X and Z	<i>Streptomyces tendae</i>	Peptidyl nucleoside	<i>C. albicans</i>	Inhibition of chitin synthesis	[78]
Tyrocidines (A, B, C)	<i>Brevibacillus parabrevis</i>	Cyclodecapeptides, β -sheet, 10 amino acids	<i>C. albicans</i> , <i>F. solani</i> , <i>B. cinerea</i>	Membrane lysis	[79,80]
<i>Fungal peptides</i>					
Echinocandin B	<i>Aspergillus nidulans</i>	Cyclic lipopeptide	<i>C. albicans</i>	Inhibition of glucan synthesis	[81]
Aureobasidin A	<i>Aureobasidium pullulans</i>	Cyclic depsipeptide	<i>C. neoformans</i>	Interferes with actin assembly, delocalization of chitin, interferes with sphingolipid synthesis	[82,83]
PAF	<i>Penicillium chrysogenum</i>	Cys-rich	<i>A. fumigatus</i>	Membrane polarisation and activation of ion channels	[84]

Antifungal peptides of plant origin

Antifungal peptides sourced from plants form the majority in the antifungal peptide library. Nonetheless, their potential antimicrobial benefits in medical mycology have largely been unexplored [75,76]. This is because, until recently, fungi were considered as predominantly phytopathogens and as such most of the research regarding their antimicrobial activities had centred on phytopathogens.

Plants produce diverse highly basic, cysteine rich peptides known as defensins whose antimicrobial activity is predominantly antifungal (Table 1.1) [59]. The mode of action of many of the plant defensins has been well characterised and is believed to involve interaction with specific lipid domains of the fungal plasma membrane [85]. Plant defensins are also categorised as either morphogenic or non-morphogenic depending on whether or not antifungal activity is accompanied by morphological changes such as hyphal hyper-branching [86].

DmAMP1, a plant defensin from *Dahlia merckii*, was shown to interact with the sphingolipid mannosyldiinositolphosphorylceramide (M(IP)₂C) [60] resulting in biphasic membrane permeabilisation in *Saccharomyces cerevisiae* [87]. The interaction of *DmAMP1* with M(IP)₂C was found to be enhanced in the presence of equimolar concentrations of ergosterol and M(IP)₂C [60].

RsAFP2 is a 50 amino acid defensin that is isolated from the seeds of the radish plant (*Raphanus sativus*) [61]. Like *DmAMP1*, it also induces biphasic membrane permeabilization but through interaction with glucosylceramides [62]. Furthermore, in *C. albicans*, *RsAFP2* causes morphological alterations [88] and induces the production of endogenous reactive oxygen species (ROS)[61].

PvD1, a plant defensin that is found in *Phaseolus vulgaris* seeds [89], was shown to induce membrane permeabilisation in several *Fusarium* and *Candida* spp. by interacting with glucosylceramides as well as ergosterol [63]. Disorganisation in the cytoplasm content and plasma membrane of *C. albicans* were also observed after treatment with *PvD1*. In addition, *PvD1* was able to induce the production of ROS and nitric oxide in *C. albicans* and *F. oxysporum* [63].

NaD1 is a plant defensin that is isolated from the flower *Nicotiana glauca* [90]. It has exhibited potent antifungal activity against numerous agronomically relevant filamentous fungi. The

antifungal activity was elicited by permeabilising the fungal membrane which resulted in granulation of the cytoplasm and cell death [64].

Insect-derived antifungal peptides

Due to the absence of a specialised immune system in insects, innate immunity forms the basis of protection against pathogenic attack. This innate defence system heavily relies on the production of a cocktail of AMPs targeting various pathogens.

Drosomycin is an inducible 5 kDa peptide consisting of eight cysteine residues and is produced by the fruit fly *Drosophila melanogaster* [65]. It has displayed very potent fungicidal activity at low micromolar concentrations against filamentous fungi and yeasts [66,91,92]. Its membranolytic mode of action is facilitated by the interaction with sphingolipids located in the fungal membrane [65,66]. Cohen *et al.* [93] observed that drosomycin interacts with the voltage gated sodium channels in *D. melanogaster* and hypothesised that this interaction contributes its antifungal activity.

Cecropins are linear 4 kDa peptides that have been isolated from haemolymph of the giant silk moth, *Hyalopora cecropia* [94]. They have demonstrated lethal activity against *Aspergillus* and *Fusarium* spp., with the plasma membrane being their target [67,95]. It has also been shown that they are not toxic to mammalian cells at their fungicidal dosages [96,97].

Thanatin is a cyclic, non-haemolytic 21 residue peptide isolated from the insect *Posidus maculiventris* [98]. It is sequentially, structurally and functionally different from all the other insect AMPs but closely resembles the brevenins, which are frog secreted antimicrobial peptides. This peptide is fungicidal against *B. cinerea*, *N. crassa* and *A. fumigatus* but has no activity against yeasts such as *S. cerevisiae* [99].

Antifungal peptides of animal origin

Amphibian-derived antifungal peptides

Amphibians synthesise and secrete antimicrobial peptides to protect themselves against microbial invasion. Several families of antifungal peptides have been isolated from amphibians [67,76,100].

The first reported antifungal peptides from amphibians were the magainins which are produced by the African clawed tree frog, *Xenopus laevis* [75,76]. They are linear, amphipathic peptides enriched in glycine and serine amino acids. They have exhibited antifungal activity against *C. neoformans*, *S. cerevisiae* and *C. albicans*. [101]. They are selective for microbial membranes, but

their therapeutic index is too low for them to be used for the treatment of systemic infections in humans [58]. Magainins act by rupturing the membrane as well as interfering with DNA integrity [68].

Another frog species, *Phyllomedusa sauvagii* (the South American arboreal frog) secretes a group of antimicrobial peptides known as the dermaseptins. These peptides are linear and rich in lysine residues. Their fungicidal activity against filamentous fungi and yeasts has been reported. They employ a lytic mode of action whereby they destabilise fungal membrane architecture through interaction with membrane sterols [67,69].

Brevenins and bombinins are also amphibian produced peptides that have shown potent anti-*Candida* activity. They are found in the skin secretion of the frogs belonging to the *Rana* and *Bombina* genera respectively. However, brevenins are highly haemolytic at low micromolar concentrations whereas bombinins are not [100,102].

Mammalian-derived antifungal peptides

Even though mammals have a highly specialised acquired defence system, innate immunity is still very crucial in conferring protection against pathogenic microbes. It is through this innate immune system that a host of antimicrobial peptides are produced. A wide variety of antifungal peptides have been isolated from several mammalian species such as humans, cows, pigs, rabbits and chickens.

The largest group of mammalian AMPs are the defensins which consist of six highly conserved cysteine residues that are stabilised by three disulphide bridges. The defensins are divided into three subfamilies: α , β , and θ defensins [103]. Human neutrophils constitutively express the α defensins HNP1-4 while HD5 and HD6 are constitutively expressed by the Paneth's cells. HNP1 and HNP2 have exhibited strong anti-*Candida* activity while HNP3 potently inhibited *C. neoformans* [104,105]. Membrane pore formation as well as inhibition of protein and nucleic acid synthesis have been identified to be the mechanisms employed by these peptides for antimicrobial activity [56,70]. In addition, rabbit produced α defensins, NP1-3 effectively killed *C. albicans* and *A. fumigatus* [71,106]. It was shown that NP1 and 2 interact with chitin which suggests the possible involvement of the fungal cell wall in their mode of action [71].

The β -defensin peptide family found in humans comprises six peptides namely HBD1-6. HBD1-3 have been shown to possess excellent antifungal activity against *C. albicans*, *C.krusei* and *C. parapsilosis* [107,108]. The activity in *C. albicans* was shown to involve membrane

permeabilisation linked to inhibition of fungal cell metabolism [109]. Protegrins and gallinacins, which are β -defensins produced by pigs and chickens, respectively, have inhibitory activity against *C. albicans* [110–112].

Another class of mammalian produced antifungal peptides are the cathelicidins. LL-37, the only cathelicidin expressed in humans, is produced by proteolytic cleavage of the protein hCAP18 [113]. It is a broad-spectrum antimicrobial peptide that has shown membrane mediated activity against *C. albicans* [114–116]. Cattle and pigs, on the other hand, produce several kinds of cathelicidins with diverse structures and antimicrobial activities. BMAP-27, BMAP-28 and SMAP-29 are bovine α -helical peptides that have demonstrated considerable membrane permeabilising activity towards *C. albicans* and *C. neoformans*, but not against filamentous fungi [117]. Indolicidin, another bovine derived tryptophan rich peptide belonging to cathelicidin family of peptides is highly lethal against *C. neoformans* but moderately lethal towards *Candida* spp. [117]. It forms an extended wedge-type conformation in the presence of plasma membranes [118]. Tritrypticin, the porcine analogue of indolicidin, was reported to have weak activity against both *A. fumigatus* and *C. albicans* [119].

Humans also produce a group of cationic peptides known as histatins which possess a high content of histidine residues. Histatins exhibit strong candidacidal activity [120,121]. They have also shown great antifungal activity against *C. neoformans* [122] and *A. fumigatus* [123]. The mechanism by which histatins exert their antifungal activity has been postulated to involve interaction with an energised fungal membrane and internalisation into the cytoplasm [74].

Antifungal peptides of microbial origin

Bacterial-derived antifungal peptides

Several bacterial species are sources of a variety of AFPs with excellent activities against pathogenic fungi. The iturins and bacillomycin peptides, which were among the first isolated AFPs, are products of the soil bacterium *Bacillus subtilis* [124]. The iturin family, which comprises iturin A, C, D, E, bacillomycin D, F, L, mycosubtilin and bacillopeptin, is a group of cyclic lipopeptides whose antimicrobial activity is primarily antifungal with little effect on bacteria. Iturins act by introducing ion conducting pores in the cytoplasmic membrane thereby increasing the leakage of K^+ [33,58,75,76]. Iturin A was found to have potent antifungal activity against *A. flavus* and *F. moniliforme* [125]. Bacillomycin F effectively inhibits *A. niger*, *C. albicans* and *S. cerevisiae* [77]. Unfortunately, the downside of these peptides is that they are very haemolytic [126].

Pseudomonas syringae produces a class of cyclic lipodepsinonapeptides known as syringomycins, which are amongst the most potent bacterial AFPs [126]. Members of the syringomycin family (syringomycin E, syringotoxin B and syringostatin A) have displayed excellent *in vitro* activity against clinically relevant isolates of *Candida*, *Aspergillus* and *C. neoformans* species [127]. The mode of action of syringomycins involves the alteration of membrane potential and subsequent disruption of membrane function through formation of ion conducting pores in the membrane [128,129]

Nikkomycins are peptidyl nucleoside inhibitors of the enzyme involved in the biosynthesis of chitin, which is an essential fungal cell wall component. They are produced by *Streptomyces tendae* [78,130]. Nikkomycins have shown significant growth inhibitory activity against *C. albicans* both *in vitro* and *in vivo* and are not cytotoxic to human cells [131]. Closely related to the nikkomycins are the polyoxins which are produced by *Streptomyces cacaoi*. Their mechanism of action is very similar to that of the nikkomycins [132].

Brevibacillus parabrevis produces a group of small, cyclic β -sheet peptides known as tyrocidines [133]. These peptides have demonstrated potent growth inhibitory activity against filamentous phytopathogenic fungi such as *F. solani* and *B. cinerea* [79,80]. They were also shown to be active against the human pathogens, *C. albicans* and *A. fumigatus* [57,79]. Their antifungal activity is elicited via rapid membrane permeabilisation.

Fungal-derived antifungal peptides

By far, the most potent AFPs are those produced by fungi themselves. Examples include peptides such as the echinocandins produced by *Aspergillus nidulans*, aureobasidins, AcAFP, AFP, ANAFP and PAF [81,134–137].

The echinocandins are diverse group of cyclic lipopeptides that interfere with the biosynthesis of the fungal cell wall by inhibiting the enzyme 1,3 β -glucan synthase [81]. Peptides that make up this family include the native echinocandins (A, B and C) and other closely related peptides that possess a modified echinocandin B core such as pneumocandins, mulundocandins, aculeacins and WF11899 [76]. Amongst the native echinocandins, analogues of echinocandin B have the greatest potency and have been used as a template for developing new drugs. Caspofungin (second generation pneumocandin), micafungin and anidulafungin (both echinocandins) are currently the only peptide-based antifungal agents approved for the treatment of invasive mycoses [58]. Echinocandins are currently the drugs of choice for the treatment of invasive candidiasis due to

their potent fungicidal activity against most of the *Candida* spp. including those that are resistant to fluconazole or amphotericin B [49,58]. However, they are fungistatic towards *Aspergillus* spp. and are only prescribed as alternative therapy for invasive aspergillosis [35,58]. *Cryptococcus* spp. are intrinsically insensitive to echinocandins [42].

The other *Aspergillus* spp. from which antifungal peptides have been isolated are *A. clavatus*, *A. giganteus* and *A. niger* which produce AcAFP, AFP and ANAFP, respectively [134–136]. These peptides have displayed excellent inhibitory activities against a multitude of filamentous fungi including *A. fumigatus* [138,139].

Aureobasidins are cyclic lipodepsipeptides that are synthesised by *Aureobasidium pullulans* and effectively inhibit *Candida* spp. and *C. neoformans* [137]. It is believed that they act by interfering with the synthesis of sphingolipids, altering the assembly of actin and delocalisation chitin in cell walls [82,83].

Penicillium chrysogenum produces a low molecular weight cysteine-rich antifungal protein known as PAF [140]. PAF has been shown to inhibit *A. fumigatus*, amongst other opportunistic pathogens. Its proposed mechanism of action involves membrane polarization and activation of ion channels [84].

Based on the highlighted potencies of various antifungal peptides towards a great many fungal pathogens, it is safe to conclude that antifungal peptides bear the potential to become the urgently needed antifungal therapeutic agents. Further characterisation of their properties and mode of action is essential for their development into antifungal agents. As such, the research reported in this thesis was conducted with the aim of enhancing the understanding of the properties of small aromatic peptides and elucidating their potential use as antifungal therapy.

1.6 Antifungal potential of small aromatic peptides

Natural cyclodecapeptides: Tyrocidines and analogues

The tyrocidines and analogues are a group of cyclic decapeptides with broad and potent antimicrobial activity. They were first isolated in 1939 by Dubos [141] as constituents of tyrothricin, a peptide complex produced by the soil bacterium *Brevibacillus parabrevis* [141,142]. Tyrothricin is composed of approximately 40-60% tyrocidines and 10-20% linear gramicidins [142]. Tyrothricin successfully became the first antibiotic to be approved for clinical use despite it

being discovered a decade after penicillin [141,143]. However due to its haemolytic activity [144], clinical application of tyrothricin was restricted to topical and oral use [145–147].

Structural properties

Tyrocidines and their analogues are β -sheet cyclic peptides composed of ten amino acid residues [142,143]. The structural characterisation done by Tang *et al.*[143], indicated the existence of different analogues with a conserved amino acid sequence (cyclo-[f¹P²X³x⁴N⁵Q⁶X⁷V⁸O⁹L¹⁰]) (Table 1.2. Figure 1.2), varying only in positions three, four, seven and nine. The variability in the aromatic residue in the seventh position is the basis upon which the decapeptides are named, with the Y-containing peptides named tyrocidines, the W-containing peptides named tryptocidines and the F-containing peptides named phenycidines. Variation in the aromatic dipeptide moiety in positions three and four determines the letter assigned to the different analogues. The analogues containing the (Ff) moiety are denoted A analogues, while those containing (Wf) and (Ww) moieties are denoted as B and C analogues, respectively. Lastly, the amino acid residue in the ninth position determines whether a subscript follows the letter designated to the analogues. For instance, tyrocidine A (Figure 1.2) has an Orn residue while tyrocidine A₁ has a Lys residue in the same position [143,148,149]. The tyrocidines (tyrocidine A, A₁, B, B₁, C and C₁) are naturally abundant within the tyrocidine mixture whereas the phenycidines and tryptocidines are found in lesser quantities [143,148]. The amino acid sequence of tyrocidines and their analogues is 50% homologous to that of gramicidin S, an antimicrobial peptide synthesised by *Bacillus brevis* whose sequence is cyclo-(VOLfPVOLfP) [150]. It has been observed that under physiological conditions, tyrocidine A assumes a β -sheet conformation with two β -turns [151,152]. This secondary structure is also conserved in the other analogues [153].

Biological activity

The natural cyclodecapeptides have displayed activity towards a broad spectrum of pathogens which incorporates bacteria, fungi and parasites. Following their discovery, Dubos [141] reported on the potent antibacterial activity of tyrocidines against the Gram-positive bacteria *Diplococcus pneumoniae*, *Streptococcus haemolyticus* and *Staphylococcus aureus*. This activity against Gram-positive species has been corroborated by other studies as activity against *Listeria monocytogenes*, *Micrococcus luteus*, *S. aureus* and *Streptococcus pyogenes* has also been reported [154,155]. However, it has been shown that the tyrocidines are not as effective against Gram-negative bacteria such as *Escherichia coli*, *Klebsiella pneumoniae* and *Haemophilus influenza* [141,155].

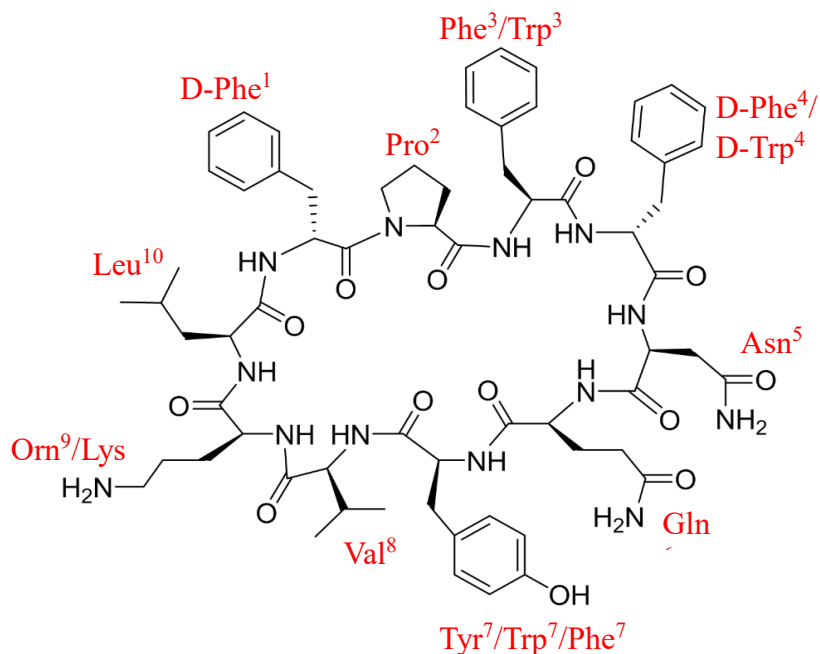


Figure 1.2: Cyclodecapeptide structure showing the variable positions with the possible amino acid substitutions for the major tyrocidines and analogues

In addition to antibacterial activity, the cyclodecapeptides have also exhibited antifungal activity. Tyrocidines inhibited the germination and growth of *Neurospora crassa* [156]. Tyrocidine mixture (Trc mix) and individual tyrocidine analogues were inhibitory to the growth of a range of filamentous fungi and their activities were significantly greater than that of bifonazole, a commercial antifungal agent from the azole group [79,80]. Tyrocidines have also demonstrated synergism with clinical antifungal drugs, amphotericin B and caspofungin [57]. It was shown that combinations of these drugs with tyrocidines were highly effective at inhibiting the growth of planktonic *C. albicans* cells and formation of biofilm as well as eradicating already formed biofilms *in vitro*. Furthermore, the combination of tyrocidine A with caspofungin displayed *in vivo* activity against *C. albicans* [57].

Interestingly, the cyclodecapeptides have also exhibited noteworthy activity, with IC₅₀ values in the nanomolar concentration range, against *Plasmodium falciparum*, one of the parasitic protozoan species responsible for the pathogenesis of malaria in humans [157]. Unfortunately, because of their haemolytic [142,157,158], and leukocytolytic activity [159], they cannot be used

systemically. Nevertheless, there is ongoing research within our group which aims to eliminate this unwanted toxicity via modification and formulation.

Table 1.2: Summary of peptides identified in the tyrothricin complex

Identity	Abbreviation	Sequence ^a	Theoretical Monoisotopic M_r ^b	Relative abundance ^c
Major Tyrocidines				
Tyrocidine C ₁	YC ₁	<i>Cyclo</i> -(fPW _w NQYVKL)	1361.692	30
Tyrocidine C	YC	<i>Cyclo</i> -(fPW _w NQYVOL)	1347.676	100
Tyrocidine B ₁	YB ₁	<i>Cyclo</i> -(fPW _f NQYVKL)	1322.681	44
Tyrocidine B ₁ '	YB ₁ '	<i>Cyclo</i> -(fPF _w NQYVKL)	1322.681	5.8
Tyrocidine B	YB	<i>Cyclo</i> -(fPW _f NQYVOL)	1308.655	109
Tyrocidine B'	YB'	<i>Cyclo</i> -(fPF _w NQYVOL)	1308.655	14
Tyrocidine A ₁	YA ₁	<i>Cyclo</i> -(fPF _f NQYVKL)	1283.670	39
Tyrocidine A	YA	<i>Cyclo</i> -(fPF _f NQYVOL)	1269.653	88
Tyrocidine Analogues				
Tryptocidine C	WC	<i>Cyclo</i> -(fPW _w NQWVOL)	1370.692	23
Tryptocidine C ₁	WC ₁	<i>Cyclo</i> -(fPW _w NQWVKL)	1384.708	2.3
Tryptocidine B	WB	<i>Cyclo</i> -(fPW _f NQWVOL)	1331.681	26
Tryptocidine B ₁	WB ₁	<i>Cyclo</i> -(fPW _f NQWVKL)	1345.697	13
Tryptocidine A	WA	<i>Cyclo</i> -(fPF _f NQWVOL)	1292.647	15
Tryptocidine A ₁	WA ₁	<i>Cyclo</i> -(fPF _f NQWVKL)	1306.686	<1
Phenycidine A	WA	<i>Cyclo</i> -(fPF _f NQFVOL)	1253.660	3.1
Phenycidine A ₁	WA ₁	<i>Cyclo</i> -(fPF _f NQFVKL)	1267.675	<1
Linear Gramicidins				
Val – Gramicidin A	VGA	VGALAvVvWLWLWLW	1881.078	44
Val – Gramicidin B	VGB	VGALAvVvWLFLWLW	1842.067	4.1
Val – Gramicidin C	VGC	VGALAvVvWLYLWLW	1858.062	24
Gramicidin S	GS	<i>Cyclo</i> -(fPVOLfPVOL)	1140.704	-

^a The peptide sequences are as given by Tang *et al.* [143]. Amino acids are denoted using the standard one letter abbreviations with lowercase letters representing D-amino acids and uppercase letters representing L-amino acids.

^b Theoretical monoisotopic mass (M_r) was calculated as the sum of the molecular weights of the constituent amino acids.

^c Peptide abundance is expressed relative to the abundance of tyrocidine C [143].

Mode of action

For many cationic AMPs, membrane action leading to cell lysis is regarded as the principal mode of action. Data from numerous studies indicates that the killing and/or inhibitory mechanisms of the natural cyclodecapeptides involve membranolysis [57,79,80,155,156,160]. Wenzel *et al.* [161] recently showed that tyrocidine A and tyrocidine C formed defined ion-conducting pores which have a major influence on phospholipid head-group orientation, yet the exact nature by which microbial inhibition occurs is not fully understood.

Interestingly, it has been argued that there is no correlation between tyrocidine activity and lysis and that lysis is only a secondary process that results from the activity of the target cells' own autolytic enzymes [141]. Dubos *et al.* [154] showed that tyrocidines inhibit the metabolic reactions of *S. aureus* and *S. pyogenes*, substantiating the proposition that tyrocidines may employ alternate mechanisms of action in addition to lytic action. These mechanisms may depend upon an initial interaction with membrane followed by translocation into the intracellular space. Alternatively, the tyrocidines may remain bound to cell membrane components and interfere with their function without necessarily rupturing the membrane. Wenzel *et al.* [161] showed that the tyrocidines cause a loss of membrane proteins from bacterial membranes, as well as influence certain intracellular protein and the chromatin packing.

It has been shown that in addition to membrane lysis, interaction with the β -glucans may play role in the antifungal activity of tyrocidines against *F. solani*. β -glucans are essential components of the fungal cell wall. Treatment of hyphae with β -glucanase inhibited the activity of the tyrocidines against *F. solani* [80]. In the same study, tyrocidines induced alterations in the morphology of fungal hyphae which could be attributed to the interference with Ca^{2+} gradients, actin polymerisation, cell cycle or sterol rich plasma membrane domains. It was also observed that the presence of Ca^{2+} diminished antifungal activity suggesting a possible interference with the processes that generate and maintain Ca^{2+} gradients [80].

Tyrocidines were also reported to have induced the production of ROS in *C. albicans* biofilms. However, it was observed ROS was not essential for biofilm eradication as the tyrocidines maintained their activity in the presence of an antioxidant [57].

It has also been hypothesised that tyrocidines could possibly interfere with nucleic acid and protein metabolism. Tyrocidines are known to interact with DNA in the organism that produces them, and this interaction leads to the repression of RNA transcription [162,163]. Moreover, the inhibition of DNA, RNA and protein synthesis in *N. crassa* by tyrocidine substantiated this hypothesis [156].

The antiplasmodial activity of tyrocidines was attributed to the inhibition of *P. falciparum* development and arrest of the intraerythrocytic parasite lifecycle rather than haemolysis [157]. In a different study, tryptocidine C distorted the lipid structures found within the food vacuole of malaria parasites [158]. This finding implied the possibility of a molecular target existing within the food vacuole.

There is clearly increasing evidence that suggests the utilisation of more than one mode of action against pathogens by the cyclodecapeptides. If this is the case, then the likelihood of pathogens developing resistance against them is greatly reduced making them attractive candidates for therapeutic drug development.

Synthetic Arginine and Tryptophan rich peptides: RW-hexapeptides

Although a vast number of natural antimicrobial peptides with excellent activities against pathogenic microbes have been identified, very few have successfully made it through the drug discovery pipeline and have been granted approval for clinical use [58]. This is mainly due to inherent toxicity towards eukaryotic cells and unfavourable pharmacokinetic properties. Moreover, many naturally occurring peptides are relatively large hence their production on a large scale is often difficult and costly [51,164,165]. But these limitations could be overcome by developing smaller AMPs with favourable toxicity and pharmacokinetic profiles. Synthetic combinatorial chemistry technology has enabled the identification and development of many such small AMPs.

Of interest are small peptides that possess a high content of arginine and tryptophan residues in their primary structures as similar motifs have been identified within naturally occurring AMPs such as lactoferricin, indolicidin and tritrypticin and are believed to be the core of antimicrobial activity [166]. Through screening of different synthetic combinatorial libraries, several hexapeptides sequences rich in Arg and Trp residues were identified as having the highest antimicrobial activity [167–170]. One such hexapeptide is *N*-acetylated Arg-Arg-Trp-Trp-Arg-Phe-amide (Ac-RRWRF-NH₂) whose antimicrobial activity has been illustrated [169]. Using this hexapeptide as a template, various sequence and structural analogues have been designed and investigated for antibacterial activity by our research collaborators. However, their antifungal activity has not been elucidated. As such, it is the goal of this study is to elucidate the antifungal activity as well as the mechanism of action of these analogues. These peptides will be referred to as RW-hexapeptides.

Structural properties of RW-hexapeptides

RW-hexapeptides that are the focus of the research reported in Chapter 2-4 are either linear or cyclic (Figure 1.3). Linear RW peptides are analogues of the Ac-RRWRF-NH₂ peptide whose amino acid sequences vary slightly from that of the original peptide. They are amidated at the carboxyl end and acetylated at the amino end. Amidation at the carboxyl end has previously been illustrated to be essential for high antimicrobial activity [171]. Cyclic RW-hexapeptides, on the

other hand, are both structural and sequential analogues of Ac-RRWRF-NH₂. The parent cyclic RW-hexapeptide, cyclo-RRWRF was derived from its linear analogue through head-to-tail cyclisation [164].

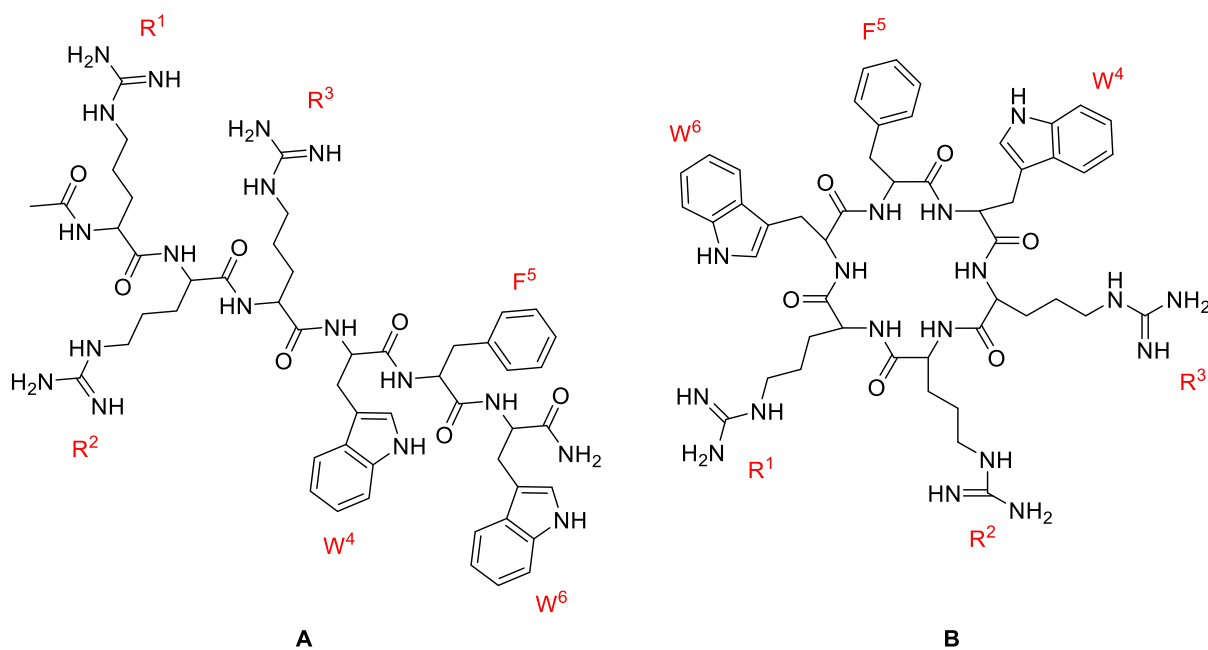


Figure 1.3 Structures of A) Ac-RRRWWF B) cyclo-RRRWWF. Amino acids are indicated by standard one letter amino acid abbreviations. Structures were drawn using ChemBioDraw Ultra 13.0 (Cambridge Soft®, UK).

RW-hexapeptides have a relatively simple and conserved primary structure comprising six amino acid residues, with Arg and Trp being the predominant residues. These residues give the hexapeptides their amphipathic nature and therefore, modulate antimicrobial activity. It is believed that the positively charged side chain of Arg attracts the peptide to negatively charged membrane components such as lipopolysaccharide and phospholipid head groups facilitating an initial interaction with target membranes. The interaction is then maintained by Trp whose bulky hydrophobic side chain prefers to associate with the interfacial regions of the lipid bilayers [164,171]. In some analogues, one or more Arg residues are replaced with Lys while Phe or Tyr replace Trp as the aromatic residues. Substitutions of this nature have resulted in altered antimicrobial and haemolytic activities, illustrating that amphipathicity alone is not enough for activity [164]. Rather, a fine balance between the cationic and lipophilic properties is necessary to achieve maximum antimicrobial activity and minimal host toxicity.

Linear and cyclic RW-hexapeptides have different secondary structures. The secondary structure of Ac-RRWWRF-NH₂ has been shown to be undefined (disordered) in aqueous solution but becomes more ordered in a membrane-mimicking environment [172]. Conversely, cyclo-RRWWRF has been reported to have an ordered secondary structure in either environment. In fact, the cyclic peptide has been proposed to have a β -sheet backbone that is stabilised by two β -turns [173].

Biological activity

The activity of synthetic RW-hexapeptides against microbes has been the subject of numerous investigations. Like natural AMPs, some of the RW-hexapeptides have broad spectrum antimicrobial activity while others are highly selective for certain target organisms.

Blondelle *et al.* [169] identified a series of peptides with the sequence Ac-RRWWCX-NH₂ where X denotes any of the 20 natural amino acids. These peptides were tested for antimicrobial activity against two Gram-positive species (*S. aureus* and *Streptococcus sanguis*), two Gram-negative species (*Pseudomonas aeruginosa* and *E. coli*) and the yeast, *C. albicans*. In general, they were inhibitory towards all microorganisms tested and did not show specificity towards any organism. In a different study, higher antimicrobial activity was observed against *S. aureus* than against *P. aeruginosa* and *E. coli* [171].

PAF26, an all D-amino acid peptide that was identified by a combinatorial approach exhibited strong antifungal activity against filamentous fungal phytopathogens *B. cinerea*, *Penicillium italicum* and *Penicillium digitatum*. It also inhibited *E.coli* and *S. cerevisiae* but with much lower efficacy highlighting its selectivity towards certain filamentous fungi [174]. It should be noted that PAF26 is D-amino acid analogue of Ac-RKKWWF-NH₂ which is one of the peptides that will be investigated in this study.

For the cyclic RW-hexapeptides, antibacterial activity has largely been the centre of focus. Their inhibitory activity against *Bacillus subtilis*, *E. coli* and *L. monocytogenes* has been reported [158,164,175,176]. In fact, they have demonstrated better activity than their linear counterparts. In studies conducted by Dathe *et al.* [164,175], linear peptides were moderately active towards *B. subtilis* and inactive against *E. coli*. Upon cyclisation, improved antibacterial activity and selectivity were noted.

Apart from their high antimicrobial activity, the absence of toxicity towards mammalian cells makes RW-hexapeptides very attractive leads compounds for drug development. Multiple

investigators have tested different RW-hexapeptides for haemolytic activity and all their results indicated little to no haemolysis activity [164,169,171,175].

Mode of action

The high content of cationic and hydrophobic residues renders the RW-hexapeptides structurally suited for membrane activity [177]; yet it has been illustrated several times that they do not exert their antimicrobial activity through membrane permeabilisation. PAF26 was shown to be inefficient at facilitating the uptake of SYTOX Green at sub-MIC concentrations that inhibited the growth and induced morphological alterations in *P. digitatum* hyphae. This indicated that membrane permeabilisation is low at concentrations that inhibit fungal growth [178]. Ac-RRWWFR-NH₂ was also quite inefficient at inducing leakage of calcein from large unilamellar vesicles composed of POPG/POPC (1:1); an indication of membrane disruption not being the main mode of action [179]. The low membrane permeabilising ability of RW-hexapeptides was further demonstrated when low levels of propidium iodide were detected inside *E. coli* after treatment with cyclo-RRRWWF (cWWF) at its minimum inhibitory concentration (MIC) [180].

While membrane lysis is not the primary mode of action of RW-hexapeptides, the exact manner in which they elicit antimicrobial activity has not been fully elucidated. Efforts to improve the understanding of how these peptides kill their targets have yielded evidence of novel mechanisms which appear to be target and peptide specific [176,177,181,182].

Peptide translocation across the bacterial membrane was ruled out as a possible mechanism of action of cWWF against *B. subtilis* after fluorescence could not be detected within the cytoplasm following treatment of bacteria with cWWF labelled with nitrobenzoxadiazole (NBD-cWWF). This indicated that the fluorescent labelled cWWF had not traversed the *B. subtilis* membrane [177]. However, the peptide was observed to accumulate within the lipid bilayer; specifically, in cardiolipin rich domains. Based on this observation, the cytoplasmic membrane was postulated to be the target of the cyclic peptide [177]. Confirmation of the membrane as the target was later provided by Scheinpflug *et al.* [176] who reported that the action of cWWF against *B. subtilis* involved a rapid reduction of membrane fluidity. Changes in fluidity resulted in the formation of distinct membrane domains which differ in local membrane fluidity, disorganisation of membrane proteins and ultimately, cell autolysis.

On the other hand, it appears that RW-hexapeptides exert their antifungal activity in a completely different manner. A multistep mechanism involving interaction of peptide with the fungal cell

envelope, internalisation of the peptide and disruption of intracellular processes has been suggested for PAF26 and derivatives [181]. Munoz *et al.* [178] was able to show the translocation of a FITC-labelled PAF26 into the cytoplasm of *P. digitatum*. They also observed that PAF26 altered the morphology of *P. digitatum* hyphae as was indicated by dichotomous tip branching and swelling of hyphae with abnormal chitin deposition. These observations were indicative of changes in the structure of the cell wall and showed that the fungal cell wall is not only the first line of interaction with the peptide but a target as well. Results from other investigations reveal that PAF26 interferes with various intracellular processes. There is evidence of interference with responses to DNA damage, Arg homeostasis, ribosome biogenesis and unfolded protein stress responses in *S. cerevisiae* [183]. Additionally, the effects of treating *N. crassa* with PAF26 included increased production of endogenous ROS and nitric oxide as well as a dose dependent disruption of calcium homeostasis [184,185].

From the above, it is possible to deduce that the antifungal and antibacterial activities of RW hexapeptides are elicited differently. The mechanism of action could also be dependent on the nature of the peptide (cyclic versus linear). This underscores the importance of both target cell and peptide properties on antimicrobial activity.

1.7 Concluding remarks

Fungal pathogens and the systemic infections they cause are a global health burden that needs to be addressed with urgency. To do this, new antifungal therapeutics agents with novel mechanism of action need to be developed. Natural cyclodecapeptides (tyrocidines and analogues) and RW-hexapeptides are potential candidates for development as antifungal agents based on their potent antimicrobial activities. For this reason, it is highly essential that their antifungal activity as well as mode of action be characterised, as this information is pertinent to the future development of any drug.

1.8 References

- [1] J.R. Perfect, The antifungal pipeline: a reality check, *Nature Reviews Drug Discovery*, 16 (2017) 603–616.
- [2] G.D. Brown, D.W. Denning, N.A.R. Gow, S.M. Levitz, M.G. Netea, T.C. White, Hidden killers: Human fungal infections, *Science Translational Medicine*, 4 (2012).
- [3] G.D. Brown, D.W. Denning, S.M. Levitz, Tackling human fungal infections, *Science*, 336 (2012) 647–647.
- [4] S. Campoy, J.L. Adrio, Antifungals, *Biochemical Pharmacology*, 133 (2017) 86–96.

- [5] M.A. Pfaller, D.J. Diekema, Epidemiology of invasive mycoses in North America, *Critical Reviews in Microbiology*, 36 (2010) 1–53.
- [6] N. Robbins, G.D. Wright, L.E. Cowen, Antifungal drugs: The current armamentarium and development of new agents, *American Society of Microbiology*, (2016) 903–922.
- [7] J.P. Latgé, *Aspergillus fumigatus* and aspergillosis, *Clinical Microbiology Reviews*, 12 (1999) 310–350.
- [8] J.-P. Latg, *Aspergillus fumigatus*, a saprotrophic pathogenic fungus, *Mycologist*, 17 (2003) 56–61.
- [9] A. Chakrabarti, S.S. Chatterjee, A. Das, M.R. Shivaprakash, Invasive aspergillosis in developing countries, *Medical Mycology*, 49 (2011) S35–S47.
- [10] A. Brahm, H. Segal, Aspergillosis, *New England Journal of Medicine*, 18360 (2009) 1870–1884.
- [11] D.W. Denning, Therapeutic outcome in invasive aspergillosis, *Clinical Infectious Diseases*, 23 (1996) 608–615.
- [12] T.F. Patterson, W.R. Kirkpatrick, M. White, J.W. Hiemenz, J.R. Wingard, B. Dupont, M.G. Rinaldi, D.A. Stevens, J.R. Graybill, Invasive aspergillosis. Disease spectrum, treatment practices, and outcomes, *Medicine*, 79 (2000) 250–260.
- [13] M.A. Pfaller, P.G. Pappas, J.R. Wingard, Invasive fungal pathogens: current epidemiological trends, *Clinical Infectious Diseases*, 43 (2006) S3–S14.
- [14] D.W. Denning, Invasive aspergillosis, 26 (1998) 781–803.
- [15] K. V Ramana, S. Kandi, V. Bhartkumar P, C. V Sharada, R. Rao, R. Mani, S. D Rao, Invasive fungal infections: A comprehensive review, *American Journal of Infectious Diseases and Microbiology*, 1 (2013) 64–69.
- [16] T. Frieden, Antibiotic resistance threats in the United States, Centers for Disease Control and Prevention, US Department of Health and Human Services: Atlanta, GA, (2013).
- [17] T.A. Clark, R.A. Hajjeh, Recent trends in the epidemiology of invasive mycoses, *Current Opinion in Infectious Diseases*, 15 (2002) 569–574.
- [18] N.P. O’Grady, M. Alexander, E.P. Dellinger, J.L. Gerberding, S.O. Heard, D.G. Maki, H. Masur, R.D. McCormick, L.A. Mermel, M.L. Pearson, I.I. Raad, A. Randolph, R.A. Weinstein, Guidelines for the prevention of intravascular catheter-related infections, *Clinical Infectious Diseases*, 35 (2002) 1281–1307.
- [19] M.A. Pfaller, D.J. Diekema, Rare and emerging opportunistic fungal pathogens: concern for resistance beyond *Candida albicans* and *Aspergillus fumigatus*, *Journal of Clinical Microbiology*, 42 (2004) 4419–4431.
- [20] M.J. Ruping, J.J. Vehreschild, O.A. Cornely, Patients at high risk of invasive fungal infections: when and how to treat, *Drugs*, 68 (2008) 1941–1962.
- [21] J.J. Castón-Osorio, A. Rivero, J. Torre-Cisneros, Epidemiology of invasive fungal infection, *International Journal of Antimicrobial Agents*, 32 (2008) S103-109.
- [22] H.M. Blumberg, W.R. Jarvis, J.M. Soucie, J.E. Edwards, J.E. Patterson, M.A. Pfaller, M.S. Rangel-Frausto, M.G. Rinaldi, L. Saiman, R.T. Wiblin, R.P. Wenzel, Risk factors for

- candidal bloodstream infections in surgical intensive care unit patients: the NEMIS prospective multicenter study, *Clinical Infectious Diseases*, 33 (2001) 177–186.
- [23] D. Abi-Said, E. Anaissie, O. Uzun, I. Raad, H. Pinzowski, S. Vartivarian, The epidemiology of hematogenous candidiasis caused by different *Candida* species, *Clinical Infectious Diseases*, 24 (1997) 1122–1128.
- [24] P.G. Pappas, J.H. Rex, J. Lee, R.J. Hamill, R.A. Larsen, W. Powderly, C.A. Kauffman, N. Hyslop, J.E. Mangino, S. Chapman, H.W. Horowitz, J.E. Edwards, W.E. Dismukes, A prospective observational study of candidemia: epidemiology, therapy, and influences on mortality in hospitalized adult and pediatric patients, *Clinical Infectious Diseases*, 37 (2003) 634–643.
- [25] O. Gudlaugsson, S. Gillespie, K. Lee, J. V. Berg, J. Hu, S. Messer, L. Herwaldt, M. Pfaller, D. Diekema, Attributable mortality of nosocomial candidemia, revisited, *Clinical Infectious Diseases*, 37 (2003) 1172–1177.
- [26] F. Lanternier, S. Cypowyj, C. Picard, J. Bustamante, O. Lortholary, J.-L. Casanova, A. Puel, Primary immunodeficiencies underlying fungal infections, *Current Opinion in Pediatrics*, 25 (2013) 736–47.
- [27] J. Bogaerts, D. Rouvroy, H. Taelman, A. Kagame, M.A. Aziz, D. Swinne, J. Verhaegen, AIDS-associated cryptococcal meningitis in Rwanda (1983–1992): epidemiologic and diagnostic features, *Journal of Infection*, 39 (1999) 32–37.
- [28] C.M. Schutte, C.H. Van der Meyden, D.S. Magazi, The impact of HIV on meningitis as seen at a South African Academic Hospital (1994 to 1998), *Infection*, 28 (2000) 3–7.
- [29] B.J. Park, K.A. Wannemuehler, B.J. Marston, N. Govender, P.G. Pappas, T.M. Chiller, Estimation of the current global burden of cryptococcal meningitis among persons living with HIV/AIDS, *Aids*, 23 (2009) 525–30.
- [30] R.S. Heyderman, I.T. Gangaidzo, J.G. Hakim, J. Mielke, A. Taziwa, P. Musvaire, V.J. Robertson, P.R. Mason, Cryptococcal meningitis in human immunodeficiency virus-infected patients in Harare, Zimbabwe, *Clinical Infectious Diseases*, 26 (1998) 284–9.
- [31] D.J. Sloan, V. Parris, Cryptococcal meningitis: epidemiology and therapeutic options, *Clinical Epidemiology*, 6 (2014) 169–182.
- [32] WHO | Global Burden of Disease (GBD) 2002 estimates, WHO, (2014).
- [33] M. Rautenbach, A.M. Troskie, J.A. Vosloo, Antifungal peptides: To be or not to be membrane active, *Biochimie*, 130 (2016) 132–145.
- [34] D.A. Enoch, H.A. Ludlam, N.M. Brown, Invasive fungal infections: a review of epidemiology and management options, *Journal of Medical Microbiology*, 55 (2006) 809–818.
- [35] J.E. Nett, D.R. Andes, Antifungal agents: spectrum of activity, pharmacology, and clinical indications, *Infectious Disease Clinics*, 30 (2016) 51–83.
- [36] W.I. Gruszecki, M. Gagos, M. Herec, P. Kernen, Organization of antibiotic amphotericin B in model lipid membranes. A mini review, *Cellular and Molecular Biology Letters*, 8 (2003) 161–170.
- [37] L. Ostrosky-Zeichner, A. Casadevall, J.N. Galgiani, F.C. Odds, J.H. Rex, An insight into

- the antifungal pipeline: selected new molecules and beyond, *Nature Reviews Drug Discovery*, 9 (2010) 719–727.
- [38] T.M. Anderson, M.C. Clay, A.G. Cioffi, K.A. Diaz, G.S. Hisao, M.D. Tuttle, A.J. Nieuwkoop, G. Comellas, N. Maryum, S. Wang, B.E. Uno, E.L. Wildeman, T. Gonen, C.M. Rienstra, M.D. Burke, Amphotericin forms an extramembranous and fungicidal sterol sponge, *Nature Chemical Biology*, 10 (2014) 400–406.
- [39] A. Lemke, A.F. Kiderlen, O. Kayser, Amphotericin B, *Applied Microbiology and Biotechnology*, 68 (2005) 151–162.
- [40] J.N. Day, T.T.H. Chau, M. Wolbers, P.P. Mai, N.T. Dung, N.H. Mai, N.H. Phu, H.D. Nghia, N.D. Phong, C.Q. Thai, L.H. Thai, L. V. Chuong, D.X. Sinh, V.A. Duong, T.N. Hoang, P.T. Diep, J.I. Campbell, T.P.M. Sieu, S.G. Baker, N.V.V. Chau, Combination antifungal therapy for cryptococcal meningitis, *New England Journal of Medicine*, 368 (2013) 1291–1302.
- [41] A. Ray, S. Anand, Recent trends in antifungal therapy: focus on systemic mycoses, *The Indian Journal of Chest Diseases & Allied Sciences*, 42 (2000) 357–366.
- [42] Y. Chang, S. Yu, J. Heitman, M. Wellington, New facets of antifungal therapy, *Virulence*, 8 (2017) 222–236.
- [43] P.L. Shao, L.M. Huang, P.R. Hsueh, Recent advances and challenges in the treatment of invasive fungal infections, *International Journal of Antimicrobial Agents*, 30 (2007) 487–495.
- [44] P.K. Shukla, P. Singh, R.K. Yadav, S. Pandey, S.S. Bhunia, Past, present, and future of antifungal drug development, *Communicable Diseases of the Developing World*, (2018) 125–167.
- [45] P. Vandeputte, S. Ferrari, A.T. Coste, Antifungal resistance and new strategies to control fungal infections, *International Journal of Microbiology*, 2012 (2011).
- [46] D.W. Denning, Echinocandin antifungal drugs, *The Lancet*, 362 (2003) 1142–1151.
- [47] G.M. Keating, D.P. Figgitt, Caspofungin, *Drugs*, 63 (2003) 2235–2263.
- [48] A. Gullo, Invasive fungal infections, *Drugs*, 69 (2009) 65–73.
- [49] P.G. Pappas, C.A. Kauffman, D.R. Andes, C.J. Clancy, K.A. Marr, L. Ostrosky-Zeichner, A.C. Reboli, M.G. Schuster, J.A. Vazquez, T.J. Walsh, T.E. Zaoutis, J.D. Sobel, Clinical practice guideline for the management of candidiasis: 2016 update by the Infectious Diseases Society of America, *Clinical Infectious Diseases*, 62 (2015) e1–e50.
- [50] R.E.W. Hancock, R. Lehrer, Cationic peptides: a new source of antibiotics, *Trends in Biotechnology*, 16 (1998) 82–88.
- [51] J.P. Bradshaw, Cationic Antimicrobial peptides, *BioDrugs*, 17 (2003) 233–240.
- [52] L.O. Brandenburg, J. Merres, L.J. Albrecht, D. Varoga, T. Pufe, Antimicrobial peptides: multifunctional drugs for different applications, *Polymers*, 4 (2012) 539–560.
- [53] R.E. Hancock, Peptide antibiotics, *Lancet*, 349 (1997) 418–422.
- [54] R.E.W. Hancock, D.S. Chapple, Peptide Antibiotics, *Antimicrobial Agents and Chemotherapy*, 43 (1999) 1317–1323.

- [55] H. Jenssen, P. Hamill, R.E.W. Hancock, Peptide antimicrobial agents, *Clinical Microbiology Reviews*, 19 (2006) 491–511.
- [56] K.A. Brogden, Antimicrobial peptides: Pore formers or metabolic inhibitors in bacteria?, *Nature Reviews Microbiology*, 3 (2005) 238–250.
- [57] A.M. Troskie, M. Rautenbach, N. Delattin, J.A. Vosloo, M. Dathe, B.P.A. Cammue, K. Thevissen, Synergistic activity of the tyrocidines, antimicrobial cyclodecapeptides from *Bacillus aneurinolyticus*, with amphotericin B and caspofungin against *Candida albicans* biofilms, *Antimicrobial Agents and Chemotherapy*, 58 (2014) 3697–3707.
- [58] A. Matejuk, Q. Leng, M.D. Begum, M.C. Woodle, P. Scaria, S.T. Chou, A. Mixson, Peptide-based antifungal therapies against emerging infections, *Drugs of the Future*, 35 (2010) 197.
- [59] N. Hegedüs, F. Marx, Antifungal proteins: more than antimicrobials?, *Fungal Biology Reviews*, 26 (2013) 132–145.
- [60] K. Thevissen, I.E.J.A. François, J.Y. Takemoto, K.K. Ferket, E.M. Meert, B.P. Cammue, DmAMP1, an antifungal plant defensin from dahlia (*Dahlia merckii*), interacts with sphingolipids from *Saccharomyces cerevisiae*, *FEMS Microbiology Letters*, 226 (2003) 169–173.
- [61] A.M. Aerts, I.E.J.A. François, E.M.K. Meert, Q.T. Li, B.P.A. Cammue, K. Thevissen, The antifungal activity of RsAFP2, a plant defensin from *Raphanus sativus*, involves the induction of reactive oxygen species in *Candida albicans*, *Journal of Molecular Microbiology and Biotechnology*, 13 (2007) 243–247.
- [62] K. Thevissen, F.R. Terras, W.F. Broekaert, Permeabilization of fungal membranes by plant defensins inhibits fungal growth, *Applied and Environmental Microbiology*, 65 (1999) 5451–8.
- [63] E.O. Mello, S.F.F. Ribeiro, A.O. Carvalho, I.S. Santos, M. Da Cunha, C. Santa-Catarina, V.M. Gomes, Antifungal activity of PvD1 defensin involves plasma membrane permeabilization, inhibition of medium acidification, and induction of ROS in fungi cells, *Current Microbiology*, 62 (2011) 1209–1217.
- [64] N.L. Van Der Weerden, R.E.W. Hancock, M.A. Anderson, Permeabilization of fungal hyphae by the plant defensin NaD1 occurs through a cell wall-dependent process, *Journal of Biological Chemistry*, 285 (2010) 37513–37520.
- [65] P. Fehlbaum, P. Bulet, L. Michaut, M. Lagueux, W.F. Broekaert, C. Hetru, J.A. Hoffmann, Insect immunity. Septic injury of drosophila induces the synthesis of a potent antifungal peptide with sequence homology to plant antifungal peptides, *Journal of Biological Chemistry*, 269 (1994) 33159–33163.
- [66] Z.-T. Zhang, S.-Y. Zhu, Drosomycin, an essential component of antifungal defence in *Drosophila*, *Insect Molecular Biology*, 18 (2009) 549–556.
- [67] A.J. De Lucca, J.M. Bland, T.J. Jacks, C. Grimm, T.J. Walsh, Fungicidal and binding properties of the natural peptides cecropin B and dermaseptin, *Medical Mycology*, 36 (1998) 291–298.
- [68] C.O. Morton, A. Hayes, M. Wilson, B.M. Rash, S.G. Oliver, P. Coote, Global phenotype screening and transcript analysis outlines the inhibitory mode(s) of action of two amphibian-derived, alpha-helical, cationic peptides on *Saccharomyces cerevisiae*,

- Antimicrobial Agents and Chemotherapy, 51 (2007) 3948–3959.
- [69] A. Mor, K. Hani, P. Nicolas, The vertebrate peptide antibiotics dermaseptins have overlapping structural features but target specific microorganisms, *Journal of Biological Chemistry*, 269 (1994) 31635–31641.
- [70] R.I. Lehrer, A. Barton, K.A. Daher, S.S. Harwig, T. Ganz, M.E. Selsted, Interaction of human defensins with *Escherichia coli*. Mechanism of bactericidal activity, *The Journal of Clinical Investigation*, 84 (1989) 553–561.
- [71] S.M. Levitz, M.E. Selsted, T. Ganz, R.I. Lehrer, R.D. Diamond, *In vitro* killing of spores and hyphae of *Aspergillus fumigatus* and *Rhizopus oryzae* by rabbit neutrophil cationic peptides and bronchoalveolar macrophages, *Journal of Infectious Diseases*, 154 (1986) 483–489.
- [72] C.H. Kirkpatrick, I. Green, R.R. Rich, A.L. Schade, Inhibition of growth of *Candida albicans* by iron-unsaturated lactoferrin: relation to host-defense mechanisms in chronic mucocutaneous candidiasis, *Journal of Infectious Diseases*, 124 (1971) 539–544.
- [73] K.A. Zarembek, J.A. Sugui, Y.C. Chang, K.J. Kwon-Chung, J.I. Gallin, Human polymorphonuclear leukocytes inhibit *Aspergillus fumigatus* conidial growth by lactoferrin-mediated iron depletion, *Journal of Immunology*, 178 (2007) 6367–6373.
- [74] A.B. Mochon, H. Liu, The antimicrobial peptide histatin-5 causes a spatially restricted disruption on the *Candida albicans* surface allowing rapid entry of the peptide into the cytoplasm, *PLoS Pathogens*, 4 (2008) e1000190.
- [75] K. Ajesh, K. Sreejith, Peptide antibiotics: An alternative and effective antimicrobial strategy to circumvent fungal infections, *Peptides*, 30 (2009) 999–1006.
- [76] A.J. De Luca, T.J. Walsh, Antifungal peptides: Origin, activity, and therapeutic potential, *Revista Iberoamericana de Micologia*, 17 (2000) 116–120.
- [77] A. Mhammedi, F. Peypoux, F. Besson, G. Michel, Bacillomycin, a new antibiotic of iturin group: isolation and characterisation, *The Journal of Antibiotics*, 35 (1982) 306–311.
- [78] T. Chapman, O. Kinsman, J. Houston, Chitin biosynthesis in *Candida albicans* grown *in vitro* and *in vivo* and its inhibition by nikkomycin Z, *Antimicrobial Agents and Chemotherapy*, 36 (1992) 1909–1914.
- [79] M. Rautenbach, A.M. Troskie, J.A. Vosloo, M.E. Dathe, Antifungal membranolytic activity of the tyrocidines against filamentous plant fungi, *Biochimie*, 130 (2016) 122–131.
- [80] A.M. Troskie, A. de Beer, J.A. Vosloo, K. Jacobs, M. Rautenbach, Inhibition of agronomically relevant fungal phytopathogens by tyrocidines, cyclic antimicrobial peptides isolated from *Bacillus aneurinolyticus*, *Microbiology*, 160 (2014) 2089–2101.
- [81] D. Cappelletty, K. Eiselstein-McKittrick, The echinocandins, *Pharmacotherapy*, 27 (2007) 369–388.
- [82] M. Endo, K. Takesako, I. Kato, H. Yamaguchi, Fungicidal action of aureobasidin A, a cyclic depsipeptide antifungal antibiotic, against *Saccharomyces cerevisiae*, *Antimicrobial Agents and Chemotherapy*, 41 (1997) 672–676.
- [83] M.M. Nagiec, E.E. Nagiec, J.A. Baltisberger, G.B. Wells, R.L. Lester, R.C. Dickson, Sphingolipid synthesis as a target for antifungal drugs complementation of the inositol

- phosphorylceramide synthase defect in a mutant strain of *Saccharomyces cerevisiae* by the AUR1 gene, *The Journal of Biological Chemistry*, 272 (1997) 9809–9817.
- [84] F. Marx, The *Penicillium chrysogenum* antifungal protein PAF , a promising tool for the development of new antifungal therapies and fungal cell biology studies, *Cellular and Molecular Life Sciences*, 65 (2008) 445–454.
- [85] K. Thevissen, K.K.A. Ferket, I.E.J.A. François, B.P.A. Cammue, Interactions of antifungal plant defensins with fungal membrane components, *Peptides*, 24 (2003) 1705–1712.
- [86] B. Thomma, B. Cammue, K. Thevissen, Plant defensins, *Planta*, 216 (2002) 193–202.
- [87] K. Thevissen, F.R.G. Terras, W.F. Broekaert, Permeabilization of fungal membranes by plant defensins inhibits fungal growth, *Applied and Environmental Microbiology*, 65 (1999) 5451–5458.
- [88] K. Thevissen, P. de Mello Tavares, D. Xu, J. Blankenship, D. Vandenbosch, J. Idkowiak-Baldys, G. Govaert, A. Bink, S. Rozental, P.W.J. de Groot, T.R. Davis, C.A. Kumamoto, G. Vargas, L. Nimrichter, T. Coenye, A. Mitchell, T. Roemer, Y.A. Hannun, B.P.A. Cammue, The plant defensin RsAFP2 induces cell wall stress, septin mislocalization and accumulation of ceramides in *Candida albicans*, *Molecular Microbiology*, 84 (2012) 166–180.
- [89] P.D. Games, I.S. dos Santos, É.O. Mello, M.S.S. Diz, A.O. Carvalho, G.A. de Souza-Filho, M. Da Cunha, I.M. Vasconcelos, B. dos S. Ferreira, V.M. Gomes, Isolation, characterization and cloning of a cDNA encoding a new antifungal defensin from *Phaseolus vulgaris* L seeds, *Peptides*, 29 (2008) 2090–2100.
- [90] N.L. Van Der Weerden, F.T. Lay, M.A. Anderson, The plant defensin, NaD1, enters the cytoplasm of *Fusarium oxysporum* hyphae, *The Journal of Biological Chemistry*, 283 (2008) 14445–14452.
- [91] L. Michaut, P. Fehlbaum, M. Moniatte, A. Van Dorsselaer, J.-M. Reichhart, P. Bulet, Determination of the disulfide array of the first inducible antifungal peptide from insects: drosomycin from *Drosophila melanogaster*, *FEBS Letters*, 395 (1996) 6–10.
- [92] B. Lemaitre, J.M. Reichhart, J.A. Hoffmann, *Drosophila* host defense: differential induction of antimicrobial peptide genes after infection by various classes of microorganisms, *Proceedings of the National Academy of Sciences*, 94 (1997) 14614–14619.
- [93] L. Cohen, Y. Moran, A. Sharon, D. Segal, D. Gordon, M. Gurevitz, Drosomycin, an innate immunity peptide of *Drosophila melanogaster*, interacts with the fly voltage-gated sodium channel, *Journal of Biological Chemistry*, 284 (2009) 23558–23563.
- [94] D. Hultmark, H. Steiner, T. Rasmuson, H.G. Boman, Insect immunity. Purification and properties of three inducible bactericidal proteins from hemolymph of immunized pupae of *Hyalophora cecropia*, *European Journal of Biochemistry*, 106 (2005) 7–16.
- [95] A.J. DeLucca, J.M. Bland, T.J. Jacks, C. Grimm, T.E. Cleveland, T.J. Walsh, Fungicidal activity of cecropin A, *Antimicrobial Agents and Chemotherapy*, 41 (1997) 481–483.
- [96] A. Giacometti, O. Cirioni, R. Ghiselli, C. Viticchi, F. Mocchegiani, A. Riva, V. Saba, G. Scalise, Effect of mono-dose intraperitoneal cecropins in experimental septic shock, *Critical Care Medicine*, 29 (2001) 1666–1669.

- [97] A.J. Moore, D.A. Devine, M.C. Bibby, Preliminary experimental anticancer activity of cecropins, *Peptide Research*, 7 (1994) 265–9.
- [98] N. Mandard, P. Sodano, H. Labbe, J.-M. Bonmatin, P. Bulet, C. Hetru, M. Ptak, F. Vovelle, Solution structure of thanatin, a potent bactericidal and fungicidal insect peptide, determined from proton two-dimensional nuclear magnetic resonance data, *European Journal of Biochemistry*, 256 (1998) 404–410.
- [99] P. Fehlbaum, P. Bulet, S. Chernysh, J.P. Briand, J.P. Roussel, L. Letellier, C. Hetru, J.A. Hoffmann, Structure-activity analysis of thanatin, a 21-residue inducible insect defense peptide with sequence homology to frog skin antimicrobial peptides, *Proceedings of the National Academy of Sciences*, 93 (1996) 1221–1225.
- [100] M. Simmaco, G. Kreil, D. Barra, Bombinins, antimicrobial peptides from *Bombina* species, *Biochimica et Biophysica Acta - Biomembranes*, 1788 (2009) 1551–1555.
- [101] M. Zasloff, Magainins, a class of antimicrobial peptides from *Xenopus* skin: isolation, characterization of two active forms, and partial cDNA sequence of a precursor, *Proceedings of the National Academy of Sciences*, 84 (1987) 5449–5453.
- [102] T. Pál, B. Abraham, Á. Sonnevend, P. Jumaa, J.M. Conlon, Brevinin-1BYa: a naturally occurring peptide from frog skin with broad-spectrum antibacterial and antifungal properties, *International Journal of Antimicrobial Agents*, 27 (2006) 525–529.
- [103] J.J. Schneider, A. Unholzer, M. Schaller, M. Schäfer-Korting, H.C. Korting, Human defensins, *Journal of Molecular Medicine*, 83 (2005) 587–595.
- [104] T. Ganz, M.E. Selsted, D. Szklarek, S.S. Harwig, K. Daher, D.F. Bainton, R.I. Lehrer, Defensins. Natural peptide antibiotics of human neutrophils, *The Journal of Clinical Investigation*, 76 (1985) 1427–1435.
- [105] R.I. Lehrer, T. Ganz, D. Szklarek, M.E. Selsted, Modulation of the in vitro candidacidal activity of human neutrophil defensins by target cell metabolism and divalent cations, *The Journal of Clinical Investigation*, 81 (1988) 1829–1835.
- [106] M.E. Selsted, D. Szklarek, T. Ganz, R.I. Lehrer, Activity of rabbit leukocyte peptides against *Candida albicans*, *Infection and Immunity*, 49 (1985) 202–206.
- [107] Z. Feng, B. Jiang, J. Chandra, M. Ghannoum, S. Nelson, A. Weinberg, Human beta-defensins: Differential activity against candidal species and regulation by *Candida albicans*, *Journal of Dental Research*, 84 (2005) 445–450.
- [108] S. Joly, C. Maze, P.B. McCray, J.M. Guthmiller, Human beta-defensins 2 and 3 demonstrate strain-selective activity against oral microorganisms, *Journal of Clinical Microbiology*, 42 (2004) 1024–1029.
- [109] V. Krishnakumari, N. Rangaraj, R. Nagaraj, Antifungal activities of human beta-defensins HBD-1 to HBD-3 and their C-terminal analogs Phd1 to Phd3, *Antimicrobial Agents and Chemotherapy*, 53 (2009) 256–260.
- [110] Y. Cho, J.S. Turner, N.N. Dinh, R.I. Lehrer, Activity of protegrins against yeast-phase *Candida albicans*, *Infection and Immunity*, 66 (1998) 2486–2493.
- [111] V.N. Kokryakov, S.S.L. Harwig, E.A. Panyutich, A.A. Shevchenko, G.M. Aleshina, O. V. Shamova, H.A. Korneva, R.I. Lehrer, Protegrins: leukocyte antimicrobial peptides that combine features of corticostatic defensins and tachyplesins, *FEBS Letters*, 327 (1993)

- 231–236.
- [112] S.S.L. Harwig, K.M. Swiderek, V.N. Kokryakov, L. Tan, T.D. Lee, E.A. Panyutich, G.M. Aleshina, O. V. Shamova, R.I. Lehrer, Gallinacins: cysteine-rich antimicrobial peptides of chicken leukocytes, *FEBS Letters*, 342 (1994) 281–285.
- [113] A. Nijnik, R.E. Hancock, The roles of cathelicidin LL-37 in immune defences and novel clinical applications, *Current Opinion in Hematology*, 16 (2009) 41–47.
- [114] B. López-García, P.H.A. Lee, K. Yamasaki, R.L. Gallo, Anti-fungal activity of cathelicidins and their potential role in *Candida albicans* skin infection, *Journal of Investigative Dermatology*, 125 (2005) 108–115.
- [115] S.R. Ordonez, I.H. Amarullah, R.W. Wubbolts, E.J.A. Veldhuizen, H.P. Haagsman, Fungicidal mechanisms of cathelicidins LL-37 and CATH-2 revealed by live-cell imaging, *Antimicrobial Agents and Chemotherapy*, 58 (2014) 2240–2248.
- [116] D. Vandamme, B. Landuyt, W. Luyten, L. Schoofs, A comprehensive summary of LL-37, the lactoferrin human cathelicidin peptide, *Cellular Immunology*, 280 (2012) 22–35.
- [117] M. Benincasa, M. Scocchi, S. Pacor, A. Tossi, D. Nobili, G. Basaglia, M. Buseti, R. Gennaro, Fungicidal activity of five cathelicidin peptides against clinically isolated yeasts, *Journal of Antimicrobial Chemotherapy*, 58 (2006) 950–959.
- [118] M.E. Selsted, M.J. Novotny, W.L. Morris, Y.Q. Tang, W. Smith, J.S. Cullor, Indolicidin, a novel bactericidal tridecapeptide amide from neutrophils, *Journal of Biological Chemistry*, 267 (1992) 4292–4295.
- [119] C. Lawyer, S. Pai, M. Watabe, P. Borgia, T. Mashimo, L. Eagleton, K. Watabe, Antimicrobial activity of a 13 amino acid tryptophan-rich peptide derived from a putative porcine precursor protein of a novel family of antibacterial peptides, *FEBS Letters*, 390 (1996) 95–98.
- [120] R. Rayhan, L. Xu, R.P. Santarpia, C.A. Tylenda, J.J. Pollock, Antifungal activities of salivary histidine-rich polypeptides against *Candida albicans* and other oral yeast isolates, *Oral Microbiology and Immunology*, 7 (1992) 51–52.
- [121] J.J. Pollock, L. Denepitiya, B.J. MacKay, V.J. Iacono, Fungistatic and fungicidal activity of human parotid salivary histidine-rich polypeptides on *Candida albicans*, *Infection and Immunity*, 44 (1984) 702–7.
- [122] H. Tsai, L.A. Bobek, Human salivary histatin-5 exerts potent fungicidal activity against *Cryptococcus neoformans*, *Biochimica et Biophysica Acta - General Subjects*, 1336 (1997) 367–369.
- [123] E.J. Helmerhorst, I.M. Reijnders, W. van't Hof, I. Simoons-Smit, E.C. Veerman, A. V Amerongen, Amphotericin B- and fluconazole-resistant *Candida* spp, *Aspergillus fumigatus*, and other newly emerging pathogenic fungi are susceptible to basic antifungal peptides, *Antimicrobial Agents and Chemotherapy*, 43 (1999) 702–704.
- [124] C.D. Sumi, B.W. Yang, I.-C. Yeo, Y.T. Hahm, Antimicrobial peptides of the genus *Bacillus* : a new era for antibiotics, *Canadian Journal of Microbiology*, 61 (2015) 93–103.
- [125] M.A. Klich, A.R. Lax, J.M. Bland, Inhibition of some mycotoxigenic fungi by iturin A, a peptidolipid produced by *Bacillus subtilis*, *Mycopathologia*, 116 (1991) 77–80.

- [126] C.L. Bender, F. Alarcón-Chaidez, D.C. Gross, *Pseudomonas syringae* phytotoxins: mode of action, regulation, and biosynthesis by peptide and polyketide synthetases, *Microbiol. Mol. Biol. Rev.*, 63 (1999) 266–292.
- [127] K.N. Sorensen, K.H. Kim, J.Y. Takemoto, *In vitro* antifungal and fungicidal activities and erythrocyte toxicities of cyclic lipodepsinonapeptides produced by *Pseudomonas syringae* pv *syringae*, *Antimicrobial Agents and Chemotherapy*, 40 (1996) 2710–2713.
- [128] L. Zhang, J.Y. Takemoto, Mechanism of action of *Pseudomonas syringae* phytotoxin, syringomycin. Interaction with the plasma membrane of wild-type and respiratory-deficient strains of *Saccharomyces cerevisiae*, *Biochimica et Biophysica Acta - Biomembranes*, 861 (1986) 201–204.
- [129] A.M. Feigin, J.Y. Takemoto, R. Wangspa, J.H. Teeter, J.G. Brand, Properties of voltage-gated ion channels formed by syringomycin E in planar lipid bilayers, *Journal of Membrane Biology*, 149 (1996) 41–47.
- [130] R.K. Li, M.G. Rinaldi, *In vitro* antifungal activity of nikkomycin Z in combination with fluconazole or itraconazole, *Antimicrobial Agents and Chemotherapy*, 43 (1999) 1401–1405.
- [131] K. Gull, Mechanism of action of nikkomycin and the peptide transport system of *Candida albicans*, *Journal of General Microbiology*, 131 (1985) 775–780.
- [132] R.J. Mehta, W.D. Kingsbury, J. Valenta, P. Actor, Anti-*Candida* activity of polyoxin: example of peptide transport in yeasts, *Antimicrobial Agents and Chemotherapy*, 25 (1984) 373–374.
- [133] R.J. Dubos, R.D. Hotchkiss, The production of bactericidal substances by aerobic sporulating *Bacilli*, *The Journal of Experimental Medicine*, 73 (1941) 629–640.
- [134] S. Wnendt, N. Ulbrich, U. Stahl, Molecular cloning, sequence analysis and expression of the gene encoding an antifungal-protein from *Aspergillus giganteus*, *Current Genetics*, 25 (1994) 519–523.
- [135] D. Gun Lee, S. Yub Shin, C.-Y. Maeng, Z. Zhu Jin, K. Lyong Kim, K.-S. Hahm, Isolation and characterization of a novel antifungal peptide from *Aspergillus niger*, *Biochemical and Biophysical Research Communications*, 263 (1999) 646–651.
- [136] H. Skouri-Gargouri, A. Gargouri, First isolation of a novel thermostable antifungal peptide secreted by *Aspergillus clavatus*, *Peptides*, 29 (2008) 1871–1877.
- [137] Y. Yoshikawa, K. Ikai, Y. Umeda, A. Ogawa, K. Takesako, I. Kato, H. Naganawa, Isolation, structures, and antifungal activities of new aureobasidins, *The Journal of Antibiotics*, 46 (1993) 1347–1354.
- [138] F. Marx, Small, basic antifungal proteins secreted from filamentous ascomycetes: a comparative study regarding expression, structure, function and potential application, *Applied Microbiology and Biotechnology*, 65 (2004) 133–142.
- [139] V. Meyer, A small protein that fights fungi: AFP as a new promising antifungal agent of biotechnological value, *Applied Microbiology and Biotechnology*, 78 (2008) 17–28.
- [140] F. Marx, H. Haas, M. Reindl, G. Stöffler, F. Lottspeich, B. Redl, Cloning, structural organization and regulation of expression of the *Penicillium chrysogenum* paf gene encoding an abundantly secreted protein with antifungal activity, *Gene*, 167 (1995) 167–

171.

- [141] R.J. Dubos, Studies on bactericidal agent extracted from a soil *Bacillus*: 1 Preparation of the agent. Its activity in vitro, *The Journal of Experimental Medicine*, 70 (1939) 1–10.
- [142] D. Hotchkiss, R. Dubos, The isolation of bactericidal substances from cultures from *Bacillus brevis*, *The Journal of Biological Chemistry*, 141 (1941) 155–162.
- [143] X.-J. Tang, P. Thibault, R.K. Boyd, Characterisation of the tyrocidine and gramicidin fractions of the tyrothricin complex from *Bacillus brevis* using liquid chromatography and mass spectrometry, *International Journal of Mass Spectrometry and Ion Processes*, 122 (1992) 153–179.
- [144] K.P. Dimick, The hemolytic action of gramicidin and tyrocidine, *Experimental Biology and Medicine*, 78 (1951) 782–784.
- [145] W. Wigger-Alberti, M. Stauss-Grabo, K. Grigo, S. Atiye, R. Williams, H.C. Korting, Efficacy of a tyrothricin-containing wound gel in an abrasive wound model for superficial wounds, *Skin Pharmacology and Physiology*, 26 (2013) 52–56.
- [146] J. Henderson, The status of tyrothricin as an antibiotic agent for topical application, *Journal of the American Pharmaceutical Association*, 35 (1946) 141–147.
- [147] G. Kagan, L. Huddlestone, P. Wolstencroft, Two lozenges containing benzocaine assessed in the relief of sore throat, *Journal of International Medical Research*, 10 (1982) 443–446.
- [148] A.M. Troskie, Tyrocidines, cyclic decapeptides produced by soil bacilli, as potent inhibitors of fungal pathogens, PhD Thesis, Department of Biochemistry, University of Stellenbosch, (2013), <http://hdl.handle.net/10019.1/86162>
- [149] W. Van Rensburg, Characterization of natural antimicrobial peptides adsorbed to different matrices, MSc Thesis, Department of Biochemistry, University of Stellenbosch, (2015). <http://hdl.handle.net/10019.1/97929>
- [150] G.F. Gause, M.G. Brazhnikova, Gramicidin S: origin and mode of action, *Lancet*, 244 (1944) 715–716.
- [151] P.J. Loll, E.C. Upton, V. Nahoum, N.J. Economou, S. Cocklin, The high resolution structure of tyrocidine A reveals an amphipathic dimer, *Biochimica et Biophysica Acta - Biomembranes*, 1838 (2014) 1199–1207.
- [152] M. Kuo, W.A. Gibbons, Total assignments, including four aromatic residues, and sequence confirmation of the decapeptide tyrocidine A using difference double resonance. Qualitative nuclear overhauser effect criteria for beta turn and antiparallel beta-pleated sheet conformation, *Journal of Biological Chemistry*, 254 (1979) 6278–6287.
- [153] G. Munyuki, G.E. Jackson, G.A. Venter, K.E. Kövér, L. Szilágyi, M. Rautenbach, B.M. Spathelf, B. Bhattacharya, D. Van Der Spoel, β -sheet structures and dimer models of the two major tyrocidines, antimicrobial peptides from *Bacillus aneurinolyticus*, *Biochemistry*, 52 (2013) 7798–7806.
- [154] R.J. Dubos, R.D. Hotchkiss, A.F. Coburn, The effect of gramicidin and tyrocidine on bacterial metabolism, *Journal of Biological Chemistry*, 146 (1942) 421–426.
- [155] B.M. Spathelf, M. Rautenbach, Anti-listerial activity and structure-activity relationships of the six major tyrocidines, cyclic decapeptides from *Bacillus aneurinolyticus*, *Bioorganic*

- and Medicinal Chemistry, 17 (2009) 5541–5548.
- [156] B. Mach, C.W. Slayman, Mode of action of tyrocidine on *Neupospora*, *Biochimica et Biophysica Acta*, 124 (1966) 351–361.
- [157] M. Rautenbach, N.M. Vlok, M. Stander, H.C. Hoppe, Inhibition of malaria parasite blood stages by tyrocidines, membrane-active cyclic peptide antibiotics from *Bacillus brevis*, *Biochimica et Biophysica Acta - Biomembranes*, 1768 (2007) 1488–1497.
- [158] A.N.-N. Leussa, Characterisation of small cyclic peptides with antimalarial and antilisterial activity PhD Thesis, Department of Biochemistry, University of Stellenbosch, (2014), <http://hdl.handle.net/100191/86161>.
- [159] C.H. Rammelkamp, L. Weinstein, Toxic effects of tyrothricin, gramicidin and tyrocidine, *Journal of Infectious Diseases*, 71 (1942) 166–173.
- [160] A.N. yango N. Leussa, M. Rautenbach, Detailed SAR and PCA of the tyrocidines and analogues towards leucocin A-sensitive and leucocin A-resistant *Listeria monocytogenes*, *Chemical Biology & Drug Design*, 84 (2014) 543–557.
- [161] M. Wenzel, M. Rautenbach, J.A. Vosloo, T. Siersma, C.H.M. Aisenbrey, E. Zaitseva, W.E. Laubscher, W. van Rensburg, J.C. Behrends, B. Bechinger, L.W. Hamoen, The multifaceted antibacterial mechanisms of the pioneering peptide antibiotics tyrocidine and gramicidin S, *MBio*, 9 (2018) 1–20.
- [162] A. Bohg, H. Ristow, Tyrocidine-induced modulation of the DNA conformation in *Bacillus brevis*, *European Journal of Biochemistry*, 170 (1987) 253–258.
- [163] A. Bohg, H. Ristow, DNA-supercoiling is affected in vitro by the peptide antibiotics tyrocidine and gramicidin, *European Journal of Biochemistry*, 160 (1986) 587–591.
- [164] M. Dathe, H. Nikolenko, J. Klose, M. Bienert, Cyclization increases the antimicrobial activity and selectivity of arginine- and tryptophan-containing hexapeptides, *Biochemistry*, 43 (2004) 9140–9150.
- [165] A.K. Marr, W.J. Gooderham, R.E. Hancock, Antibacterial peptides for therapeutic use: obstacles and realistic outlook, *Current Opinion in Pharmacology*, 6 (2006) 468–472.
- [166] D.I. Chan, E.J. Prenner, H.J. Vogel, Tryptophan- and arginine-rich antimicrobial peptides: structures and mechanisms of action, *Biochimica et Biophysica Acta (BBA) - Biomembranes*, 1758 (2006) 1184–1202.
- [167] B. López-García, L. González-Candelas, E. Pérez-Payá, J.F. Marcos, Identification and characterization of a hexapeptide with activity against phytopathogenic fungi that cause postharvest decay in fruits, *The American Phytopathological Society*, 13 (2000) 837–846.
- [168] S.E. Blondelle, R.A. Houghten, Novel antimicrobial compounds identified using synthetic combinatorial library technology, *Trends in Biotechnology*, 14 (1996) 60–65.
- [169] S.E. Blondelle, E. Takahashi, K.T. Dinh, R.A. Houghten, The antimicrobial activity of hexapeptides derived from synthetic combinatorial libraries, *Journal of Applied Bacteriology*, 78 (1995) 39–46.
- [170] R.A. Houghten, J.R. Appel, S.E. Blondelle, J.H. Cuervo, C.T. Dooley, C. Pinilla, The use of synthetic peptide combinatorial libraries for the identification of bioactive peptides, *BioTechniques*, 13 (1992) 412–21.

- [171] M.B. Strøm, Ø. Rekdal, J.S. Svendsen, Antimicrobial activity of short arginine- and tryptophan-rich peptides, *Journal of Peptide Science*, 8 (2002) 431–437.
- [172] W. Jing, H.N. Hunter, J. Hagel, H.J. Vogel, The structure of the antimicrobial peptide Ac-RRWRF-NH₂ bound to micelles and its interactions with phospholipid bilayers, *Journal of Peptide Research*, 61 (2003) 219–229.
- [173] C. Appelt, A. Wessolowski, J.A. Söderhäll, M. Dathe, P. Schmieder, Structure of the antimicrobial, cationic hexapeptide cyclo(RRWRF) and its analogues in solution and bound to detergent micelles, *ChemBioChem*, 6 (2005) 1654–1662.
- [174] B. López-García, E. Pérez-Payá, J.F. Marcos, Identification of novel hexapeptides bioactive against phytopathogenic fungi through screening of a synthetic peptide combinatorial library, *Applied and Environmental Microbiology*, 68 (2002) 2453–2460.
- [175] A. Wessolowski, M. Bienert, M. Dathe, Antimicrobial activity of arginine- and tryptophan-rich hexapeptides: the effects of aromatic clusters, D-amino acid substitution and cyclization, *Journal of Peptide Research*, 64 (2004) 159–169.
- [176] K. Scheinpflug, M. Wenzel, O. Krylova, J.E. Bandow, M. Dathe, H. Strahl, Antimicrobial peptide cFWF kills by combining lipid phase separation with autolysis, *Scientific Reports*, 7 (2017) 44332.
- [177] K. Scheinpflug, O. Krylova, H. Nikolenko, C. Thurm, M. Dathe, Evidence for a novel mechanism of antimicrobial action of a cyclic R-,W-rich hexapeptide, *PLoS ONE*, 10 (2015) 1–16.
- [178] A. Muñoz, B. López-García, J.F. Marcos, Studies on the mode of action of the antifungal hexapeptide PAF26, *Antimicrobial Agents and Chemotherapy*, 50 (2006) 3847–3855.
- [179] A.J. Rezansoff, H.N. Hunter, W. Jing, I.Y. Park, S.C. Kim, H.J. Vogel, Interactions of the antimicrobial peptide Ac-FRWHR-NH₂ with model membrane systems and bacterial cells, *Journal of Peptide Research*, 65 (2005) 491–501.
- [180] C. Junkes, R.D. Harvey, K.D. Bruce, R. Dölling, M. Bagheri, M. Dathe, Cyclic antimicrobial R-, W-rich peptides: the role of peptide structure and E coli outer and inner membranes in activity and the mode of action, *European Biophysics Journal*, 40 (2011) 515–528.
- [181] A. Muñoz, M. Gandía, E. Harries, L. Carmona, N.D. Read, J.F. Marcos, Understanding the mechanism of action of cell-penetrating antifungal peptides using the rationally designed hexapeptide PAF26 as a model, *Fungal Biology Reviews*, 26 (2013) 146–155.
- [182] A. Muñoz, E. Harries, A. Contreras-Valenzuela, L. Carmona, N.D. Read, J.F. Marcos, Two functional motifs define the interaction, internalization and toxicity of the cell-penetrating antifungal peptide PAF26 on fungal cells, *PLoS ONE*, 8 (2013) 1–11.
- [183] B. López-García, M. Gandía, A. Muñoz, L. Carmona, J.F. Marcos, A genomic approach highlights common and diverse effects and determinants of susceptibility on the yeast *Saccharomyces cerevisiae* exposed to distinct antimicrobial peptides, *BMC Microbiology*, 10 (2010) 289.
- [184] L. Carmona, M. Gandía, B. López-García, J.F. Marcos, Sensitivity of *Saccharomyces cerevisiae* to the cell-penetrating antifungal peptide PAF26 correlates with endogenous nitric oxide (NO) production, *Biochemical and Biophysical Research Communications*, 417 (2012) 56–61.

- [185] A. Muñoz, J.F. Marcos, N.D. Read, Concentration-dependent mechanisms of cell penetration and killing by the de novo designed antifungal hexapeptide PAF26, *Molecular Microbiology*, 85 (2012) 89–106.

Chapter 2

Production, purification and chemical characterisation of natural and synthetic peptides

2.1 Introduction

Over the last couple of decades, the incidence of systemic mycoses amongst the human population has increased, concomitantly with an increase in the mortalities due to these mycoses. It is estimated that approximately one and a half million individuals succumb to systemic mycoses annually [1]. This is attributed to the growing population of immunocompromised individuals who are susceptible to infections caused by fungi and the increasing frequency of antimycotic resistant pathogens [2]. A major concern is that new antimycotic agents which can combat resistant pathogens are lacking and no new antimycotic drug has entered the market in over a decade. As such, the dire need for novel antimycotic agents has motivated this research study in which the potential of selected peptides to act as antifungal agents was determined by investigating their antifungal activity against *A. fumigatus*, a human fungal pathogen.

The peptides that were selected for this study belong to two distinct groups, namely the cyclodecapeptides (tyrocidines and analogues) and the RW-hexapeptides. Cyclodecapeptides are a family of structurally related cyclic peptides that are produced naturally by the soil bacterium *Br. parabrevis* [3]. They are produced in conjunction with linear gramicidins and together they form the tyrothricin complex which was the first clinically used antibiotic [3–5]. On the other hand, the linear and cyclic RW-hexapeptides are synthetic peptides that are derivatives of a hexapeptide that was identified through screening of a synthetic combinatorial library [6].

Both groups of peptides have previously been shown to exhibit excellent antimicrobial activity. Their activities against bacterial pathogens, as well as selected fungal phytopathogens are well documented in literature [5,7–15]. On the contrary, research regarding antifungal activity against human fungal pathogens has been limited to a few studies. To date, the antifungal activity of tyrocidines against a human fungal pathogen has only been investigated by our group [16,17]. As for the RW-hexapeptides in our library, data pertaining to their activity towards human fungal pathogens are lacking.

Before the biological activity of any peptide can be ascertained, it is of utmost importance that the peptide be in a high state of purity. This is because a peptide's biological effect can only be deemed accurate if the peptide is of acceptable purity. The standard practice in our research group is that

a peptide needs to be at least 90% pure by peptide composition, as determined by a stringent quality control (QC) regime. Two techniques that are indispensable to the purification and characterisation of peptides are high performance liquid chromatography (HPLC) and mass spectrometry, specifically electrospray ionisation mass spectrometry (ESMS). In this study, an optimised semi-preparative reversed phase HPLC methodology was employed to purify individual tyrocidines and analogues from crude peptide mixtures that were extracted from cultures of *Br. parabrevis*. Our stringent QC entailed ultra-performance liquid chromatography (UPLC) linked to high resolution electrospray mass spectrometry (ESMS) (denoted as UPLC-MS) and was used to determine the success of the purification protocol and confirm identity and purity of all the peptides in this study.

Table 2.1: Summary of the small antimicrobial peptides rich in aromatic residues selected for this study.

Peptide	Sequence	Structure	Monoisotopic M_r
<i>Tyrocidines and analogues</i>			
Tyrocidine A (YA)	fPffNQYVOL	Cyclic	1269.6546
Tyrocidine B (YB)	fPWfNQYVOL	Cyclic	1308.6655
Tyrocidine C (YC)	fPWwNQYVOL	Cyclic	1347.6764
Tryptocidine C (WC)	fPWwNQWVOL	Cyclic	1370.6924
<i>Synthetic RW-hexapeptides</i>			
cKRK	KRKWFW	Cyclic	931.5181
cRKK	RKKWFW	Cyclic	931.5181
cWFW	RRRWFW	Cyclic	987.5304
cWRW	RWRWRW	Cyclic	1026.5413
cWWW	RRRWWW	Cyclic	1026.5413
cWYW	RRRWYW	Cyclic	1003.5253
Ac-KRK	Ac-KRKWFW-NH ₂	Linear	990.5552
Ac-RKK	Ac-RKKWFW-NH ₂	Linear	990.5552
Ac-WFW	Ac-RRRWFW-NH ₂	Linear	1046.5675
Ac-WRW	Ac-RWRWRW-NH ₂	Linear	1085.5775
Ac-WWW	Ac-RRRWWW-NH ₂	Linear	1085.5775
Ac-WYW	Ac-RRRWYW-NH ₂	Linear	1062.5624

Amino acids in the peptide sequences are denoted by their conventional one letter abbreviations except for Ornithine which is denoted as O. Lower case letters are indicative of D-amino acids while uppercase letters indicate L-amino acids, Ac denotes *N*-acetyl or acetylated *N*-terminal and NH₂ denotes amidated or acid amide C-terminal

2.2 Materials

Peptide production

Br. parabrevis 5618-DSM strain was obtained from Leibniz Institute DSMZ – German Collection of Microorganisms and Cell Cultures. Merck (Darmstadt, Germany) supplied tryptone soy broth (TSB), agar and the following components of the TGS (tryptone glucose salt) medium: tryptone, glucose, potassium dihydrogen orthophosphate (KH₂PO₄), magnesium sulphate heptahydrate (MgSO₄·7H₂O), ferrous (II) sulphate (FeSO₄), manganese sulphate (MnSO₄) and calcium chloride (CaCl₂). Potassium chloride for the TGS medium as well as L-tryptophan and L-phenylalanine were supplied by Sigma (St. Louis, USA). Petri dishes were purchased from Greiner Bio-one (Frickenhausen, Germany) whilst Falcon® tubes were provided by Becton Dickson Labware (Lincoln Park, USA). Lasec (Cape Town, South Africa) provided 0.22 µm cellulose acetate syringe filters.

Extraction, purification and analysis of peptides

All solvent preparation was done using analytical grade water that had undergone reverse osmosis followed by filtration through a Millipore Milli-Q water purification system (Milford, USA). Acetonitrile (HPLC-grade, far UV cut-off of 190 nm) was supplied by Romil Limited (Cambridge, UK). Merck (Darmstadt, Germany) supplied ethanol (EtOH), hydrochloric acid and sodium chloride (NaCl). Activated carbon was supplied by Lurgi (Frankfurt, Germany). Trifluoroacetic acid (TFA >98%), diethyl ether, acetone, methanol (>99.9%) and commercial tyrothricin were obtained from Sigma (St. Louis, USA). Waters-Millipore (Milford, USA) supplied the following chromatography columns: Nova-Pak C₁₈ semi-preparative reversed phase HPLC column ((6 µm particle size, 60 Å pore size, 7.8 mm x 300 mm and an ACQUITY UPLC® bridged ethyl hybrid (BEH) C₁₈ column (1.7 µm particle size, 2.1 mm x 100 mm). HVLP membrane filters (0.45µm) were also obtained from Waters-Millipore (Milford, USA). Electrospray mass spectrometry was performed using a Waters Synapt G2 mass spectrometer. The synthetic cyclic peptides, except cWWW2, cWRW2 and cWYW were sourced from Leibniz, Germany. GL Biochem Limited (Shanghai, China) supplied the synthetic linear hexapeptides and the cyclic peptides, cWWW2, cWRW2 and cWYW.

2.3 Methods

Pre-culturing of the producer organism

Br. parabrevis 5618-DSM from freezer stocks was streaked onto TSB agar plates (3% w/v TSB, 1.5% w/v agar) using sterile culturing techniques. The plates were incubated at 37 °C for 48 hours.

Single colonies were selected and used to inoculate 20 mL of TSB broth. The inoculated broth was incubated at 37 °C with shaking at 150 rpm until an optical density (OD) reading between 0.6 and 0.9 at 595 nm was reached (approximately 16 hours). Fresh TSB was used to dilute the inoculated broth until the OD reading was at 0.20. This dilution was then used as the starter culture for tyrocidine production.

Production and extraction of peptides from cultures of *Br. parabrevis*

Three TGS media solutions were prepared and sterilised by autoclaving. Two of the autoclaved media solutions were then supplemented with either 16.5 mM Trp or 22 mM Phe. The amino acids were filter sterilised. The third TGS medium solution was not supplemented with any amino acid. Peptide production cultures were started by inoculating all TGS media solutions with a 1% (v/v; relative to final volume of production culture) starter culture of *Br. parabrevis*. After inoculation, the cultures were incubated at 37 °C for ten days.

An optimised extraction method [3,18] was used to isolate the produced peptides. This optimised method is currently protected by a non-disclosure agreement with BIOPEP™, University of Stellenbosch. Therefore, a detailed description of the methodology cannot be provided. The biomass was extracted by employing a stepwise methodology relying on the solubility of the tyrothricin peptides. The dry extract of tyrothricin contained both tyrocidine and linear gramicidin fractions. To separate the two fractions, the extract was washed with a combination of diethyl ether and acetone. Tyrocidines are precipitated out of solution while gramicidins remained in solution. The precipitate was dried under nitrogen gas, resuspended in acetonitrile solution and lyophilised.

Semi-preparative RP-HPLC of tyrocidines and analogues

Purification of the crude extracts obtained from the non-supplemented and Phe-supplemented cultures was achieved by semi-preparative reversed-phase high performance liquid chromatography (RP-HPLC). The chromatography system, which was controlled by MAXIMA software, consisted of two Waters 510 pumps, a Waters 440 ultraviolet (UV) detector set at 254 nm and a Nova-Pak C₁₈ semi-preparative RP-HPLC column (6 µm particle size, 60 Å pore size, 300 mm × 7.8 mm). A similar chromatography system which was under the control of Millennium software and was connected to a Waters 717 Autosampler was used to purify the crude extracts obtained from the Trp-supplemented culture. Samples to be purified were dissolved in 50% (v/v) acetonitrile (ACN) and centrifuged for 10 minutes at 10 000×g before 100 µL aliquots at 10 mg/mL were injected onto the semi-preparative RP-HPLC column. A non-linear gradient elution

method with two solvents, solvent A (0.001% (v/v) TFA) and solvent B (90% (v/v) ACN, 10% (v/v) Solvent A), was employed for the separation of peptides (Table 2.2). The solvent flow rate was set at 3 mL/minute and the column temperature was set to 35 °C.

Fractions whose purity was found to be unsatisfactory had to undergo a second round of purification which was performed on the chromatography system controlled by Millennium software. All parameters of the protocol were kept constant except the concentration of the samples injected was adjusted to 4 mg/mL.

Table 2.2: Gradient elution method used for semi-preparative RP-HPLC

Time (min)	% Solvent A	% Solvent B	Gradient curve type*
0.0	50	50	-
0.5	50	50	-
23	20	80	Concave
24	0	100	Linear
26	0	100	-
30	50	50	Linear
35	50	50	-

*HPLC gradient programme from Waters™.

ESMS and UPLC-MS analysis of peptides

Prior to RP-HPLC purification, crude extracts were analysed using ESMS and UPLC-MS to confirm peptide production and establish the profile of the produced peptides. After purification, ESMS and UPLC-MS analyses were used to establish the success of the purification procedure. Samples to be analysed were prepared in 5% (v/v) ACN in analytical grade water to concentrations of 1.0 mg/mL (crude extracts) and 0.20 mg/mL (purified extracts).

For ESMS, the analysis was carried out in a Waters Quadrupole Time-of-flight (Q-TOF) Synapt G2 mass spectrometer by injecting 2-5 µL samples directly onto a Z-spray electrospray ionisation source with a set temperature of 120 °C. The cone and capillary voltages were set to 15 V and 3 kV respectively. Desolvation was done at 275 °C using nitrogen gas. Data was acquired by scanning through a mass to charge (m/z) range of 300-2000 in positive ion mode.

UPLC-MS analyses were carried using a Waters Acquity UPLC™ chromatography system coupled to the Waters Quadrupole Time-of-flight (Q-TOF) Synapt G2 mass spectrometer. Separation was achieved by running samples through an Acquity UPLC® BEH C₁₈ column for 18 minutes. The column temperature was set to 60 °C. A linear gradient elution method (Table 2.3) was employed in which the mobile phase, comprising 1% (v/v) formic acid in analytical grade water (eluant A) and ACN (eluant B), with flow through the column at a rate of 0.3 mL/min.

Table 2.3: Gradient programme used for analysis of peptides by UPLC

Time (min)	% eluant A	% eluant B	Gradient curve type*
0.0	100	0	-
0.5	100	0	linear
1.0	70	30	linear
10.0	40	60	linear
15.0	20	80	linear
15.1	100	0	linear
18.0	100	0	-

*HPLC gradient programme from Waters™.

Data Analysis

GraphPad Prism® 6.0 (GraphPad software, San Diego, USA) was used to graphically represent purification data obtained from semi-preparative RP-HPLC. Analysis of ESMS and UPLC-MS data was done by using MassLynx™ software V4.1.

2.4 Results and Discussion

Part 1: Production, purification and characterisation of tyrocidines and analogues

Analysis of crude extracts

Extraction of peptide biomass from cultures of *Br. parabrevis* yielded crude mixtures composed of various tyrocidines and analogues as well as linear gramicidin A. The exact composition of these crude extracts was determined by UPLC-MS and is shown in Figure 2.1 and Table 2.4.

The bacterial culture that received no amino acid supplementation produced a wide range of tyrocidines and analogues across all three of the A, B and C peptide subfamilies. In contrast, amino acid supplementation caused an apparent shift in the production profile of the tyrocidines and analogues. Supplementation with 22.5 mM Phe resulted in the predominant production of tyrocidine A analogues with extremely low quantities of the tyrocidine B analogues. On the other hand, supplementation with 16.5 mM Trp favoured the production of tyrocidine C analogues. Supplementation with the two amino acids also influenced the production of linear VGA. In comparison to the non-supplemented culture, supplementation with phenylalanine inhibited the production of VGA while supplementation with tryptophan increased the production. These results are consistent with the findings of Vosloo *et al.* [19].

As highlighted in Table 2.4, the peptide profile of the extract from the non-supplemented culture is comparable to that of the extract from the study conducted by Tang *et al.* [4]. The differences in the relative abundances could be attributed to different culturing conditions such as different

bacterial strains for peptide production, different nutrient media and different incubation conditions. This shows that the culturing conditions of *Br. parabrevis* also influence the peptide production profile.

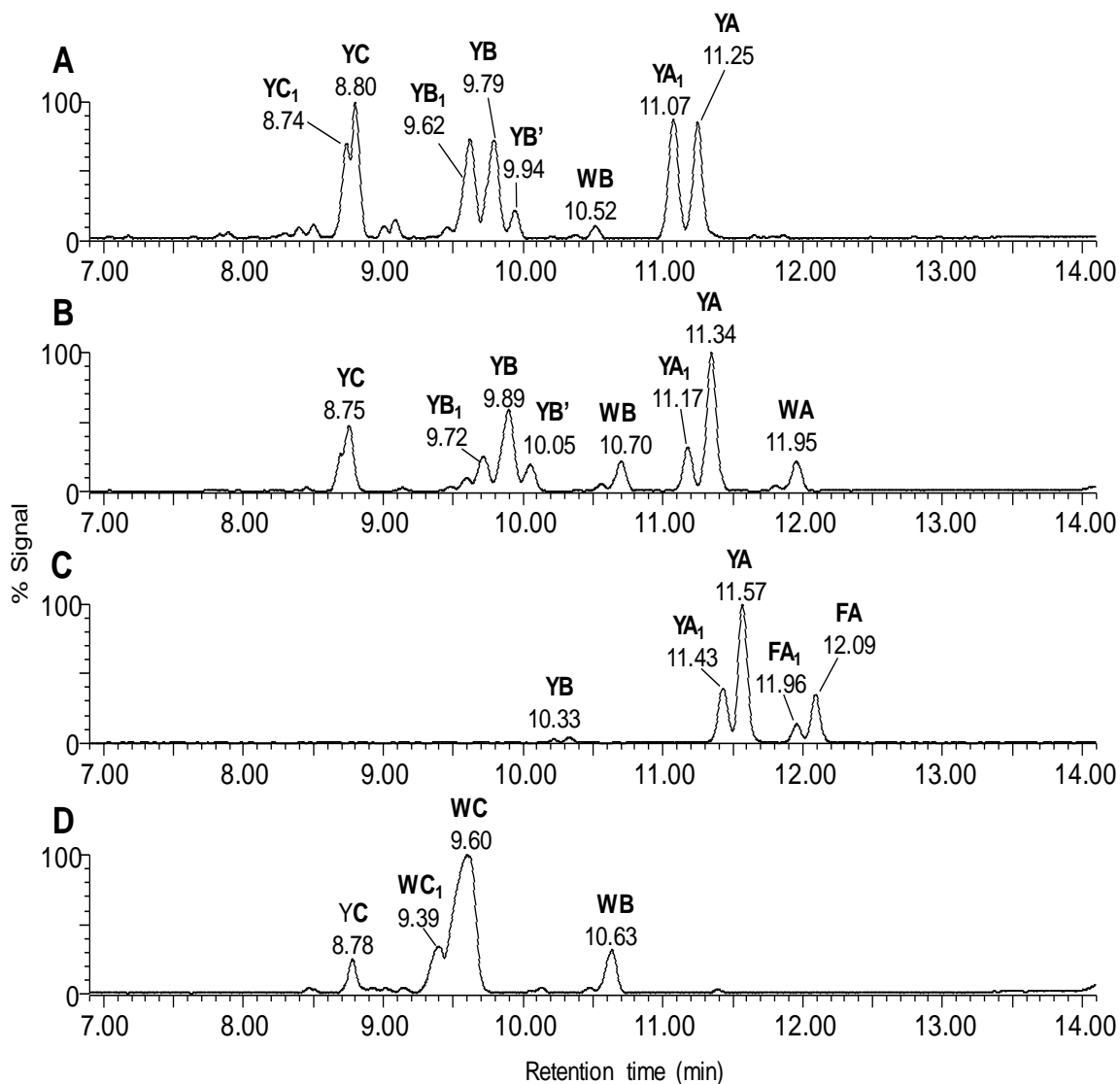


Figure 2.1: UPLC-MS chromatograms showing the composition of the crude peptide mixtures extracted from cultures of *Br. parabrevis*.

A) Tyrocidine mixture (Tmix) purified from commercial tyrothricin complex.

B) Crude extracts from the non-supplemented cultures.

C) Crude extracts from the cultures supplemented with 22 mM phenylalanine.

D) Crude extracts from the cultures supplemented with 16.5 mM tryptophan.

The letters Y, W and F denote the tyrocidine, tryptocidine and phenicydine analogues respectively, which differ in the aromatic amino acid residue at position 7. The letters A, B and C denote the A, B and C analogues respectively which differ in their content of aromatic residues at the 3rd and 4th positions. The subscript 1 is used to denote the Lys containing analogues.

Table 2.4: Comparative analysis of the peptide content of crude culture extracts, commercial tyrocidine mixture and the tyrothricin extract reported by Tang *et al.* [4]

Peptide Identity	% Abundance ^a			Commercial tyrocidine mixture ^b	Tang <i>et al.</i> (1992)
	Non-supplemented culture	22 mM Phe supplemented	16.5 mM Trp supplemented		
Tyrocidine C ₁	4.0			11.0	4.8
Tyrocidine C	11.3		6.2	14.5	16.0
Tryptocidine C ₁	<1		13.2	<1	<1
Tryptocidine C	2.4		66.4	1.1	3.7
Tyrocidine B ₁	7.4	1.0		15.2	7.0
Tyrocidine B	19.3	1.8		15.2	17.4
Tyrocidine B'	5.4			3.6	2.2
Tryptocidine B ₁	1.2			<1	2.1
Tryptocidine B	5.8		9.9	1.5	4.1
Tyrocidine A ₁	7.8	22.0		16.1	6.2
Tyrocidine A	26.0	51.0		16.1	14.0
Tryptocidine A ₁	1.0			<1	
Tryptocidine A	6.0			<1	2.4
Phenycidine A ₁		6.7			
Phenycidine A		17.5			<1
Val-Gramicidin A	<1		1.7		7.0

^a % Relative abundance was determined by expressing the peak area of each peptide as a percentage of the sum of the peak areas of all peptides present in the extract. It was assumed that the response factors of all peptides are similar due to their analogous structures.

^b The commercial tyrocidine mixture consists of only the tyrocidine containing fraction of the commercial tyrothricin complex.

Purification of single peptides by semi-preparative RP-HPLC

The goal was to purify the major tyrocidines (A, B and C) from the crude extract obtained from the non-supplemented culture. From the first round of semi-preparative HPLC purification, ten fractions were collected (Figure 2.2) and analysed by UPLC-MS to determine identity and purity. Only those fractions with a purity of 60% and/or greater in respect of the targeted single peptides were selected for a second round of purification. The selected fractions were fraction 3 (tyrocidine C), 5 and 6 (tyrocidine B) and 8 and 9 (tyrocidine A) (summarised in Table 2.5).

The first round of semi-preparative RP-HPLC purification of the crude extract from the Phe-supplemented culture yielded ten fractions (Figure 2.3). From these, only fractions 7 to 9 had

purities greater than 70% according to UPLC-MS analyses with respect to tyrocidine A and phenycidine A, and were subjected to a second round of purification. Fractions 7 and 8 contained tyrocidine A and A₁ while fraction 9 contained tyrocidine A and phenycidine A (Table 2.5). However, the phenycidine-containing fraction was not taken into the second round of purification because of low yield.

Seven fractions were collected from the semi-preparative RP-HPLC purification of the crude extract from the Trp-supplemented cultures (Figure 2.4). The peptides of interest from this extract were tryptocidine C and tyrocidine C. Tryptocidine C was present in fractions 5 and 6 at purities of greater than 90% according to UPLC-MS analyses (Table 2.5). As such, there was no need for an additional round of purification. The tyrocidine C containing fraction (fraction 3) was subjected to a second round of purification since its purity was below 90%.

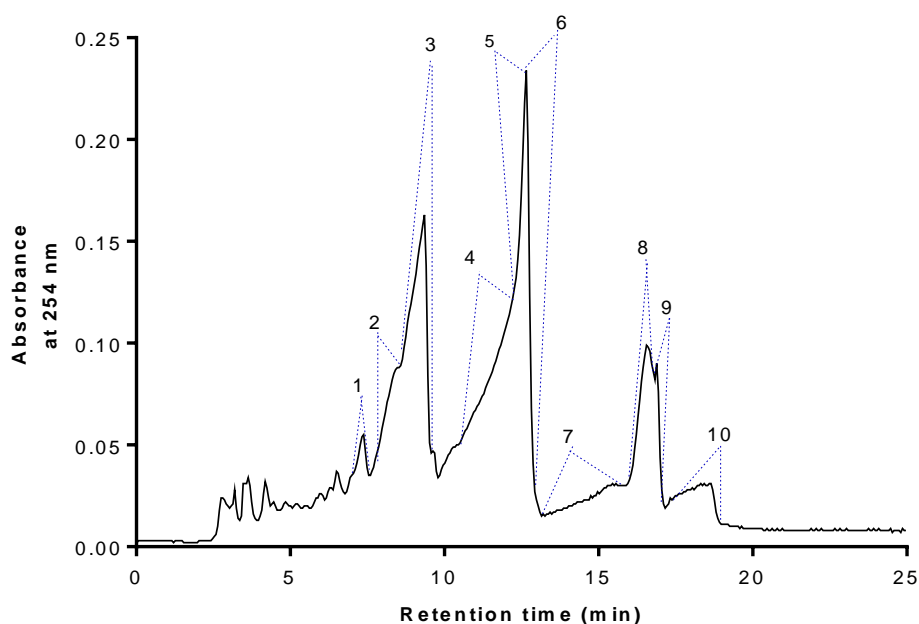


Figure 2.2: Chromatogram showing the semi-preparative RP-HPLC purification of individual peptides from the crude mixture extracted from the non-supplemented cultures of *Br. parabrevis*. The numbers 1-10 denote the fractions that were collected during purification.

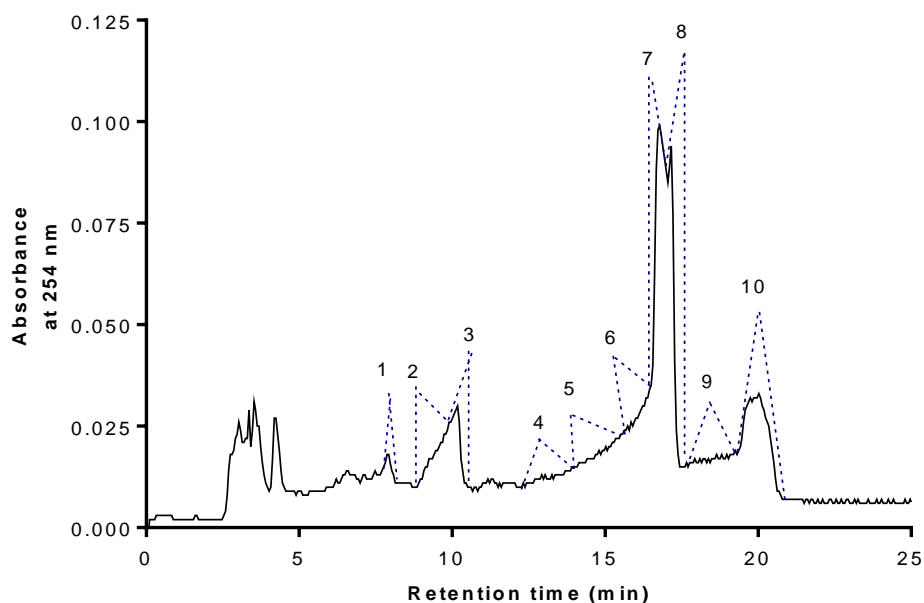


Figure 2.3: Chromatogram showing the semi-preparative RP-HPLC purification of individual peptides from the crude mixture extracted from the cultures of *Br. parabrevis* supplemented with 22 mM phenylalanine. The numbers 1-10 denote the fractions that were collected during purification.

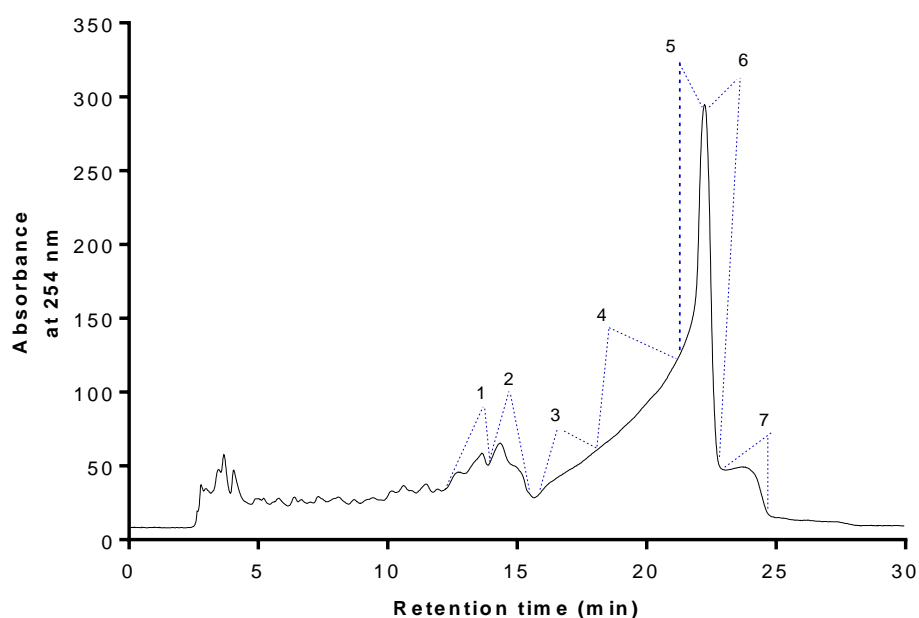


Figure 2.4: Chromatogram showing the semi-preparative RP-HPLC purification of individual peptides from the crude mixture extracted from the cultures of *Br. parabrevis* supplemented with 16.5 mM tryptophan. The numbers 1-7 denote the fractions that were collected in this round of purification.

Table 2.5: Summary of the peptide composition of each of the fractions collected during semi-preparative HPLC purification of the three culture extracts.

Origin of crude extract	RP-HPLC fraction	Peptide composition ^a
Non-supplemented culture	1	13 YC, 32 YC ₁
	2	48 YC, 52 YC ₁
	3	63 YC, 25 YC ₁
	4	40 YB, 31 YB ₁ , 26 YB ₁ '
	5	63 YB, 20 YB', 18 YB ₁
	6	66 YB, 21 WC, 6 WC ₁
	7	56 YA, 39 YA ₁
	8	75 YA, 22 YA ₁ , 2 WB
	9	76 YA, 3 YA ₁ , 18 WB
	10	ND ^b
22 mM Phe-supplemented	1*	YB
	2	ND ^b
	3	ND ^b
	4*	YA, YA ₁
	5	64 YA, 30 YA ₁
	6	58 YA, 40 YA ₁
	7	85 YA, 15 YA ₁
	8	83 YA, 2 YA ₁ , 10 FA
	9	18 YA, 78 FA
	10*	FA, WA
16.5 mM Trp-supplemented	1	68 YC, 14 YC ₁ , 4 WC ₁
	2*	YC, VGA
	3*	WC, WC ₁
	4	73 WC, 27 WC ₁
	5	92 WC, 8 WC ₁
	6	90 WC, 6 WC ₁ , 2 WB
	7*	WB

^a Peptide composition is expressed as a percentage contribution (number before peptide abbreviation) and was determined via UPLC-MS analysis. The letters Y, W and F denote the tyrocidine, tryptocidine and phenylicidine analogues respectively, which differ in the aromatic amino acid residue at position 7. The letters A, B and C denote the A, B and C analogues respectively which differ in their content of aromatic residues at the 3rd and 4th positions. The subscript 1 is used to denote the Lys containing analogues.

^b ND – not determined. Fractions were not analysed due to low yields obtained during purification.

* These fractions were analysed by ESMS alone and not subjected to UPLC-MS due to their low peptide content, therefore the percentage peptide composition was not ascertained.

UPLC-MS analysis of purified single peptides

Following one or two rounds of semi-preparative HPLC purification, UPLC-MS analyses were carried out to determine the success of the purification steps. The final UPLC-MS analyses of the four peptides that were selected for this study, YA, YB, YC and WC are represented in Figures 2.5-2.8.

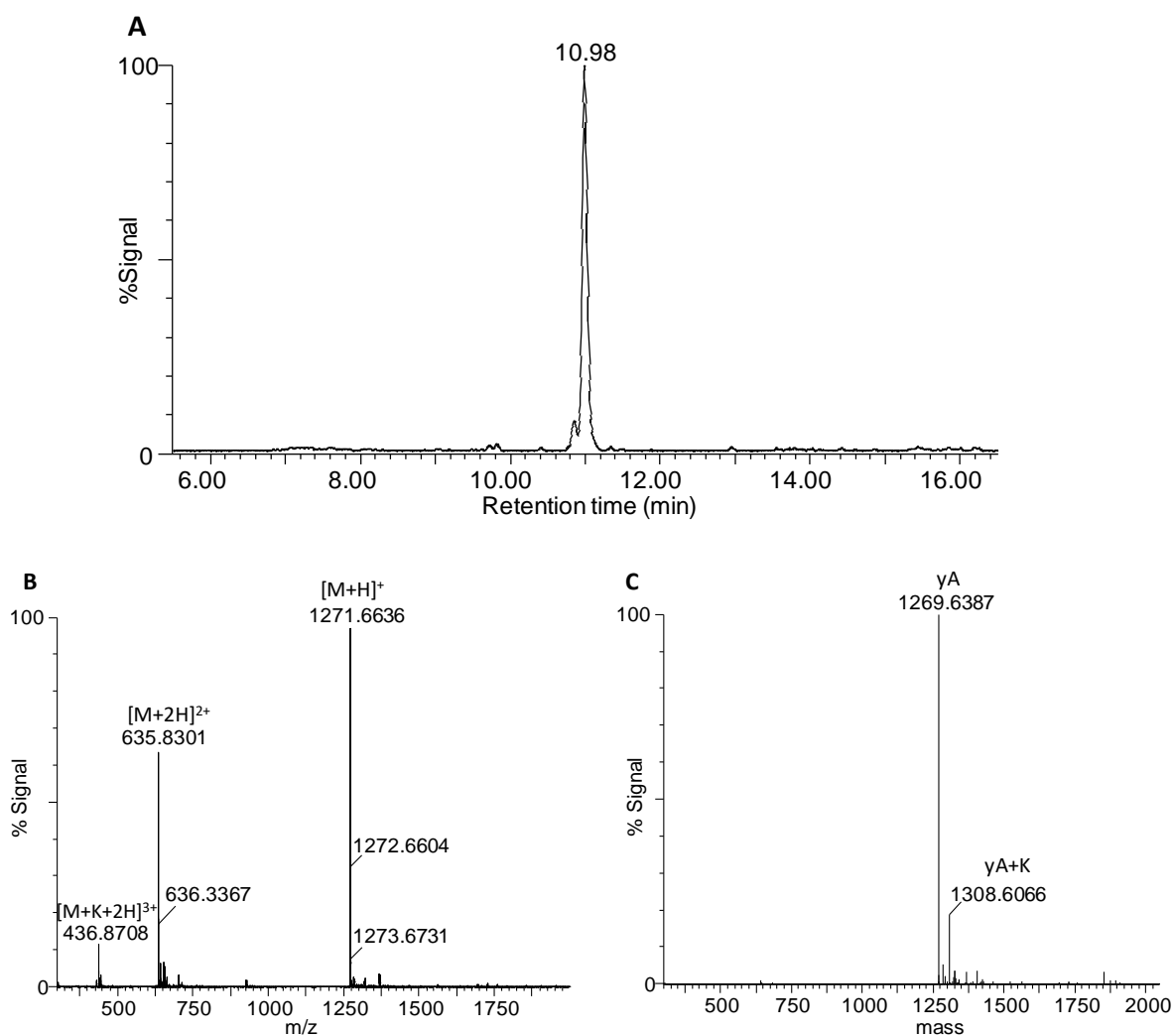


Figure 2.5: UPLC-MS analysis of the purified tyrocidine A (YA).

A) UPLC chromatogram of the purified tyrocidine A (200 $\mu\text{g/mL}$; 5 μL injection volume) indicating an elution time of 10.98 minutes.

B) ESMS positive ion spectrum of the elution peak of tyrocidine A indicating the singly charged molecular ions $[M+H]^+$, doubly charged molecular ions $[M+2H]^{2+}$ and triply charged molecular ions $[M+K+2H]^{3+}$.

C) The MaxEnt 3 generated ESMS mass spectrum of tyrocidine A depicting the experimental monoisotopic molecular mass.

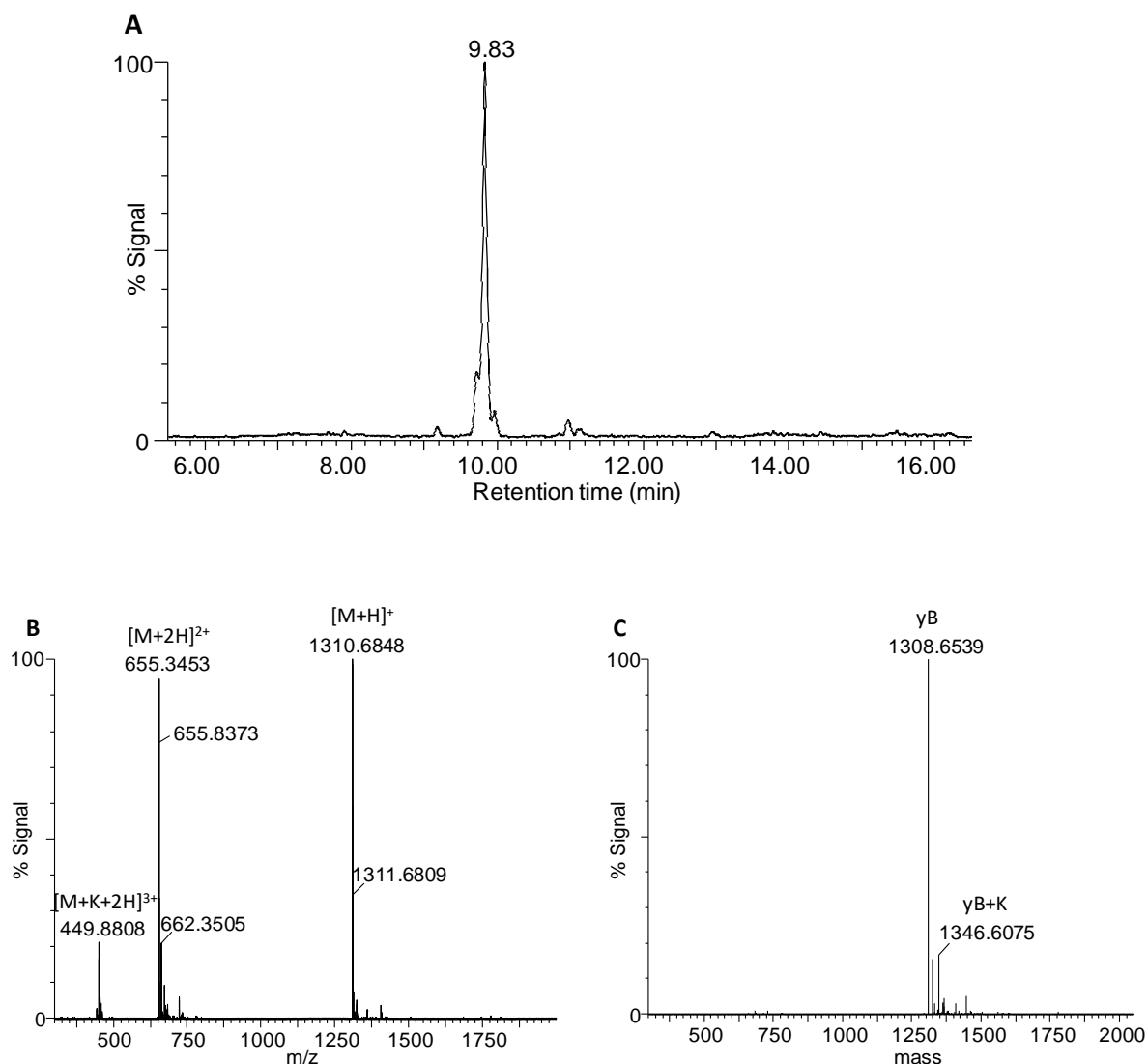


Figure 2.6: UPLC-MS analysis of the purified tyrocidine B (YB).

A) UPLC chromatogram of the purified tyrocidine B (200 $\mu\text{g/mL}$; 5 μL injection volume) indicating an elution time of 9.83 minutes.

B) ESMS positive ion spectrum of the elution peaks of tyrocidine B, B₁ and B' indicating the singly charged molecular ions $[\text{M}+\text{H}]^+$, doubly charged molecular ions $[\text{M}+2\text{H}]^{2+}$ and triply charged molecular ions $[\text{M}+\text{K}+2\text{H}]^{3+}$.

C) The MaxEnt 3 generated ESMS mass spectrum of tyrocidine B/B₁ complex depicting the experimental monoisotopic molecular masses.

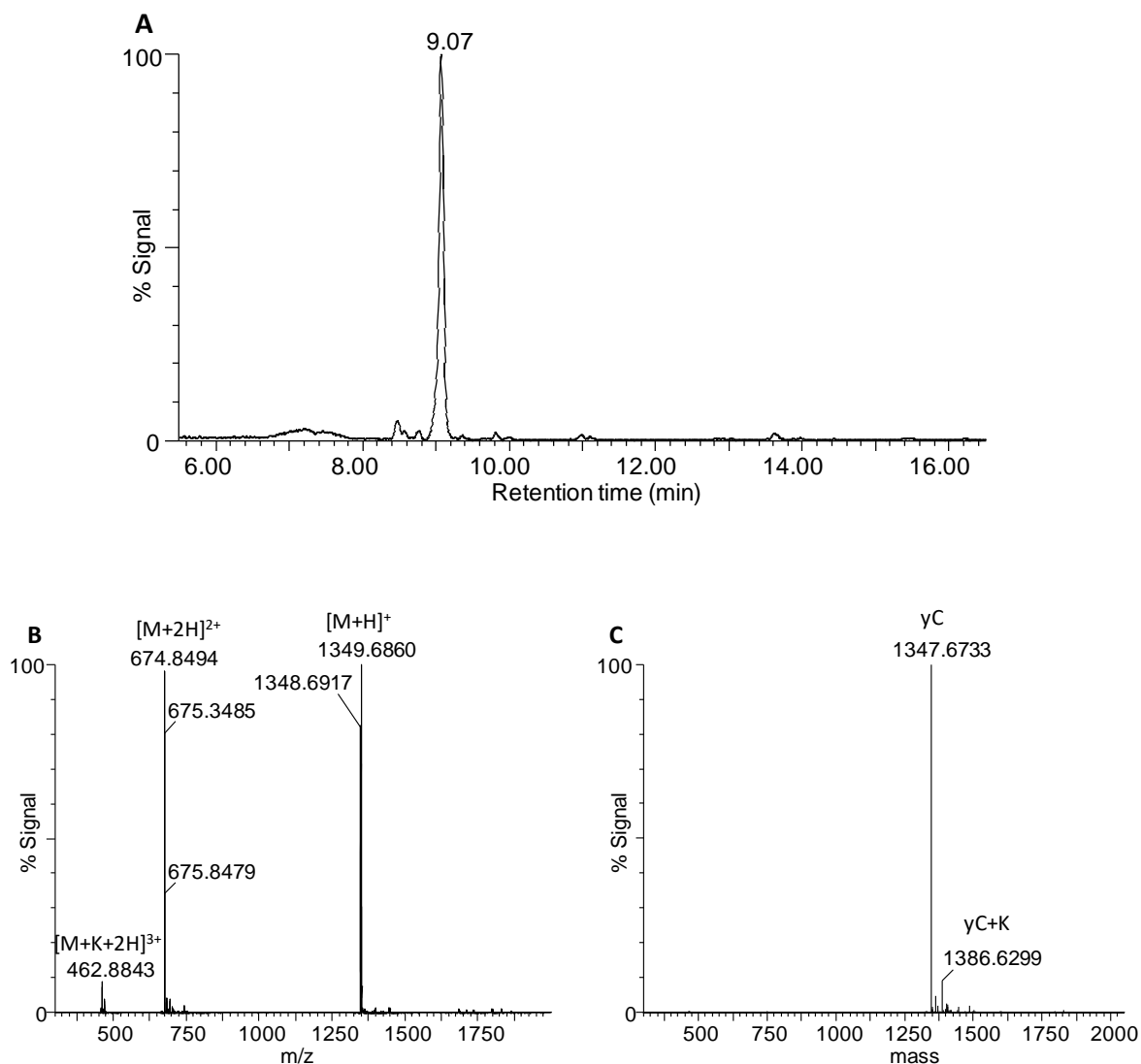


Figure 2.7: UPLC-MS analysis of the purified tyrocidine C (YC).

A) UPLC chromatogram of the purified tyrocidine C (200 $\mu\text{g/mL}$; 5 μL injection volume) indicating an elution time of 9.07 minutes.

B) ESMS positive ion spectrum of the elution peak of tyrocidine C indicating the singly charged molecular ions $[\text{M}+\text{H}]^+$, doubly charged molecular ions $[\text{M}+2\text{H}]^{2+}$ and triply charged molecular ions $[\text{M}+\text{K}+2\text{H}]^{3+}$.

C) The MaxEnt 3 generated ESMS mass spectrum of tyrocidine A depicting the experimental monoisotopic molecular mass.

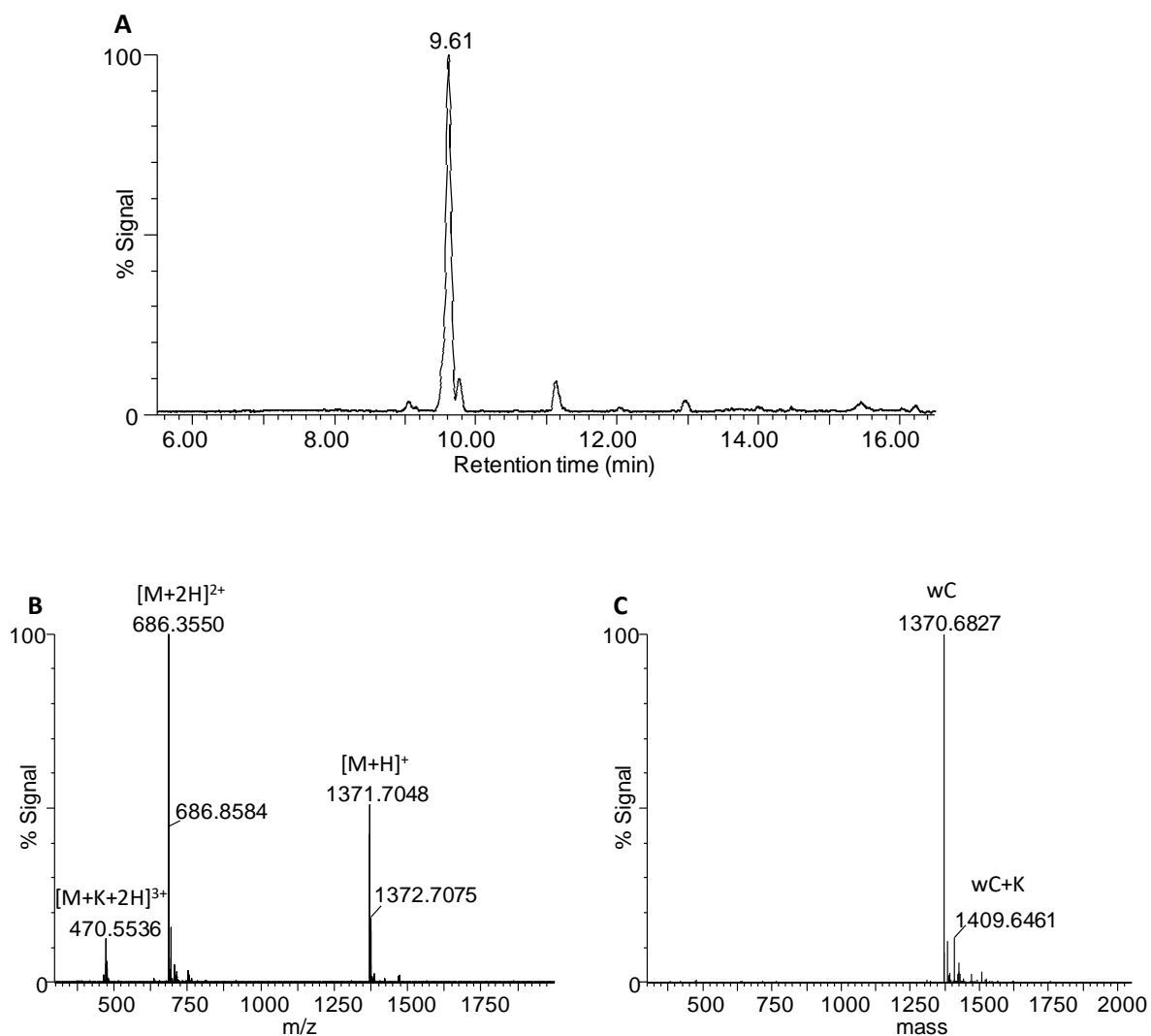


Figure 2.8: UPLC-MS analysis of the purified tryptocidine C (WC).

A) UPLC chromatogram of the purified tryptocidine C (200 $\mu\text{g/mL}$; 5 μL injection volume) indicating an elution time of 9.61 minutes.

B) ESMS positive ion spectrum of the elution peak of tryptocidine C indicating the singly charged molecular ions $[M+H]^+$, doubly charged molecular ions $[M+2H]^{2+}$ and triply charged molecular ions $[M+K+2H]^{3+}$.

C) The MaxEnt 3 generated ESMS mass spectrum of tryptocidine C depicting the experimental monoisotopic molecular mass.

Overall, purification of the tyrocidines and analogues from crude culture extracts was successful. Three out of the four purified peptides attained purities greater than 90% with respect to the single peptide. Only tyrocidine B could not be purified to over 90% due to the presence of the tyrocidine B₁. The two peptides are highly similar in their amino acid sequences differing only by a single amino acid substitution of Orn to Lys in tyrocidine B₁. Ultimately, a single methylene (CH₂) group differentiates the two peptides. This renders their separation on a semi-preparative column difficult often necessitating the use of an analytical HPLC column and reduction in the loading concentrations [16,20,21].

Based on the observed retention times, order of retention of the four peptides on the UPLC column was consistent with literature [16,17,20–22]. Tyrocidine A was retained the longest followed by tyrocidine B, tryptocidine C and tyrocidine C, respectively. These differences in the retention times are indicative of the different hydrophobic properties of the tyrocidines and analogues imposed by the variable positions in the amino acid sequence. The three tyrocidines (YA, YB and YC) differ from each other at positions three and four which comprise the aromatic dipeptide moiety. YA contains only Phe residues (Ff), while YC contains only Trp residues (Ww). YB contains both Trp and Phe (Wf). The hydrophobicities of the three aromatic amino acids follows the trend F>W>Y on the hydrophobic scale [23]. Based on this, YC is relatively polar in comparison to the other two analogues hence a shorter retention time. YA is relatively more hydrophobic and is thus retained the longest on the UPLC column. Tryptocidine C (WC) differs from YC at position seven where it contains a Trp residue in place of Tyr. Because Trp is relatively more hydrophobic than Tyr [23], the retention time of WC is greater than that of YC.

Mass spectrometric analyses revealed that all four peptides form singly, doubly and triply charged ion species. The ions carrying the single and double charges are derived from the single and double protonation of the peptide. On the other hand, the ionic species carrying the triple charge contain two protons and a potassium ion. The relative abundances of the three ionic species on the mass spectra highlights the differential ionisation pattern amongst the four peptides. All peptides exhibited relatively low tendencies to carry triple charges. However, YA appears to carry a single charge more readily than it does a double charge while WC readily carries a double charge over a single charge. The abundances of the singly and doubly charged ionic species on the mass spectra of YB and YC appeared to be relatively equal. The MaxEnt 3 mathematic algorithm in the Masslynx Software was used to calculate the monoisotopic masses of the peptides thereby confirming the identity of the peptides. This mass was then compared to the theoretical

monoisotopic masses of the peptides to determine mass accuracy (Table 2.6). The mass error for all peptides was generally found to be less 15 ppm which indicated that the correct peptides were isolated and that they were chemically intact. It is specifically important to determine the chemical integrity of the peptides as our research group found that the tyrocidines tend to get deaminated at the Asn and/or Gln residues and, in some instances, are oxidised at the aromatic residues

Table 2.6: Summary of the characterisation of the tyrocidines and analogues purified for use in this study

Peptide identity (Abbreviation)	Source culture	Experimental M_r (Theoretical M_r) ^a	Mass accuracy (ppm)	UPLC Retention time (min)	UPLC- MS % Purity ^b
Tyrocidine A (YA)	Non-supplemented/ 22 mM Phe supplemented	1269.6387 (1269.6546)	13.8	10.98	93
Tyrocidine B/B₁ (YB/YB1)	Non-supplemented	1308. 6539/1322.6812 (1308.6655/1322.6610)	8.9/ -15.3	9.83	97 (85/12)
Tyrocidine C (YC)	Non-supplemented/ 16.5 mM Trp supplemented	1347.6733 (1347.6764)	2.3	9.07	97
Tryptocidine C (WC)	16.5 mM Trp supplemented	1370.6827 (1370.6924)	7.1	9.61	90

^aExperimental monoisotopic mass was determined by ESMS whereas theoretical monoisotopic mass was calculated by summing the monoisotopic masses of the constituent amino acids of each peptide.

^b% Purity was calculated by expressing the peak area of the peptide's elution peak as a percentage of total of the peak areas of all the peaks integrated on the chromatogram.

Part two: Chemical characterisation of the synthetic hexapeptides

Because the RW-synthetic hexapeptides were sourced from elsewhere, it was necessary to confirm their identity and state of purity as well as determine their chemical characteristics. This was done by ESMS and UPLC-MS analyses which are represented in Figures 2.9-2.23.

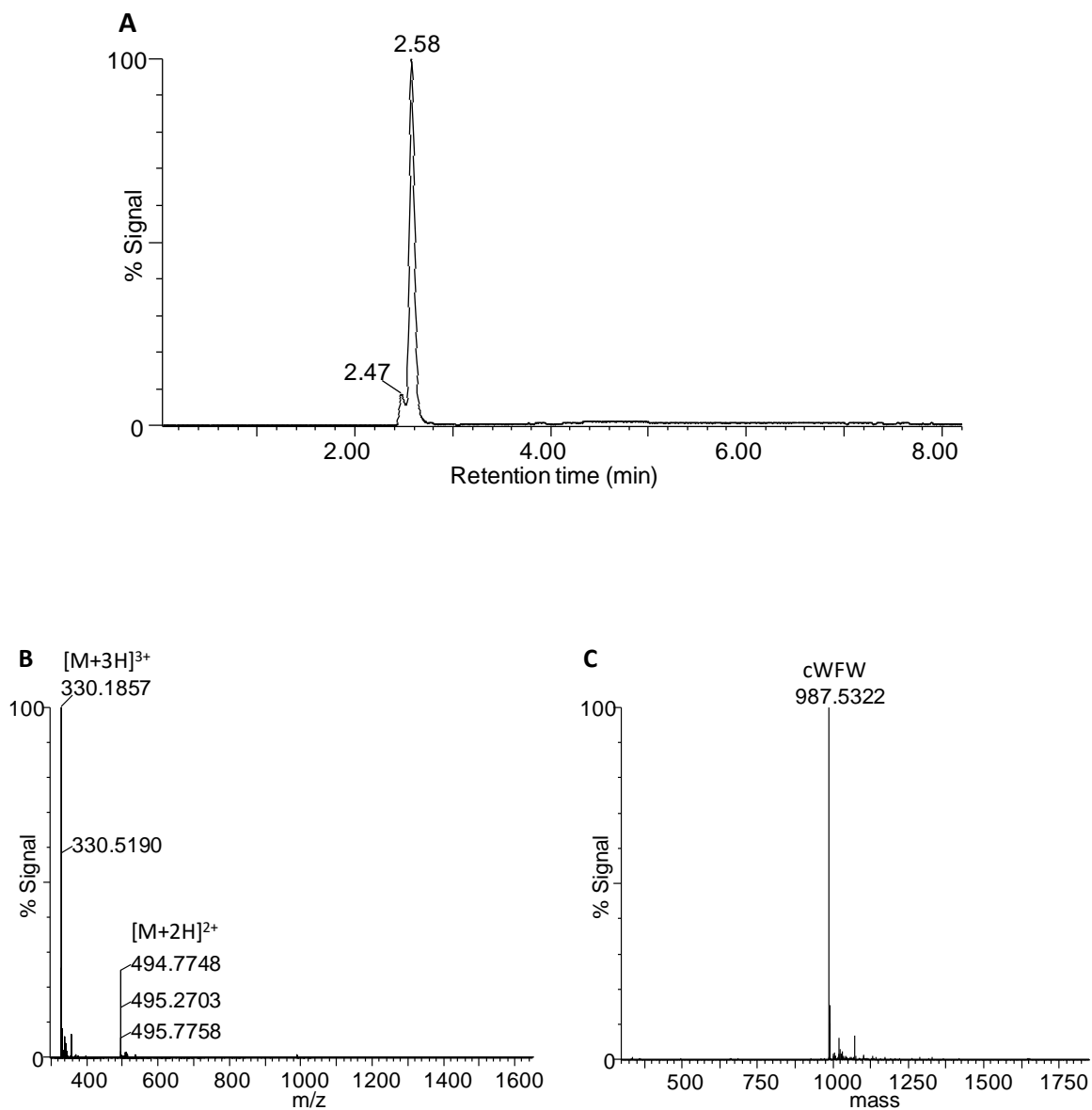


Figure 2.9: UPLC-MS analysis of cWFW.

A) UPLC chromatogram of cWFW (200 $\mu\text{g/mL}$; 5 μL injection volume) indicating an elution time of 2.58 minutes.

B) ESMS positive ion spectrum of the elution peak of cWFW indicating the doubly charged molecular ions $[\text{M}+2\text{H}]^{2+}$ and triply charged molecular ions $[\text{M}+3\text{H}]^{3+}$.

C) The MaxEnt 3 generated ESMS mass spectrum of cWFW depicting the experimental monoisotopic molecular mass.

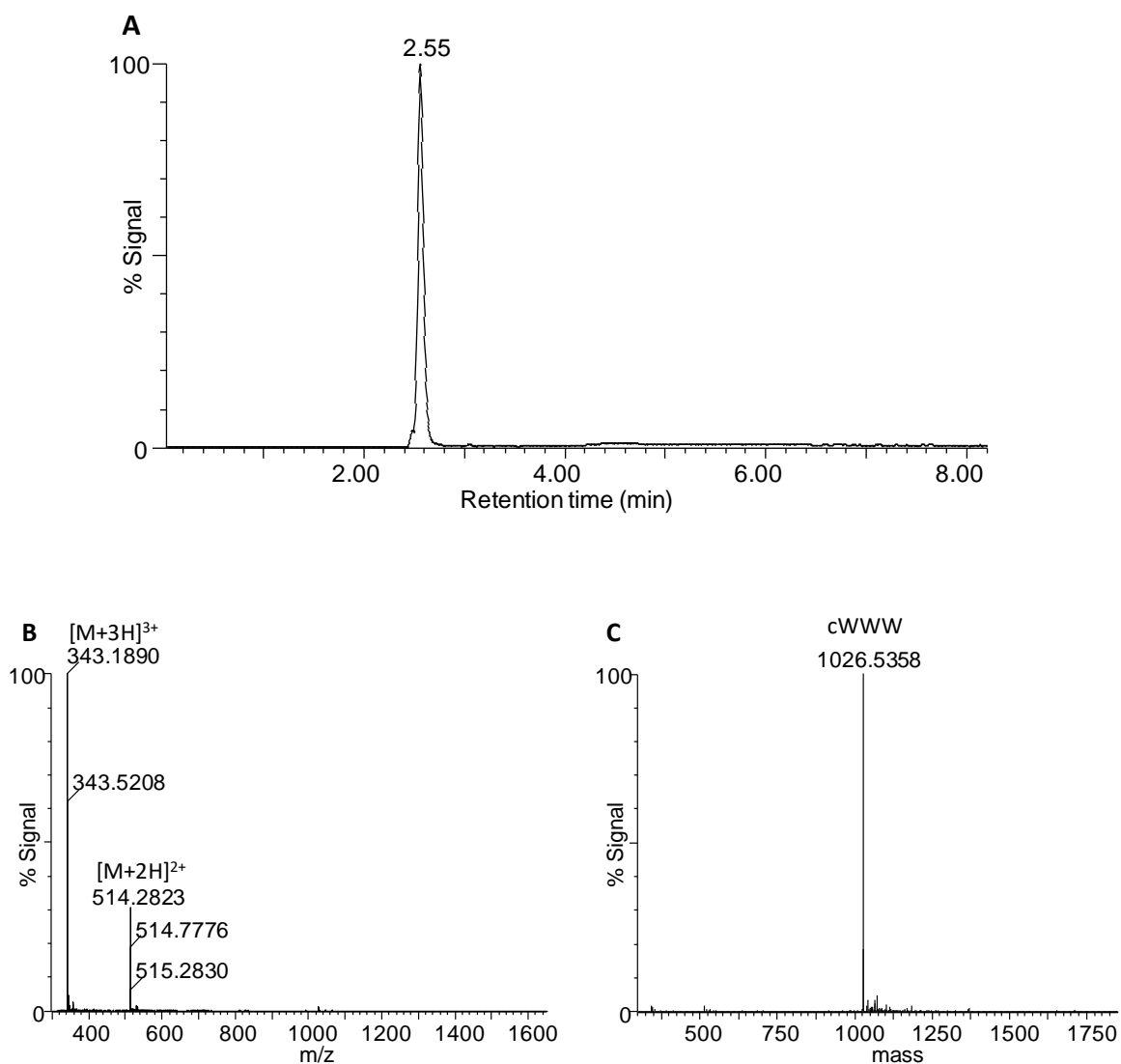


Figure 2.10: UPLC-MS analysis of *cWWW1*, a preparation from the *Dathe* group.

A) UPLC chromatogram of *cWWW* (200 $\mu\text{g/mL}$; 5 μL injection volume) indicating an elution time of 2.55 minutes.

B) ESMS positive ion spectrum of the elution peak of *cWWW* indicating the doubly charged molecular ions $[\text{M}+2\text{H}]^{2+}$ and triply charged molecular ions $[\text{M}+3\text{H}]^{3+}$.

C) The MaxEnt3 generated ESMS mass spectrum of *cWWW* depicting the experimental monoisotopic molecular mass.

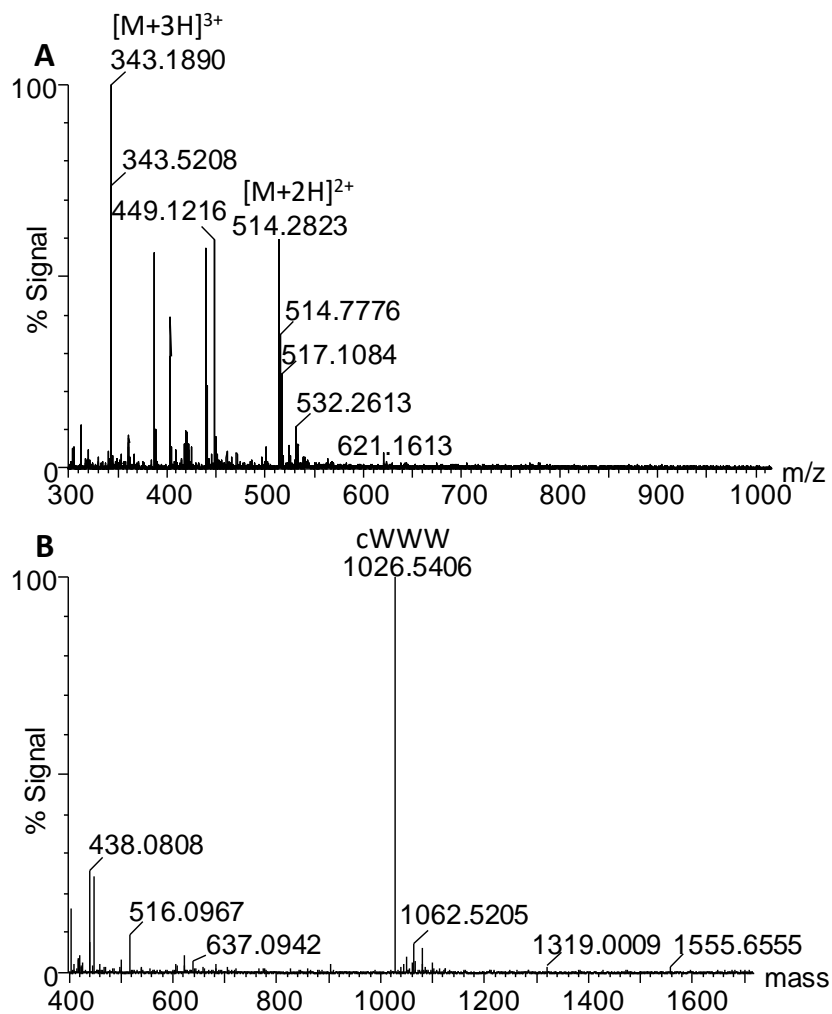


Figure 2.11: ESMS analysis of *cWWW2*, a preparation from *GL Biochem*.

A) ESMS positive ion spectrum of the elution peak of *cWWW* indicating the doubly charged molecular ions $[M+2H]^{2+}$, the triply charged molecular ions $[M+3H]^{3+}$ and contaminating ions. B) The MaxEnt3 generated ESMS mass spectrum of *cWWW* depicting the experimental monoisotopic molecular mass as well as the monoisotopic molecular masses of contaminants.

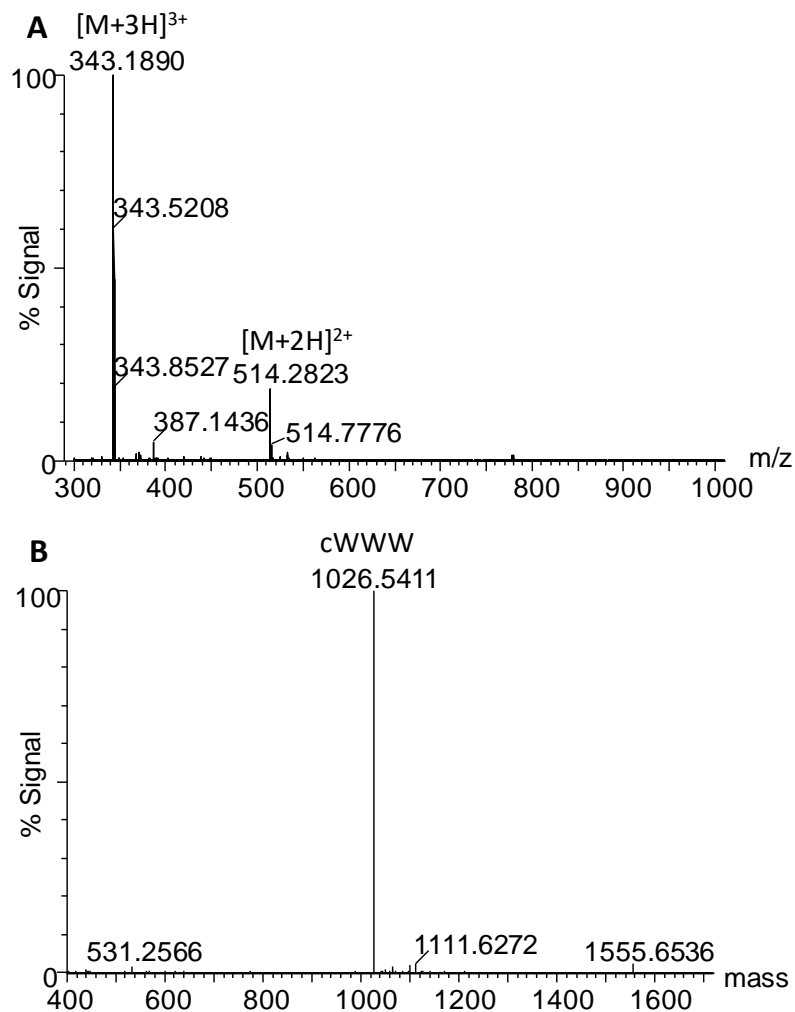


Figure 2.12: ESMS analysis of *cWWW3*, a preparation from *GL Biochem*.

A) ESMS positive ion spectrum of the elution peak of *cWWW* indicating the doubly charged molecular ions $[M+2H]^{2+}$, triply charged molecular ions $[M+3H]^{3+}$ and contaminating ions.

B) The MaxEnt 3 generated ESMS mass spectrum of *cWWW* depicting the experimental monoisotopic molecular mass as well as the monoisotopic molecular masses of contaminants.

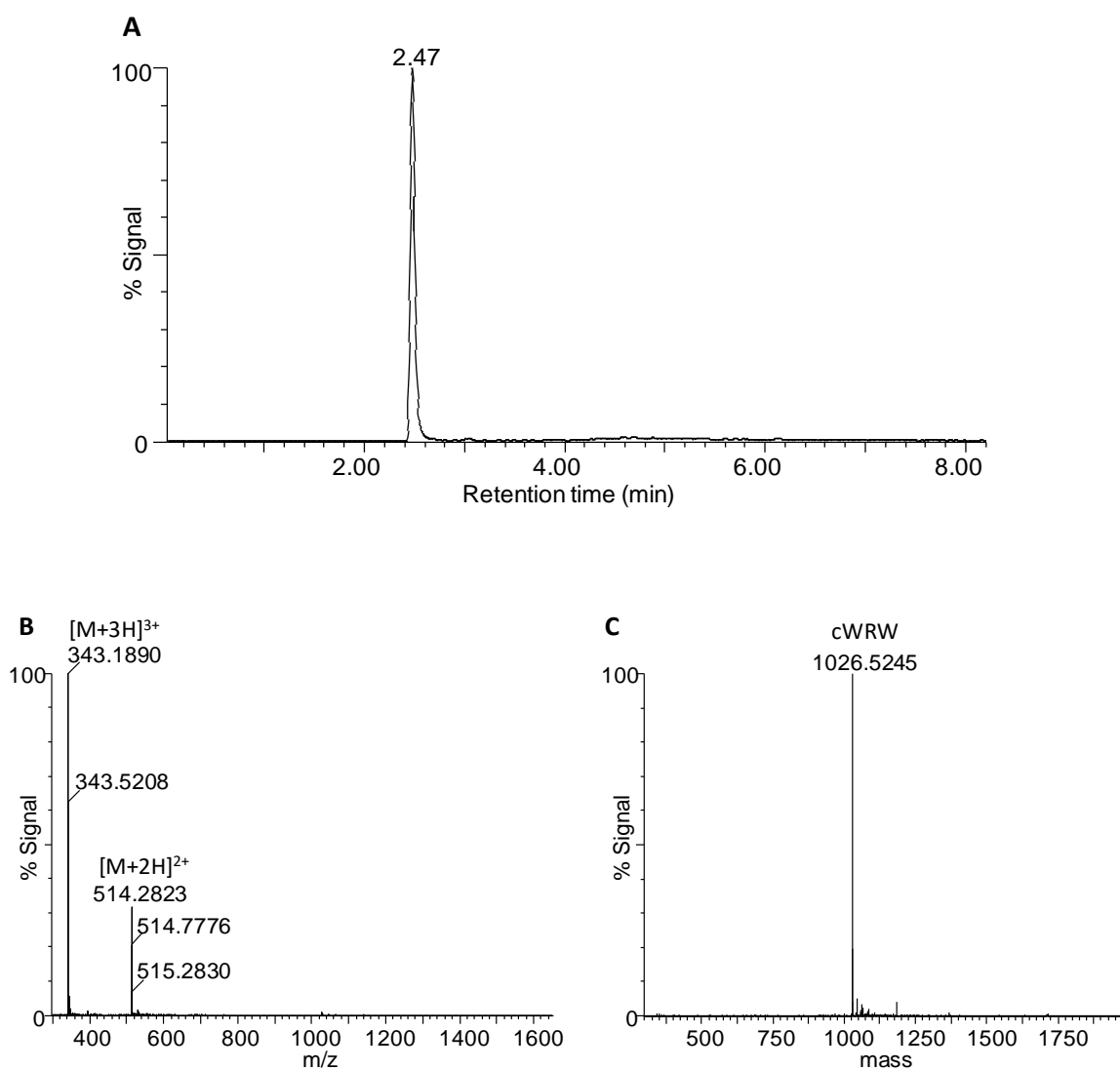


Figure 2.13: UPLC-MS analysis of *cWRW1*, a preparation from the *Dathe* group.

A) UPLC chromatogram of *cWRW* (200 $\mu\text{g/mL}$; 5 μL injection volume) indicating an elution time of 2.47 minutes.

B) ESMS positive ion spectrum of the elution peak of *cWRW* indicating the doubly charged molecular ions $[\text{M}+2\text{H}]^{2+}$ and triply charged molecular ions $[\text{M}+3\text{H}]^{3+}$.

C) The MaxEnt 3 generated ESMS mass spectrum of *cWRW* depicting the experimental monoisotopic molecular mass.

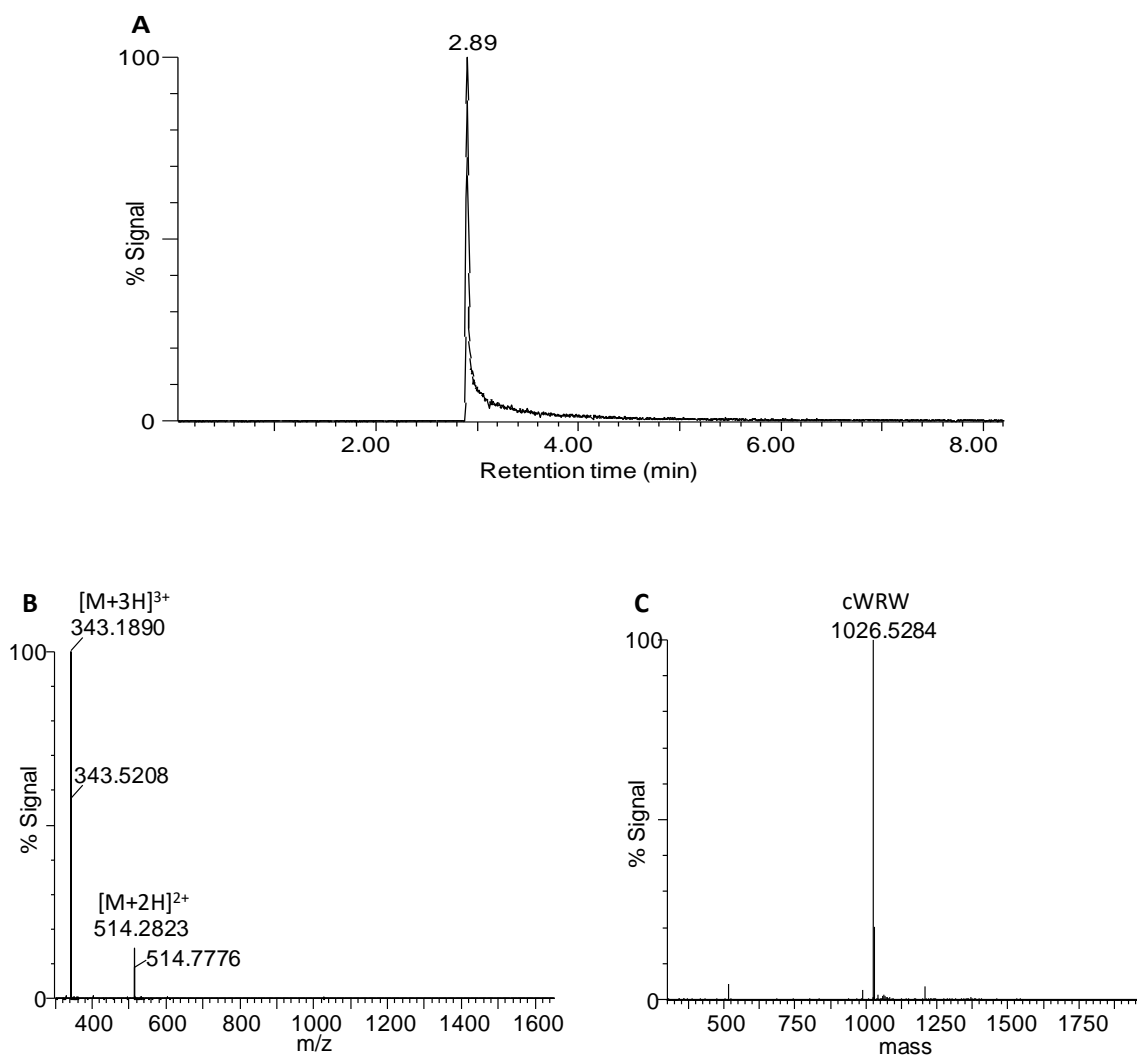


Figure 2.14: UPLC-MS analysis of cWRW2, a preparation from GL Biochem.

A) UPLC chromatogram of cWRW (200 $\mu\text{g/mL}$; 5 μL injection volume) indicating an elution time of 2.89 minutes.

B) ESMS positive ion spectrum of the elution peak of cWRW indicating the doubly charged molecular ions $[M+2H]^{2+}$ and triply charged molecular ions $[M+3H]^{3+}$.

C) The MaxEnt 3 generated ESMS mass spectrum of cWRW depicting the experimental monoisotopic molecular mass.

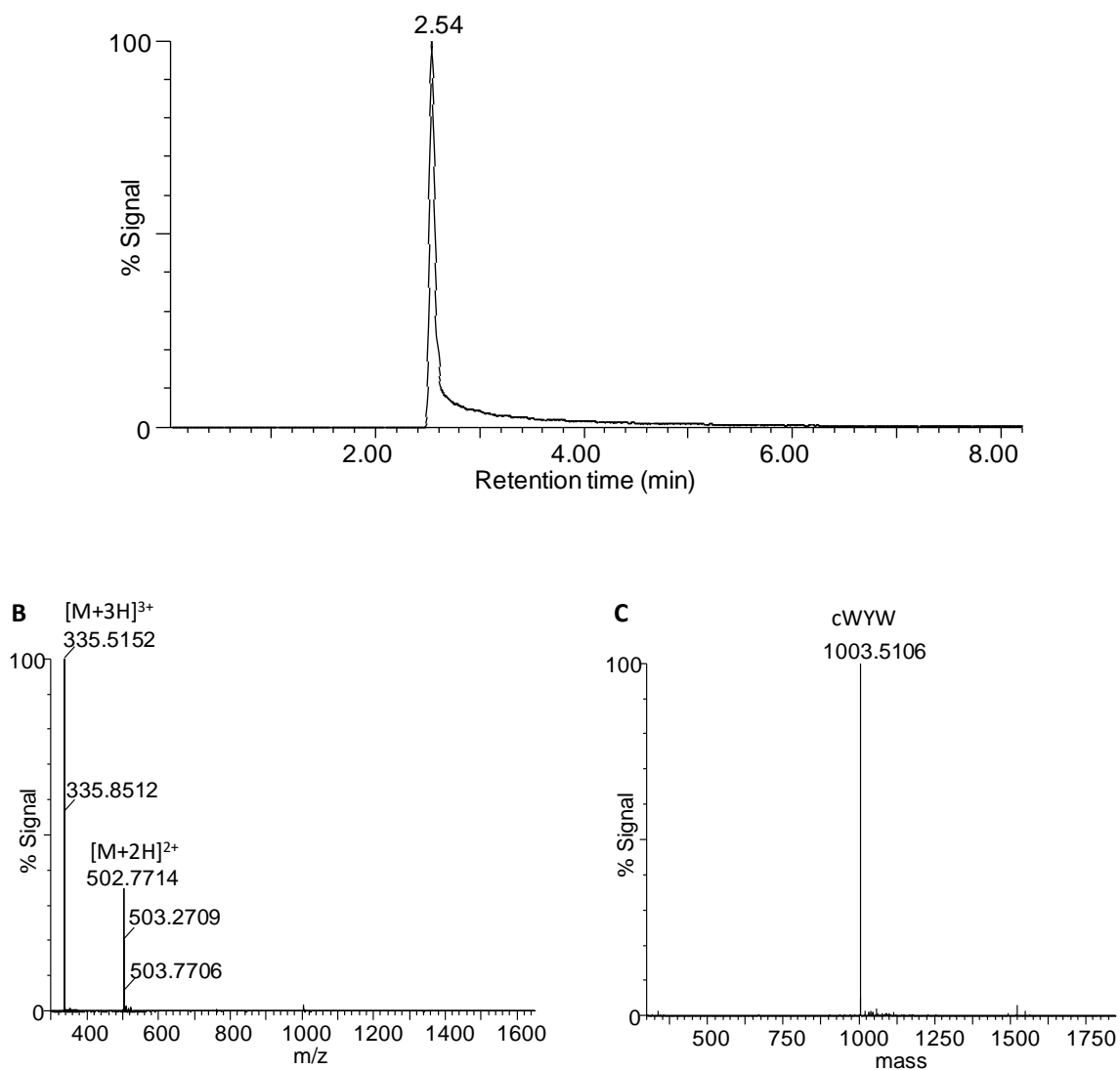


Figure 2.15: UPLC-MS analysis of cWYW.

A) UPLC chromatogram of cWYW (200 $\mu\text{g/mL}$; 5 μL injection volume) indicating an elution time of 2.54 minutes.

B) ESMS positive ion spectrum of the elution peak of cWYW indicating the doubly charged molecular ions $[M+2H]^{2+}$ and triply charged molecular ions $[M+3H]^{3+}$.

C) The MaxEnt 3 generated ESMS mass spectrum of cWYW depicting the experimental monoisotopic molecular mass.

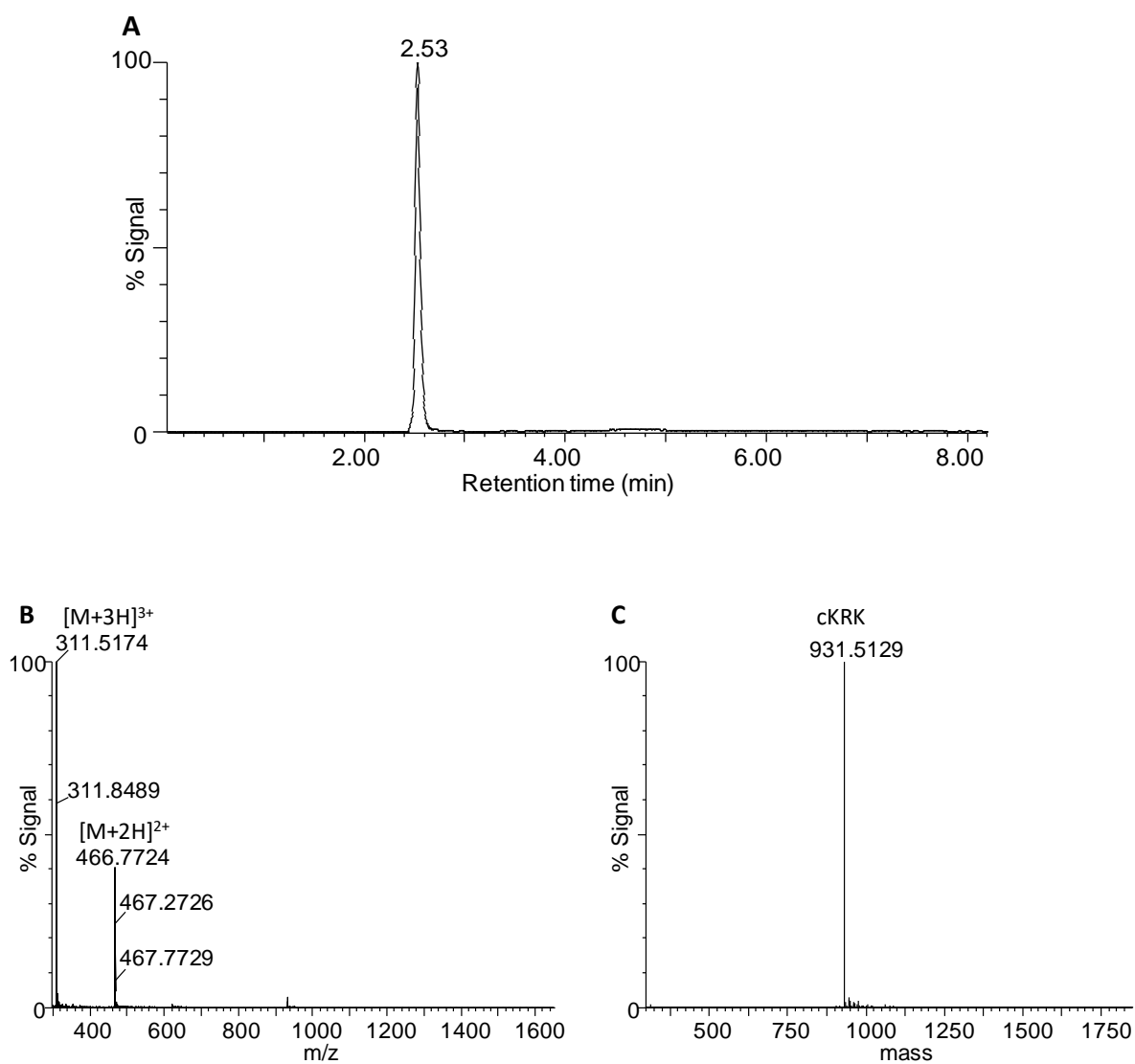


Figure 2.16: UPLC-MS analysis of *cKRK*.

A) UPLC chromatogram of *cKRK* (200 $\mu\text{g/mL}$; 5 μL injection volume) indicating an elution time of 2.53 minutes.

B) ESMS positive ion spectrum of the elution peak of *cKRK* indicating the doubly charged molecular ions $[\text{M}+2\text{H}]^{2+}$ and triply charged molecular ions $[\text{M}+3\text{H}]^{3+}$.

C) The MaxEnt 3 generated ESMS mass spectrum of *cKRK* depicting the experimental monoisotopic molecular mass.

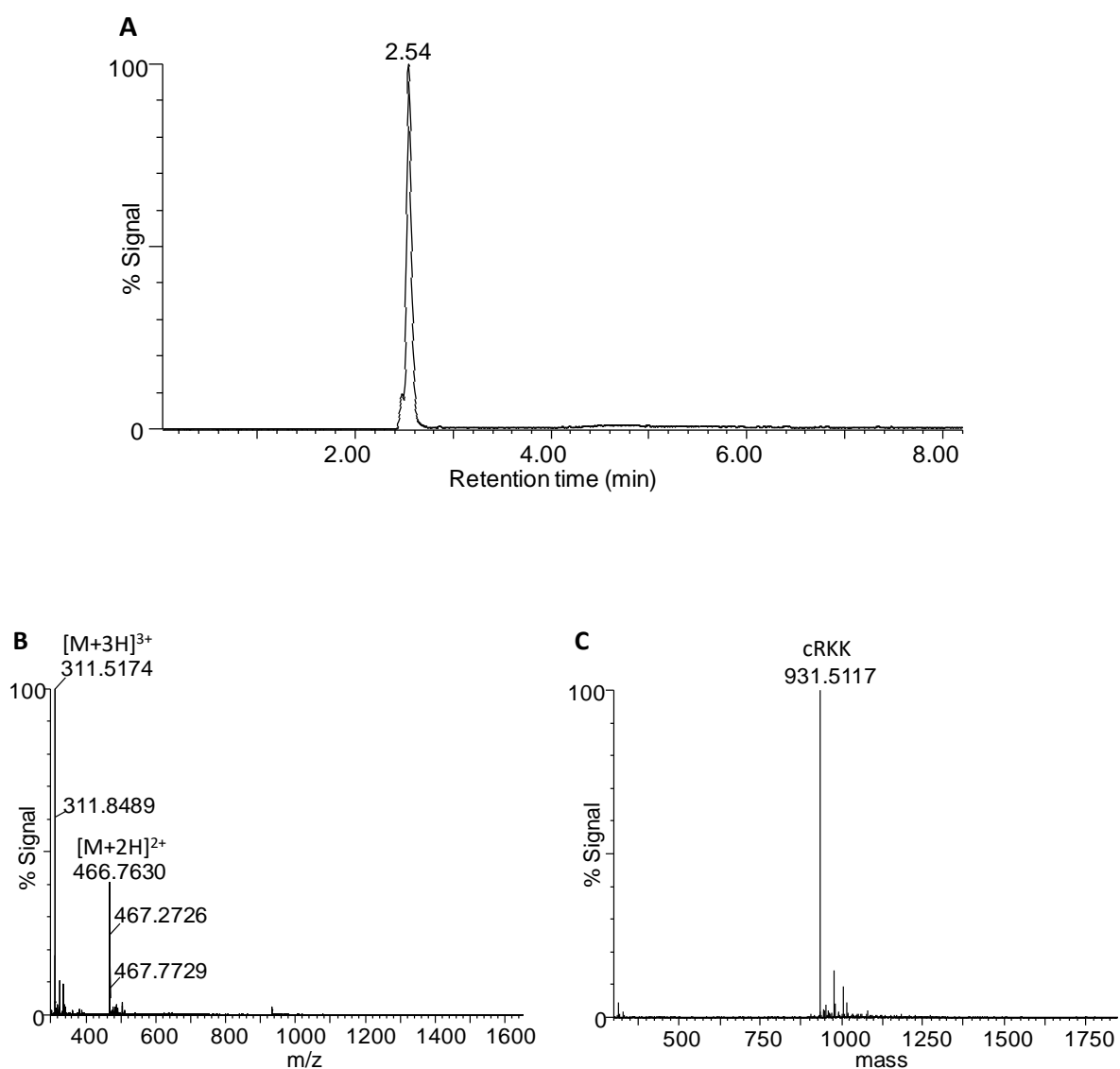


Figure 2.17: UPLC-MS analysis of cRKK.

A) UPLC chromatogram of cRKK (200 $\mu\text{g/mL}$; 5 μL injection volume) indicating an elution time of 2.53 minutes.

B) ESMS positive ion spectrum of the elution peak of cRKK indicating the doubly charged molecular ions $[\text{M}+2\text{H}]^{2+}$ and triply charged molecular ions $[\text{M}+3\text{H}]^{3+}$.

C) The MaxEnt 3 generated ESMS mass spectrum of cRKK depicting the experimental monoisotopic molecular mass.

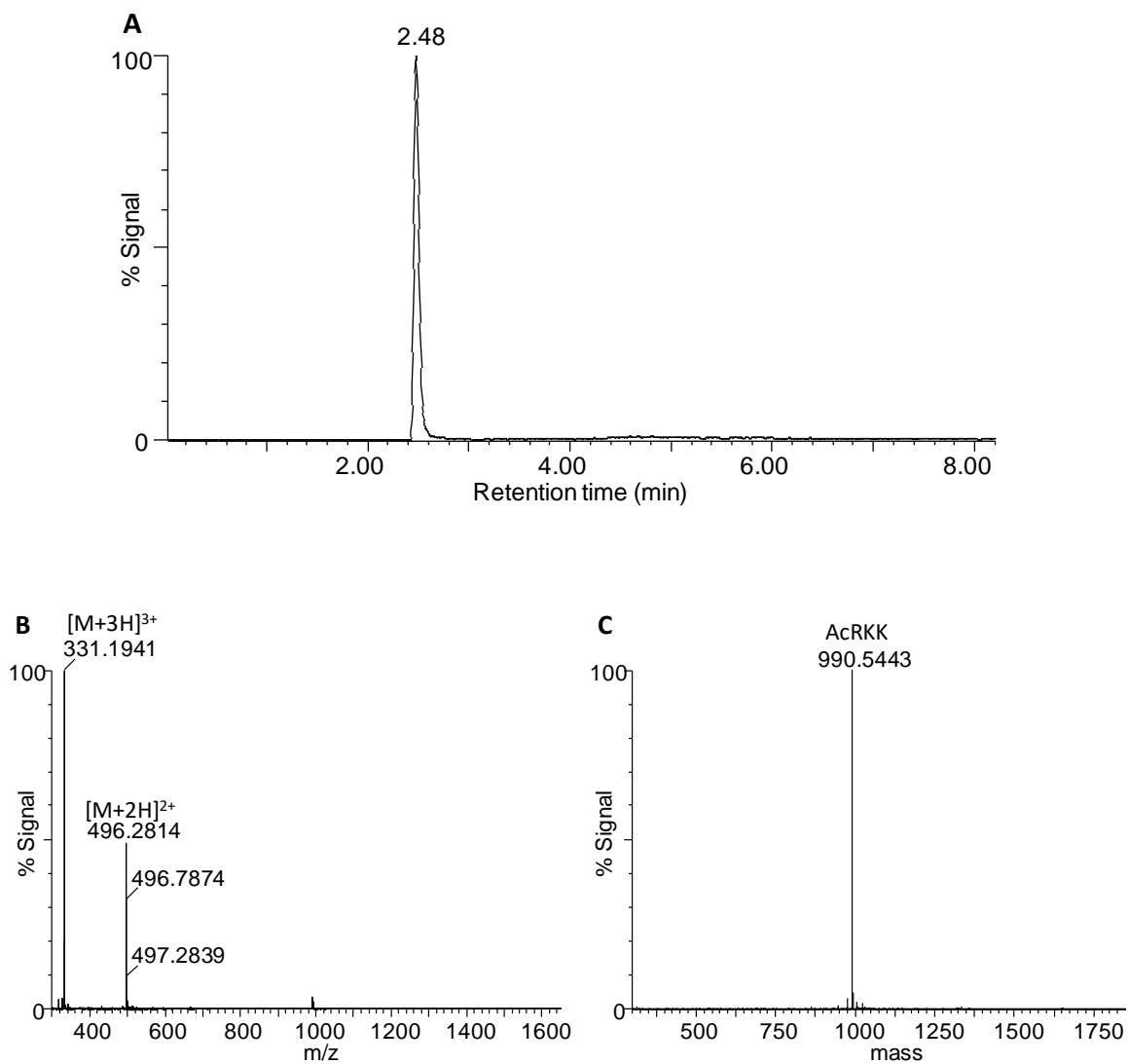


Figure 2.18: UPLC-MS analysis of AcRKK.

A) UPLC chromatogram of AcRKK (200 $\mu\text{g/mL}$; 5 μL injection volume) indicating an elution time of 2.48 minutes.

B) ESMS positive ion spectrum of the elution peak of AcRKK indicating the doubly charged molecular ions $[\text{M}+2\text{H}]^{2+}$ and triply charged molecular ions $[\text{M}+3\text{H}]^{3+}$.

C) The MaxEnt 3 generated ESMS mass spectrum of AcRKK depicting the experimental monoisotopic molecular mass.

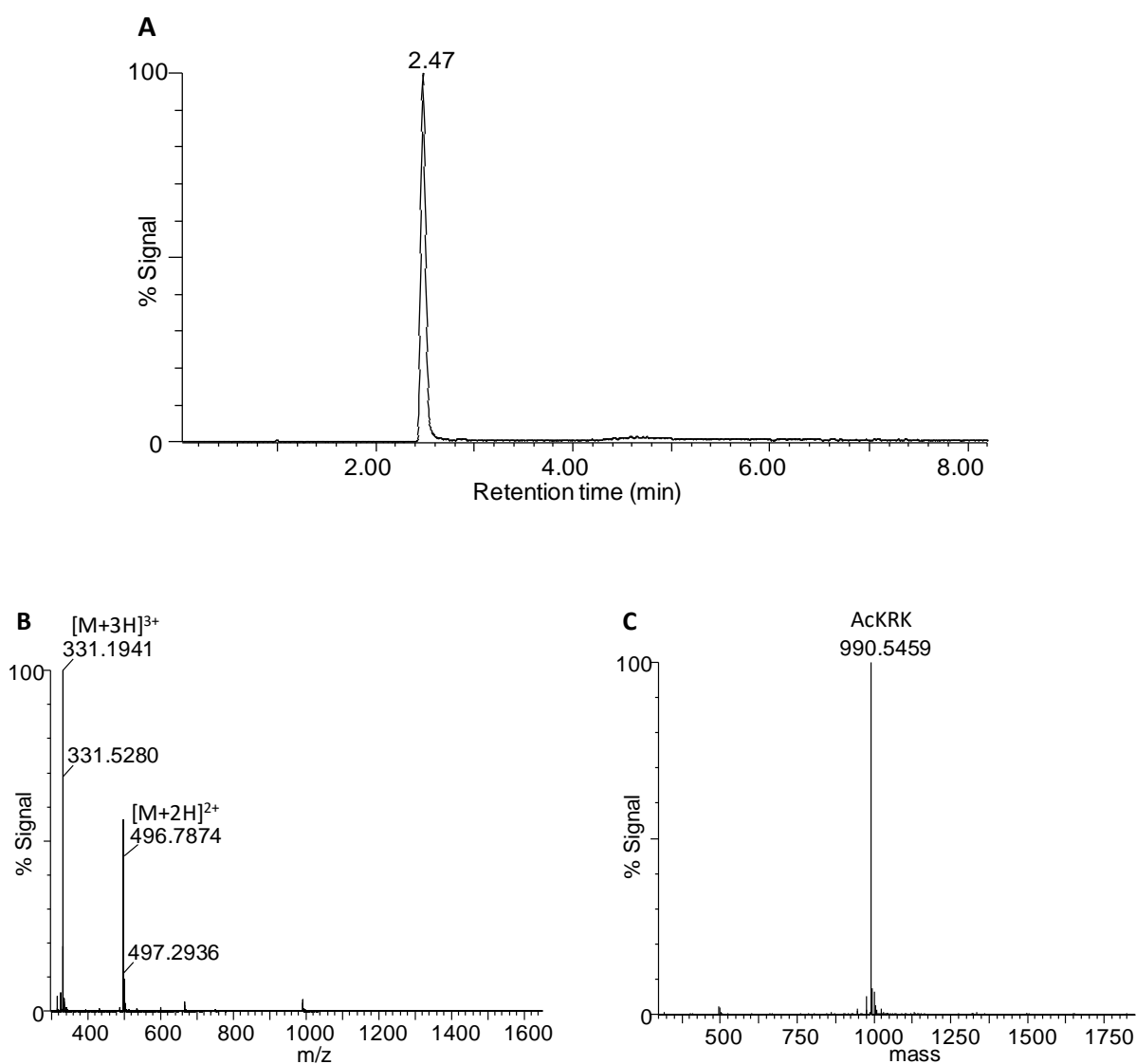


Figure 2.19: UPLC-MS analysis of AcKRK.

A) UPLC chromatogram of AcKRK (200 $\mu\text{g/mL}$; 5 μL injection volume) indicating an elution time of 2.47 minutes.

B) ESMS positive ion spectrum of the elution peak of AcKRK indicating the doubly charged molecular ions $[\text{M}+2\text{H}]^{2+}$ and triply charged molecular ions $[\text{M}+3\text{H}]^{3+}$.

C) The MaxEnt 3 generated ESMS mass spectrum of AcKRK depicting the experimental monoisotopic molecular mass.

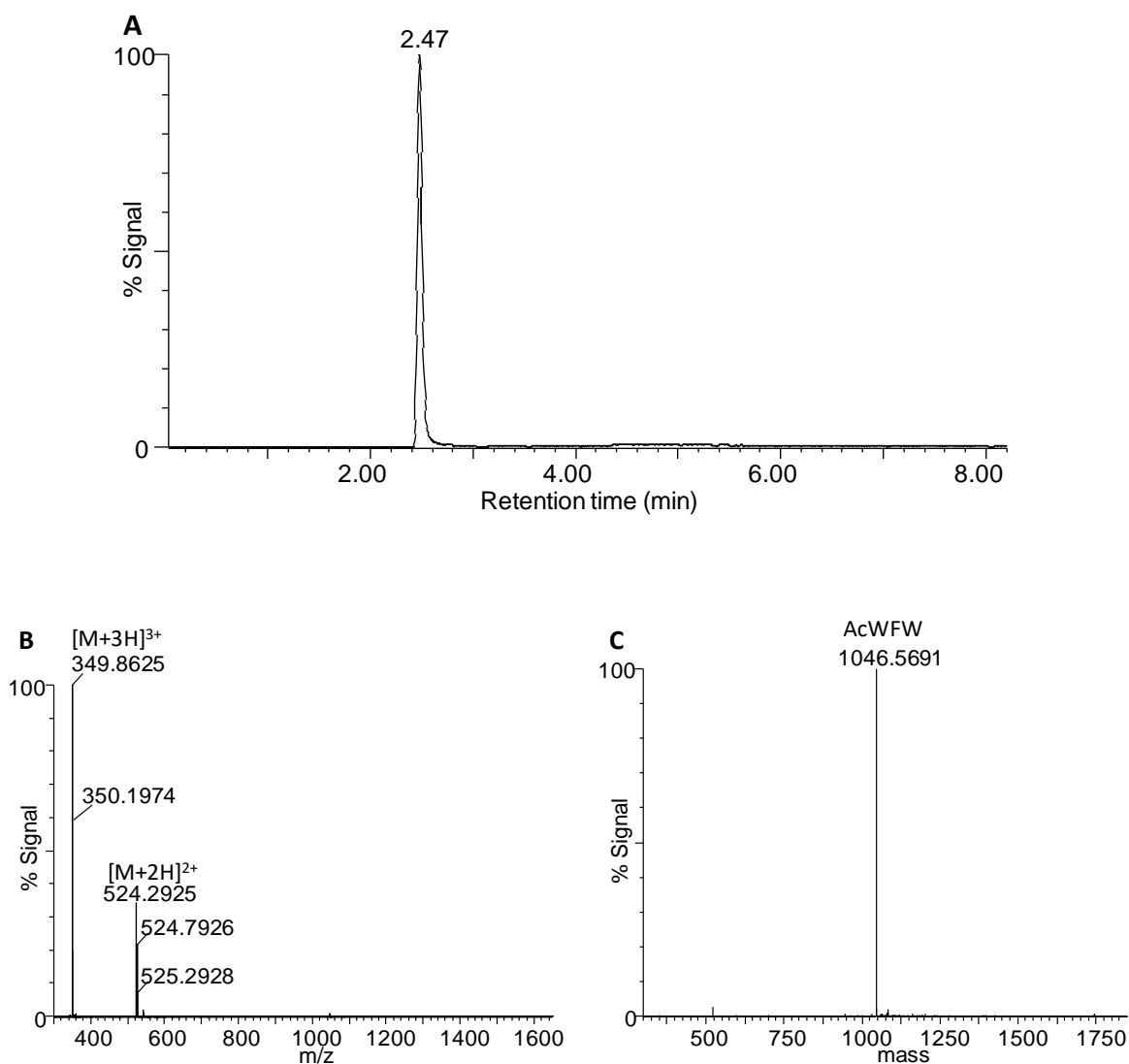


Figure 2.20: UPLC-MS analysis of AcWFW.

A) UPLC chromatogram of AcWFW (200 $\mu\text{g/mL}$; 5 μL injection volume) indicating an elution time of 2.47 minutes.

B) ESMS positive ion spectrum of the elution peak of AcWFW indicating the doubly charged molecular ions $[\text{M}+2\text{H}]^{2+}$ and triply charged molecular ions $[\text{M}+3\text{H}]^{3+}$.

C) The MaxEnt 3 generated ESMS mass spectrum of AcWFW depicting the experimental monoisotopic molecular mass.

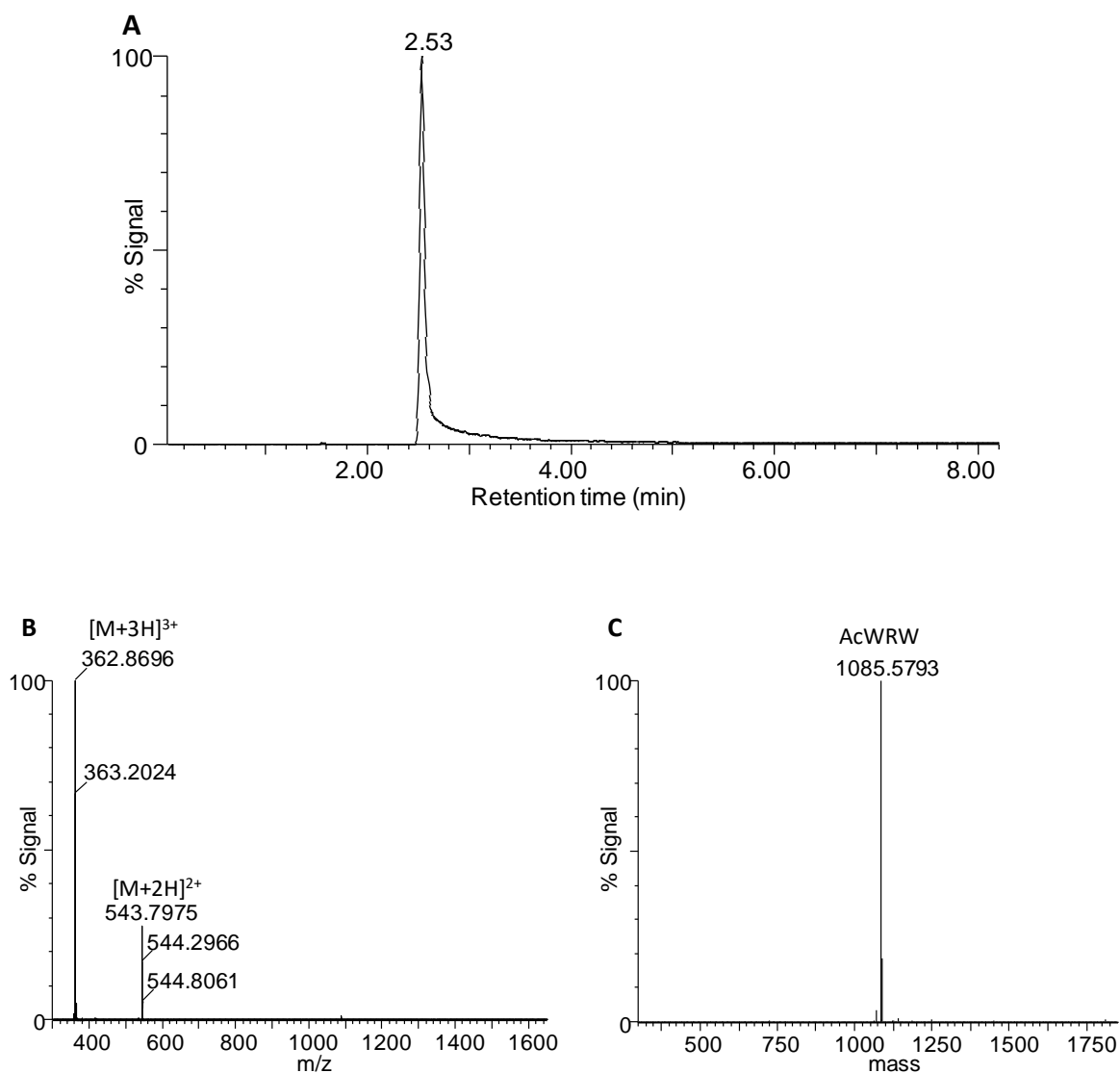


Figure 2.21: UPLC-MS analysis of AcWRW.

A) UPLC chromatogram of AcWRW (200 $\mu\text{g/mL}$; 5 μL injection volume) indicating an elution time of 2.53 minutes.

B) ESMS positive ion spectrum of the elution peak of AcWRW indicating the doubly charged molecular ions $[\text{M}+2\text{H}]^{2+}$ and triply charged molecular ions $[\text{M}+3\text{H}]^{3+}$.

C) The MaxEnt 3 generated ESMS mass spectrum of AcWRW depicting the experimental monoisotopic molecular mass.

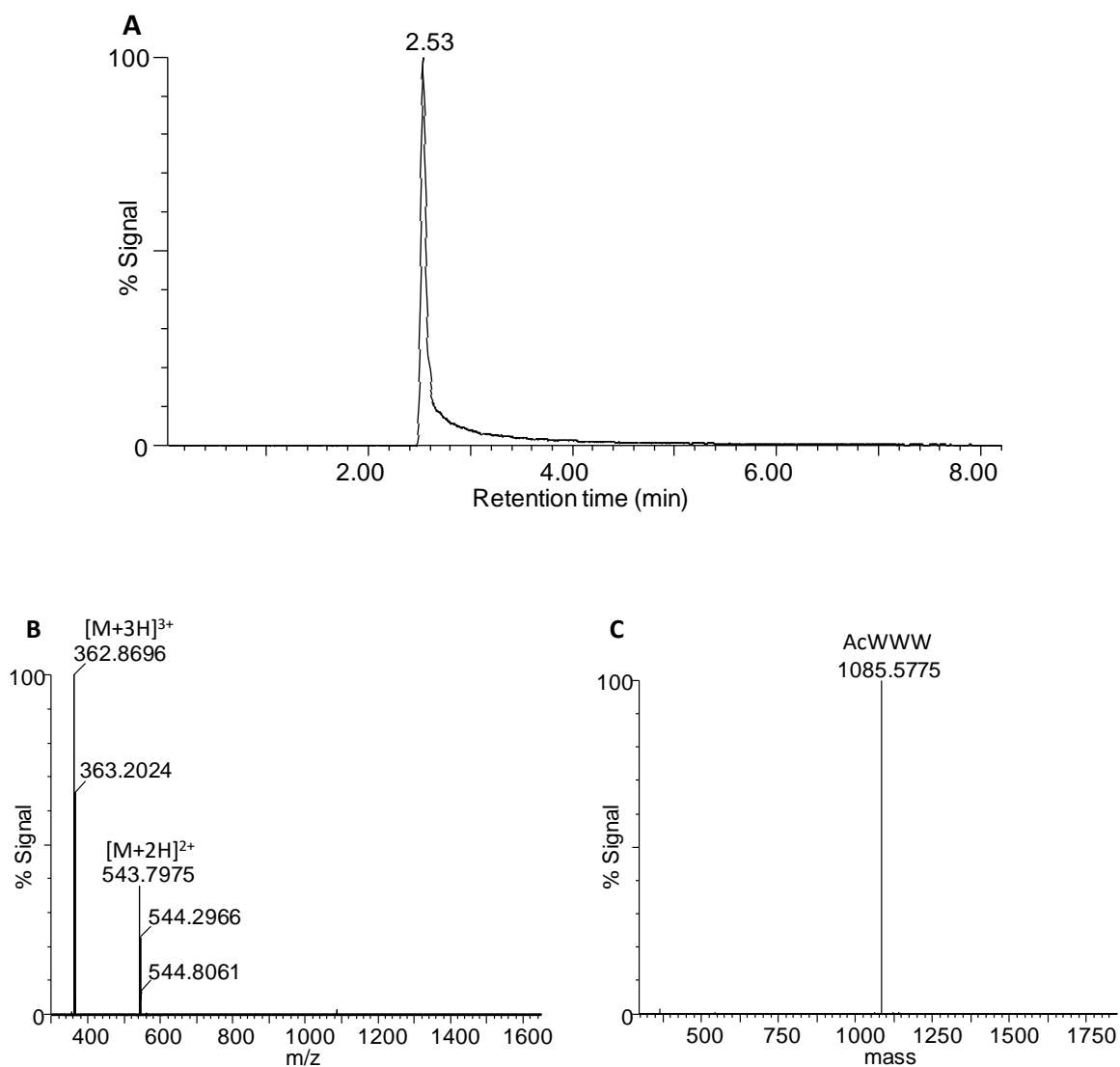


Figure 2.22: UPLC-MS analysis of AcWWW.

A) UPLC chromatogram of AcWWW (200 $\mu\text{g/mL}$; 5 μL injection volume) indicating an elution time of 2.53 minutes.

B) ESMS positive ion spectrum of the elution peak of AcWWW indicating the doubly charged molecular ions $[\text{M}+2\text{H}]^{2+}$ and triply charged molecular ions $[\text{M}+3\text{H}]^{3+}$.

C) The MaxEnt 3 generated ESMS mass spectrum of AcWWW depicting the experimental monoisotopic molecular mass.

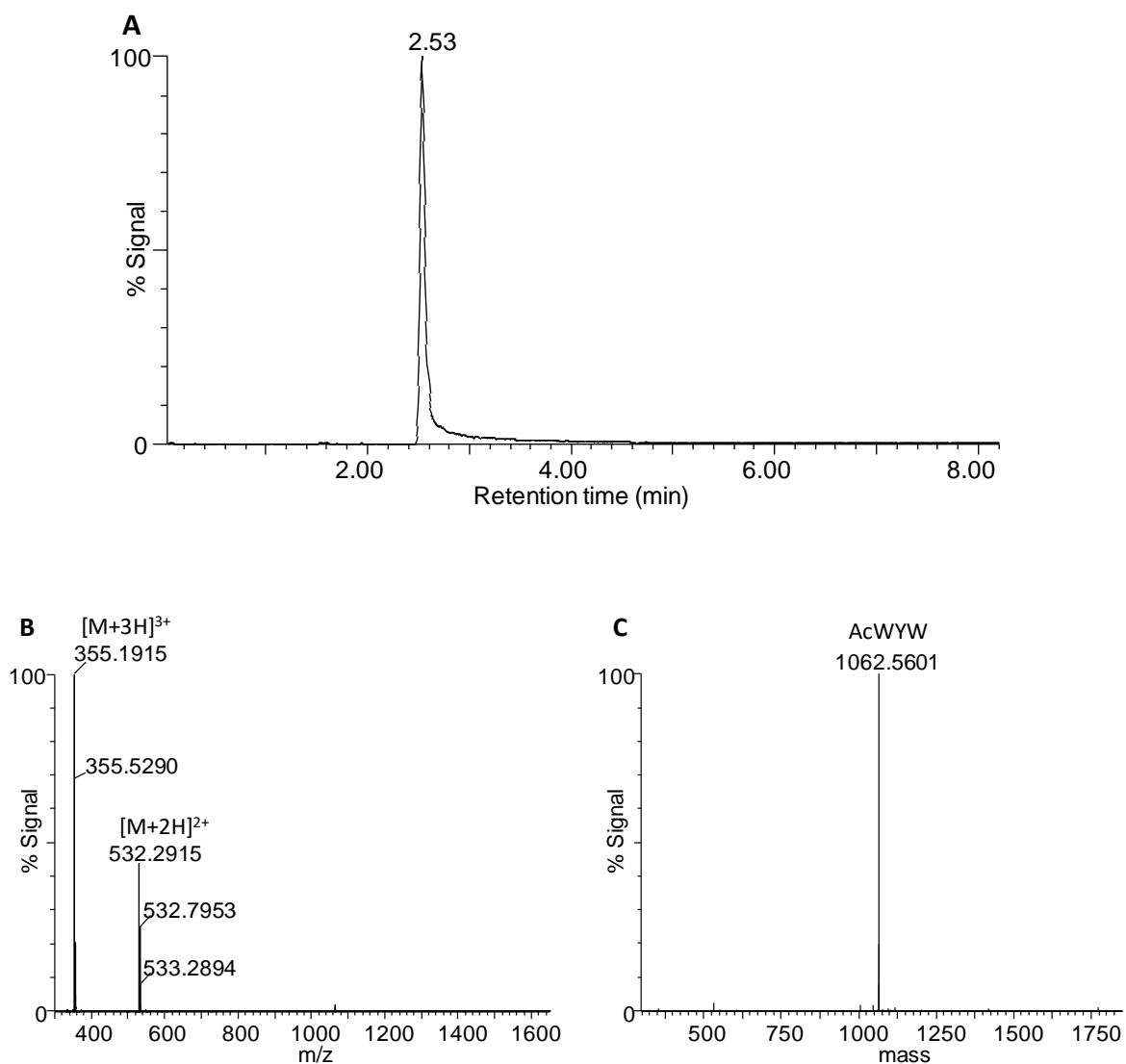


Figure 2.23: UPLC-MS analysis of AcWYW.

A) UPLC chromatogram of AcWYW (200 $\mu\text{g/mL}$; 5 μL injection volume) indicating an elution time of 2.53 minutes.

B) ESMS positive ion spectrum of the elution peak of AcWYW indicating the doubly charged molecular ions $[\text{M}+2\text{H}]^{2+}$ and triply charged molecular ions $[\text{M}+3\text{H}]^{3+}$.

C) The MaxEnt 3 generated ESMS mass spectrum of AcWYW depicting the experimental monoisotopic molecular mass.

By comparing the experimental M_r derived from ESMS to the theoretical M_r , the identities of all the peptides were successfully confirmed (Figures 2.9 – 2.23, Table 2.7). Most of the mass errors were below 15 ppm for the peptides which confirmed peptide identity and chemical integrity.

Table 2.7: Summary of the UPLC-MS characterisation of the synthetic RW-hexapeptides used in this study

Peptide identity	Structure	Experimental M_r (Theoretical M_r) ^a	Mass accuracy (ppm)	UPLC Retention time (min)	UPLC-MS % Purity ^b
Ac-KRK (Ac-KRKFW-NH ₂)	linear	990.5443 (990.5552)	11.0	2.48	>99
Ac-RKK (Ac-RKKFW-NH ₂)	linear	990.5459 (990.5552)	9.4	2.47	>99
Ac-WFW (Ac-RRRWF-NH ₂)	linear	1046.5691 (1046.5675)	-15.3	2.47	>99
Ac-WRW (Ac-RWRWR-NH ₂)	linear	1085.5793 (1085.5788)	0.46	2.53	>99
Ac-WWW (Ac-RRRWWW-NH ₂)	linear	1085.5775 (1085.5788)	1.19	2.53	97
Ac-WYW (Ac-RRRWYW-NH ₂)	linear	1062.5601 (1062.5624)	2.16	2.53	>99
cKRK (KRKFW)	cyclic	931.5129 (931.5181)	5.6	2.53	>99
cRKK (RKKFW)	cyclic	931.5117 (931.5181)	6.9	2.54	94
cWFW (RRRWF)	cyclic	987.5322 (987.5304)	-1.8	2.58	92
cWRW1 (RWRWR)	cyclic	1026.5245 (1026.5413)	16.4	2.47	>99
cWRW2 (RWRWR)	cyclic	1026.5284 (1026.5413)	12.6	2.89	>90
cWWW1 (RRRWWW)	cyclic	1026.5358 (1026.5413)	5.4	2.55	97
cWWW 2 (RRRWWW)	cyclic	1026.5406 (1026.5413)	0.7	ND	impure
cWWW 3 (RRRWWW)	cyclic	1026.5411 (1026.5413)	0.2	ND	ND
cWYW (RRRWYW)	cyclic	1003.5106 (1003.5253)	14.7	2.54	>99

^a Experimental monoisotopic mass was determined by ESMS whereas theoretical monoisotopic mass was calculated by summing the monoisotopic masses of the constituent amino acids of each peptide.

^b % Purity was calculated by expressing the peak area of the peptide's elution peak as a percentage of total of the peak areas of all the peaks integrated on the chromatogram.

Because of the three cationic residues in the RW-hexapeptides, they demonstrated a high propensity to carry multiple charges as only doubly and triply charged molecular ions were detected as shown on their mass spectra. In contrast to the mass spectra of the tyrocidines, no singly charged molecular ions or potassium adducts were detected. The UPLC chromatograms revealed that the RW-hexapeptides are much more polar in comparison to the tyrocidines. They eluted significantly earlier from the UPLC column ($R_t < 3$ minutes) than the tyrocidines ($R_t > 9$ minutes). This could be attributed to the higher proportion of the cationic amino acid residues in the sequences of the RW-hexapeptides. The contribution of polar residues to the primary structures of RW-hexapeptides is 50% compared to a 30%-40% contribution in the primary structures of the tyrocidines and analogues.

It must be noted that two peptide preparations of the WRW cyclic analogue and three preparations of the WWW cyclic analogue were characterised (Figures 2.11-2.15). The first peptide preparations (cWWW1 and cWRW1) were obtained from our research collaborators, the Dathe-group at the Leibniz Institute, Germany whereas the second and third preparations (cWWW2, cWWW3 and cWRW2) were supplied by GL Biochem Ltd (Shanghai, China). These peptide preparations from the different suppliers exhibited different chemical properties. The cWRW1 preparation from the Dathe group appeared to be slightly polar than the cWRW2 from from GL-Biochem as shown by its earlier elution from the UPLC column (Table 2.7). Given that the preparation of peptides for the UPLC-MS analyses was done in the same manner and the same protocol was utilised during the analyses, the observed anomalies can be linked to differences in the UPLC column. Alternatively, the retention difference could be due to shielding of charges by contaminants leading to an ion-pairing effect and concomitant increase in retention on the C_{18} matrix. Even though the two cWRW peptide preparations showed slightly different UPLC-MS profiles, their ESMS mass spectra were very similar as were their purities. On the other hand, the ESMS mass spectra of the three cWWW peptides were very different. The ESMS mass spectrum of cWWW2 (Figure 2.11) displayed various unidentified peaks related to impurities, which are absent in the mass spectrum of cWWW1 (Figure 2.10) and cWWW3 (Figure 2.12). However, we failed to generate a UPLC chromatogram for either cWWW2 or cWWW3. In both preparations the peptide signals were not detected during UPLC-MS at the same concentration as cWWW1. From these QC analyses it can be deduced that cWWW2 contained a large amount of impurities, resulting in a concentration that was too low for detection with UPLC-MS, therefore this preparation was discarded. The failure to generate a UPLC-MS profile for cWWW3 that is quite pure according to the direct injection ESMS is unclear. The only observation that could point to

non-ionisable impurities is that about a 20-fold lower positive ion signal was obtained for this preparation, compared to similar RW preparations at the same concentration. These impurities could also have led to ion-pairing and retention on the column and a failure to elute during the UPLC run.

With exception of cWRW2, the RW-hexapeptides had very similar retention times regardless of their cyclic or linear nature (Table 2.7). In some instances, the same retention times were observed for different peptides. It was expected that RW-hexapeptides would have similar amphipathic properties due to their highly conserved amino acid composition. The difference in their amino acid sequences is a result of either substitution of a single amino acid or just a rearrangement of amino acids. In the linear group, the most polar peptides were Ac-RKK and Ac-WFW and the least polar peptides were Ac-WWW, Ac-WRW and Ac-WYW. From the cyclic group, cWRW1 was found to be the most polar while the cWRW2 preparation was found to be the least polar.

The retention times of peptides containing the same amino acid residues, albeit arranged differently were observed to be different (cKRR vs cRKK, cWRW vs cWWW and AcKRR vs AcRKK). This indicated that the order of amino acids in the primary structure of peptides influences the amphipathic properties. However, for the Ac-WRW and Ac-WWW, rearrangement of amino acids had no effect on the amphipathicity as the two peptides had the same retention time on the UPLC column.

Generally, cyclisation increased hydrophobicity as evidenced by a slight increase in retention times of the cyclic analogues. A similar phenomenon was reported by other investigators [13,24]. Dathe *et al.* [24] suggested that the increase might related to the clustering of hydrophobic residues which in turn enhances the amphipathicity of the molecules. Strangely, for the amino acid sequence RWRWRW, a reduction in the retention time was observed upon cyclisation of the linear peptide.

2.4 Conclusion

The biological production of the natural cyclodecapeptide analogues (YA, YB, YC and WC) using cultures of *Br. parabrevis* was successful. Employing an optimised semi-preparative RP-HPLC methodology enabled the successful purification of these peptides to greater than 90% purity by peptide composition as determined by ESMS and UPLC-MS analyses. This successful purification paved way for structural characterisation and elucidation of the bioactivity which will be discussed in Chapters 3 and 4, respectively. Furthermore, the analysis of the synthetic RW-hexapeptides by

ESMS and UPLC-MS confirmed their identity and allowed the determination of their level of purity. From this study it is also clear that stringent QC is essential to ensure that peptide preparations are of high purity and quality, regardless of the supplier's data on the peptide preparation. It was established that the RW-hexapeptides, except cWWW3 had a greater than 90% purity, with the majority being greater than 99% pure. The results of the UPLC analysis also gave insight into their chemical nature. The members of this family of small peptides possess similar amphipathic properties. In addition, they are highly polar relative to the tyrocidines. Chemical characterisation as well the structural characterisation (Chapter 3) will be correlated to the observed antifungal activity of the peptides that will be presented and discussed in Chapter 4.

2.5 References

- [1] G.D. Brown, D.W. Denning, N.A.R. Gow, S.M. Levitz, M.G. Netea, T.C. White, Hidden killers: Human fungal infections, *Science Translational Medicine*, 4 (2012).
- [2] M.A. Pfaller, D.J. Diekema, Epidemiology of invasive mycoses in North America, *Critical Reviews in Microbiology*, 36 (2010) 1–53.
- [3] D. Hotchkiss, R. Dubos, The isolation of bactericidal substances from cultures from *Bacillus brevis*, *The Journal of Biological Chemistry*, 141 (1941) 155–162.
- [4] X.-J. Tang, P. Thibault, R.K. Boyd, Characterisation of the tyrocidine and gramicidin fractions of the tyrothricin complex from *Bacillus brevis* using liquid chromatography and mass spectrometry, *International Journal of Mass Spectrometry and Ion Processes*, 122 (1992) 153–179.
- [5] R.J. Dubos, Studies on bactericidal agent extracted from a soil *Bacillus*: 1 Preparation of the agent its activity in vitro, *The Journal of Experimental Medicine*, 70 (1939) 1–10.
- [6] S.E. Blondelle, R.A. Houghten, Novel antimicrobial compounds identified using synthetic combinatorial library technology, *Trends in Biotechnology*, 14 (1996) 60–65.
- [7] B.M. Spathelf, M. Rautenbach, Anti-listerial activity and structure-activity relationships of the six major tyrocidines, cyclic decapeptides from *Bacillus aneurinolyticus*, *Bioorganic and Medicinal Chemistry*, 17 (2009) 5541–5548.
- [8] M. Rautenbach, A.M. Troskie, J.A. Vosloo, M.E. Dathe, Antifungal membranolytic activity of the tyrocidines against filamentous plant fungi, *Biochimie*, 130 (2016) 122–131.
- [9] A.M. Troskie, M. Rautenbach, N. Delattin, J.A. Vosloo, M. Dathe, B.P.A. Cammue, K. Thevissen, Synergistic activity of the tyrocidines, antimicrobial cyclodecapeptides from *Bacillus aneurinolyticus*, with amphotericin B and caspofungin against *Candida albicans* biofilms, *Antimicrobial Agents and Chemotherapy*, 58 (2014) 3697–3707.
- [10] A.N. yango N. Leussa, M. Rautenbach, Detailed SAR and PCA of the tyrocidines and analogues towards leucocin A-sensitive and leucocin A-resistant *Listeria monocytogenes*, *Chemical Biology & Drug Design*, 84 (2014) 543–557.

- [11] A. Muñoz, B. López-García, J.F. Marcos, Studies on the mode of action of the antifungal hexapeptide PAF26, *Antimicrobial Agents and Chemotherapy*, 50 (2006) 3847–3855.
- [12] A. Muñoz, B. López-García, E. Pérez-Payá, J.F. Marcos, Antimicrobial properties of derivatives of the cationic tryptophan-rich hexapeptide PAF26, *Biochemical and Biophysical Research Communications*, 354 (2007) 172–177.
- [13] A. Wessolowski, M. Bienert, M. Dathe, Antimicrobial activity of arginine- and tryptophan-rich hexapeptides: The effects of aromatic clusters, D-amino acid substitution and cyclization, *Journal of Peptide Research*, 64 (2004) 159–169.
- [14] C. Appelt, A. Wessolowski, J.A. Söderhäll, M. Dathe, P. Schmieder, Structure of the antimicrobial, cationic hexapeptide cyclo(RRWRF) and its analogues in solution and bound to detergent micelles, *ChemBioChem*, 6 (2005) 1654–1662.
- [15] C. Junkes, R.D. Harvey, K.D. Bruce, R. Dölling, M. Bagheri, M. Dathe, Cyclic antimicrobial R-, W-rich peptides: The role of peptide structure and *E coli* outer and inner membranes in activity and the mode of action, *European Biophysics Journal*, 40 (2011) 515–528.
- [16] A.M. Troskie, Tyrocidines, cyclic decapeptides produced by soil bacilli , as potent inhibitors of fungal pathogens, PhD Thesis, Department of Biochemistry, University of Stellenbosch, (2013), <http://hdl.handle.net/10019.1/86162>
- [17] J.A. Vosloo, Optimised bacterial production and characterisation of natural antimicrobial peptides with potential application in agriculture, PhD Thesis, Department of Biochemistry, University of Stellenbosch, (2016), <http://hdl.handle.net/10019.1/98411>
- [18] R.J. Dubos, R.D. Hotchkiss, The production of bactericidal substances by aerobic sporulating *Bacilli*, *The Journal of Experimental Medicine*, 73 (1941) 629–640.
- [19] J.A. Vosloo, M.A. Stander, A.N.N. Leussa, B.M. Spathelf, M. Rautenbach, Manipulation of the tyrothricin production profile of *Bacillus aneurinolyticus*, *Microbiology (United Kingdom)*, 159 (2013) 2200–2211.
- [20] B. Spathelf, Qualitative structure-activity relationships of the major tyrocidines , cyclic decapeptides from *Bacillus aneurinolyticus*, PhD Thesis, Department of Biochemistry, University of Stellenbosch, (2013), <http://hdl.handle.net/10019.1/4001>
- [21] A.N.-N. Leussa, Characterisation of small cyclic peptides with antimalarial and antilisterial activity PhD Thesis, Department of Biochemistry, University of Stellenbosch, <http://hdl.handle.net/100191/86161>, (2014).
- [22] W. Van Rensburg, Characterization of natural antimicrobial peptides adsorbed to different matrices, MSc Thesis, Department of Biochemistry, University of Stellenbosch, (2015). <http://hdl.handle.net/10019.1/97929>
- [23] J. Kyte, R.F. Doolittle, S. Diego, L. Jolla, A simple method for displaying the hydrophobic character of a protein, *Journal of Molecular Biology*, 157 (1982) 105–132.
- [24] M. Dathe, H. Nikolenko, J. Klose, M. Bienert, Cyclization increases the antimicrobial activity and selectivity of arginine- and tryptophan-containing hexapeptides, *Biochemistry*, 43 (2004) 9140–9150.

Chapter 3

Structural characterisation of natural cyclodecapeptides and synthetic hexapeptides

3.1 Introduction

In the development of antimicrobial peptides for therapeutic applications, it is important to have a clear understanding of factors that govern the activity of these peptides. It has been shown that target cell properties, physicochemical properties of the peptide as well as environmental factors all play a role in the interaction between an antimicrobial peptide and its target. Intrinsic properties of a peptide that affect bioactivity are related to its conformation and include size, charge distribution, hydrophobicity, amphipathicity and secondary structure. Additionally, environmental factors such as the hydrophobicity/polarity, ionic strength and pH of a peptide's environment also have an effect on its conformation thereby influencing how it interacts with a target and ultimately, its activity [1–4]. Because of the influence of physicochemical parameters of peptides on bioactivity, their elucidation is important to better understand structure activity relationships, modulation of bioactivity and mode of action [5].

Circular dichroism (CD), a spectrophotometric character exhibited by chiral compounds, is an important technique for studying peptide and protein secondary structure. The spectrophotometric properties of the peptide bond, in particular the carbonyl group, are very sensitive to different secondary structural motifs and as a result, characteristic CD spectra exist for the various types of secondary structures found in proteins and peptides [6,7]. Because conformation dictates the nature of the CD spectra, CD can therefore be used to predict the secondary structure of peptides and to track any conformational changes induced by the environment [7]. From previous work [5,8,9], it has been reported that tyrocidines produce CD spectra that can be misinterpreted as that of α -helical structures. However, it has been shown through NMR studies [10] and X-ray crystallography [11] that they form predominantly β -sheet structures, containing type II β -turns. It has been hypothesised that the aberrant CD spectra could possibly be due to the contribution of aromatic amino acid residues, their propensity to aggregate in solution and their cyclic nature, as well as their two D-amino acids in their structure [5,8,9]. Investigations of the structure of cyclic RW-hexapeptides by CD spectroscopy have found that they have rather flexible but ordered

conformations consisting of two β -turns in aqueous solution. In lipophilic environments, the ordered conformation is maintained but the position of the β -turns is changed [12,13]. On the other hand, the structure of the linear analogues has been characterised as random/disordered in aqueous solutions. However, it has been shown that in membrane mimicking environments, they transition to ordered structures and become structurally similar to their cyclic counterparts as they adopt amphipathic conformations [14].

In addition to CD, fluorescence spectroscopy (FS) has proved to be a valuable and sensitive technique in the study of peptide structure. It relies on the intrinsic fluorescent properties of the aromatic amino acids, specifically that of Trp due to it being the dominant fluorophore in peptides and proteins [10]. Trp is quite sensitive to its local environment and any change in the local environment of Trp causes changes in its fluorescence emission spectra [10]. The spectral changes usually observed include shifting of the emission maxima and changes in the fluorescence intensity and yield which depicts either quenching or dequenching [15–17]. These changes often reflect conformational changes in peptides. Previous work has shown that both tyrocidines and RW-peptides exhibit blue shifting and fluorescence quenching when their environment changes from polar to hydrophobic [9,13]. Furthermore, in the absence of crystal structures and 2D NMR data, *de novo* low energy molecular models can be useful tools in the prediction of peptide structure. Using tailored computer software, various physicochemical attributes of molecular models can be analysed which can enhance the understanding of peptide structure.

In this study, CD spectroscopy and FS were employed for the purposes of characterising the structure of natural cyclo-decapeptides (tyrocidines and analogues) and synthetic RW-hexapeptides in different solvent environments. The RW-hexapeptides structures were also analysed *in silico* via modelling and the results of these *in silico* analyses compared to the *in vitro* analyses.

3.2 Materials

Characterisation of peptide structure was performed on two groups of peptides; namely the natural cyclo-decapeptides (tyrocidines and analogues) and the synthetic RW-hexapeptides. Three of the synthetic cyclic RW-hexapeptides (cKRK, cRKK, and cWFW) were obtained from Liebniz, Germany while cWYW, cWRW and cWWW, as well as all the linear RW-hexapeptides were

supplied by GL Biochem Limited (Shanghai, China). It should be noted that the cWRW and cWWW characterised in this chapter are from the third batch (otherwise referred to as cWRW3 and cWWW3 in Chapter 2). The tyrothricin-derived cyclodecapeptides were extracted from cultures of *Brevibacillus parabrevis* 5618-DSM and purified by semi-preparative reversed phase HPLC (described in Chapter 2). All peptides used in this investigation were at least 90% pure according to UPLC-MS analysis, with exception of cWWW from GL Biochem (referred to as cWWW3 in Chapter 2) which failed our UPLC-MS analysis although the supplier noted its purity as >95% (refer to Chapter 2). Peptide solutions were prepared using the following solvents; analytical grade water that had been purified by reverse osmosis followed by filtration through a Millipore MilliQ water purification system (Milford, USA), acetonitrile (HPLC-grade, far UV cut-off of 190 nm) supplied by Romil Limited (Cambridge, UK) and 2,2,2-trifluoroethanol purchased from Sigma (St. Louis, USA).

3.3 Methods

Molecular modelling of RW-hexapeptide structures

Using YASARA 11.3.2[®] software [18], models of RW-hexapeptide structures were generated by Prof M. Rautenbach by implementing basic principles of molecular modelling. A template model of AcWWW-amide with a β -sheet backbone structure was built as the representative starting model of the linear hexapeptides. A template model of cWWW, with two β -turns in which RW- and WR are taking part in the β -turn moieties, was built as the representative starting model of the cyclo-hexapeptides. These template models were then subjected to exhaustive molecular dynamic (MD) simulations at 298K using YASARA 2 force field [18]. Each simulation run was followed by an energy minimisation step *in vacuo*. Simulation runs were performed on the template models until successive runs yielded structures with no appreciable difference in energy and backbone structure (average RMSD < 1Å for consecutive structures). At this point, it was thus assumed that the template models had reached a global energy minimum and could be used as representative model structures. Molecular models of the other analogues in each group were derived from these low energy template structures by simply mutating the amino acid sequence accordingly and performing MD simulation runs to check whether a global energy minimum had been reached.

In this study, 15 low energy model structures were selected for each peptide and superposed onto each other to validate that similar structures were obtained. The characterisation of the 15 low energy structures of each peptide was done using YASARA 11.3.2[®] software [18]. Secondary structures and size-defining parameters (radius, surface area and volume) were determined to compare the peptides with each other.

Circular dichroism spectroscopy

Dry, analytically weighed aliquots of the cyclodecapeptides were dissolved in 50% (v/v) acetonitrile (ACN) in analytical grade water to make 2.000 mM peptide stock solutions. The stock solutions were then diluted 10× with analytical grade water so that the concentration of ACN was 5% (v/v). A final dilution with either analytical grade water or 2,2,2-trifluoroethanol (TFE) was carried out to achieve a final peptide concentration of 100.0 μM and ACN concentration of 2.5% (v/v). For the RW-peptides, 200.0 μM peptide solutions in analytical grade water were prepared prior to further dilution with either 2,2,2-TFE or analytical grade water to achieve a final peptide concentration of 100.0 μM. The peptides were analysed for circular dichroism on a Chirascan CD spectrometer (Applied Photophysics, UK) at 25 °C using a quartz cuvette with a pathlength of 0.05 cm. Three scans were performed on each sample and data collection over 185-295 nm was set at 0.5 seconds per step of 1 nm (average of 4000 data points per nm) and a bandwidth of 1 nm.

Fluorescence spectroscopy

Following CD analysis, the same peptide samples were analysed for fluorescence emission on a Varioskan[®] Flash multimode plate reader (Thermo Scientific, USA). Peptide solutions were excited at 280 nm with an excitation bandwidth of 5 nm. Acquisition of fluorescence emission data was done in the region between 300 nm and 420 nm using a step size of 2 nm. Emission scans were done in triplicate for each peptide sample.

Data analysis

Data from the peptide models was analysed in YASARA 11.3.2[®] software. GraphPad Prism[®] 6.0 (GraphPad software, San Diego, USA) was used to plot CD spectra and fluorescence emission spectra. To determine the content of the various secondary structural elements within the peptides, CDPro software package was used to deconvolute CD spectral data (240 - 185 nm). The

CONTINLL algorithm and protein reference set 4 (IBasis 4) were utilised in deconvolution process.

3.4 Results and Discussion

Molecular models of natural cyclodecapeptides

The structures of YA and YC were previously determined by nuclear magnetic resonance spectroscopy (NMR) by Munyuki *et al.* [10] and by using homology modelling [Rautenbach and Leussa, unpublished data] from the structure of YC by Munyuki *et al.* [10]. All four of the cyclodecapeptides displayed the typical β -sheet and β -turn structures as can be seen in Figure 3.1. However, none of the cyclo-decapeptides displayed overt amphipathicity in their monomeric form. Munyuki *et al.* [10] modelled the dimers of YA and YC from NMR data and showed that these structures have an amphipathic nature. Similarly, a model of a YA dimer derived from a YA crystal structure also displayed amphipathic character [11].

A summary of the structural parameters determined from the four cyclodecapeptide models is given in Table 3.1.

Table 3.1: Summary of the structural characteristics of the four cyclodecapeptides derived from model structures. Radius, surface area and volume refer to the Van der Waals radius/surface/volume.

Peptide identity	Sequence	Type	Radius (Å)	Surface area (Å ²)	Volume (Å ³)
Tyrocidine A (YA)	fPFfNQYVOL	cyclic	12.38	1130.95	1309.3
Tyrocidine B (YB)	fPWfNQYVOL	cyclic	12.23	1149.33	1344.6
Tyrocidine C (YC)	fPWwNQYVOL	cyclic	12.40	877.84	1377.6
Tryptocidine C (WC)	fPWwNQWVOL	cyclic	12.07	1161.31	1399.2

It is interesting to note that the radii of the peptides are quite similar at 12-13 Å (Table 3.1). A typical membrane is 7.5-10 nm thick (75-100 Å) [19]. This means that at least four peptide molecules would be needed to span a bilayer membrane to form the ion-conducting pores observed by Wenzel *et al.* [20].

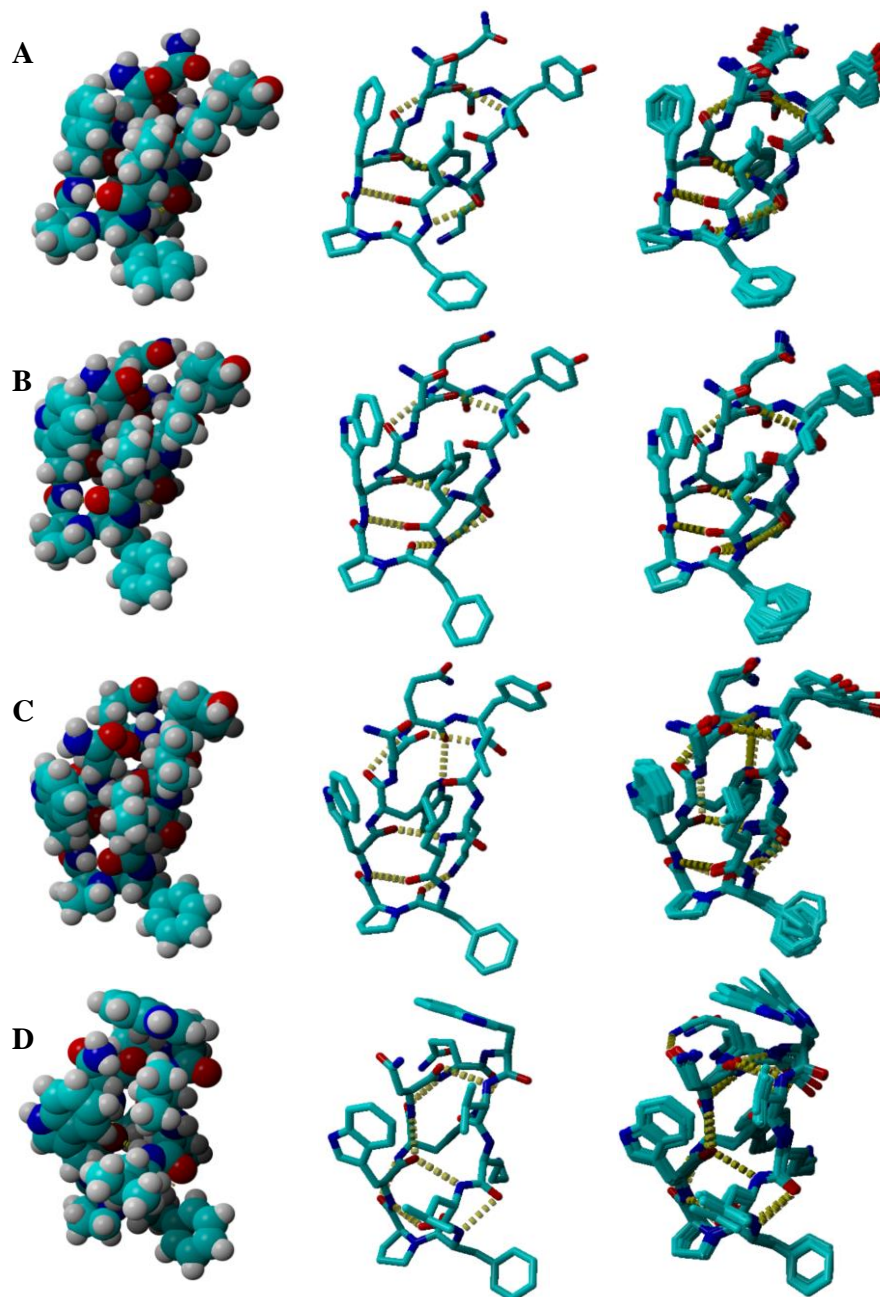


Figure 3.1: *Low energy structural models of the natural cyclodecapeptides*

A) YA, B) YB, C) YC and D) WC. The images on the left depict ball models, middle images depict stick models with the backbone hydrogen bonding highlighted and images on the right depict overlays of 10 lowest energy model structures. Carbon atoms are depicted in light blue, nitrogen in dark blue, oxygen in red and hydrogen bonds in yellow. For simplicity, hydrogen atoms are not depicted in structures.

Molecular modelling of RW-hexapeptide structures

Peptide structures were modelled exclusively for the RW-hexapeptides as the modelling of the cyclodecapeptide structures has been done previously [5,10,21]. Molecular modelling was done for the following cyclic and linear RW-hexapeptide analogues: cWFW, cWRW, cWWW, cWYW, AcWFW, AcWRW, AcWWW and AcWYW. As expected, the models showed that there, indeed, are huge structural differences between the cyclic and linear analogues. Out of the four cyclic analogues whose structures were modelled, cWFW, cWYW, cWWW exhibited a highly conserved backbone structure comprising a single β -turn and a single γ -turn (Figure 3.2A-C). The two turns were stabilised by hydrogen bonds between the amino (NH) and carbonyl (CO) groups of the peptide backbone. The β -turn was created by the formation of a hydrogen bond between the amide CO-group of Trp¹ and the amide NH-group of Arg⁴. On the other hand, hydrogen bonding between the amide NH-group of Arg⁵ and the amide CO-group of Trp¹ gave rise to the γ -turn. A third hydrogen bond which was also involved in stabilising the peptide backbone was observed between the amide CO-group of Trp³ and the amide NH-group of Arg⁵. Overall, the three model hexapeptides exhibited amphipathic structures; with the aromatics clustered on one side and the Arg residues spread out on the opposite side. The observed amphipathic structures show consistency with previous structural characterisations of these hexapeptides [12,22]. However, there is a slight discrepancy with regards to the types of turns in peptide backbone. While cWFW has previously been characterised to also contain two turns, both turns were reported to be β -turns [22].

Although the model structure for cWRW also showed an amphipathic configuration, it did not resemble the molecular models of the other cyclic analogues (Figure 3.2D). The hydrophobic aromatic residues did not truly cluster together despite being separated from the polar Arg residues. In addition, the cWRW backbone consisted of two γ -turns that were stabilised by the following hydrogen bonds: Trp³-O:HN-Trp⁵ and Arg⁴-O:HN-Arg⁶. A third hydrogen bond was also observed between the terminal NH₂ group of Arg⁴ and the amide CO-group of the same residue.

Analysis of secondary structure of these models showed cWRW to consist of solely undefined/irregular structural elements whereas the other cyclic analogues were found to have 66.6% turn structures and 33.3% undefined structures (Table 3.3). The comparative analysis of the

size parameters relating to the Van der Waals surface did not yield any clear trend (Table 3.2). Interestingly, the Van der Waals radii of the cyclic hexapeptides were very similar to radii of the cyclodecapeptides which can be attributed to the cyclic nature of their peptide backbones.

Models for the linear analogues also exhibited conservation of backbone structure amongst three of the four analogues, namely AcWFW, AcWWW and AcWYW. The structure was characterised by a single γ -turn that was stabilised by hydrogen bonding between the CO-group of the acetyl moiety and the amide NH-group of Arg². An additional hydrogen bond was common amongst all three analogues and this was between the NH-group on the indole ring of Trp⁴ and CO-group of the acetyl moiety. Other hydrogen bonds stabilised the backbone structures, but their number and location varied amongst the three analogues (Table 3.2). For instance, both AcWFW and AcWWW had three additional hydrogen bonds but different residues were involved in the bonding. AcWYW, on the other hand, only had one extra hydrogen bond. Similar to what was observed for the cyclic analogues, the structure of the model for AcWRW was vastly different from the other linear analogues. The molecular model displayed a total of six internal hydrogen bonds (Table 3.2). Two of these, which were also present in the models of the other linear analogues, were Acetyl-O:H(NE1)-Trp⁴ and Acetyl-O:HN-Arg²; with the latter stabilising the γ -turn. In addition to the γ -turn that was common to the other three analogues, the model depicted two other γ -turns. These γ -turns were a result of the following hydrogens bonds: Trp²-O:HN-Trp⁴ and Trp⁴-O:HN-Trp⁶. The models for the linear RW-hexapeptides illustrated an amphipathic conformation, albeit not as strong and defined as for the cyclic analogues. This was because at least one of the polar residues tended to associate with aromatics in the hydrophobic cluster (Figure 3.3). The amphipathic nature of the linear RW-hexapeptides has also been previously reported [23,24]. Interestingly, the secondary structures of the molecular models of all the linear analogues were found to be entirely undefined/irregular even though the models depicted clear structural distinctions between AcWRW and the other three analogues (Table 3.3). However, comparative analysis of the size parameters relating to the Van der Waals surface highlighted how different AcWRW is from its counterparts. While the radii and surface areas of AcWWW, AcWFW and AcWYW were comparable, the radius of AcWRW was considerably smaller and its surface area substantially greater. However, all four peptides had similar volumes (Table 3.2).

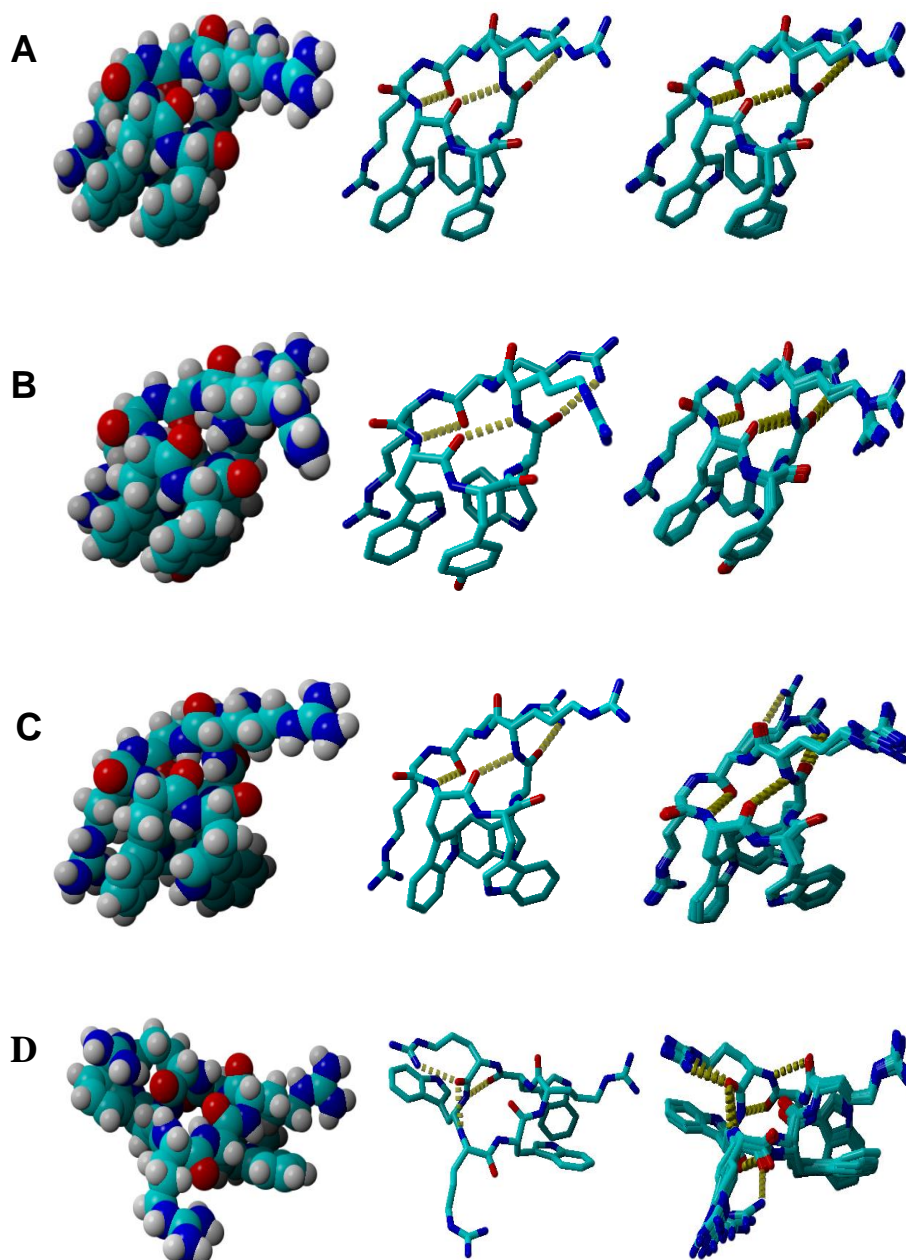


Figure 3.2: *Low energy structural models of linear RW-hexapeptides*

A) cFWF, B) cWYW, C) cWWW and D) cWRW. The images, from left to right, depict ball models, stick models with the backbone hydrogen bonding highlighted and overlays of 15 lowest energy model structures. Carbon atoms are depicted in light blue, nitrogen in dark blue, oxygen in red and hydrogen bonds in yellow. For simplicity, hydrogen atoms are not depicted in structures.

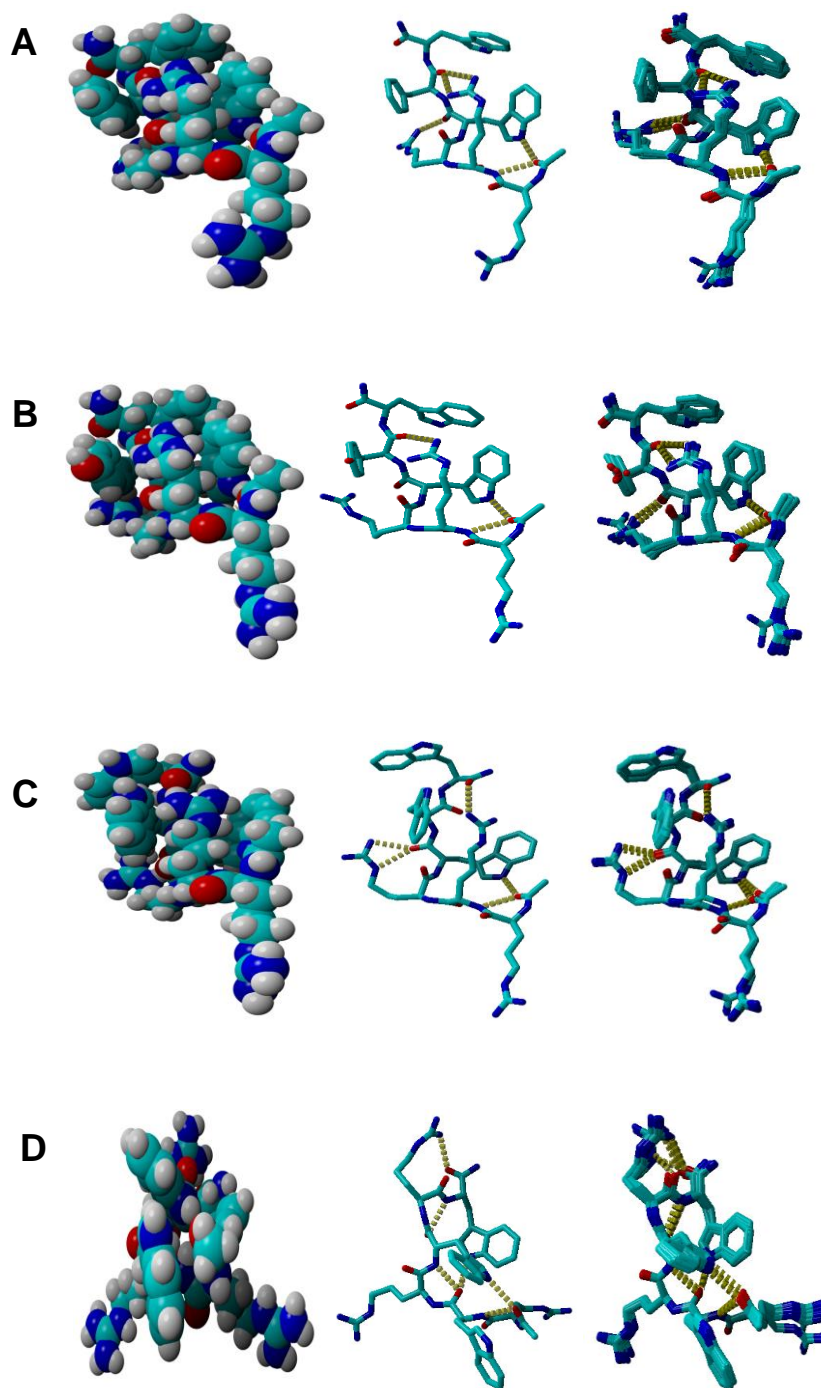


Figure 3.3: *Low energy structural models of linear RW-hexapeptides*

A) AcWFW, **B)** AcWYW, **C)** AcWWW and **D)** AcWRW. The images on the left depict ball models, middle images depict stick models with the backbone hydrogen bonding highlighted and images on the right depict overlays of 15 lowest energy model structures. Carbon atoms are depicted in light blue, nitrogen in dark blue, oxygen in red and hydrogen bonds in yellow. For simplicity, hydrogen atoms are not depicted in structures.

Table 3.2: Summary of the structural characteristics of the RW-hexapeptides derived from model structures

Peptide identity	Sequence	Type	Radius ^a (Å)	Surface area ^a (Å ²)	Volume ^a (Å ³)	Observed hydrogen bonding pattern ^b
Ac-KRK	Ac-KRKFW-NH ₂	linear	n.d ^c	n.d	n.d	n.d
Ac-RKK	Ac-RKKFW-NH ₂	linear	n.d	n.d	n.d	n.d
Ac-WFW	Ac-RRRWF-NH ₂	linear	15.03	931.94	1081.18	Ac-O:H(NE1)-Trp ⁴ , Ac-O:HN-Arg ² , Phe ⁵ -O:H ₁ N-Arg ² , Phe ⁵ -O:H ₂ N-Arg ² , Trp-O:H ₁ NArg ³
Ac-WRW	Ac-RWRWR-NH ₂	linear	12.77	993.13	1118.89	Ac-O:H(NE1)-Trp ⁴ , Ac-O:HN-Arg ² , Trp ² -O:HN-Trp ⁴ , Trp ² -O:H(NE1)-Trp ⁶ , Trp ⁴ -O:HN-Trp ⁶ , Trp ⁶ -O:H ₂ N-Arg ⁵
Ac-WWW	Ac-RRRWWW-NH ₂	linear	15.37	936.90	1111.43	Ac-O:H(NE1)-Trp ⁴ , Ac-O:HN-Arg ² , Trp ⁶ -O:H ₂ N-Arg ² , Trp ⁴ -O:H(NE)Arg ³ , Trp ⁴ -O:H ₁ N-Arg ³
Ac-WYW	Ac-RRRWYW-NH ₂	linear	15.35	943.22	1092.38	Ac-O:H(NE1)-Trp ⁴ , Ac-O:HN-Arg ² , Tyr ⁵ -O:H ₁ N-Arg ²
cKRK	KRKFW	cyclic	n.d	n.d	n.d	n.d
cRKK	RKKFW	cyclic	n.d	n.d	n.d	n.d
cWFW	RRRWF	cyclic	12.66	848.32	1017.31	Arg ⁵ -O:HN-Trp ¹ , Trp ¹ -O:HN-Arg ⁴ , Trp ³ -O:H ₂ N-Arg ⁵
cWRW	RWRWR	cyclic	12.98	919.61	1045.96	Arg ⁴ -O:H ₂ N-Arg ⁴ , Arg ⁴ -O:HN-Arg ⁶ , Trp ³ -O:HN-Trp ⁵
cWWW	RRRWWW	cyclic	12.40	871.58	1046.87	Arg ⁵ -O:HN-Trp ¹ , Trp ¹ -O:HN-Arg ⁴ , Trp ³ -O:H ₂ N-Arg ⁵
cWYW	RRRWYW	cyclic	12.04	845.79	1020.23	Arg ⁵ -O:HN-Trp ¹ , Trp ¹ -O:HN-Arg ⁴ , Trp ³ -O:H ₂ N-Arg ⁵

^aRadius, surface area and volume refer to the Van der Waals radius/surface/volume^b(NE1) refers to the amino group in the indole ring of Trp, NH refers to the amino group of the peptide backbone, NH₁ and NH₂ refer to the terminal amino groups on the Arg residues^cn.d refers to not determined

Analysis of peptide structure by Circular Dichroism

Natural cyclodecapeptides

The far UV CD spectra of the cyclodecapeptides highlighted two negative minima in the regions 208 ± 2 nm and 216 ± 2 nm, resembling spectra that are typical of α -helical structures and not β sheet structures (Figure 3.4). However, this was not an unexpected result as similar findings have been reported in literature [5,8,9]. The deviation of the CD spectra of the cyclodecapeptides from characteristic β -sheet CD spectra could be attributed to a combination of factors that interfere with CD of the peptide backbone. The aromatic amino acids present in the structures of the cyclodecapeptides possibly contribute to the atypical spectra. Aromatic amino acids are known for their optical absorption in the 210-240 nm region and several CD studies for proteins have highlighted the influence of aromatics on CD spectra in the far UV region [25–27]. For this reason, it is believed that the minima observed at the 216 ± 2 nm region could be strongly influenced by aromatic amino acids [5,9]. In addition to aromatic residues, the structures of the cyclodecapeptides consist of D-amino acid residues which most likely contribute to anomalous appearance of their CD spectra. The cyclic structures of the cyclodecapeptides are stabilised by type II β -turns which are also thought to have a contributory role towards distorting the shape of the CD spectra [28,29]. Furthermore, the cyclodecapeptides are well known for their tendency to self-assemble and form higher order structures in solution. It is thus believed that the aggregation state of the cyclodecapeptides potentially interferes with their CD spectra resulting in spectra that are unusual for β -sheet structures [8].

The two minima observed at 208 ± 2 nm and 216 ± 2 nm (Figure 3.4) are attributed to the presence of β -turns and β sheet structural elements respectively [26,28]. These two minima were of comparable negative ellipticity. In 50% TFE, a membrane mimicking solvent, the minima attributed to the β -turns were slightly blue shifted to 208 ± 2 nm and their negative ellipticities were greatly enhanced for all analogues. On the other hand, the intensity of the ellipticities at the 216 ± 2 nm minima were slightly enhanced for YA and YB while it was reduced for YC and WC. This is indicative of the higher proportion of sheet structures in the Phe-containing cyclodecapeptides relative to the analogues that lack Phe residues. The increased negative ellipticity at the 208 ± 2 nm minima indicate stabilisation of the β -turn structural elements. This conforms to the widely known secondary structure stabilising effect of TFE [28]. TFE promotes intramolecular hydrogen bonding by reducing the competitive effect of water for the peptide hydrogen bonds [4].

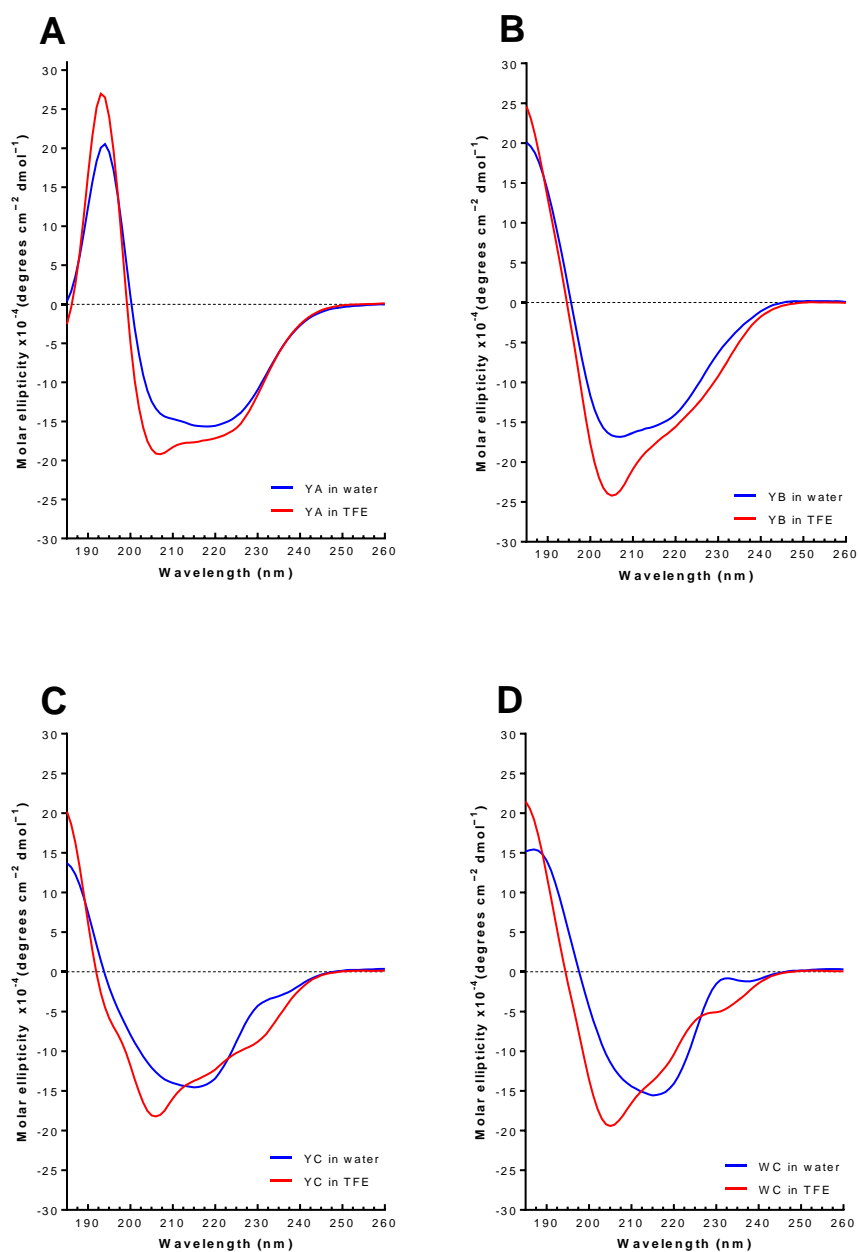


Figure 3.4: Far UV CD spectra of the cyclodecapeptide analogues [100 μ M] in an aqueous environment (water) and membrane mimicking environment (50% TFE).

A) Tyrocidine A (YA) with Phe³, Phe⁴ and Tyr⁷, **B)** Tyrocidine B (YB) with Phe³, Trp⁴ and Tyr⁷, **C)** Tyrocidine C (YC) with Trp³, Trp⁴ and Tyr⁷, **D)** Tryptocidine C (WC) with Trp³, Trp⁴, and Trp⁷. Blue curves represent CD spectra of peptides in water while red curves represent CD spectra of peptides in 50% TFE. Each CD spectra is an average of triplicate determinations.

An additional spectral feature (maximum) was observed in water for two of the Trp⁴-containing cyclodecapeptides, YC and WC which is absent in the Phe-containing peptides, YA and YB. This maximum was observed at approximately 230 nm and was well defined for WC while it appeared as a shoulder in YC. This spectral feature has previously been attributed to the contributory effect

of Trp residues because of the strong absorption of the indole ring in this spectral region. Moreover, the absence of this maximum in YA that contains no Trp-residues further strengthens the notion that this spectral feature is due to Trp residues [8]. Inversion of the 230 nm maximum to a negative minimum was observed in 50% TFE. This change in the appearance of the bands could also be indicative of changes in the orientation of the Trp side chains with respect to the peptide backbone[9].

All four cyclodecapeptides exhibited positive maxima in the lower wavelength regions of the CD spectra. For YB and YC, the maxima fell outside the CD spectral region (<185 nm) for both water and 50% TFE. For YA and WC in aqueous environment, the positive maxima were at 194 nm and 187 nm, respectively. These maxima were slightly blue shifted to 193 nm and 185 nm respectively in the TFE membrane mimicking environment. A positive maximum in the 180 nm – 190 nm region is representative of π - π^* transitions of the peptide bond [6,30].

The ellipticity ratio $\theta_{208}/\theta_{216}$ can provide important information about structural changes. The ellipticity ratios of all analogues in TFE were >1 and followed the order WC>YC>YB>YA, which is also related to the Trp content illustrating the influence of aromatic residues (Figure 3.5). Unfortunately, due to the varying contributions of the different aromatic residues towards the ellipticity at 216 nm, it is not feasible to compare the ellipticity ratios of the different cyclodecapeptides. However, comparisons can be made between the ellipticity ratios of a single peptide when in water and in 50% TFE. Changes in the ellipticity ratios can indicate alterations in the backbone structure and/or formation of higher order structures [5,9,10]. The ellipticity ratios of all the cyclodecapeptide analogues were enhanced in the TFE membrane mimicking environment implying a decreased proportion of β -sheet structures relative to β -turn structures (Figure 3.5). It is possible that TFE-induced changes in the conformation led to the formation of intermolecular hydrogen bonds and as a result the formation of higher order sheet structures. Intramolecular hydrogen bonding seems to have been promoted by TFE as indicated by the enhancement of β -turn minima at 208 nm. This change in the ellipticity ratios could be attributed to new hydrogen bonded networks that are not only β -structures, since TFE is known to promote the formation of ordered structures and hydrogen bonding [4]. YA was least influenced by solvent change which suggests that the more hydrophobic YA already had a more ordered conformation in water than the Trp-containing analogues.

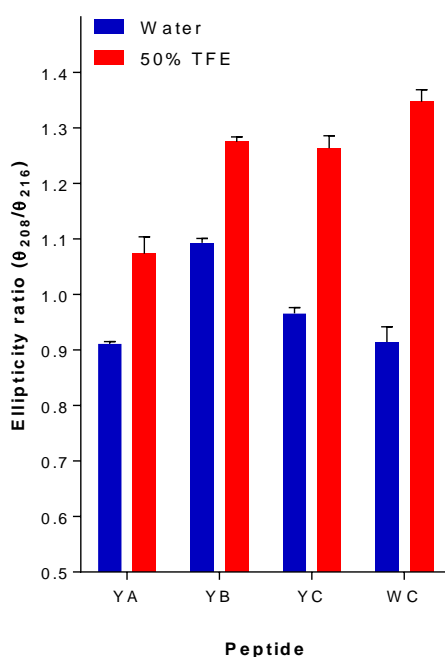


Figure 3.5: Changes in the ellipticity ratios ($\theta_{208}/\theta_{216}$) of the cyclodecapeptides induced by a membrane-mimicking environment.

Ellipticity ratios of the peptides in an aqueous environment and membrane mimicking environment are depicted in blue and red respectively. Each ratio is a mean value calculated from three spectra with error bar depicting the standard error of the mean (SEM).

It was not possible to determine the content of the different secondary structure fractions in the cyclodecapeptides from the CD spectra. This is because CDPro, a software that analyses CD spectra to estimate the content of structural elements, is not suitable to analyse oligopeptides/polypeptides consisting of unnatural and/or D-amino acids because they are not represented within its databases.

The CD of aromatic amino acids in the near UV spectral region (250 nm – 320 nm) can be utilised as a fingerprint for tertiary structure [6]. Changes in the tertiary structure often cause changes in the local environment of these aromatics which in turn leads to changes in their CD spectra [31]. It should be noted that near UV CD has the potential to detect major changes in the tertiary structure of peptides even though there may be no apparent change in the secondary structure [31,32]. This is because the tertiary structure is influenced by the orientation of side chains whereas the backbone orientation determines the secondary structure.

Although it seems as if the backbone conformations of the four cyclodecapeptides are quite stable and rigid, as expected for cyclic peptides (refer to Figure 3.1), the self-assembly structures (i.e.

dimers and higher oligomers) formed by the oligomerisation of peptide monomers are dynamic and their formation relies on both backbone interactions and interactions between the amino acid side chains. It has been shown through ESMS that the cyclodecapeptides have a high propensity to form dimers in aqueous solution, with the dimers being more dominant in the more hydrophobic analogues (YA and YB) than the polar analogues (YC and WC) [9,10]. It has been proposed that these dimers may be the active structures responsible for the antimicrobial activity of the cyclodecapeptides [10,11]. X-ray crystallography studies and NMR studies showed that the dimers are stabilised by hydrogen bonds and hydrophobic interactions between their monomeric units [10,11]. Moreover, aromatic residues play a key role in stabilising the dimer structures as they are involved in both intramolecular (residue 3) and intermolecular hydrogen bonding (residues 1 and 7) [10,11]. As such, near UV CD spectroscopy can be employed to monitor the character of aromatic amino acids in self-assembly structures such as dimers and higher order oligomers in different environments (Figure 3.5).

For YA, the shift to a membrane mimicking environment resulted in a loss of resolution of the near UV peaks observed in the aqueous environment. Moreover, the shape of the spectrum in the 260-290 nm was inverted indicating reorientation of the Tyr side-chain which could potentially indicate changes in the Tyr-dependent self-assembly structures of YA.

The spectra of YB were comparable in both solvent environments except for a slight blue shift and reduced intensity of the ellipticity between 250-260 nm in the TFE environment. This difference alludes to an altered orientation of the Phe residues. The similar near UV spectra in both solvent environments implies that the environment has little influence on the self-assembly structures of YB whose formation involves the participation of aromatic amino acid residues.

The near UV CD spectra for YC and WC showed increased ellipticity in the wavelength region between 270-290 nm (Figure 3.6). As Trp and Tyr residues are known to produce peaks in this spectral region [6], the observed enhanced ellipticities could be attributed to altered orientations of these aromatic residues. In addition, for both peptides, the shape of the peak at about 260 nm was inverted and the ellipticity decreased which is suggestive of changes in the local environment of the Phe residues. Just like YA and YB, this could potentially indicate changes in the aromatic residue-dependent self-assembly structures of YC and WC.

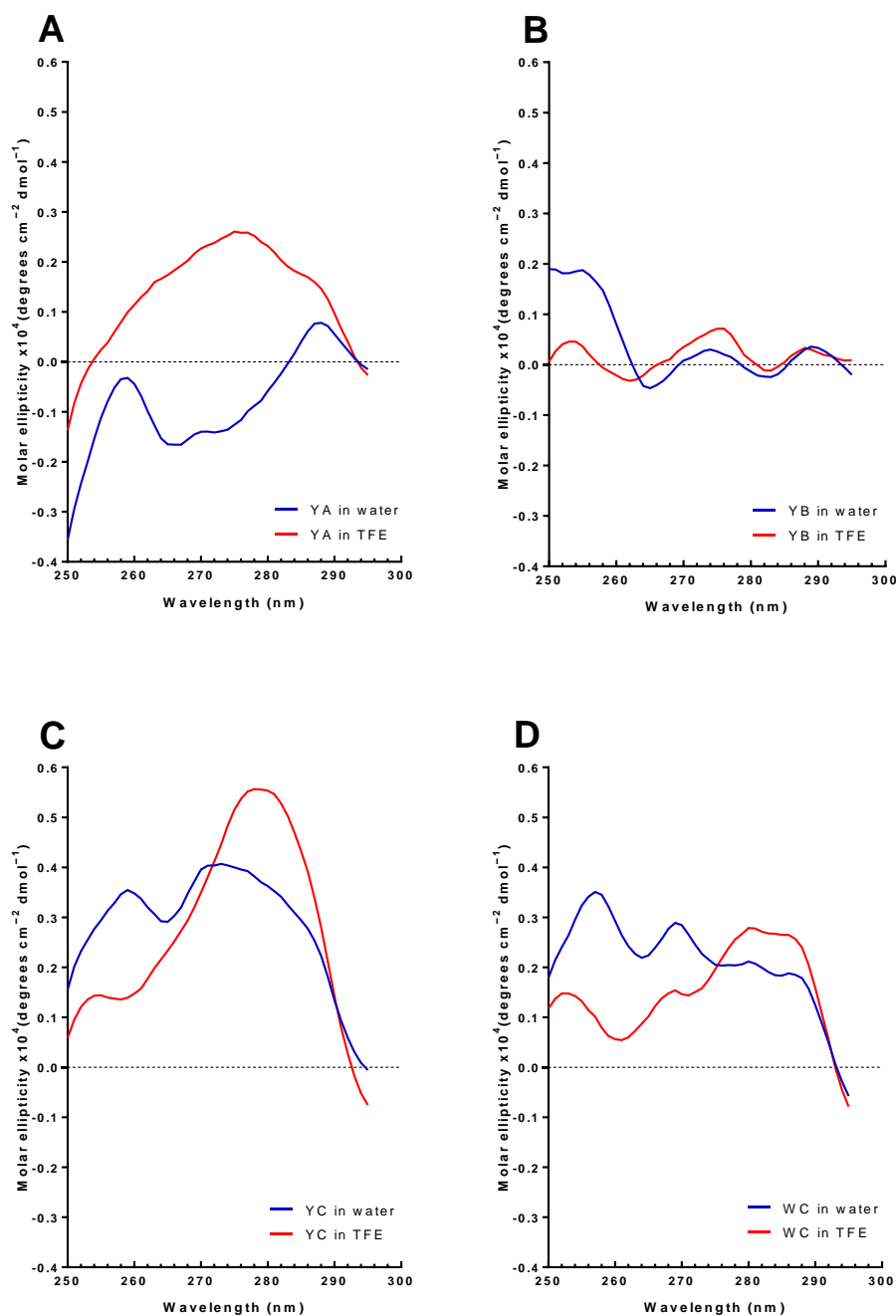


Figure 3.6: Near UV CD spectra of the cyclodecapeptide analogues [100 μM] in an aqueous environment (water) and membrane mimicking environment (50% TFE).

A) Tyrocidine A (YA) with Phe³, Phe⁴ and Tyr⁷, **B)** Tyrocidine B (YB) with Phe³, Trp⁴ and Tyr⁷, **C)** Tyrocidine C (YC) with Trp³, Trp⁴ and Tyr⁷, **D)** Tryptocidine C (WC) with Trp³, Trp⁴, and Trp⁷. Blue curves represent CD spectra of peptides in water while red curves represent CD spectra of peptides in 50% TFE. Each CD spectra is an average of triplicate determinations.

RW-hexapeptides

As with the tyrothricin-derived cyclodecapeptides, the CD spectra of the RW-hexapeptides are also anomalous. None show any clear conformity to the spectra that characterise regular structural elements such as β -sheets and α -helices. Like the cyclodecapeptides, the RW-hexapeptides are rich in aromatic side chains which can interfere with the amide CD of the peptide backbone thereby distorting the shape of the CD spectra. Moreover, according to the molecular modelling that was done for these hexapeptides, their structures consist of γ -turns. These γ -turns possibly contribute to the unusual appearance of the CD spectra of these peptides since there currently is no reference spectra for the characterisation of γ -turns.

The far UV CD spectra of the cyclic analogues in aqueous environment show minima at 203 ± 1 nm which is characteristic of β -turns (Figure 3.7). This result is consistent with previous observations [13,14,33] and can be correlated to the β -turns depicted in the molecular models discussed above. A second minimum was observed at approximately 214 nm for cWRW (Figure 3.7D), as well as for the Phe- and Lys-containing analogues (Figure 3.7 A, B and C). The minimum was observed at 225 nm and 221 nm for cWWW and cWYW respectively (Figure 3.7E and F). This second minimum can be attributed to β -sheet structures in the peptide backbone. The combination of the two minima denotes a β -turn/ β -sheet motif [4,28,29]. The second minimum can also be attributed to the contributions from the aromatic residues. This is because the CD within the 210-240 nm region can be influenced by the contribution of aromatic residues, especially Tyr and Trp, which are known to have profound absorption in this region [25]. Therefore, contributions from Tyr and Trp residues in the middle position of the aromatic tripeptide moieties of cWYW and cWWW respectively would account for the red shift, as well as the increased negative ellipticity observed at this second minimum relative to the other analogues. The analogues with Phe in this position have a reduced negative ellipticity because the absorption of Phe is not as strong as that of the other two aromatic amino acids. The intensity of this second minimum is also reduced on the cWRW spectrum because the residue in the fifth position is Arg. In 50% TFE, the negative ellipticity of both minima were enhanced. This indicates increased backbone constraints leading to stabilisation of the turn structures and β -sheet structures which is consistent with the reported stabilising effect of TFE-containing solutions on β -hairpin and β -turn structures [28,34]. For the second minimum, the enhanced ellipticity as well as the subtle red/ blue shifts could also point to changes in the orientation of the aromatic side chains.

The spectra of the Phe-containing hexapeptides appeared sufficiently similar in both water and 50% TFE alluding to a conserved structure amongst these analogues. The spectra of cWYW were also quite comparable to the spectra of the Phe-containing analogues. The only difference was the enhanced ellipticity of the second minimum which could be attributed to the contribution of its Tyr residue. This also shows how structurally similar cWYW is to the Phe-containing analogues. The molecular models also depict a conserved structure between cWFW and cWYW thereby corroborating the findings from CD.

The general shape of the CD spectra of cWWW appears considerably different from that of the Tyr and Phe-containing analogues. This difference in shape suggests a different backbone configuration for the cWWW analogue. However, based on the model structures which depict a conserved backbone structure for cWWW, cWFW and cWYW, it is expected that the CD spectra of cWWW would resemble that of the other two analogues. Interestingly, the CD spectra of the analysed cWWW preparation appear to resemble those of the linear analogue, AcWWW (discussed below). From this, it can be concluded that the cyclisation process during peptide synthesis may not have been successful and as such some of the peptide in the preparation might still be in its linear form. Additionally, the ellipticity of the cWWW preparation was observed to be substantially weaker than the ellipticities of the other cyclic analogues (Figure 3.7E). The reason for this could be the purity of this cWWW preparation (referred to as cWWW3 in Chapter 2).

From the ESMS analysis (Chapter 2), it was established that the peptide preparation showed a signal 20-fold below the signals of the other peptides. As we were unable to obtain a UPLC-MS analysis, it could mean that the preparation contained only about 5% peptide, which is well below acceptable standard of purity (must be $\geq 90\%$ peptide composition as determined by UPLC-MS). It, therefore, means that the concentration of the correct peptide was considerably less than what was calculated which resulted in the weak MS and CD signals. This is unfortunate, as the initial cWWW peptide batch (referred to as cWWW1 in Chapter 2) from Dr Margitta Dathe showed a high purity, but we had a limited amount of this peptide and it was used as one of our model peptides in Chapter 4. It is unclear which components are contributing to the mass that was weighed out for this cWWW3 peptide preparation, but it is quite possible that the supplier's synthesis procedure led to a modified peptide product with the same molecular mass as cWWW, with some residual linear peptide.

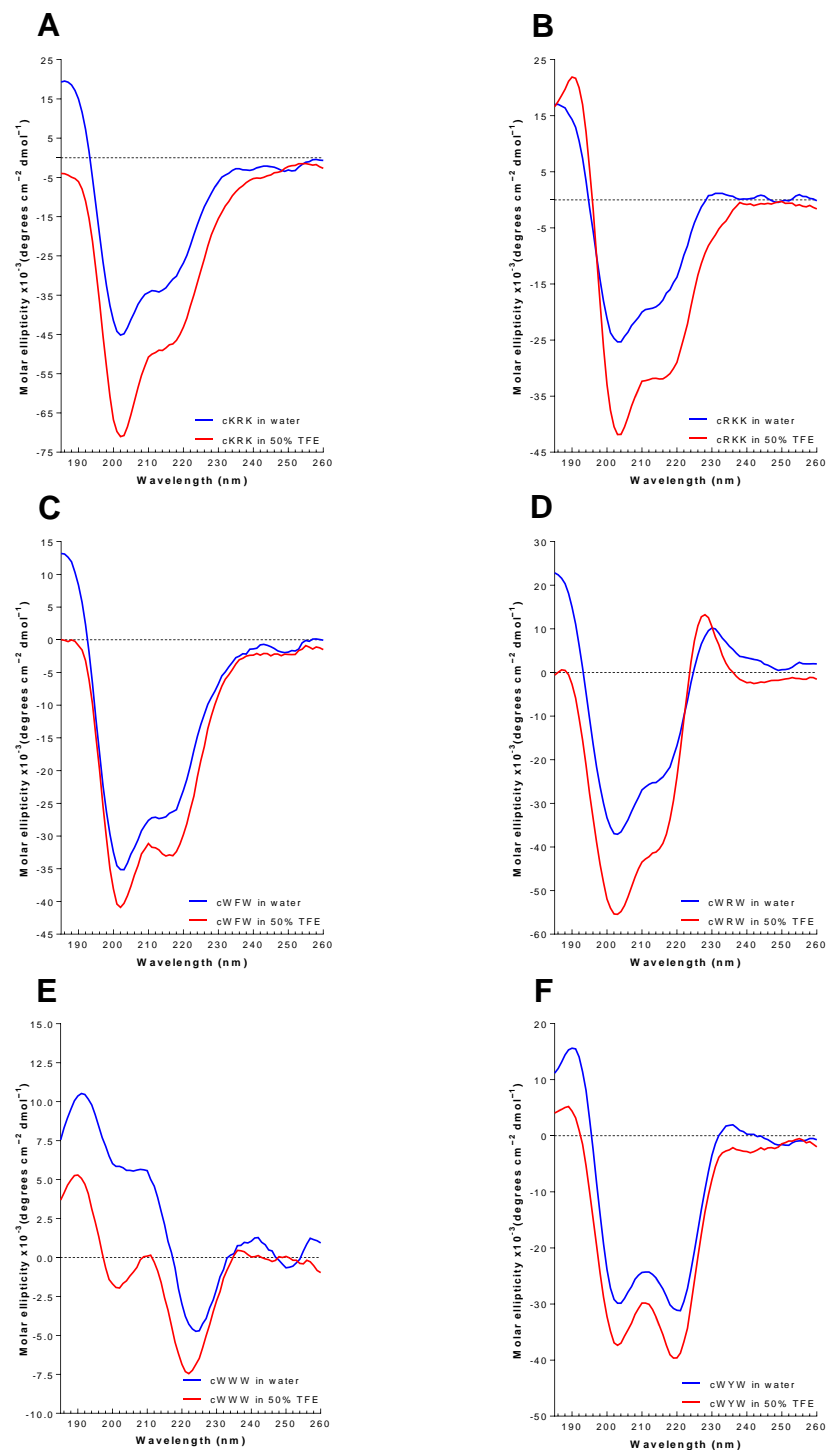


Figure 3.7: Far UV CD spectra of the cyclic RW-hexapeptide analogues at [100 μM] in an aqueous environment (water) and membrane mimicking environment (50% TFE).

A) cKRK, B) cRKK, C) cFWW, D) cWRW, E) cWWW and F) cWYW. Blue lines represent CD spectra of peptides in water while red lines represent CD spectra of peptides in 50% TFE. Each CD spectrum is an average of triplicate determinations.

cWRW was the only cyclic analogue whose spectra showed a pronounced positive maximum band at 230 nm in water and 228 nm in 50% TFE (Figure 3.7F). This maximum can also be attributed to contribution of Trp residues [32] due to the observed blue shift in the membrane mimicking environment. The exclusivity of this maximum to the spectra of cWRW highlights how structurally different this peptide is from the other analogues, which correlates well the structures of the molecular models discussed above.

The CD spectra of the linear analogues were significantly different from those of the cyclic analogues (Figure 3.8). For the Phe-containing analogues (Figure 3.8A-C) and the Tyr-containing analogues (Figure 3.8F), the CD spectra in water had three visible bands; one negative minimum at 196 ± 1 nm, a shoulder with negative ellipticity at 213 ± 1 nm and a positive maximum at 228 ± 1 nm. The combination of a negative minimum at 196 ± 1 nm and a positive maximum at 228 ± 1 nm is typical of irregular/undefined structural elements [14]. The positive maximum as well as the shoulder at 213 ± 1 nm could also represent the contributions from aromatic residues. The shoulder at 213 ± 1 nm cannot possibly be attributed to β -sheet structural elements because the analysis of secondary structure of the molecular models did not yield any β -sheet elements. Moreover, previous research has shown that structures of linear RW-hexapeptides in solution are undefined [13,14]. In a hydrophobic environment, the shapes of the CD spectra changed drastically and appeared to resemble the CD spectra of the cyclic analogues. The intensity of the negative minima at 196 ± 1 nm was reduced and red shifted to approximately 200 nm, the shoulders at 213 ± 1 nm were converted to defined minima and red shifted to 217 nm and the positive maxima at 228 ± 1 nm disappeared. These changes indicate changes in the peptide backbone structure and possible changes in the orientation of aromatic side chains [13,14]. Thus, it can be deduced that hydrophobic nature of 50% TFE induced a disordered to more ordered conformational transition in the linear RW-hexapeptides. Interestingly, the spectra of AcWWW were found to be quite comparable to that of its cyclic analogue, with minor variations (Compare Figure 3.8E with Figure 3.7E). In water, the CD spectrum of AcWWW exhibited two minima at 197 nm and 225 nm while in 50% TFE the first minimum was red shifted to 200 nm and the second was blue shifted to 223 nm. In comparison with the CD spectra of cWWW, which highlighted its minima at 202 nm and 225 nm in water and at 201 nm and 221 nm in 50% TFE, an apparent similarity is evident. This further corroborates the earlier assumption that the cWWW from the second batch was, in fact, not a cyclic peptide.

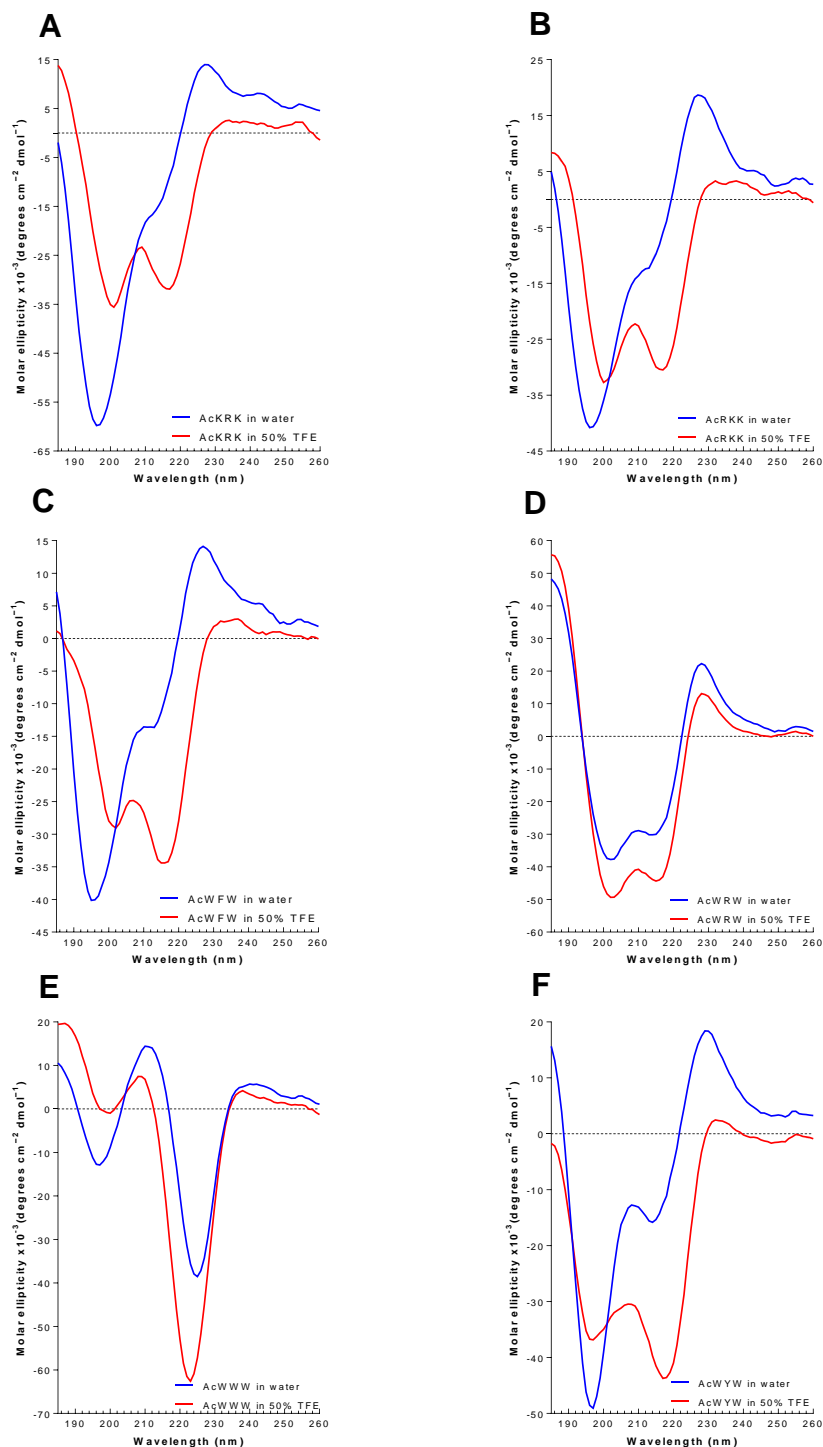


Figure 3.8: Far UV CD spectra of the linear RW-hexapeptide analogues at [100 μM] in an aqueous environment (water) and membrane mimicking environment (50% TFE).

A) AcKRK, B) AcRKK, C) AcWFW, D) AcWRW, E) AcWWW and F) AcWYW. Blue curves represent CD spectra of peptides in water while red curves represent CD spectra of peptides in 50% TFE. Each CD spectrum is an average of triplicate determinations.

For AcWRW, the shape of the spectra is virtually the same as that of the cyclic analogue (compare Figure 3.8D with Figure 3.7D). Based on this and the molecular models, it is plausible to conclude that the structures of the linear and cyclic analogues of WRW are undefined in both aqueous and membrane mimicking environments.

The CD spectra were analysed using CDPro software package to estimate the composition of various secondary structure fractions. The analysis did not yield any clear correlation with the analysis of secondary structure of the molecular models, except that both did not identify helical structures. The reason for this could be that the databases used by this software do not include structures for cyclic peptides and oligopeptides with a high content of aromatic residues thus, the software fails to accurately interpret the spectra data of such peptides. Moreover, proteins and peptides with secondary structures such as γ -turns are not well represented in the software's databases. This means that the software is unable to recognise these structural elements and may interpret them as undefined structures. On the other hand, the molecular models were constructed from basic principles using the YASARA 2 algorithm that has also been built from a protein database. The molecular models only considered intramolecular bonds, even though intermolecular bonds could also take place in solution leading to hydrogen-bonded networks and sheet structures. Because of these shortcomings, the absolute contribution of the secondary structures predicted by the CDPro and YASARA software packages must be considered with caution. The results from these calculations and prediction of secondary structures are given in Table 3.3.

Table 3.3: Analysis of secondary structure of RW-hexapeptides (H – α -helix, S – β -sheet, T – turns, U – undefined/irregular structures. The calculated/predicted content of these secondary structural elements is expressed in percentages.)

Peptide Identity	Secondary structural elements											
	CD (Water)				CD (50% TFE)				YA SARA			
Structure	H	S	T	U	H	S	T	U	H	S	T	U
Ac-KRK	0.1	61.7	2.2	36.1	0	27.1	7.6	65.4	n.d			
cKRK	0	61.5	16.9	21.6	0	56.1	33.8	10	n.d			
Ac-RKK	0.1	74.1	2.7	23.1	0	28.2	7.6	64.1	n.d			
cRKK	0.1	42.2	13.4	44.3	0	41.4	58.5	0	n.d			
Ac-WFW	0	42.4	3.7	53.8	0	27.6	16.9	55.5	0	0	0	100
cWFW	0	20.5	26	53.5	0	4.7	27	68.2	0	66.7	33.3	0
Ac-WRW	0.1	96.6	3.3	0	0	84.5	0.9	14.6	0	0	0	100
cWRW	0.1	85.3	1	13.6	0	83.9	12.9	3.3	0	0	0	100
Ac-WWW	0	9.1	3.8	87.1	0.1	14.1	7.6	78.1	0	0	0	100
cWWW	0	27.0	7.2	65.8	0	11.6	15.9	72.4	0	66.7	33.3	0
Ac-WYW	0	47.4	0	52.6	0.1	13.7	17.6	68.5	0	0	0	100
cWYW	0	32.5	3.9	63.6	0.2	32.5	19.5	47.9	0	66.7	33.3	0

If we assume that the undefined structures are actually γ -turns or new hydrogen bonded networks in TFE, then the increase in these structures, as calculated by CDPro, for most of the peptides is explained. YASARA predicted sheet and turn structures for the cyclic peptides cWYW, cWWW and cWFW. This correlated with the CDPro analysis if we only consider the results of cWYW and cWFW (as cWWW is impure), which indicated β -sheets and β -turn structures in water and/or TFE correlating with the model prediction. YASARA failed to predict the β -sheets in the linear peptides and cWRW, which could indicate that these structures are intermolecular structures in solution, as calculated with CDPro from the CD spectra.

Characterisation of the Trp environment using fluorescence spectroscopy

Natural cyclodecapeptides

In addition to CD spectroscopy, fluorescence spectroscopy was employed to gain more insight into the structural characteristics of the cyclodecapeptides in environments with different polarities. Trp fluorescence was used due to the sensitivity of the indole ring to changes in its local environment [15]. Trp experiences a fluorescence emission maximum at approximately 350 nm in water, but this maximum is blue shifted when exposed to a more hydrophobic environment [15,16]. Therefore, changes in the spectral properties of tryptophan can be used to report its location within a peptide. In turn, changes in the location of Trp residues are indicative of conformational changes within the peptide (or protein) [15].

A decrease in the total fluorescence intensity (quenching) was noted for all cyclodecapeptides when transferred from water to the TFE membrane mimicking environment relative to the aqueous environment (Figures 3.9 and 3.10). Fluorescence quenching occurs through a host of molecular interactions which include collisional quenching, energy transfer, ground state complex formation and excited state reactions [15]. The occurrence of fluorescence quenching concomitantly with a blue shift is usually associated with stacking of aromatic rings [15]. Aromatic stacking could have been facilitated by the enhanced β -turns and β -sheet structures in the TFE environment which might have caused aromatic residues to be close enough to allow stacking. Furthermore, the Trp residues could possibly be in the proximity of other chemical groups that can possibly quench their fluorescence via excited state reactions [17,35]. However, caution ought to be applied when interpreting data relating to the quenching of Trp fluorescence in TFE containing solvents as TFE has been shown to quench indole fluorescence by excited state proton transfer reactions [34]. Therefore, the observed fluorescence quenching might not necessarily be due to changes in peptide conformation but rather the quenching effect of TFE.

The three Trp-containing cyclodecapeptides showed very similar fluorescence maxima in water (Table 3.4 & Figure 3.10). All of them displayed emission maxima at 340 nm. The fact that the emission maxima of these Trp residues are blue shifted from the expected 350-353 nm when in water shows that the Trp residues are not completely exposed to water but are partially in a hydrophobic environment [16]. In 50% TFE, the maxima were blue shifted to 334 nm for YB and YC, and to 338 nm for WC. The blue shifts indicated that local environment of the Trp residues changed to a more hydrophobic one implying a change in their orientation. YA does not contain any Trp residues, therefore the fluorescence observed after excitation at 280 nm was due to its single Tyr residue. The fluorescence emission maximum of Tyr residues exposed to water is usually observed at 303 nm [15]. In this instance, the maximum was blue shifted to below 300 nm indicating that in the native conformation of the peptide, the Tyr is only partially exposed to the aqueous environment (Figure 3.9A). Because the fluorescence emission maximum fell outside the spectral range, the effect of the membrane mimicking environment on the emission could not be determined.

Table 3.4: Effect of changing the local environment of Trp residues on the fluorescence emission of the cyclodecapeptides

Peptide	$\lambda_{em\ max} \text{ (nm)}$		$\Delta \lambda_{em\ max} \text{ (nm)}$
	In water	In 50% TFE	
YA	<300	<300	0
YB	340	334	6
YC	340	334	6
WC	340	338	2

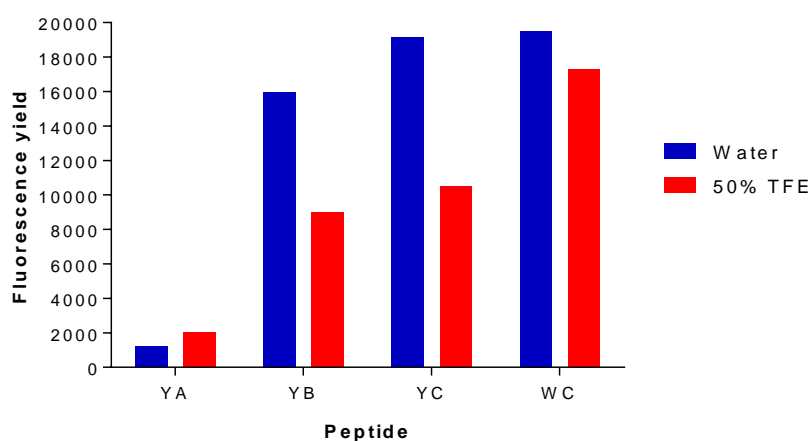


Figure 3.8: Total fluorescence yields of the cyclodecapeptide analogues with excitation at 280 nm. Fluorescence yields were obtained from emission spectra by calculating area under the curve. Blue bars are representative of the fluorescence yield produced by peptides in an aqueous environment (water) while red bars are representative of the fluorescence yield produced by peptides in a membrane-mimicking environment (50% TFE).

The observed changes in the fluorescence emission properties of the Trp side chains of YC and WC correlate well with the observed changes in their near UV CD spectra (refer to Figure 3.6). The CD spectra of both peptides in TFE highlighted enhanced ellipticities in the 280-290 nm region indicating changes in the orientation of the Trp residues which were substantiated by the observed blue shifts and reduced fluorescence yields in TFE. On the other hand, while similar changes were observed in the fluorescence emission properties of the Trp residues of YB, the near UV CD spectra of the peptide in the two solvent environments do not depict any appreciable changes with respect to the orientation of its Trp residues.

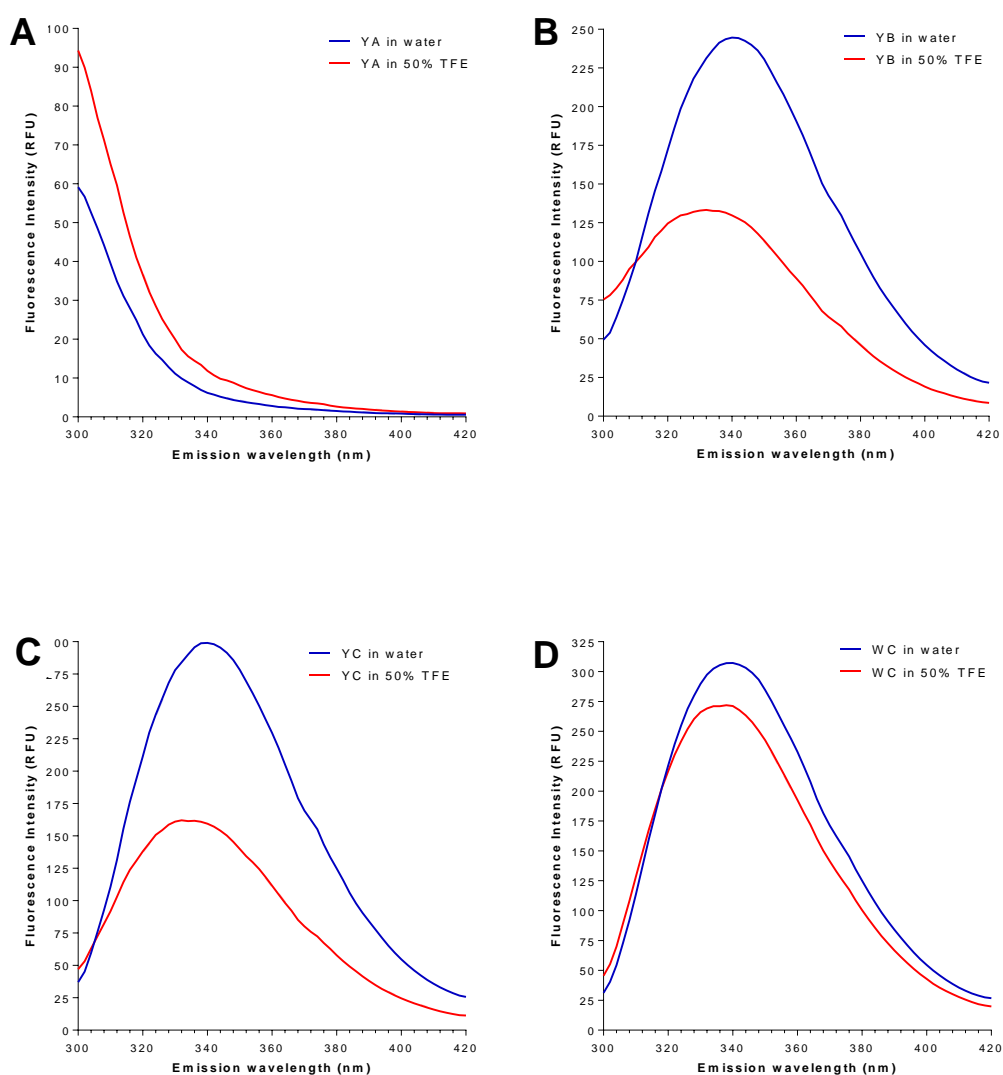


Figure 3.10: Fluorescence emission spectra of cyclodecapeptides for excitation at 280 nm

A) Tyrocidine A (YA) with Phe³, Phe⁴ and Tyr⁷, **B)** Tyrocidine B (YB) with Phe³, Trp⁴ and Tyr⁷, **C)** Tyrocidine C (YC) with Trp³, Trp⁴ and Tyr⁷, **D)** Tryptocidine C (WC) with Trp³, Trp⁴, and Trp⁷. Blue lines represent emission spectra of peptides in water while red lines represent emission spectra of peptides in 50% TFE. Fluorescence intensity is indicated in relative fluorescence units (RFU). Each fluorescence emission spectrum is an average of triplicate determinations.

RW-hexapeptides

In general, all peptides displayed maximum fluorescence emission between 348-346 nm and 346-342 nm regions in water and 50% TFE respectively (Figure 3.11, Table 3.5). The blue shift denotes a change in the environment within which Trp residues reside. This correlates well with data from CD analyses which show enhanced ellipticity of the minima localised in the 210-230 nm region when the peptides are in 50% TFE. Both observations allude to changes in the orientation of aromatic side chains and ultimately altered peptide conformations.

Table 3.5: Effect of changing the local environment of Trp residues on the fluorescence emission of RW-hexapeptides

Peptide sequence	Cyclic		$\Delta \lambda_{em\ max}$ (nm)	Linear		$\Delta \lambda_{em\ max}$ (nm)
	$\lambda_{em\ max}$ (nm)			$\lambda_{em\ max}$ (nm)		
	In water	In 50% TFE		In water	In 50% TFE	
KRKFWW	346	342	4	348	342	6
RKKFWW	348	344	4	348	342	6
RRRFWW	346	342	4	348	344	4
RWRWRW	346	342	4	346	342	4
RRRWWW	348	342	6	348	346	2
RRRWYW	346	342	4	348	346	2

The fluorescence intensities and total fluorescence yields of the linear analogues in an aqueous environment versus a membrane mimicking environment were generally comparable except for AcWRW whose fluorescence intensity and yield were enhanced by the membrane mimicking environment (Figures 3.11 & 3.12B). On the other hand, the 50% TFE led to quenching of the fluorescence intensities and decreased the total fluorescence yields of most of the cyclic analogues (Figures 3.11 & 3.11B). The molecular models of the cyclic analogues showed that the aromatic residues are clustered together in an amphipathic configuration (Refer to Figure 3.6). This proximity of aromatic residues may be responsible for the quenching effect, possibly as a consequence of aromatic ring stacking.

The fluorescence intensity and the total fluorescence yield of the cWWW analogue was appreciably reduced in comparison to the rest of the RW-hexapeptides. This confirms that the concentration of the Trp fluorophore was very low in solution which is attributable to the low purity of the peptide preparation.

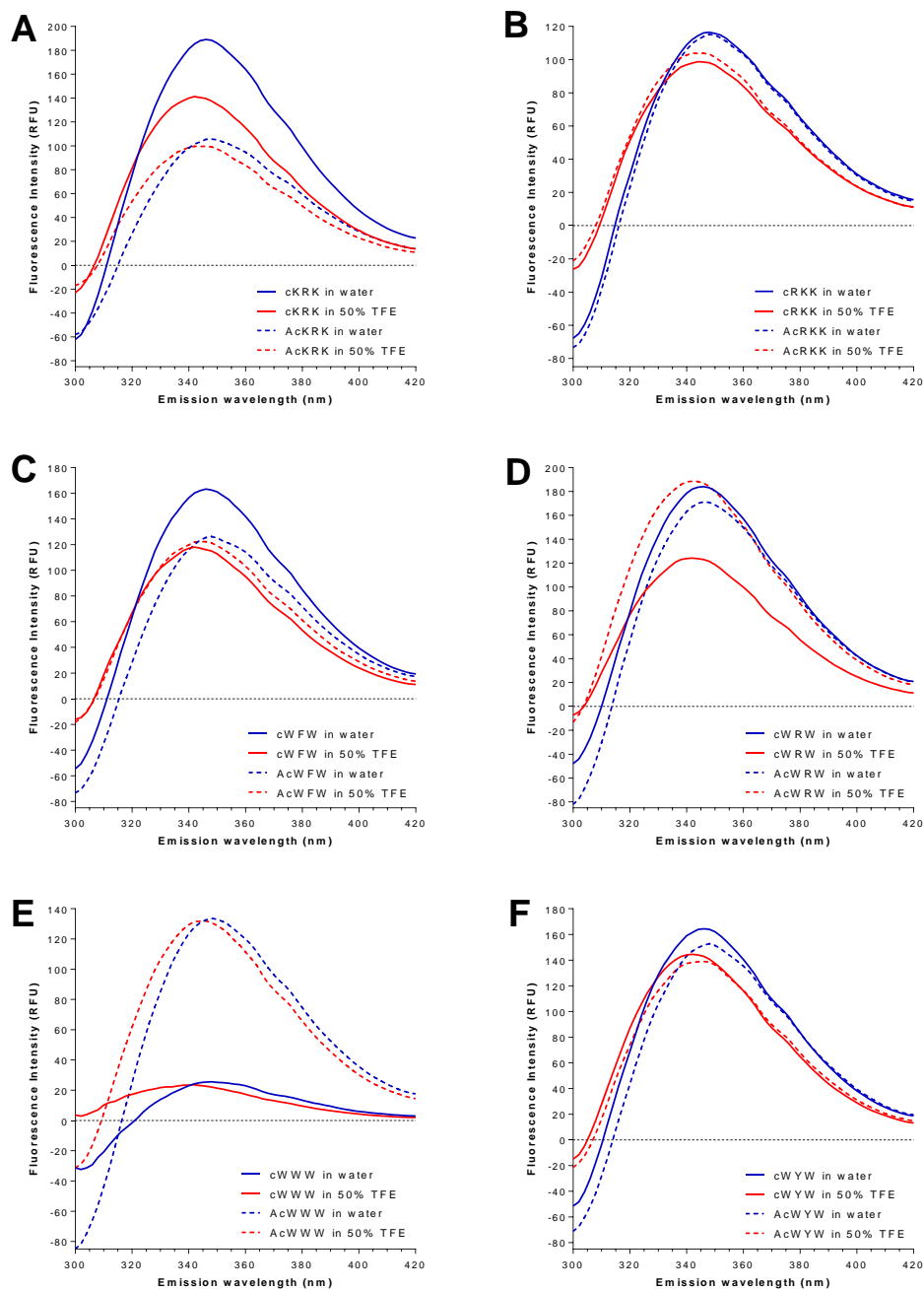


Figure 3.10: Fluorescence emission spectra of the RW-hexapeptides for excitation at 280 nm. A)-F) are fluorescence emission spectra of the cyclic and linear analogues of the same peptide. A) KRKFW, B) RKKFW, C) RRRFW, D) RWRWRW, E) RRRWW and F) RRRWYW. Blue lines represent emission spectra of peptides in water while red lines represent emission spectra of peptides in 50% TFE. Fluorescence intensity is indicated in relative fluorescence units (RFU). Each fluorescence emission spectrum is an average of triplicate determinations.

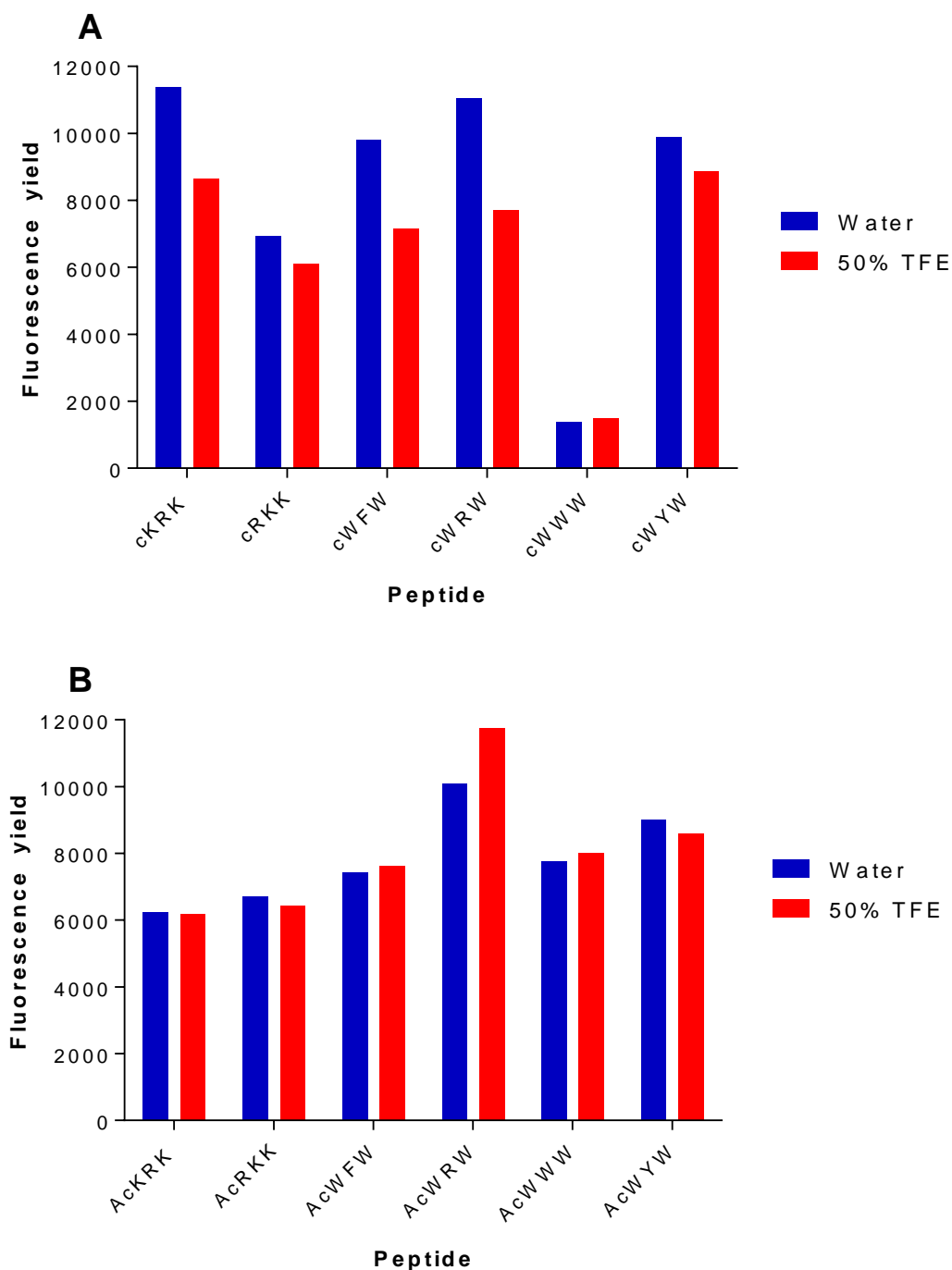


Figure 3.11: Total fluorescence yields of RW-hexapeptides for excitation at 280 nm

A) Fluorescence yields of the cyclic analogues, **B)** Fluorescence yields of the linear analogues. Fluorescence yields were obtained from emission spectra by calculating area under the curve. Blue bars are representative of the fluorescence yield produced by peptides in an aqueous environment (water) while red bars are representative of the fluorescence yield produced by peptides in a membrane-mimicking environment (50% TFE).

The fluorescence yields of the cyclic analogues, with the exception of the impure cWWW (cWWW3 preparation, refer to chapter 2), were generally higher than those of the linear analogues in the aqueous environment. This observation could be attributed to the more pronounced amphipathic configuration of the cyclic analogues brought about by the clustering of their aromatic residues. By clustering together, the exposure of the aromatic residues to water molecules is reduced hence the enhanced fluorescence yields. In TFE, however, it is not clear which group of analogues had the greatest fluorescence yields. The reason for this could be the adoption of similar structural conformations by analogues from both groups as indicated by CD spectroscopy.

3.5 Conclusion

Characterisation of the secondary structure of cyclo-decapeptides by CD spectroscopy confirmed their β -sheet structure even though their CD spectra are anomalous. The spectra exhibited two negative minima at 208 ± 2 nm and 216 ± 2 nm corresponding to β -turn and β -sheet structural elements. It is believed that the distorted β -sheet spectra are a result of the combined contribution of the aromatic sidechains, β -turns, D-amino acid residues and the aggregation of peptides in solution, all of which interfere with the CD of the peptide backbone. It was shown that in a hydrophobic environment as represented by 50% TFE, the β -turn elements of the cyclo-decapeptides are stabilised. Furthermore, the increased ellipticity ratio $\theta_{208}/\theta_{216}$ indicates increased proportions of β -turn structures relative to β -sheet structures. The near UV CD spectra of the cyclo-decapeptides clearly depicted the changes in the orientation of the aromatic residues induced by changes in the environment. Changes in the orientation of aromatic side chains are indicative of changes in tertiary structure [15], and in the case of the cyclodecapeptides this could point to increased self-assembly into oligomers placing the aromatic residues in a different environment.

For the Trp-containing cyclodecapeptides, further evidence of changes in the solution structure in a hydrophobic environment was obtained via fluorescence spectroscopy. Emission maxima were blue-shifted and quenching of fluorescence was observed in the membrane mimicking environment clearly indicating changes in the local environment of the Trp residues and hence an altered tertiary conformation.

The structural differences between the cyclic and linear analogues of the RW-hexapeptides were highlighted. In aqueous solution, cyclic analogues were found to consist of sheet and turn elements whereas the linear analogues had an undefined structure. In TFE, the cyclic analogues maintained their structure indicating a stable backbone structure while the structure of the linear analogues changed and appeared to resemble that of the cyclic analogues. This shows that a membrane

mimicking environment induces a transition from irregular to ordered structures. The exceptions to this were both WRW analogues whose structures were undefined, possibly containing a number of γ -turns in both aqueous and membrane mimicking environments. This highlights the influence of the amino acid sequence on structure. The amino acid sequence of WRW analogues is characterised by alternating Arg and Trp residues whereas the amino acid sequences of the other analogues consist of two domains; the polar and hydrophobic domains. TFE also induced changes in the orientation of aromatic side chains. This was highlighted by the changes in the intensity of the ellipticity in the 210-230 nm region on the CD spectra. Furthermore, fluorescence spectroscopy also showed that the emission maxima of the RW-hexapeptides were blue shifted in 50% TFE indicating an altered orientation of Trp side-chains. Differences in structure between the linear and cyclic analogues were also highlighted by the fact that the fluorescence emission of the cyclic analogues was quenched in the TFE environment whereas the emission of the linear analogues was not affected.

The structural properties of the cyclodecapeptides and RW-hexapeptides will be correlated to their biological activity in Chapter 4.

3.6 References

- [1] S. Rotem, I. Radzishovsky, A. Mor, Physicochemical properties that enhance discriminative antibacterial activity of short dermaseptin derivatives, *Antimicrobial Agents and Chemotherapy*, 50 (2006) 2666–72.
- [2] P.M. Hwang, H.J. Vogel, Structure-function relationships of antimicrobial peptides, *Biochemistry and Cell Biology*, 76 (1998) 235–246.
- [3] M. Jelokhani-Niaraki, E.J. Prenner, C.M. Kay, R.N. McElhaney, R.S. Hodges, Conformation and interaction of the cyclic cationic antimicrobial peptides in lipid bilayers, *Journal of Peptide Research*, 60 (2002) 23–36.
- [4] M. Jelokhani-Niaraki, E.J. Prenner, C.M. Kay, R.N. McElhaney, R.S. Hodges, L.H. Kondejewski, Conformation and other biophysical properties of cyclic antimicrobial peptides in aqueous solutions, *Journal of Peptide Research*, 58 (2001) 293–306.
- [5] B. Spathelf, Qualitative structure-activity relationships of the major tyrocidines, cyclic decapeptides from *Bacillus aneurinolyticus*, PhD Thesis, Department of Biochemistry, University of Stellenbosch, (2013), <http://hdl.handle.net/10019.1/4001>
- [6] S.M. Kelly, T.J. Jess, N.C. Price, How to study proteins by circular dichroism, *Biochimica et Biophysica Acta - Proteins and Proteomics*, 1751 (2005) 119–139.
- [7] N.J. Greenfield, Using circular dichroism spectra to estimate protein secondary structure, *Nature Protocols*, 1 (2007) 2876–2890.

- [8] S. Laiken, M. Printz, L.C. Craig, Circular dichroism of the tyrocidines and gramicidin S-A, *Journal of Biological Chemistry*, 244 (1969) 4454–4457.
- [9] J.A. Vosloo, Optimised bacterial production and characterisation of natural antimicrobial peptides with potential application in agriculture, PhD Thesis, Department of Biochemistry, University of Stellenbosch, (2016), <http://hdl.handle.net/10019.1/98411>
- [10] G. Munyuki, G.E. Jackson, G.A. Venter, K.E. Kövér, L. Szilágyi, M. Rautenbach, B.M. Spathelf, B. Bhattacharya, D. Van Der Spoel, β -sheet structures and dimer models of the two major tyrocidines, antimicrobial peptides from *Bacillus aneurinolyticus*, *Biochemistry*, 52 (2013) 7798–7806.
- [11] P.J. Loll, E.C. Upton, V. Nahoum, N.J. Economou, S. Cocklin, The high resolution structure of tyrocidine A reveals an amphipathic dimer, *Biochimica et Biophysica Acta - Biomembranes*, 1838 (2014) 1199–1207.
- [12] C. Appelt, A. Wessolowski, J.A. Söderhäll, M. Dathe, P. Schmieder, Structure of the antimicrobial, cationic hexapeptide cyclo(RRWRF) and its analogues in solution and bound to detergent micelles, *ChemBioChem*, 6 (2005) 1654–1662.
- [13] M. Dathe, H. Nikolenko, J. Klose, M. Bienert, Cyclization increases the antimicrobial activity and selectivity of arginine- and tryptophan-containing hexapeptides, *Biochemistry*, 43 (2004) 9140–9150.
- [14] M. Bagheri, S. Keller, M. Dathe, Interaction of W-substituted analogs of cyclo-RRRWFW with bacterial lipopolysaccharides: The role of the aromatic cluster in antimicrobial activity, *Antimicrobial Agents and Chemotherapy*, 55 (2011) 788–797.
- [15] J.R. Lakowicz, *Principles of Fluorescence Spectroscopy*, Springer US, Boston, MA, 2006, 10.1007/978-0-387-46312-4
- [16] E.A. Burstein, N.S. Vedenkina, M.N. Ivkova, Fluorescence and the location of tryptophan residues in protein molecules, *Photochemistry and Photobiology*, 18 (1973) 263–279.
- [17] Y. Chen, M.D. Barkley, Toward understanding tryptophan fluorescence in proteins, *Biochemistry*, 37 (1998) 9976–9982.
- [18] E. Krieger, G. Koraimann, G. Vriend, Increasing the precision of comparative models with YASARA NOVA-a self-parameterizing force field, *Proteins: Structure, Function, and Bioinformatics*, 47 (2002) 393–402.
- [19] A. Chen, V.T. Moy, Cross-linking of cell surface receptors enhances cooperativity of molecular adhesion, *Biophysical Journal*, 78 (2000) 2814–2820.
- [20] M. Wenzel, M. Rautenbach, J.A. Vosloo, T. Siersma, C.H.M. Aisenbrey, E. Zaitseva, W.E. Laubscher, W. van Rensburg, J.C. Behrends, B. Bechinger, L.W. Hamoen, The multifaceted antibacterial mechanisms of the pioneering peptide antibiotics tyrocidine and gramicidin S, *MBio*, 9 (2018) 1–20.
- [21] A.N.-N. Leussa, Characterisation of small cyclic peptides with antimalarial and antilisterial activity, PhD Thesis, Department of Biochemistry, University of Stellenbosch, (2014), <http://hdl.handle.net/100191/86161>

- [22] C. Appelt, A. Wessolowski, M. Dathe, P. Schmieder, Structures of cyclic, antimicrobial peptides in a membrane-mimicking environment define requirements for activity, *Journal of Peptide Science*, 14 (2008) 524–527.
- [23] W. Jing, H.N. Hunter, J. Hagel, H.J. Vogel, The structure of the antimicrobial peptide Ac-RRWRF-NH₂ bound to micelles and its interactions with phospholipid bilayers, *Journal of Peptide Research*, 61 (2003) 219–229.
- [24] A.J. Rezansoff, H.N. Hunter, W. Jing, I.Y. Park, S.C. Kim, H.J. Vogel, Interactions of the antimicrobial peptide Ac-FRWWHR-NH₂ with model membrane systems and bacterial cells, *Journal of Peptide Research*, 65 (2005) 491–501.
- [25] C. Krittani, W.C. Johnson, Correcting the circular dichroism spectra of peptides for contributions of absorbing side chains, *Analytical Biochemistry*, 253 (1997) 57–64.
- [26] R.W. Woody, Circular dichroism, in: *Methods in Enzymology*, 1995: pp. 34–71.
- [27] M.C. Manning, R.W. Woody, Theoretical study of the contribution of aromatic side chains to the circular dichroism of basic bovine pancreatic trypsin inhibitor, *Biochemistry*, 28 (1989) 8609–8613.
- [28] L.H. Kondejewski, M. Jelokhani-Niaraki, S.W. Farmer, B. Lix, C.M. Kay, B.D. Sykes, R.E.W. Hancock, R.S. Hodges, Dissociation of antimicrobial and hemolytic activities in cyclic peptide diastereomers by systematic alterations in amphipathicity, *Journal of Biological Chemistry*, 274 (1999) 13181–13192.
- [29] D.L. Lee, J.P.S. Powers, K. Pfliegerl, M.L. Vasil, R.E.W. Hancock, R.S. Hodges, Effects of single D-amino acid substitutions on disruption of β -sheet structure and hydrophobicity in cyclic 14-residue antimicrobial peptide analogs related to gramicidin S, *Journal of Peptide Research*, 63 (2004) 69–84.
- [30] S. Kelly, N. Price, The use of circular dichroism in the investigation of protein structure and function, *Current Protein & Peptide Science*, 1 (2000) 349–384.
- [31] A.J.S. Jones, Analysis of polypeptides and proteins, *Advanced Drug Delivery Reviews*, 10 (1993) 29–90.
- [32] N. Sreerama, M.C. Manning, M.E. Powers, J.X. Zhang, D.P. Goldenberg, R.W. Woody, Tyrosine, phenylalanine, and disulfide contributions to the circular dichroism of proteins: Circular dichroism spectra of wild-type and mutant bovine pancreatic trypsin inhibitor, *Biochemistry*, 38 (1999) 10814–10822.
- [33] K. Scheinpflug, H. Nikolenko, I. V. Komarov, M. Rautenbach, M. Dathe, What goes around comes around: a comparative study of the influence of chemical modifications on the antimicrobial properties of small cyclic peptides, *Pharmaceuticals*, 6 (2013) 1130–1144.
- [34] Y. Chen, B. Liu, M.D. Barkley, Trifluoroethanol quenches indole fluorescence by excited-state proton transfer, *Journal of the American Chemical Society*, 117 (1995) 5608–5609.
- [35] J.H. Lakey, E.M. Raggett, Measuring protein—protein interactions, *Current Opinion in Structural Biology*, 8 (1998) 119–123.

Chapter 4

Characterisation of biological activity and mode of action of natural cyclodecapeptides and synthetic RW-hexapeptides

4.1 Introduction

The recent years have seen an unprecedented rise in the population of immunocompromised individuals [1]. Concomitantly, there has been a surge in the incidence of fungal infections. Of great concern are the invasive fungal infections due to their extremely high mortality rates [2]. An example of such infections is invasive aspergillosis which is caused by the human fungal pathogen, *A. fumigatus*. Invasive aspergillosis poses the greatest challenge in cancer and transplant patients. More than 50% of individuals that are diagnosed with this infection succumb to it, even when they receive treatment. However, in the absence of treatment, the case fatalities can be 100% [2,3]. The fact that the mortality rates are still very high despite treatment highlights the limitations of the existing antifungal therapeutic arsenal. Because of this, novel therapeutic options with alternative mechanisms of action are urgently required for the effective management of invasive fungal infections.

Antimicrobial peptides (AMPs) can potentially be the armament required in the fight against invasive fungal infections. AMPs are rendered attractive for therapeutic development by their high antimicrobial potency, rapid killing kinetics, which involve the utilisation of multiple modes of action and limited potential for the development of resistance [4,5]. Furthermore, AMPs can possibly improve the activity of conventional therapeutics thus making them attractive for use in combination therapy [6]. A plethora of natural and synthetic AMPs with antifungal activity have been discovered, but the focus of this investigation are the tyrocidines and analogues (natural cyclodecapeptides) and the synthetic RW-hexapeptides.

The tyrocidines and analogues are a group of structurally related cyclodecapeptides that were discovered as part of the tyrothricin complex that was isolated from cultures of a soil bacterium, *Bacillus brevis* [7], later reclassified as *Brevibacillus parabrevis* [8]. Since their discovery over seven decades ago, these cyclodecapeptides have illustrated broad spectrum antimicrobial activity [7,9–14]. Nonetheless, there is very little literature on the antifungal activity of the natural cyclodecapeptides. Most of the work on the characterisation of their antifungal activity has been done by our group [12–14].

The synthetic RW-hexapeptides are a relatively new group of AMPs that are derivatives of a linear hexapeptide (Ac-RRWWRF-NH₂) that was identified in the screening of a synthetic combinatorial library [15]. Their amino acid sequences closely resemble a motif that is recurrent in some natural AMPs such as lactoferricin, indolicidin and tritrypticin and to which their antimicrobial activity has been attributed. The RW-hexapeptides have exhibited tremendous antibacterial activity against Gram-positive and Gram-negative bacteria [11,16–18]. A few of the linear RW-hexapeptide analogues were found to have antifungal activity [19–21], but the antifungal activity of the cyclic RW-hexapeptides remains uncharacterised.

The need for the development of new antifungal agents coupled with the largely unexplored antifungal potential of the cyclodecapeptides and the RW-hexapeptides was the motivation for this investigation. In this chapter, the characterisation of the biological activity of the aforementioned peptides, as well as a partial characterisation of their mode of action are presented.

4.2 Materials

Peptides utilised in this study were purified and characterised as described in Chapter 2. These included two tyrocidine analogues (YA, YB) and tryptocidine C (WC), as well as the twelve synthetic RW-hexapeptides. Five of the six cyclic RW-hexapeptide preparations were donated by Dr Margitta Dathe (Leipzig Institute, Germany), while cWYW and the six linear peptide preparations were from GL-Biochem (Shanghai, China). Gramicidin S (GS) was purchased from Sigma Aldrich (Steinheim, Germany). *Aspergillus fumigatus* ATCC 204305 was obtained from the American Type culture Collection (ATCC) (Manassas, VA, USA). Sterile water was prepared by reverse osmosis followed by filtration through a Millipore MilliQ® water purification system (Milford, USA). Potato dextrose broth (PDB), agar, and Tween-20 were supplied by Fluka (Buchs, Switzerland). Polypropylene 96-well microtiter black plates were purchased from Nunc (Roskilde, Denmark) while polystyrene 96-well microtiter clear plates were obtained from Corning Incorporated (Corning, USA). Sterile petri dishes were obtained from Lasec (South Africa) and Falcon tubes were supplied by Becton Dickson Labware (Lincoln Park, USA). Sigma Aldrich (St Louis, USA) supplied gentamycin, RPMI 1640 medium, resazurin sodium salt and 2',7'-dichlorofluorescein diacetate (H₂DCFDA). SYTOX Green was from Lonza (Walkersville, USA) while ascorbic acid was obtained from Roth (Karlsruhe, Germany). Components of phosphate buffered saline (KH₂PO₄, Na₂HPO₄, NaCl and KCl) as well as ethanol (>99.8%) were supplied by Merck (Darmstadt, Germany). A+ packed erythrocytes from anonymous donors (containing 300 mL erythrocytes, 100 mL saline-adenine-glucose-mannitol red blood cell preservation solution

and 63.0 mL citrate phosphate dextrose anticoagulant) were obtained from the Western Cape Blood Services in South Africa.

4.3 Methods

Peptide preparation

Dry, analytically weighed aliquots of peptides were used to make up peptide solutions. Preparation of 4.00 mM stock solutions of the natural cyclodecapeptides was done by dissolving dry peptide aliquots in 60% (v/v) EtOH in water. This was followed by a 4× dilution step to achieve a final peptide concentration of 1.00 mM in 15% (v/v) EtOH in water. Stock solutions (1.00 mM) of the synthetic peptides were prepared by dissolving dry aliquots of peptide into water. Gramicidin S was prepared either like the cyclodecapeptides or the hexapeptides. All peptide preparations were done in pyrolyzed glassware to limit contamination with detergents and pyrogens. All the prepared peptide solutions (1.00 mM) were subjected to serial doubling dilution steps in 96-well microtiter plates so that the peptide concentration ranged between 1.00 mM – 0.0078 mM. Dilutions were carried using the same solvent in which the peptides had been dissolved.

For the studies that were performed using peptide combinations, 1.00 mM stock solutions of tryptocidine C (WC) and each of the selected RW-hexapeptides (cWWW, cWRW, AcWWW and AcWRW) were mixed together in a 1:1 ratio so that the concentration of each peptide in the mixture was 0.5 mM. Serial doubling dilutions of these peptide combinations were then prepared so that the final peptide concentration range in the dilution plate was 0.5 mM – 0.0039 mM.

Culturing of fungi and spore harvesting

Aspergillus fumigatus was cultured from dormant spores. Cultures were grown at 25 °C on potato dextrose agar (PDA) plates containing gentamycin for 10 days until sporulation. Spores were harvested using 5 ml of sterile Tween-20 water (0.1%, v/v). They were left to hydrate overnight at 4 °C prior to counting using a haemocytometer. A spore concentration of 2.0×10^4 spores/mL was used in all the assays.

Microdilution broth assays to investigate inhibition of the germination and growth of *A. fumigatus* spores

Spore suspensions containing 2.0×10^4 spores/mL were prepared in half-strength potato dextrose broth (50% PDB in water; v/v) solutions. Subsequently, 90 µL of spore suspensions were pipetted into the wells of microtiter plates followed by the addition of 10 µL of peptide solutions. The growth control wells contained spore suspensions but received no peptide. Instead, they received

10 µL of 15% EtOH or sterile water for the assays involving cyclodecapeptides and hexapeptides respectively. To control for sterility, 10 µL of either 15% EtOH or sterile water were added to 90 µL of spore free 50% PDB. These wells represented the background. Microtiter plates were then covered with aluminium foil and incubated at 25 °C for 48 hours after which light dispersion was spectrophotometrically determined at 595 nm using a Spark™ 10M multimode microplate reader. Growth inhibition was determined according to the following equation:

$$\% \text{ growth inhibition} = 100 - \frac{100 \times (A_{595} \text{ of well} - \text{mean } A_{595} \text{ of background})}{(\text{mean } A_{595} \text{ of growth wells} - \text{mean } A_{595} \text{ of background})}$$

Microdilution broth assays to determine metabolic inhibition of *A. fumigatus* hyphae

The activity of selected peptides (wC, cWWW, cWRW, AcWRW and AcWWW) against *A. fumigatus* hyphae was determined by measuring the effect of peptide treatment on fungal metabolic activity. This was achieved by using resazurin as a metabolic indicator. Spores of *A. fumigatus* (2.0×10^4 spores/mL) were incubated in 96-well black microtiter plates containing 50% PDB solution (90 µL/well) at 25 °C for 30 h to get hyphae growing. To control for sterility, four wells on the microtiter plate received 50% PDB media without spores. Hyphae were then treated for two hours with either 10 µL of peptide solutions in 15% EtOH or 10 µL of 15% EtOH. Gramicidin S was the activity control for metabolic inhibition. Subsequently, hyphae were washed three times with phosphate-buffered saline (PBS). This was followed by the addition of resazurin solution (10 µL of 1.0 mg resazurin sodium salt in 1.00 mL water) to 90 µL of PBS- hyphae suspension. Following a 3-hour incubation at 37 °C in the dark, fluorescence readings were taken using the Spark™ 10M multimode microplate reader with excitation and emission wavelengths set at 540 nm and 590 nm respectively. Inhibition of metabolic activity was calculated as follows:

$$\% \text{ metabolic inhibition} = 100 - \frac{100 \times (Em_{590} \text{ of well} - \text{mean } Em_{590} \text{ of background})}{(\text{mean } Em_{590} \text{ of metabolically active} - \text{mean } Em_{590} \text{ of background})}$$

with the background being represented by the wells that contained no hyphae and the metabolically active wells represented by wells that contained hyphae but received no peptide treatment.

Haemolysis assay

Preparation of human erythrocytes was done according to a previously described methodology [22]. Briefly, with strict adherence to ethical regulations, A+ packed erythrocytes were obtained from the Western Cape Blood Services in South Africa. The erythrocytes were washed twice with RPMI media and the remaining cells were resuspended in the RPMI media. Prior to the assay, the

erythrocyte suspension was briefly centrifuged at 1200×g for 3 minutes. Subsequently, a 2% haematocrit suspension was prepared by adding erythrocytes to PBS solution in a falcon tube. Into the wells of 96-well microtiter plates was pipetted 90 µL of the haematocrit suspension followed by 10 µL of peptide solutions. Preparation of peptide solutions was exactly as for the antifungal assays. The controls for haemolysis activity were gramicidin S (100% haemolysis) and sterile water (0% haemolysis). The erythrocyte-containing microtiter plates were incubated at 37 °C for 2 hours after which they were centrifuged at 900×g for 10 minutes. From them, 10 µL of supernatant was extracted and added to 90 µL of fresh PBS in microtiter plates. Subsequently, optical absorbance at 415 nm was spectrophotometrically determined using a Spark™ 10M multimode microplate reader. Haemolytic activity was determined as follows:

$$\% \text{ haemolysis} = 100 \times \frac{(A_{415} \text{ of well} - \text{mean } A_{415} \text{ of background})}{(\text{mean } A_{415} \text{ of complete lysis} - \text{mean } A_{415} \text{ of background})}$$

Time course kinetic study to investigate membrane permeabilisation

Spores of *A. fumigatus* in 5% PDB solution (2×10^4 spores/mL) were left to grow at 25 °C for 30 hours. Hyphae were then treated with 10× stock solutions of peptide (0.25 mM) prepared as described above. Simultaneously, SYTOX Green dye was added to the hyphae at a final concentration of 0.5 µM. Measurement of fluorescence emission was immediately commenced using a Spark™ multimode microplate reader with 485 nm and 538 nm set as the excitation and emission wavelengths respectively. Fluorescence readings were taken over a 60-minute period with 2-minute intervals. Sterile water was used as the no lysis control while WC was the control for total lysis.

Spectrofluorometric determination of ROS production

Spores of *A. fumigatus* (2.0×10^4 spores/mL) were incubated for 30 hours at 25 °C in 96-well microtiter plates containing 90 µL of 50% PDB. Hyphae were then treated with 10 µL of 10× stock solutions of peptides resulting in final concentrations ranging from 100.0 µM to 0.78 µM. Hyphae that served as the negative controls for peptide treatment were treated with the same volume of 15% EtOH. Treated hyphae were incubated at 25 °C for 3 hours after which the hyphae were washed three times with phosphate-buffered saline (PBS). Ten microlitres of 2',7'-dichlorofluorescein diacetate (H₂DCFDA) were then added to 90 µL of a PBS-hyphae suspension and incubated for a further 1 hour at 37 °C. Accumulation of reactive oxygen species (ROS) was determined by measuring fluorescence emission using the Spark™ 10M multimode microplate reader with excitation and emission wavelengths set at 485 nm and 540 nm respectively. To

determine whether the observed fluorescence was due to accumulation of ROS induced by peptides, hyphae were pre-treated with peptide in the presence of ascorbic acid (10 mM) before incubation with H₂DCFDA.

Data Analysis

GraphPad Prism® 6.0 (GraphPad software, San Diego, USA) was used to plot data from dose response assays. Data from growth inhibition, metabolic inhibition and haemolysis assays were fitted onto sigmoidal curve using non-linear regression. The curves were defined by the equation:

$$Y = \frac{\text{bottom} + (\text{top} - \text{bottom})}{1 + 10^{\log IC_{50} \times \text{Activity slope}}}$$

All curves had a slope set to <7. The midpoint between top and bottom plateaus represents the IC₅₀ or HC₅₀, which are activity parameters representing the concentrations necessary to cause 50% growth and metabolic inhibition or 50% haemolysis.

The IC₅₀ values calculated from data of the dose response assays involving peptide combinations were used to calculate fractional inhibitory concentrations (FIC) and fractional inhibitory indices (FICI). FICI values are used to classify the type of interactions between the peptides in combination mixture as synergistic, antagonistic or additive. The interactions are indicated as follows: FICI ≤ 0.5 indicates absolute synergism, 1 > FICI > 0.5 indicates slight synergism, FICI = 1 indicates additive or no interactions, 1 < FICI < 4 indicates slight antagonism and FICI ≥ 4 indicates absolute antagonism [11,23]. The equations below represent how the FIC and FICI are calculated;

$$FIC (A) = \frac{IC50 (A \text{ in } A + B \text{ combination})}{IC50 \text{ of } A \text{ alone}}$$

$$FIC (B) = \frac{IC50 (B \text{ in } A + B \text{ combination})}{IC50 \text{ of } B \text{ alone}}$$

$$FICI = FIC (A) + FIC (B)$$

Data from the membrane permeability kinetic assay was plotted onto a one phase association curve according to the equation:

$$Y = Y_{max} \times (1 - e^{(-K.X)})$$

Statistical data analysis was also done using GraphPad Prism® 6.0. The analyses included standard error of the mean (SEM), one-way ANOVA and multiple t-tests.

4.4 Results and Discussion

Part 1: Characterisation of biological activity

*Growth inhibition of *A. fumigatus* spores*

The growth inhibitory activity of three cyclodecapeptides (YA, YB and WC) and twelve RW-hexapeptides against *A. fumigatus* spores was characterised. Due to the low yield obtained from semi-preparative RP-HPLC, YC was depleted during structural characterisation (described in Chapter 3) hence its biological activity could not be assessed. Gramicidin S (GS), an analogous cyclodecapeptide with 50% sequence identity to the Trcs, was utilised as the positive control for antifungal activity in all experiments. Antifungal activity was determined by considering the two activity parameters, IC_{50} and IC_{max} which define the concentrations causing 50% and 100% growth inhibition respectively. IC_{max} is calculated from the dose response curve and represents a calculated MIC (minimum inhibitory concentration).

Cyclodecapeptides

All the cyclodecapeptides potently inhibited the growth of *A. fumigatus* spores (Table 4.1). Their growth inhibitory activity was characterised by IC_{50} and IC_{max} values in the low micromolar range (<10 μ M). The potency of the cyclodecapeptides followed the trend YB>YA>WC. In a study conducted by Vosloo [24], a similar trend was observed, albeit slightly lower IC_{50} and IC_{max} values were reported for the growth inhibition of *A. fumigatus* spores. Antifungal activity of all cyclodecapeptides was comparable and there were no statistically significant differences in their IC_{50} values ($P>0.05$; refer to Table 4.6 in addendum for statistical analysis). This can be attributed to the high similarity in amino acid sequence as well the conserved β -sheet structure among the cyclodecapeptide analogues [24–26]. Furthermore, antifungal activity seems to be modulated by amphipathicity. Comparison of the UPLC retention times (Chapter 2) of the three cyclodecapeptide analogues shows YB to be the intermediate analogue in terms of hydrophobicity and hydrophilicity suggesting a higher degree of amphipathicity.

RW-hexapeptides

For peptides designed to target bacterial pathogens [11], the cyclohexapeptides displayed profound growth inhibitory activity towards *A. fumigatus*, as summarised in Table 4.1. For all but cRKK, the IC_{50} and IC_{max} values were <10 μ M and ≤ 20 μ M respectively, indicating a close similarity in their activity. The two most active analogues were cWWW and cWRW, unlike with antibacterial activity where cFWW was found to be the most active analogue (Table 4.1).

Nevertheless, the antifungal activity of cWFW was not significantly different from that of cWWW and cWRW ($P > 0.05$; refer to Table 4.7 in addendum for statistical analysis).

The two most active peptides, cWRW and cWWW, contain the same amino acid residues, which are Arg and Trp, but differ in the order of arrangement of these residues. Based on the potent activity displayed by these two RW-hexapeptide analogues, it can therefore be hypothesised that Arg and Trp are the two most important residues for antifungal activity. The importance of Arg is further underscored by the fact that the two Lys-containing analogues exhibit the least potency in inhibiting the germination and growth of *A. fumigatus* from spores. Additionally, the statistical similarity between the IC_{50} and IC_{max} values of cWRW and cWWW suggests that the order of the residues may not be important for antifungal activity given that the residue content is identical. It must be noted that the cWRW and cWWW that were tested for activity were from the batch that was provided by Dr Margitha Dathe (referred to as cWWW1 and cWRW1 in Chapter 2).

The slight differences noted in the growth inhibitory activity of the three analogues with a mutation in the middle aromatic residue of the aromatic tripeptide moiety (cWFW, cWWW and cWYW) show that the identity of aromatic residue in this position may be influential in the modulation of activity. The results indicated that Trp is the most preferred residue in this position, followed by Phe and lastly Tyr (Table 4.1, refer to Table 4.7 in addendum for statistical analysis).

The activity of some of the cyclohexapeptides was quite comparable to that of the cyclodecapeptides. According to the one-way ANOVA statistical analysis performed on the IC_{50} values, the activity of the three most active cyclohexapeptides (cWWW, cWRW and cWFW) was similar to that of the cyclodecapeptides (Table 4.1, refer to Table 4.8 in addendum for statistical analysis).

On the other hand, the activity of linear RW-hexapeptides was found to be significantly lower than that of the cyclodecapeptides. Furthermore, they demonstrated reduced antifungal potency characterised by IC_{50} values that were 2- to 4-fold higher than those of the corresponding cyclic analogues (Table 4.1). This highlights the activity enhancing effect of cyclisation on the RW-hexapeptides. Dathe *et al.* [17] also reported improved antibacterial activity of the RW-hexapeptides upon cyclisation.

Table 4.1: Summary of the germination and growth inhibitory activity of the cyclodecapeptides and RW-hexapeptides towards *A. fumigatus* spores. The values of the activity parameters, IC_{50} and IC_{max} , are expressed in μM and represent the mean \pm SEM of n biological repeats, each with between 3-6 technical repeats.

Description	Peptide	$IC_{50} \pm$ SEM (n)	$IC_{max} \pm$ SEM (n)	Dose response curves
Natural cyclodecapeptides	YA	3.9 ± 1.1 (3)	5.4 ± 0.4 (3)	
	YB	2.9 ± 1.1 (3)	4.5 ± 0.5 (3)	
	WC	5.3 ± 1.0 (3)	7.4 ± 0.2 (3)	
Positive control	GS	4.6 ± 1.1 (6)	7.2 ± 0.9 (6)	
Synthetic cyclic RW-hexapeptides	cKRK	9.8 ± 0.8 (3)	20.4 ± 1.5 (3)	
	cRKK	12.1 ± 1.3 (3)	26.0 ± 3.9 (3)	
	cWFW	7.8 ± 0.6 (3)	17.2 ± 2.9 (3)	
	cWRW	7.0 ± 0.6 (4)	13.2 ± 1.6 (4)	
	cWWW	5.9 ± 0.6 (4)	9.3 ± 1.0 (4)	
	cWYW	9.3 ± 0.2 (3)	18.9 ± 1.8 (3)	
Synthetic Linear RW-hexapeptides	AcKRK	28.3 ± 2.3 (3)	54.6 ± 5.0 (3)	
	AcRKK	48.2 ± 3.2 (3)	68.6 ± 5.5 (3)	
	AcWFW	21.4 ± 2.4 (3)	59.3 ± 12 (3)	
	AcWRW	12.6 ± 0.9 (3)	26.0 ± 0.7 (3)	
	AcWWW	13.0 ± 1.0 (3)	26.6 ± 1.2 (3)	
	AcWYW	27.1 ± 2.9 (3)	71.4 ± 11 (3)	

Based on the structural models of the RW-hexapeptides (Chapter 3), the higher activity of the cyclic analogues can possibly be attributed to their more pronounced amphipathic conformation. Nonetheless, the same trend of activity was observed for the linear RW-hexapeptides as was for the cyclic RW-hexapeptides, with AcWWW and AcWRW exhibiting the greatest antifungal activity. It was interesting to note that AcRKK exhibited the least potency against *A. fumigatus* spores. AcRKK is the L-form analogue of the D-amino acid peptide PAF26, a synthetic peptide that was discovered by screening a synthetic combinatorial library for antifungal peptides. It has shown potent to moderate activity against various filamentous fungal pathogens [20].

Antifungal activity against A. fumigatus hyphae

The effect of WC and selected RW-hexapeptide analogues (WRW and WWW) on the hyphae of *A. fumigatus* was investigated using the resazurin assay [27]. In this assay, the metabolic reduction of resazurin (blue) to resorufin (pink, fluorescent) is used as measure of the cells' metabolic activity (redox potential) and in turn their viability [27,28]. The only peptides that effectively arrested the metabolic activity of the fungal hyphae within the range of peptide concentrations tested were cWWW and WC (Table 4.2 and Figure 4.1). However, their activities were significantly different ($P < 0.05$; refer to Table 4.12 in addendum for statistical analysis). The activity of WC against *A. fumigatus* hyphae was more than four-fold greater than that of cWWW (Table 4.2). Moreover, WC exhibited greater activity than the control (GS), while cWWW was less active. The other three RW-hexapeptide analogues had minimal to no activity towards *A. fumigatus* hyphae.

In this study all the peptides exhibited lower IC_{50} values for germination and growth inhibition of *A. fumigatus* spores, compared to the inhibition of hyphal metabolic activity (Table 4.2). The hyphal growth forms of fungi are normally more resistant to antifungal treatments [29,30]. However, an encouraging result is that for WC, this difference is not statistically significant ($P > 0.05$; refer to Table 4.13 in addendum for statistical analysis). This illustrates that WC is equally as effective at inhibiting the growth of spores, as it is at abolishing metabolic activity in hyphae. A non-discriminatory membranolytic mode of action of WC may account for the observed similarity in the activity towards spores and hyphae.

Table 4.2: Comparison of the activity of peptides against *A. fumigatus* spores and hyphae. All IC₅₀ values are in μM units and represent the mean \pm SEM of n biological repeats, each repeat consisting of 3-6 technical repeats.

Peptides	Metabolic inhibition of hyphae	Germination and growth inhibition of spores
	IC ₅₀ \pm SEM (n)	IC ₅₀ \pm SEM (n)
WC	6.2 \pm 1.1 (3)	5.3 \pm 1.0 (3)
cWRW	>100 (3)	7.0 \pm 0.6 (4)
cWWW	28.3 \pm 1.1 (3)	5.9 \pm 0.6 (4)
AcWRW	>100 (3)	26.0 \pm 0.7 (3)
AcWWW	>100 (3)	26.6 \pm 1.2 (3)
GS	15.7 \pm 1.1 (3)	4.6 \pm 1.1 (6)

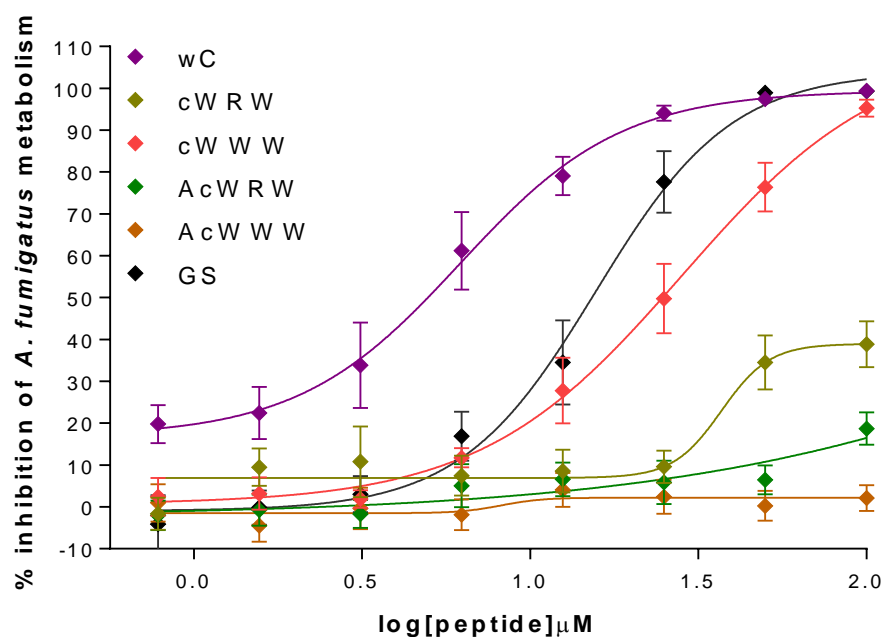


Figure 4.1: Inhibition of the metabolic activity of *A. fumigatus* hyphae.

Thirty-hour old *A. fumigatus* hyphae were treated for 2 hours with selected peptides followed by a 2-hour incubation with resazurin solution to evaluate metabolic activity. Peptide concentrations ranged between 100.0-0.79 μM . Each data point is representative of the mean \pm SEM of triplicate biological assays with triplicate technical repeats per assay.

Conversely, the RW-hexapeptide analogues are not as effective at inhibiting the metabolic activity of hyphae, as they are at inhibiting the growth of spores (Table 4.2, Figure 4.1). This loss of antifungal activity towards fungal hyphae by the RW-hexapeptides may be an indication that the target upon which they act in spores may be absent, present in lower concentration, shielded or modified in hyphae.

Evaluation of the toxicity of the cyclodecapeptides and the RW-hexapeptides

Evaluation of peptide toxicity was achieved by assessing the haemolytic activity elicited by the peptide groups towards human erythrocytes. The haemolytic activity of the cyclodecapeptides has been well characterised previously [22,31,32] and has been shown to compare well with that of GS, which was used as the positive control for haemolysis in this investigation. As expected, the cyclodecapeptides displayed haemolytic activity that was quite prominent and highly comparable to the activity of GS (Table 4.3). The HC_{50} values of all the analogues were below 20 μ M and were confined within a narrow concentration range. However, according to one-way ANOVA, a significant difference exists between the activities of YB and WC ($P < 0.05$; refer to Table 4.14 in addendum for statistical analysis). The activity of the cyclodecapeptides followed the same trend that was depicted for the growth inhibition of *A. fumigatus* spores, with $YB > YA > WC$. On this premise, it can be inferred that both the antifungal and haemolytic activities are governed by the same factors. Additionally, the pronounced haemolytic activity of the tyrocidines can be ascribed to their previously characterised membranolytic mode of action [10,13].

Conversely, the RW-hexapeptides exhibited very little haemolytic activity, maintaining consistency with the findings of other investigators [17,18] (Table 4.3). Because of their low haemolytic activity, it was not possible to fit the data obtained from dose response assays onto sigmoidal curves and in turn, determine HC_{50} . In order to assess the unique haemolytic properties of each hexapeptide analogue, % haemolysis induced at 100 μ M was taken into consideration. In general, the linear analogues exhibited less haemolytic activity in comparison to their cyclic counterparts. This indicates that while cyclisation enhances antimicrobial activity, it also enhances their toxicity thereby compromising some of their selectivity. However, the difference in activity between the cyclic and linear RW-hexapeptides is not statistically significant ($P > 0.05$), except for the RKK and WWW analogues (Table 4.3, refer to Table 4.15 in addendum for statistical analysis). It was also established that the Lys-containing analogues induced greater haemolysis over the Arg-containing analogues. Based on this and the antifungal data, it can thus be concluded the roles of the two basic amino acid residues in peptides are juxtaposed. While Arg appears to promote antimicrobial activity, Lys promotes peptide toxicity against human erythrocytes.

It appears that aromatic residues have an influential role in the haemolytic activity of the RW-hexapeptides, as they do in their antifungal activity. As shown in Table 4.3, the haemolytic activity of the WWW analogues was approximately four-fold higher than that of WFW and WYW analogues indicating that the nature of the aromatic residue in the middle position of the aromatic

Table 4.3: Summary of the haemolytic activity of the cyclodecapeptides and RW-hexapeptides towards human erythrocytes. The values of the activity parameter, HC_{50} , are expressed in μM and haemolysis activity at $100 \mu\text{M}$ is given in percentages. All values represent the mean \pm SEM of n biological repeats, each with between 3-6 technical repeats.

Description	Peptide	$HC_{50} \pm \text{SEM}$ (n)	%Haemolysis at $100 \mu\text{M} \pm$ SEM (n)	Dose response curves
Natural cyclo- decapeptides	YA	11.6 ± 1.2 (3)	103 ± 1.8 (3)	
	YB	8.3 ± 1.1 (3)	97.6 ± 2.7 (3)	
	WC	15.8 ± 1.3 (3)	93.1 ± 2.3 (3)	
Positive control	GS	12.9 ± 1.03 (11)	101 ± 1.5 (11)	
Synthetic cyclic RW- hexapeptides	cKRK	>100 (4)	10.0 ± 1.4 (4)	
	cRKK	>100 (4)	22.5 ± 2.9 (4)	
	cWFW	>100 (4)	4.5 ± 1.0 (4)	
	cWRW	>100 (4)	1.0 ± 0.7 (4)	
	cWWW	>100 (4)	20.4 ± 3.4 (4)	
	cWYW	>100 (4)	4.9 ± 2.0 (4)	
Synthetic Linear RW- hexapeptides	AcKRK	>100 (4)	6.6 ± 1.8 (4)	
	AcRKK	>100 (4)	5.9 ± 1.7 (4)	
	AcWFW	>100 (4)	1.2 ± 0.8 (4)	
	AcWRW	>100 (4)	1.8 ± 0.8 (4)	
	AcWWW	>100 (4)	5.1 ± 1.6 (4)	
	AcWYW	>100 (4)	1.0 ± 0.3 (4)	

tripeptide moiety influences the haemolytic activity of these peptides. From this and the antifungal activity data, it can be concluded that while Trp may be the best aromatic residue for antifungal activity, its presence in this position compromises selectivity.

Determination of peptide selectivity

For future therapeutic development, it is of utmost importance that antimicrobial peptides display higher selectivity for the microbial target. *In vitro* selectivity can be determined by comparing a peptide's (or compound's) antimicrobial activity to its toxicity against a selected host/human cell type. For the cyclodecapeptides, the *in vitro* selectivity parameter was determined by using the antifungal activity parameter, IC₅₀ to the haemolytic toxicity parameter, HC₅₀ (Figure 4.2, Table 4.4). All three natural cyclodecapeptides exhibited similar levels of low selectivity for the fungal target as indicated by their selectivity indices of values of approximately 3 (Table 4.4). This low selectivity can be attributed to a non-discriminatory membranolytic mode of action.

On the other hand, the RW-hexapeptides demonstrated a high degree of selectivity for the fungal target. Because the HC₅₀ could not be determined, the selectivity of the RW-hexapeptides was established by considering the growth inhibitory activity and haemolytic activity at 100 µM (the highest concentration tested in the dose response assays) (Table 4.4).

Table 4.4: Summary of the calculated selectivity parameters

Cyclo-decapeptide	Selectivity (HC₅₀/IC₅₀)	Cyclo-hexapeptide	Selectivity*	Linear hexapeptide	Selectivity*
YA	3.01	cKRK	9.23	AcKRK	14.6
YB	2.83	cRKK	4.20	AcRKK	14.9
WC	3.01	cWFW	20.4	AcWFW	80.1
GS	2.81	cWRW	94.2	AcWRW	56.7
* <u>Antifungal activity at 100 µM</u> Haemolysis at 100 µM		cWWW	4.4	AcWWW	19.5
		cWYW	19.7	AcWYW	98.7

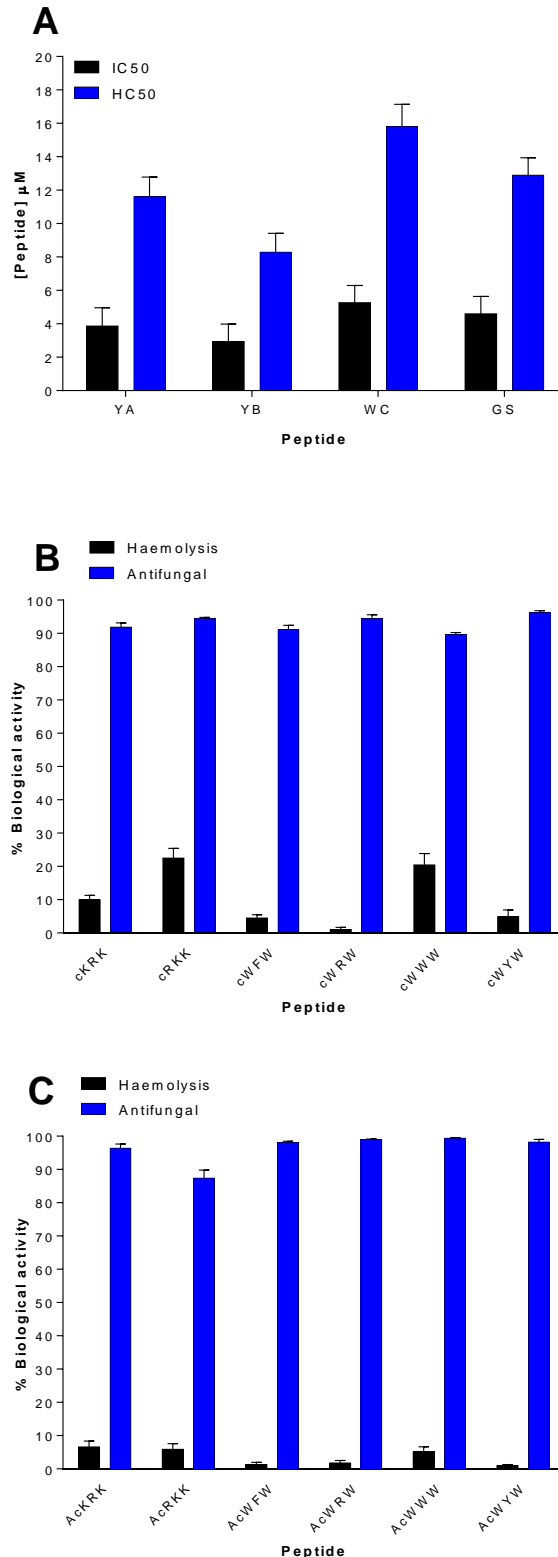


Figure 4.2: Comparison of the antifungal and haemolytic activities to establish peptide selectivity.

A) Selectivity of the cyclodecapeptides depicted as a comparison between the activity parameters IC₅₀ (antifungal) and HC₅₀ (haemolysis).

B) Selectivity of cyclic RW-hexapeptides depicted as comparison between the antifungal and haemolytic activities at 100 μM.

C) Selectivity of cyclic RW-hexapeptides depicted as comparison between the antifungal and haemolytic activities at 100 μM.

In Figure 4.2 it is quite clear that at the same peptide concentration antifungal activity was significantly greater than the haemolytic activity, for all the peptides. However, the RW hexapeptides exhibited much better selectivity than the cyclodecapeptides (Figure 4.2, Table 4.4). This selectivity is an indication that the target of the RW-hexapeptides in *A. fumigatus* is absent in human erythrocytes. The differences in the selectivity exhibited by the two peptide groups (cyclodecapeptides vs RW-hexapeptides) could possibly allude to distinctly different mechanisms of action.

Antifungal activity of peptide combinations

Having established the activity of single peptides in each of the three groups, it was decided to investigate the activity of selected peptides when used in combination. This was motivated by the fact that combination therapy can potentially boost activity and minimise the development of antimicrobial resistance, concomitantly. In addition, postulations regarding the modes of action of each of the peptides in a combination pair can be made based on the nature of interactions between two peptides. Synergistic interactions often indicate distinct modes of action, while additive interactions may suggest similar modes of action or a shared target. Antagonistic interactions suggest a shared target but different or opposing modes of action.

From the cyclodecapeptides, WC was selected as the representative analogue. This decision was based on the fact that all three cyclodecapeptides displayed similar growth inhibitory activity against *A. fumigatus* spores and WC was the most selective analogue. From the RW-hexapeptide library cWWW and cWRW and their linear analogues were selected, as they were the most active analogues in their respective categories.

Based on the FIC indices (FICIs) and isobologram shapes of the peptide combinations, the interactions turned out to be slightly antagonistic ($1 < \text{FICI} < 4$) [11,23] (Table 4.5). The antagonism seemed to increase with an increasing WC concentration. Since cyclodecapeptides are known to have a membranolytic mode of action [10,13], it is possible that this lytic action of WC prevented the RW-hexapeptides from accessing their target; a target which could potentially be located within the membrane or inside the fungal cell. The higher the concentration of WC, the greater its lytic action and the more the RW-hexapeptide analogues are impeded from accessing their target resulting in an increase in their FICs and ultimately a greater FICI.

Table 4.5: Summary of the characterisation of the nature of interactions between WC and selected RW-hexapeptide analogues. FIC values and FIC indices were calculated from three biological repeats (each with four technical replicates) of growth inhibition assays towards *A. fumigatus* spores.

Peptide	WC:RW peptide ratio	FIC (WC) \pm SEM	FIC (RW peptide) \pm SEM	FIC Index \pm SEM	Isobologram
cWRW	3:1	0.898 \pm 0.127	0.198 \pm 0.001	1.09 \pm 0.128	
	1:1	0.693 \pm 0.097	0.443 \pm 0.022	1.14 \pm 0.119	
	1:3	0.345 \pm 0.039	0.666 \pm 0.035	1.01 \pm 0.074	
AcWRW	3:1	1.30 \pm 0.072	0.136 \pm 0.029	1.44 \pm 0.101	
	1:1	0.990 \pm 0.114	0.300 \pm 0.036	1.29 \pm 0.15	
	1:3	0.591 \pm 0.111	0.515 \pm 0.07	1.11 \pm 0.181	
cWWW	3:1	1.15 \pm 0.132	0.291 \pm 0.015	1.44 \pm 0.147	
	1:1	0.681 \pm 0.132	0.504 \pm 0.030	1.19 \pm 0.162	
	1:3	0.339 \pm 0.047	0.765 \pm 0.010	1.10 \pm 0.057	
AcWWW	3:1	1.09 \pm 0.102	0.092 \pm 0.011	1.18 \pm 0.113	
	1:1	1.02 \pm 0.190	0.251 \pm 0.029	1.27 \pm 0.219	
	1:3	0.565 \pm 0.081	0.427 \pm 0.062	0.992 \pm 0.143	

In all combinations, the best FICI was found to be at 1:3 where it was shown to be an additive interaction (Table 4.5). The addition of 25% WC to, for example, 75% cWRW in a formulation would ensure that such a combination will be effective against both spores and hyphae. Such a combination would also hypothetically lower the toxicity, although this must still be determined.

Part 2: Mode of action studies

Investigation of the membranolytic action of RW-hexapeptides

After establishing that the RW-hexapeptides had profound growth inhibitory activity against *A. fumigatus* spores, it was befitting that an investigation be carried out to gain more insight on how this inhibitory action is exerted. Given their low haemolytic activity, and low permeabilising effect on lipid model membranes, RW-hexapeptides are believed to act via a non-membrane permeabilisation mode of action. However, it was necessary to establish whether this assumption holds true when it comes to their activity against fungal pathogens.

SYTOX Green, a membrane impermeable dye, was employed in the investigation of the membrane integrity of peptide treated *A. fumigatus* hyphae. In this instance, WC was utilised as the lysis positive control due to its known permeabilising effect on the cell membrane [6]. As shown in Figures 4.3 and 4.4A, some of the RW-hexapeptide analogues induced membrane permeation to a certain extent. In comparison to WC, this membrane permeation was negligible as depicted by the low fluorescence intensity of SG. Statistical analysis using one-way ANOVA revealed a significant difference in the uptake of SG by WC and the RW-hexapeptide analogues ($P < 0.001$; refer to Table 4.16 in addendum for statistical analysis). Figure 4.3B shows the rate of permeabilisation that was calculated by analysing data obtained within the first 10 minutes of the time course study using first order kinetics. As expected, WC exhibited a much higher permeabilisation rate than the RW-hexapeptides. This result therefore confirms the hypothesis that membrane lysis is not the dominant mode of action of the RW-hexapeptides.

It is important to note that these results do not indicate the absence of membrane permeabilisation. Rather, they portray a much slower induction of membrane permeabilisation by the RW-hexapeptide analogues. This means that even though membrane permeabilisation may not be considered as the primary means by which the RW-hexapeptides act, it should not be completely ruled out as it could potentially be an additional mechanism of action. Alternatively, membrane permeabilisation could be a secondary effect of their primary mode of action.

Amongst the RW-hexapeptides, the Lys-containing analogues induced a higher uptake of the dye as indicated by the observed maximum fluorescence intensity of SG hyphae treated with these analogues. They also permeabilised the hyphal membrane at a much faster rate than the other RW-hexapeptide analogues. This result correlated with the higher haemolytic activity observed for the Lys-analogues.

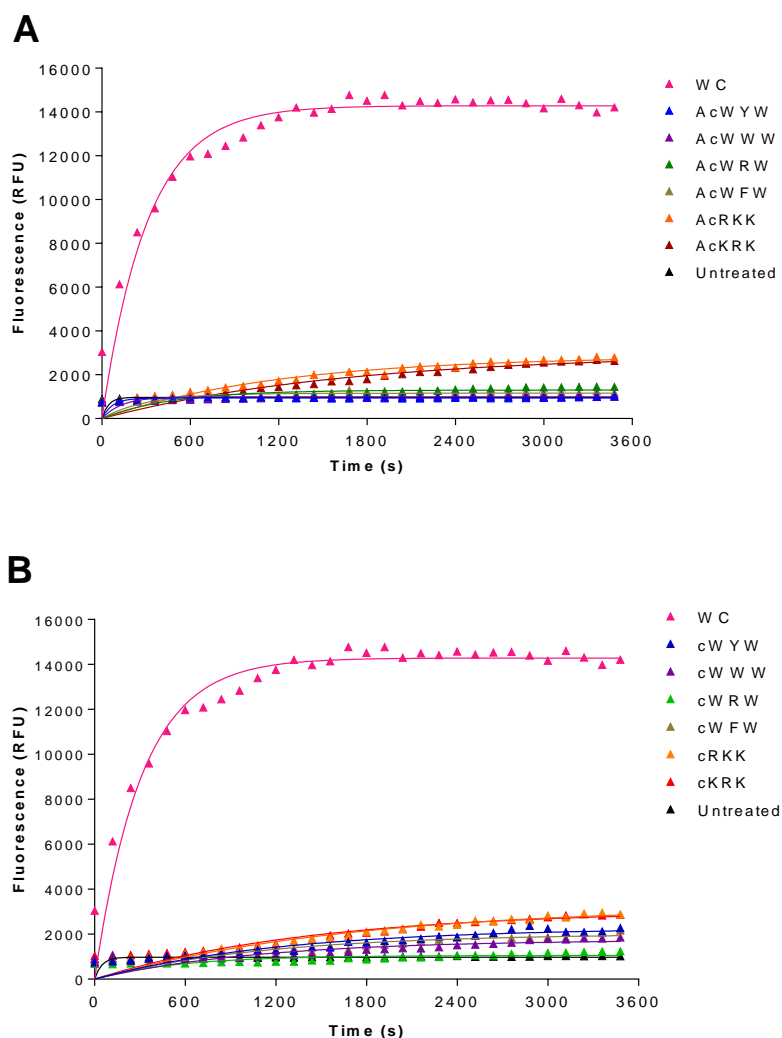


Figure 4.3: Time course kinetics of SYTOX Green (SG) uptake by peptide treated *A. fumigatus* hyphae.

A) SG uptake by linear RW-hexapeptides B) SG uptake by cyclic RW-hexapeptides.

A. fumigatus hyphae (30 hours old) were simultaneously treated with 25 μ M peptide and 0.5 μ M SG. Monitoring of SG uptake commenced immediately and lasted for 60 minutes, with fluorescence readings being recorded at 2-minute intervals. Tryptocidine C (WC) served as the positive control for lysis.

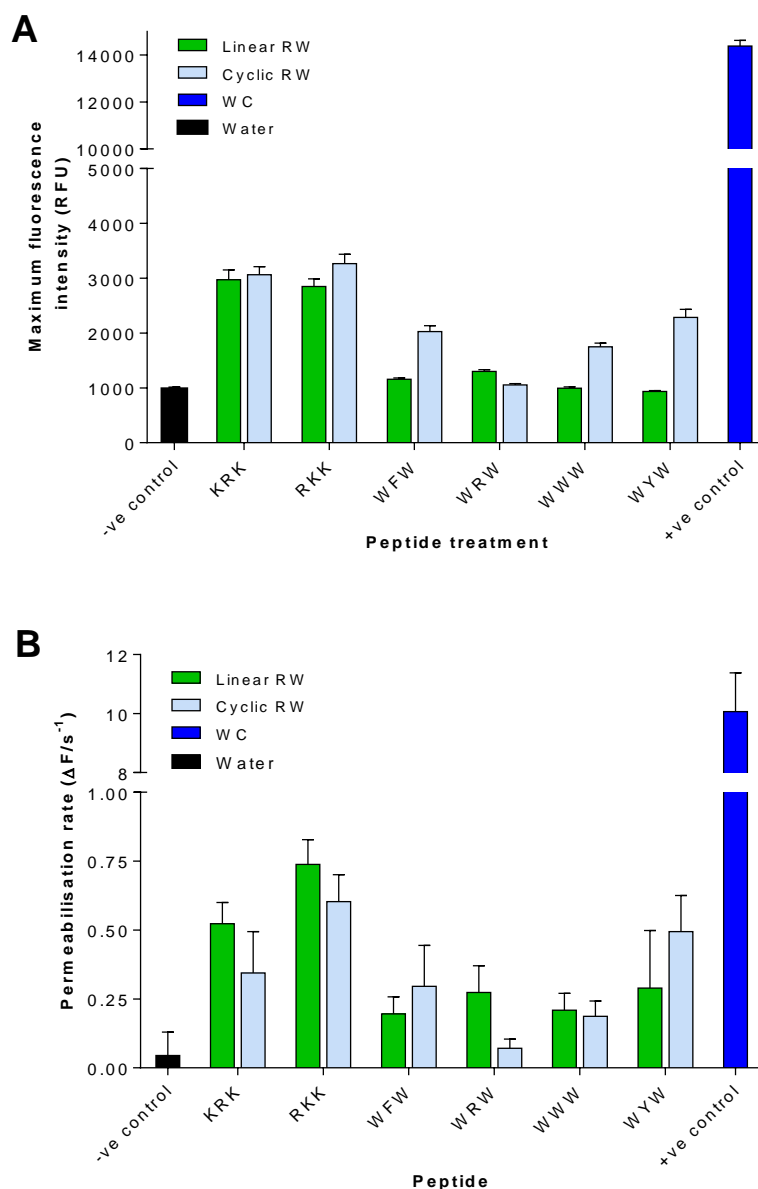


Figure 4.4: Permeabilisation of *A. fumigatus* membrane by RW-hexapeptides.

A) Maximum fluorescence intensity of SG dye observed in *A. fumigatus* hyphae after one hour of treatment with 25 μM peptide and 0.5 μM SG.

B) Rate of SG uptake by *A. fumigatus* hyphae treated with 25 μM peptide, depicted as rate of membrane permeabilisation.

The linear and cyclic analogues of the Lys-containing peptides exhibited statistically similar membrane permeabilising effects. However, the cyclic analogues cWFW, cWYW, and cWWW induced a significantly greater total uptake of SG than their linear counterparts, correlating with their higher haemolytic activity. In contrast, the membrane permeabilising activity of cWRW was significantly less than that of its linear analogue, also correlating with their haemolytic activities.

Peptide induced accumulation of ROS in *A. fumigatus* hyphae

Apoptosis or programmed cell death is a carefully controlled process that can be triggered by the intracellular accumulation of toxins such as reactive oxygen species (ROS) [33]. Several antifungal agents have been shown to induce the accumulation of reactive oxygen species in the cells of susceptible fungi [12,34–37]. On account of this, the two most active RW-hexapeptides from each of the two RW-hexapeptide categories, together with WC were tested for their ability to induce the accumulation of reactive oxygen species in the hyphae of *A. fumigatus*. Figure 4.5 shows a significantly enhanced accumulation of ROS species in the hyphae treated with cWWW and WC relative to the untreated control (refer to Table 4.18 in addendum for statistical analysis). The quantities of ROS were severely reduced upon addition of a known antioxidant, Vitamin C (ascorbic acid).

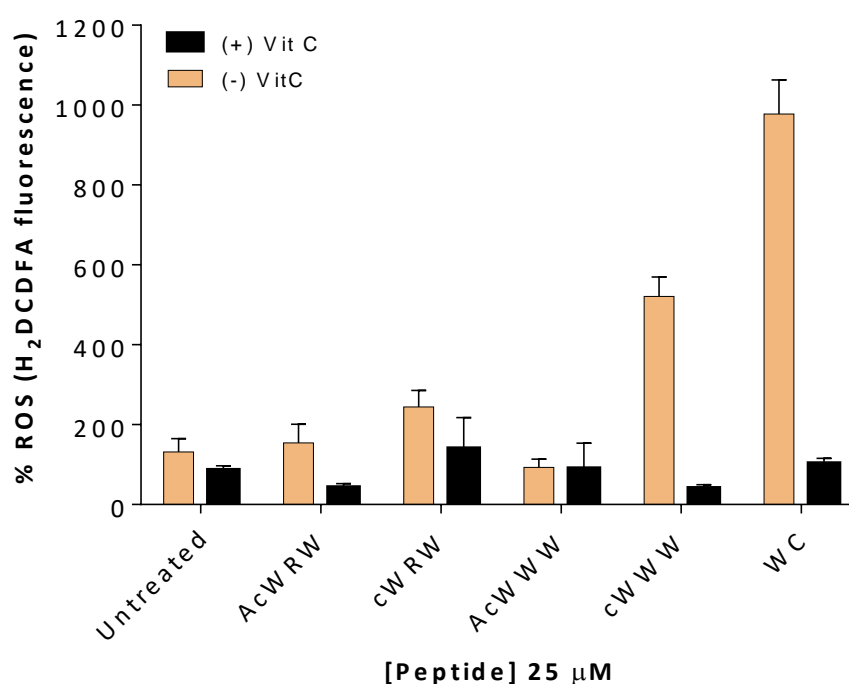


Figure 4.5: Induction of ROS in peptide treated *A. fumigatus* hyphae.

A. fumigatus hyphae (30 hours old) were treated with 25 μ M of peptide (WC, cWRW, cWWW, AcWRW and AcWWW) in the presence or absence of the antioxidant ascorbic acid (Vit C) prior to staining with 10 mM H₂DCFDA. Orange and black bars are representative of the %ROS produced in the absence and presence of antioxidant, respectively. Each data point represents the mean of three biological repeats (with four technical repeats) \pm SEM.

In a study conducted by Troskie *et al.* [12], the antifungal activity of cyclodecapeptides towards *C. albicans* cells was found to be independent of their induction of ROS. The investigators thus

concluded that the induction of ROS may be a secondary effect of cyclodecapeptides, such as WC. Because of this, it was necessary to determine whether the observed increase in ROS accumulation that was induced by cWWW and WC was linked to their antifungal activity. Unfortunately, we were unable to obtain another cWWW preparation with reproducible activity. Two attempts to obtain another viable batch of this expensive peptide were fruitless. Consequently, the role of ROS in the antifungal activity of these two peptides will only be evaluated in a future study when we have obtained good quality cWWW preparation and produced and purified more WC .

4.5 Conclusion

The natural cyclodecapeptides exhibited excellent and highly comparable antifungal activity against *A. fumigatus*. The results correlated well with previous studies on the antifungal activity of these natural peptides [12–14]. All the cyclodecapeptide analogues potently inhibited the growth of *A. fumigatus* spores as indicated by their extremely low IC₅₀ and IC_{max} values. In addition to inhibiting the growth of spores, WC demonstrated equally potent activity towards *A. fumigatus* hyphae, as well as the highest selectivity of the group of cyclodecapeptides tested. Because of this potent antifungal activity, this natural cyclodecapeptide has the potential for further development as an antifungal agent. However, its high haemolytic activity continues to derail its development as an agent for systemic application. Nonetheless, there are ongoing efforts in our group aimed at eliminating undesirable toxicity by selective formulation.

The RW-hexapeptides also exhibited profound growth inhibitory activity against *A. fumigatus* spores. In fact, the activity of three of the cyclic analogues was comparable to that of the natural cyclodecapeptides. The cyclic analogues demonstrated superior activity to the linear analogues, which highlighted the activity enhancing effect of cyclisation that has been reported previously [17]. The importance of Trp residues in antifungal activity was highlighted by the superior activity of the WRW and WWW analogues over the WFW and WYW analogues. Moreover, the greater antifungal activity exhibited by the WWW analogues over the WFW and WYW analogues also highlighted that Trp is the most preferred aromatic residue in the middle position of the aromatic tripeptide moiety for antifungal activity. However, it was shown that Trp compromises selectivity as it increases the toxicity of the RW-hexapeptides. Arg residues were also shown to be important for antifungal activity as the Arg-containing analogues demonstrated better activity in comparison to the Lys-containing analogues.

Unfortunately, the antifungal activity of the RW-hexapeptide analogues was drastically diminished against *A. fumigatus* hyphae. Apart from cWWW, none of the lead RW-hexapeptide analogues could effectively inhibit the metabolism of *A. fumigatus* hyphae. Even for cWWW, the activity decreased four-fold. Based on these observations, it is believed that the target of RW-hexapeptide analogues is either altered, shielded, present at a lower concentration or absent in fungal hyphae hence the reduction in their activity. Unlike the natural cyclodecapeptides, RW-hexapeptides displayed little to no haemolytic activity. This low haemolytic activity coupled with their excellent fungal growth inhibitory activity makes them very attractive for further development as antifungal agents for systemic use. Their high selectivity confers them an advantage over the natural cyclodecapeptides when it comes to potential systemic use.

The RW-hexapeptides also induced minimal uptake of SG indicating that they are not as effective as the cyclodecapeptides at permeabilising the membrane. Taken together, the low haemolytic activity and the low permeabilisation of fungal membrane illustrate that membrane permeabilisation is not the primary mode of action of the RW-hexapeptides. Interestingly, the natural cyclodecapeptides and the RW-hexapeptides could potentially have a common mechanism of action. WC and the lead RW-hexapeptide analogues induced the accumulation of ROS in *A. fumigatus* hyphae. However, more experiments are needed to establish if the observed ROS induction is linked to the antifungal activity of these peptides.

The interactions between WC and the RW-hexapeptide analogues were found to be slightly antagonistic, in general. The antagonism can be attributed to the high membranolytic activity of WC. It is postulated that by lysing the highly sensitive membrane of the fungal hyphal apex (growth point), WC hindered the RW-hexapeptide analogues from reaching their target. However, it was noted that FICIs of the peptide combinations in the 1:3 ratio had FICIs that were very close to 1; an indication that the interactions were additive. Based on the selectivity of the RW-hexapeptides and the antifungal activity of the combinations with WC, a good lead formulation for further development would be cWRW and WC. Given the additivity of activity at the 1:3 peptide ratio, it can be hypothesised that the WC:cWRW combination has the potential to reduce the toxicity of WC while still maintaining antifungal activity against both hyphae and spores.

4.6 References

- [1] M.A. Pfaller, D.J. Diekema, Epidemiology of invasive mycoses in North America, *Critical Reviews in Microbiology*, 36 (2010) 1–53.
- [2] G.D. Brown, D.W. Denning, N.A.R. Gow, S.M. Levitz, M.G. Netea, T.C. White, Hidden

- killers: Human fungal infections, *Science Translational Medicine*, 4 (2012).
- [3] D.W. Denning, Therapeutic outcome in invasive aspergillosis, *Clinical Infectious Diseases*, 23 (1996) 608–615.
- [4] K.A. Brogden, Antimicrobial peptides: Pore formers or metabolic inhibitors in bacteria?, *Nature Reviews Microbiology*, 3 (2005) 238–250.
- [5] R.E. Hancock, Peptide antibiotics, *Lancet*, 349 (1997) 418–422.
- [6] A.M. Troskie, Tyrocidines, cyclic decapeptides produced by soil bacilli, as potent inhibitors of fungal pathogens, PhD Thesis, Department of Biochemistry, University of Stellenbosch, (2013), <http://hdl.handle.net/10019.1/86162>
- [7] R.J. Dubos, Studies on bactericidal agent extracted from a soil *Bacillus*: 1 Preparation of the agent. Its activity in vitro, *The Journal of Experimental Medicine*, 70 (1939) 1–10.
- [8] O. Shida, H. Takagi, K. Kadowaki, K. Komagata, Proposal for two new genera, *Brevibacillus* gen nov and *Aneurinibacillus* gen nov, *International Journal of Systematic Bacteriology*, 46 (1996) 939–946.
- [9] R.J. Dubos, R.D. Hotchkiss, A.F. Coburn, The effect of gramicidin and tyrocidine on bacterial metabolism, *Journal of Biological Chemistry*, 146 (1942) 421–426.
- [10] B.M. Spathelf, M. Rautenbach, Anti-listerial activity and structure-activity relationships of the six major tyrocidines, cyclic decapeptides from *Bacillus aneurinolyticus*, *Bioorganic and Medicinal Chemistry*, 17 (2009) 5541–5548.
- [11] A.N.-N. Leussa, Characterisation of small cyclic peptides with antimalarial and antilisterial activity PhD Thesis, Department of Biochemistry, University of Stellenbosch, (2014), <http://hdl.handle.net/100191/86161>.
- [12] A.M. Troskie, M. Rautenbach, N. Delattin, J.A. Vosloo, M. Dathe, B.P.A. Cammue, K. Thevissen, Synergistic activity of the tyrocidines, antimicrobial cyclodecapeptides from *Bacillus aneurinolyticus*, with amphotericin B and caspofungin against *Candida albicans* biofilms, *Antimicrobial Agents and Chemotherapy*, 58 (2014) 3697–3707.
- [13] A.M. Troskie, A. de Beer, J.A. Vosloo, K. Jacobs, M. Rautenbach, Inhibition of agronomically relevant fungal phytopathogens by tyrocidines, cyclic antimicrobial peptides isolated from *Bacillus aneurinolyticus*, *Microbiology*, 160 (2014) 2089–2101.
- [14] M. Rautenbach, A.M. Troskie, J.A. Vosloo, M.E. Dathe, Antifungal membranolytic activity of the tyrocidines against filamentous plant fungi, *Biochimie*, 130 (2016) 122–131.
- [15] S.E. Blondelle, R.A. Houghten, Novel antimicrobial compounds identified using synthetic combinatorial library technology, *Trends in Biotechnology*, 14 (1996) 60–65.
- [16] A. Wessolowski, M. Bienert, M. Dathe, Antimicrobial activity of arginine- and tryptophan-rich hexapeptides: The effects of aromatic clusters, D-amino acid substitution and cyclization, *Journal of Peptide Research*, 64 (2004) 159–169.
- [17] M. Dathe, H. Nikolenko, J. Klose, M. Bienert, Cyclization increases the antimicrobial activity and selectivity of arginine- and tryptophan-containing hexapeptides, *Biochemistry*, 43 (2004) 9140–9150.
- [18] K. Scheinpflug, H. Nikolenko, I. V. Komarov, M. Rautenbach, M. Dathe, What goes around comes around: a comparative study of the influence of chemical modifications on the antimicrobial properties of small cyclic peptides, *Pharmaceuticals*, 6 (2013) 1130–1144.
- [19] A. Muñoz, B. López-García, J.F. Marcos, Studies on the mode of action of the antifungal

- hexapeptide PAF26, *Antimicrobial Agents and Chemotherapy*, 50 (2006) 3847–3855.
- [20] B. López-García, E. Pérez-Payá, J.F. Marcos, Identification of Novel Hexapeptides Bioactive against Phytopathogenic Fungi through Screening of a Synthetic Peptide Combinatorial Library, *Applied and Environmental Microbiology*, 68 (2002) 2453–2460.
- [21] A. Muñoz, J.F. Marcos, N.D. Read, Concentration-dependent mechanisms of cell penetration and killing by the de novo designed antifungal hexapeptide PAF26, *Molecular Microbiology*, 85 (2012) 89–106.
- [22] M. Rautenbach, N.M. Vlok, M. Stander, H.C. Hoppe, Inhibition of malaria parasite blood stages by tyrocidines, membrane-active cyclic peptide antibiotics from *Bacillus brevis*, *Biochimica et Biophysica Acta - Biomembranes*, 1768 (2007) 1488–1497.
- [23] F.C. Odds, Synergy, antagonism, and what the checkerboard puts between them, *Journal of Antimicrobial Chemotherapy*, 52 (2003) 1–1.
- [24] J.A. Vosloo, Optimised bacterial production and characterisation of natural antimicrobial peptides with potential application in agriculture, PhD Thesis, Department of Biochemistry, University of Stellenbosch, (2016), <http://hdl.handle.net/10019.1/98411>
- [25] S. Laiken, M. Printz, L.C. Craig, Circular dichroism of the tyrocidines and gramicidin S-A, *Journal of Biological Chemistry*, 244 (1969) 4454–4457.
- [26] G. Munyuki, G.E. Jackson, G.A. Venter, K.E. Kövér, L. Szilágyi, M. Rautenbach, B.M. Spathelf, B. Bhattacharya, D. Van Der Spoel, β -sheet structures and dimer models of the two major tyrocidines, antimicrobial peptides from *Bacillus aneurinolyticus*, *Biochemistry*, 52 (2013) 7798–7806.
- [27] T.L. Riss, R.A. Moravec, A.L. Niles, S. Duellman, H.A. Benink, T.J. Worzella, L. Minor, Cell viability assays, Eli Lilly & Company and the National Center for Advancing Translational Sciences, 2004.
- [28] J. O'Brien, I. Wilson, T. Orton, F. Pognan, Investigation of the Alamar Blue (resazurin) fluorescent dye for the assessment of mammalian cell cytotoxicity, *European Journal of Biochemistry*, 267 (2000) 5421–5426.
- [29] C. Lass-Flörl, M. Nagl, E. Gunsilius, C. Speth, H. Ulmer, R. Würzner, In vitro studies on the activity of amphotericin B and lipid-based amphotericin B formulations against *Aspergillus* conidia and hyphae In vitro-Empfindlichkeit von *Aspergillus*-Konidien und -Hyphen gegenüber Amphotericin B und Amphotericin B-Lipidpräparationen, *Mycoses*, 45 (2002) 166–169.
- [30] J. Guarro, C. Llop, C. Aguilar, I. Pujol, Comparison of in vitro antifungal susceptibilities of conidia and hyphae of filamentous fungi, *Antimicrobial Agents and Chemotherapy*, 41 (1997) 2760–2.
- [31] C.H. Rammelkamp, L. Weinstein, Toxic effects of tyrothricin, gramicidin and tyrocidine, *Journal of Infectious Diseases*, 71 (1942) 166–173.
- [32] B. Spathelf, Qualitative structure-activity relationships of the major tyrocidines, cyclic decapeptides from *Bacillus aneurinolyticus*, PhD Thesis, Department of Biochemistry, University of Stellenbosch, (2013), <http://hdl.handle.net/10019.1/4001>
- [33] É. Leiter, H. Szappanos, C. Oberparleiter, L. Kaiserer, L. Csernoch, T. Pusztahelyi, T. Emri, I. Pócsi, W. Salvenmoser, F. Marx, Antifungal protein PAF severely affects the integrity of the plasma membrane of *Aspergillus nidulans* and induces an apoptosis-like phenotype, *Antimicrobial Agents and Chemotherapy*, 49 (2005) 2445–2453.

- [34] A.J. Phillips, I. Sudbery, M. Ramsdale, Apoptosis induced by environmental stresses and amphotericin B in *Candida albicans*, *Proceedings of the National Academy of Sciences*, 100 (2003) 14327–14332.
- [35] I. Francois, B. Cammue, M. Borgers, J. Ausma, G. Dispersyn, K. Thevissen, Azoles: mode of antifungal action and resistance development. Effect of miconazole on endogenous reactive oxygen species production in *Candida albicans*, *Anti-Infective Agents in Medicinal Chemistry*, 5 (2006) 3–13.
- [36] K. De Brucker, B.P.A. Cammue, K. Thevissen, Apoptosis-inducing antifungal peptides and proteins, *Biochemical Society Transactions*, 39 (2011) 1527–1532.
- [37] A.M. Aerts, I.E.J.A. François, E.M.K. Meert, Q.T. Li, B.P.A. Cammue, K. Thevissen, The antifungal activity of RsAFP2, a plant defensin from *Raphanus sativus*, involves the induction of reactive oxygen species in *Candida albicans*, *Journal of Molecular Microbiology and Biotechnology*, 13 (2007) 243–247.

4.7 Addendum

Table 4.6: Summary of the P-values obtained from the statistical analysis of the germination and growth inhibitory activity of the cyclodecapeptides against *A. fumigatus* spores. Statistical significance was determined by performing one-way ANOVA (using the Bonferroni's multiple comparisons test) on the IC₅₀ values. "ns" denotes a P-value > 0.05.

	YB	WC	GS
YA	ns	ns	ns
YB		ns	ns
WC			ns

Table 4.7: Summary of the P-values obtained from the statistical analysis of the germination and growth inhibitory activity of the cyclic RW-hexapeptides against *A. fumigatus* spores. Statistical significance was determined by performing one-way ANOVA (using the Bonferroni's multiple comparisons test) on the IC₅₀ values. "ns" denotes a P-value > 0.05.

	cRKK	cWFW	cWRW	cWWW	cWYW
cRKK	ns	ns	ns	0.03	ns
cRKK		0.02	0.003	0.0004	ns
cWFW			ns	ns	ns
cWRW				ns	ns
cWWW					ns

Table 4.8: Summary of the P-values obtained from the statistical comparison of the activities of the cyclic RW-hexapeptides and cyclodecapeptides in inhibiting the germination and growth *A. fumigatus* spores. Statistical significance was determined by performing one-way ANOVA (using the Bonferroni's multiple comparisons test) on the IC₅₀ values. "ns" denotes a P-value > 0.05.

	YA	YB	WC	GS
cRKK	0.02	0.003	ns	0.02
cRKK	0.0003	<0.0001	0.003	0.0001
cWFW	ns	ns	ns	ns
cWRW	ns	ns	ns	ns
cWWW	ns	ns	ns	ns
cWYW	0.04	0.008	ns	0.04

Table 4.9: Summary of the P-values obtained from the statistical analysis of the germination and growth inhibitory activity of the linear RW-hexapeptides against *A. fumigatus* spores. Statistical significance was determined by performing one-way ANOVA (using the Bonferroni's multiple comparisons test) on the IC₅₀ values. "ns" denotes a P-value > 0.05.

	AcRKK	AcWFW	AcWRW	AcWWW	AcWYW
AcRKK	0.0006	ns	0.004	0.006	ns
AcRKK		<0.0001	<0.0001	<0.0001	0.0003
AcWFW			ns	ns	ns
AcWRW				ns	0.008
AcWWW					0.009

Table 4.10: Summary of the P-values obtained from the statistical comparison of the activities of the linear RW-hexapeptides and cyclodecapeptides in inhibiting the germination and growth *A. fumigatus* spores. Statistical significance was determined by performing One-way ANOVA (using the Bonferroni's multiple comparisons test) on the IC₅₀ values. "ns" denotes a P-value > 0.05.

	YA	YB	WC	GS
AcKRK	<0.0001	<0.0001	<0.0001	<0.0001
AcRKK	<0.0001	<0.0001	<0.0001	<0.0001
AcWFW	<0.0001	<0.0001	0.0001	<0.0001
AcWRW	ns	0.04	ns	ns
AcWWW	ns	0.03	ns	0.04
AcWYW	<0.0001	<0.0001	<0.0001	<0.0001

Table 4.11: Summary of the P-values obtained from the statistical comparison of the activities of the linear and cyclic RW-hexapeptides at inhibiting the germination and growth *A. fumigatus* spores. Statistical significance was determined by performing multiple t-tests (using the Sidak-Bonferroni method) on the IC₅₀ values. "ns" denotes a P-value > 0.05.

Peptides	Significant	P-value
cKRK vs AcKRK	Yes	0.002
cRKK vs AcRKK	Yes	0.0005
cWFW vs AcWFW	Yes	0.006
cWRW vs AcWRW	Yes	0.003
cWWW vs AcWWW	Yes	0.0009
cWYW vs AcWYW	Yes	0.004

Table 4.12: Summary of the P-values obtained from the statistical analysis of the inhibition of the metabolic activity of *A. fumigatus* hyphae by selected peptides. Statistical significance was determined by performing one-way ANOVA (using the Bonferroni's multiple comparisons test) on the IC₅₀ values. "ns" denotes a P-value > 0.05.

	cWWW	cWRW	AcWWW	AcWRW	GS
WC	<0.0001	<0.0001	<0.0001	<0.0001	0.0001
cWWW		<0.0001	<0.0001	<0.0001	<0.0001
cWRW			<0.0001	<0.0001	<0.0001
AcWWW				<0.0001	<0.0001
AcWRW					<0.0001

Table 4.13: Summary of the P-values obtained from the statistical comparison of the inhibitory activities of the selected peptides against *A. fumigatus* spores and hyphae. Statistical significance was determined by performing multiple t-tests (using the Sidak-Bonferroni method) on the IC₅₀ values. "ns" denotes a P-value > 0.05.

Peptides	Significant?	P-value
cWWW	Yes	<0.0001
cWRW	Yes	<0.0001
AcWWW	Yes	<0.0001
AcWWW	Yes	<0.0001
WC	No	0.5
GS	Yes	0.0003

Table 4.14: Summary of the P-values obtained from the statistical analysis of the haemolytic activity of the cyclodecapeptides against towards human erythrocytes. Statistical significance was determined by performing one-way ANOVA (using the Bonferroni's multiple comparisons test) on the HC₅₀ values. "ns" denotes a P-value > 0.05.

	YB	WC	GS
YA	ns	ns	ns
YB		0.0001	0.04
WC			ns

Table 4.15: Summary of the P-values obtained from the statistical comparison of the haemolytic activities of the linear and cyclic RW-hexapeptides towards human erythrocytes. Statistical significance was determined by performing multiple t-tests (using the Sidak-Bonferroni method) on the percentage haemolysis induced at 100 µM. "ns" denotes a P-value > 0.05.

Peptides	Significant?	P-value
cKRK vs AcKRK	No	0.1
cRKK vs AcRKK	Yes	<0.0001
cWFW vs AcWFW	No	0.01
cWRW vs AcWRW	No	0.5
cWWW vs AcWWW	Yes	0.0003
cWYW vs AcWYW	No	0.07

Table 4.16: Summary of the P-values obtained from the statistical comparison of the membrane permeabilising activity of the RW-hexapeptides with that of WC. Statistical significance was determined by performing one-way ANOVA (using the Bonferroni's multiple comparisons test) on the total fluorescence intensity of SYTOX Green. "ns" denotes a P-value > 0.05.

Peptide compared to WC	Significant?	P-value
AcKRK	Yes	<0.0001
AcRKK	Yes	<0.0001
AcWFW	Yes	<0.0001
AcWRW	Yes	<0.0001
AcWWW	Yes	<0.0001
AcWYW	Yes	<0.0001
cKRK	Yes	<0.0001
cRKK	Yes	<0.0001
cWFW	Yes	<0.0001
cWRW	Yes	<0.0001
cWWW	Yes	<0.0001
cWYW	Yes	<0.0001

Table 4.17: Summary of the P-values obtained from the statistical comparison of the membrane permeabilising activities of the linear and cyclic RW-hexapeptides. Statistical significance was determined by performing multiple t-tests (using the Sidak-Bonferroni method) on the total fluorescence intensity of SYTOX Green. “ns” denotes a P-value > 0.05.

Peptides	Significant?	P-value
cKRK vs AcKRK	No	0.7
cRKK vs AcRKK	No	0.07
cWFW vs AcWFW	Yes	<0.0001
cWRW vs AcWRW	Yes	<0.0001
cWWW vs AcWWW	Yes	<0.0001
cWYW vs AcWYW	Yes	<0.0001

Table 4.18: Summary of the P-values obtained from the statistical comparison of the accumulation of ROS species in peptide treated hyphae versus untreated hyphae. Statistical significance was determined by performing one-way ANOVA (using the Bonferroni’s multiple comparisons test) on the percentage ROS accumulated. “ns” denotes a P-value > 0.05.

Peptide compared to untreated control	Significant?	P-value
AcWRW	No	>0.05
AcWWW	No	>0.05
cWRW	No	>0.05
cWWW	Yes	<0.0001
WC	Yes	<0.0001

Table 4.19: Summary of the P-values obtained from the statistical comparison of the accumulation of ROS species in peptide treated hyphae in the presence versus absence of the antioxidant, Vitamin C. Statistical significance was determined by performing multiple t-tests (using the Sidak-Bonferroni method) on the total fluorescence intensity of SYTOX Green. “ns” denotes a P-value > 0.05.

Peptide	Significant	P-value
AcWRW	No	>0.05
AcWWW	No	>0.05
cWRW	No	>0.05
cWWW	Yes	<0.0001
WC	Yes	<0.0001

Chapter 5

Conclusions and recommendations for future studies

5.1 Introduction

An unprecedented global increase in the incidence of systemic fungal infections which has occurred in concurrence with a rising population of immunocompromised individuals has necessitated the search for novel agents of antifungal therapy [1–3]. Currently available therapeutic options have failed to effectively manage systemic fungal infections which are associated with high mortality rates due to modest activity against fungal pathogens and/or significant host toxicity [2]. Antimicrobial peptides (AMPs), regarded as Nature's very own antibiotics, are thus believed to be a potential solution to the threat of pathogenic fungi due to their highlighted potent and broad-spectrum antimicrobial activity [4–6]. On this premise, we set out to investigate the potential of small AMPs (natural cyclodecapeptides and RW-hexapeptides) for development as antifungal agents by characterising their antifungal activity against *Aspergillus fumigatus*. *A. fumigatus* is implicated in the pathogenesis of invasive aspergillosis, a deadly systemic fungal infection [7,8].

The investigation of the antifungal activity of the peptides was preceded by their chemical and structural characterisation. Chemical characterisation is essential to ascertain purity and chemical integrity as these properties influence the biological activity of peptides. The RW-hexapeptides only needed chemical characterisation as they were acquired elsewhere. The cyclodecapeptides had to be produced and extracted from cultures of *Brevibacillus parabrevis* first before they were purified and characterised chemically. Following successful chemical characterisation, the peptides were characterised structurally using biophysical methods in order to investigate the role of structure in peptide activity. Finally, an investigation into their antifungal activity against *A. fumigatus* spores and hyphae was carried out. Subsequently, a partial characterisation of the mode of action was done to gain insight into how antifungal activity is exerted.

5.2 Experimental conclusions

Production, purification and chemical characterisation of natural cyclodecapeptides

The tailored production of natural cyclodecapeptide analogues from amino acid supplemented cultures of *Br. parabrevis* was successful. From the analysis of the three culture extracts, it was evident that amino acid supplementation shifted the production profile of the cyclodecapeptides in fashion that is similar to what was reported by Vosloo *et al.* [9]. Supplementation with 16.5

mM Trp favoured the production of YC analogues, specifically WC while an increased production of YA analogues was observed in the extract obtained from cultures supplemented with 22 mM Phe. Purification of individual peptides using semi-preparative reversed phase HPLC was successful for most of the analogues as their UPLC-MS analyses confirmed their purities to be greater than 90% (specific peptide in composition). YB is the only analogue whose purity was below 90% as its complete separation from the closely related tyrocidine B₁ could not be achieved even after two rounds of purification. Thus, it would be ideal to optimise the HPLC purification methodology to ensure complete resolution between tyrocidine B and tyrocidine B₁ in future. The yield of tyrocidine C was low in production which prevented the investigation of its antifungal activity. This analogue is difficult to obtain in sufficient quantities via microbial culture production. Future studies could utilise different Trp:Phe ratios that would favour the production of YC by the producer cultures, as suggested by Vosloo *et al.* [9].

Chemical characterisation of RW-hexapeptides

Most of the RW-hexapeptide preparations passed our stringent quality control (QC) assessment as they were found to have purities of greater than 90%, according to UPLC-MS analysis. However, the two peptide preparations of the cWWW analogue that were obtained from GL Biochem failed our stringent QC tests. ESMS analysis of cWWW2 revealed the presence of various unidentified impurities in the peptide preparation. While the ESMS spectrum of cWWW3 appeared similar to that of the pure cWWW1, the positive ion signal was approximately 20-fold lower than expected, which could be an indication of the presence of non-ionisable impurities in the peptide preparation. The low positive ion signal and the failure to generate a UPLC-MS profile for cWWW3 are indications that the correct peptide was present only in very low quantities in the preparation which translated to a low purity.

In Chapter 4, cWWW was found to be the most active RW-hexapeptide analogue against *A. fumigatus* spores and hyphae making it a lead peptide for further development as an antifungal therapeutic agent. Because of this, it is quite important to obtain a pure preparation of this analogue as it would allow further characterisation of its activity and mode of action. In future, it would be ideal to synthesise the peptide in the BIOPEP facility as GL-Biochem are clearly struggling to synthesise cWWW correctly, and Dr Margitta Dathe's group in Leibniz have terminated their projects on the RW-hexapeptides.

UPLC-MS analysis showed the RW-hexapeptides to be highly polar as indicated by their early elution from the UPLC column ($R_t < 3$ minutes). The comparable retention times of the RW-

hexapeptide analogues was an indication of their similar amphipathic properties. However, the cyclic analogues exhibited slightly greater hydrophobicity in comparison to the linear analogues as indicated by their longer retention on the C₁₈ matrix during UPLC analysis. Dathe *et al.* [10] postulated that this increase in hydrophobicity could be attributed to the clustering of aromatic residues and could result in a slight enhancement of the amphipathicity of the cyclic analogues. The results from our molecular modelling experiments (Chapter 3) confirmed this hypothesis as the models of the cyclic hexapeptides exhibited a more defined amphipathic conformation than models of the linear analogues.

Structural characterisation of cyclodecapeptides

The results of the structural characterisation of the cyclodecapeptides showed consistency with previous findings [11–13]. The secondary structure of the cyclodecapeptides was found to be conserved and to consist of β -turn and β -sheet elements. In TFE, increased negative ellipticity at the 208 nm minima was observed which indicated an increase in β -turns and hydrogen bonded networks. TFE also promoted the formation of higher order sheet structures among the cyclodecapeptide analogues as indicated by the increased ellipticity ratios ($\theta_{208}/\theta_{216}$). Formation of higher order sheet structures was consistent with the propensity of the cyclodecapeptides to self-assemble in solution [14]. It was established from near UV CD spectroscopy and FS that self-assembly of the cyclodecapeptides is influenced by the nature of their solvent environment. Changes were observed in the shapes of the near UV CD spectra and fluorescence emission spectra of the cyclodecapeptides when their solvent environment changed. These changes pointed to the reorientation of aromatic side chains which would occur if there is an increased formation of self-assembly structures and/or alteration in the tertiary structure.

Structural characterisation of RW-hexapeptides

Characterisation of the structures of the RW-hexapeptides highlighted fundamental differences between the linear and cyclic analogues. From the *in silico* molecular modelling, the secondary structure of the molecular models of the cyclic analogues depicted a β -turn and γ -turn while the models of the linear analogues depicted only γ -turns. Analysis of secondary structure using the modelling software YASARA, indicated the secondary structure of the cyclic analogues to be composed of turn and β -sheet structures. A β -turn β -sheet motif was also represented on their CD spectra in water [15,16]. *In silico* analysis of the secondary structural composition of the linear analogues indicated only undefined elements which could be the γ turns. The shapes of their CD spectra in water were reminiscent of undefined/irregular structures [17,18]. However, a huge

change in spectral shape was observed when the solvent environment of the linear analogues changed to TFE indicating that their structures had changed significantly. This is in stark contrast to the cyclic analogues whose CD spectra did not change much in TFE indicating the stability of the backbone structure which could be attributed to the two turns in their backbone and confinement in a cyclic structure. FS also highlighted structural differences between the linear and cyclic RW-hexapeptides. While the fluorescence emission maximum of all the analogues were blue-shifted in TFE, only the cyclic analogues experienced quenching of their total fluorescence intensity.

In future, the use of model membranes is recommended when characterising the structure of peptides with CD and FS as opposed to a membrane-mimicking solvent such as TFE as they better represent the architecture of a true membrane and would give a more accurate representation of the structures adopted by peptides in a membrane environment. Advanced 2D-NMR spectroscopy of the peptides in different solvents would also be beneficial to refine the *in silico* models of the peptides.

Biological activity of peptides

In general, the cyclodecapeptides and the RW-hexapeptides displayed excellent antifungal activity against *A. fumigatus*. The cyclodecapeptides were, however, the most active followed by the cyclic RW-hexapeptides and lastly, the linear RW-hexapeptides. The activity of the most active cyclic RW-hexapeptides (cWRW, cWWW and cWFW) compared well with that of the cyclodecapeptides as indicated by the similarity of the IC₅₀ values for germination and growth inhibition of *A. fumigatus* spores. The superior activity of the cyclic analogues over the linear analogues was attributed to their more pronounced amphipathicity. Amongst the RW-hexapeptides, the WRW and WWW cyclic and linear analogues exhibited the most profound germination and growth inhibitory activity against *A. fumigatus* spores highlighting the important role of Arg and Trp residues in antifungal activity. Superior activity was observed for the Arg-containing analogues over the analogues containing Lys residues. In addition, the analogues that had only Trp as their aromatic residue had better activity than analogues with Phe and Tyr. Taken together, these two observations suggest that the antifungal activity of the RW-hexapeptides is not determined by amphipathicity alone but by specific residues.

Consistent with the findings from previous investigations [19,20], the natural cyclodecapeptides were found to be toxic as they exhibited haemolytic activity. This toxicity continues to derail their potential development as antifungal agents for the treatment of systemic infections. Conversely,

the RW-hexapeptides demonstrated limited haemolytic activity which is also consistent with previous findings [10,21]. Their low propensity to lyse human erythrocytes renders them more attractive for development as therapeutic agents for systemic use.

Investigation of the antifungal activity of peptide combinations showed the peptide interactions of the 1:3 peptide combinations of WC and each of the lead RW-hexapeptide analogues to be additive. Based on this observation, it is proposed that a combination of WC and cWRW at this ratio would be worth considering for further development as an antifungal agent. Hypothetically, such a combination would eliminate the high toxicity of WC but maintain the high antifungal potency towards spores and hyphae. It would therefore be ideal to develop such a formulation for the treatment of systemic infections, as well as topical infections such as foot and mouth ulcers caused by fungal infections. Further investigations of this proposed combination towards other fungal pathogens (*Candida* spp. and *Cryptococcus* spp.) and optimisation of the formulation are thus recommended.

Investigation of membrane permeabilisation as a mode of action showed that for the RW-hexapeptides, it is not the primary mode of action. The low uptake of SG indicated their inability to effectively disrupt the membrane integrity of the *A. fumigatus* hyphae. On the other hand, WC effectively permeabilised the membrane of *A. fumigatus* hyphae and induced rapid uptake of SG. This result was consistent with the previously reported membranolytic mode of action of the cyclodecapeptides [6]. The observed lytic action or lack thereof directly correlated to the haemolytic activity of all peptides.

WC and cWWW increased the accumulation of ROS in *A. fumigatus* hyphae. Moreover, they were the only two peptides that exhibited activity against fungal hyphae. Together, these results indicate the possible involvement of ROS in the execution of WC and cWWW's antifungal activity. However, further investigations are required to ascertain whether the increased production of ROS is linked to the antifungal activity of the peptides as Troskie *et al.* [22] found that the antifungal activity of some cyclodecapeptide analogues was not related to their ROS induction in *C. albicans*.

5.3 Last word

This study has highlighted the potent antifungal activity of the cyclodecapeptides and the RW-hexapeptides thus confirming our hypothesis that AMPs could potentially be developed as novel therapeutic agents to be used in the therapy of the rampant systemic fungal infections. The membrane action of the cyclodecapeptides has also been highlighted. However, the mode action

of the RW-hexapeptides still remains a mystery warranting further investigations into their mode of action.

5.4 References

- [1] J.L. Xie, E.J. Polvi, T. Shekhar-Guturja, L.E. Cowen, Elucidating drug resistance in human fungal pathogens, *Future Microbiology*, 9 (2014) 523–42.
- [2] Y. Chang, S. Yu, J. Heitman, M. Wellington, New facets of antifungal therapy, *Virulence*, 8 (2017) 222–236.
- [3] L. Ostrosky-Zeichner, A. Casadevall, J.N. Galgiani, F.C. Odds, J.H. Rex, An insight into the antifungal pipeline: selected new molecules and beyond, *Nature Reviews Drug Discovery*, 9 (2010) 719–727.
- [4] W. Danders, M. a Marahiel, M. Krause, N. Kosui, T. Kato, N. Izumiya, H. Kleinkauf, Antibacterial action of gramicidin S and tyrocidines in relation to active transport, in vitro transcription, and spore outgrowth, *Antimicrobial Agents and Chemotherapy*, 22 (1982) 785–790.
- [5] M. Rautenbach, N.M. Vlok, M. Stander, H.C. Hoppe, Inhibition of malaria parasite blood stages by tyrocidines, membrane-active cyclic peptide antibiotics from *Bacillus brevis*, *Biochimica et Biophysica Acta - Biomembranes*, 1768 (2007) 1488–1497.
- [6] M. Rautenbach, A.M. Troskie, J.A. Vosloo, M.E. Dathe, Antifungal membranolytic activity of the tyrocidines against filamentous plant fungi, *Biochimie*, 130 (2016) 122–131.
- [7] J.-P. Latg, *Aspergillus fumigatus*, a saprotrophic pathogenic fungus, *Mycologist*, 17 (2003) 56–61.
- [8] J.P. Latgé, *Aspergillus fumigatus* and aspergillosis, *Clinical Microbiology Reviews*, 12 (1999) 310–350.
- [9] J.A. Vosloo, M.A. Stander, A.N.N. Leussa, B.M. Spathelf, M. Rautenbach, Manipulation of the tyrothricin production profile of *Bacillus aneurinolyticus*, *Microbiology*, 159 (2013) 2200–2211.
- [10] M. Dathe, H. Nikolenko, J. Klose, M. Bienert, Cyclization increases the antimicrobial activity and selectivity of arginine- and tryptophan-containing hexapeptides, *Biochemistry*, 43 (2004) 9140–9150.
- [11] G. Munyuki, G.E. Jackson, G.A. Venter, K.E. Kövér, L. Szilágyi, M. Rautenbach, B.M. Spathelf, B. Bhattacharya, D. Van Der Spoel, β -sheet structures and dimer models of the two major tyrocidines, antimicrobial peptides from *Bacillus aneurinolyticus*, *Biochemistry*, 52 (2013) 7798–7806.
- [12] J.A. Vosloo, Optimised bacterial production and characterisation of natural antimicrobial peptides with potential application in agriculture, PhD Thesis, Department of Biochemistry, University of Stellenbosch, (2016), <http://hdl.handle.net/10019.1/98411>
- [13] B. Spathelf, Qualitative structure-activity relationships of the major tyrocidines , cyclic

- decapeptides from *Bacillus aneurinolyticus*, PhD Thesis, Department of Biochemistry, University of Stellenbosch, (2013), <http://hdl.handle.net/10019.1/4001>
- [14] S. Laiken, M. Printz, L.C. Craig, Circular dichroism of the tyrocidines and gramicidin S-A, *Journal of Biological Chemistry*, 244 (1969) 4454–4457.
- [15] D.L. Lee, J.P.S. Powers, K. Pfliegerl, M.L. Vasil, R.E.W. Hancock, R.S. Hodges, Effects of single D-amino acid substitutions on disruption of β -sheet structure and hydrophobicity in cyclic 14-residue antimicrobial peptide analogs related to gramicidin S, *Journal of Peptide Research*, 63 (2004) 69–84.
- [16] L.H. Kondejewski, M. Jelokhani-Niaraki, S.W. Farmer, B. Lix, C.M. Kay, B.D. Sykes, R.E.W. Hancock, R.S. Hodges, Dissociation of antimicrobial and hemolytic activities in cyclic peptide diastereomers by systematic alterations in amphipathicity, *Journal of Biological Chemistry*, 274 (1999) 13181–13192.
- [17] S.M. Kelly, T.J. Jess, N.C. Price, How to study proteins by circular dichroism, *Biochimica et Biophysica Acta - Proteins and Proteomics*, 1751 (2005) 119–139.
- [18] N.J. Greenfield, Using circular dichroism spectra to estimate protein secondary structure, *Nature Protocols*, 1 (2007) 2876–2890.
- [19] A.N.-N. Leussa, Characterisation of small cyclic peptides with antimalarial and antilisterial activity, PhD Thesis, Department of Biochemistry, University of Stellenbosch, (2014), <http://hdl.handle.net/100191/86161>,
- [20] B.M. Spathelf, M. Rautenbach, Anti-listerial activity and structure-activity relationships of the six major tyrocidines, cyclic decapeptides from *Bacillus aneurinolyticus*, *Bioorganic and Medicinal Chemistry*, 17 (2009) 5541–5548.
- [21] K. Scheinpflug, H. Nikolenko, I. V. Komarov, M. Rautenbach, M. Dathe, What goes around comes around-A comparative study of the influence of chemical modifications on the antimicrobial properties of small cyclic peptides, *Pharmaceuticals*, 6 (2013) 1130–1144.
- [22] A.M. Troskie, M. Rautenbach, N. Delattin, J.A. Vosloo, M. Dathe, B.P.A. Cammue, K. Thevissen, Synergistic activity of the tyrocidines, antimicrobial cyclodecapeptides from *Bacillus aneurinolyticus*, with amphotericin B and caspofungin against *Candida albicans* biofilms, *Antimicrobial Agents and Chemotherapy*, 58 (2014) 3697–3707.